



Technical University of Munich

TUM School of Life Sciences

**Unravelling the fate of tramadol in plants: Insights into the  
removal efficiency and the role of plant-bacterial interaction in  
the phytoremediation process**

**David Mamdouh Khalaf Kamel**

Complete reprint of the dissertation approved by the TUM School of Life Sciences of the  
Technical University of Munich for the award of the doctoral degree

**Doktor der Naturwissenschaften (Dr. rer. nat.)**

Chair: Prof. Dr. Kurt-Jürgen Hülsbergen

Examiners:

1. apl. Prof. Dr. Peter Schröder

2. Prof. Dr. Jürgen Geist

The dissertation was submitted to the Technical University of Munich on 25.09.2023 and  
accepted by the TUM School of Life Sciences on 13.12.2023



## Table of Contents

Abstract .....	V
Zusammenfassung .....	VII
I. List of Abbreviations .....	X
II. List of Figures .....	XI
<b>1. Introduction .....</b>	<b>1</b>
1.1. Climate change and water scarcity .....	1
1.2. Reuse of wastewater as a solution for the water scarcity problem .....	1
1.3. Contaminants of emerging concern (CECs) .....	1
1.4. The opioid Tramadol (TRD) .....	2
1.5. Phytoremediation as a solution for PPCPs removal .....	4
1.6. Impact of PPCPs on plant health.....	6
1.7. Role of beneficial bacteria in enhancing phytoremediation of xenobiotics .....	8
1.8. Impact of PPCPs on bacterial communities associated with plant roots .....	10
1.9. Aim of the Thesis .....	12
<b>2. Materials and methods .....</b>	<b>13</b>
2.1. Experimental designs .....	13
2.1.1. Removal of TRD by plants and its interaction with other contaminants (M1) .....	13
2.1.2. Effect of TRD on plant performance and root-associated bacterial community (M2) .....	13
2.1.3. Plant-bacterial interaction to enhance removal and metabolization of TRD (M3-in preparation for publication) .....	14
2.2. Samples (liquid, root and shoot) preparation for injection .....	15
2.3. Plant analysis .....	16
2.3.1. Evaluation of root activity (in M1 appendix) .....	16
2.3.2. Accumulation and translocation of TRD (in M1 appendix) .....	16
2.3.3. Extraction of crude enzymes (in M2 appendix) .....	16
2.3.4. Measured enzymes (in M2 appendix) .....	17
2.4. Bacterial analysis .....	18
2.4.1. Screening for plant growth promoting (PGP) traits (in M3 appendix) .....	18
2.4.2. Screening for <i>in vitro</i> TRD removal (in M3 appendix) .....	19
2.4.3. Molecular identification of bacterial endophytes (in M3 appendix) .....	19
2.4.4. Identification of root-associated bacterial communities .....	20

2.5. Analytical instrument setup and conditions (M1, M2 and M3) .....	21
2.6. Statistical analyses .....	22
<b>3. Manuscript Overview .....</b>	<b>24</b>
<b>4. General Discussion .....</b>	<b>28</b>
4.1. TRD uptake/removal in short-term and hydroponic experiments .....	29
4.2. Effect of TRD on GPX, CAT and GST plant enzymes .....	32
4.3. TRD effect on root-associated bacterial community .....	35
4.4. Isolation of endophytic bacteria from TRD-exposed plants and their PGP characteristics .....	38
4.5. <i>In vitro</i> and <i>in vivo</i> removal of TRD using endophytic bacterial isolates.....	39
4.6. Quantification of TRD and its O- and N-demethylated metabolites in barley tissues ....	42
<b>5. Conclusion and Recommendations .....</b>	<b>44</b>
III. References .....	46
IV. Acknowledgement.....	73
V. Appendix	
i.    Appendix M1 (Manuscript I)	
Appendix M1 (Supplements I)	
ii.   Appendix M2 (Manuscript II)	
Appendix M2 (Supplements II)	
iii.  Appendix M3 (Manuscript III, in preparation for publication)	
Appendix M3 (Supplements III)	

## **Abstract**

With a growing global population and climate change, the pressure on freshwater demand is expected to increase significantly and subsequently water scarcity problems will become more serious especially in arid and semi-arid regions. Hence, the safe reuse of treated wastewater has been considered as one of the promising techniques to overcome these problems. However, inadequate treatment of wastewater may lead to contamination of water resources with poorly degradable or recalcitrant compounds such as pharmaceuticals. Tramadol (TRD), as one of these compounds, has been frequently detected in various water resources due to the massive abuse and inadequate removal by conventional wastewater treatment plants. While the toxicity of TRD has been addressed in aquatic organisms, there is limited research regarding its presence and behaviour in plants. Therefore, during this study we studied the removal of TRD using barley seedlings in hydroponic cultures with environmentally relevant TRD concentrations, analyzed its distribution in plant parts (root and shoot) besides evaluating its effect on selected plant enzymes and root-associated bacterial communities in young barley plants. To uncover the potential cooperation between bacteria and plants to enhance the removal of TRD, a hydroponic inoculation experiment was conducted with bacterial endophytes obtained from the roots of TRD-contaminated plants. Later in the experiment, we investigated the metabolization of TRD in plant tissues and how inoculation with bacterial endophytes affected this process.

The ability of separated roots from barley and cattail plants to transport TRD was proven in a short-term uptake experiment, using the Pitman chamber technique, with a transport rate of TRD up to 5.18 and 5.79  $\mu\text{g g}^{-1}$  root fresh weight  $\text{day}^{-1}$ , respectively. Moreover, subsequent experiments using the same technique and plant species showed strong inhibition in TRD transport after exposing these excised roots to a mixture of TRD either with venlafaxine (VEN; having a similar chemical structure as TRD) or quinidine (Q; used as an inhibitor for cellular organic cation transporters). Barley seedlings showed high removal efficiency towards TRD up to 89.13 % during 15 days after exposure to environmentally relevant concentrations of this compound. Furthermore, TRD was detected in root and shoot tissues of barley seedlings which demonstrates the easy access of TRD into seedlings' roots as well as the tendency of TRD to translocate into the shoots.

Further experiments in the current thesis revealed the accumulation of TRD inside root tissues of barley plants over time (12 and 24 days) inside total roots fresh weights (FW). In addition, TRD seemed to induce the activities of guaiacol peroxidase, catalase and glutathione S-transferase in tissues of young barley plants after exposure to TRD. Not only

TRD stimulates the activity of these enzymes but it also alters the root-associated bacterial communities. TRD led to a significant impact on beta diversity of root-associated bacteria communities. The relative abundances results showed that Xanthomonadaceae was the dominating family in roots of TRD-treated plants after 24 days. Interestingly, certain amplicon sequence variants (ASVs) were differentially abundant in barley roots exposed to TRD in comparison with controls at both time points (12 and 24 days).

Furthermore, recovered endophytic bacterial isolates, from TRD-exposed cattail roots, showed positive results on the *in vitro* tests for plant growth promotion, besides the potential of some isolates to partially remove TRD in the presence of glucose or L(-)malic acid disodium (malate) as carbon source. Inoculating barley seedlings with single, dual or mixture of bacterial isolates enhanced the removal efficiency of TRD ( $1 \text{ mg L}^{-1}$ ) in hydroponic cultures compared to non-inoculated plants. Dually inoculated plants showed the highest removal efficiency (87.53 %), whilst the highest concentrations of TRD in seedlings' tissues were recorded in shoots of plants inoculated with a mixture of selected bacterial endophytes ( $255.87 \text{ } \mu\text{g TRD}$  in total shoot FW). Moreover, O- and N-desmethyltramadol (ODTRD and NDTRD, respectively) metabolites were detected and quantified in roots and shoots of barley seedlings regardless of their status of inoculation with bacterial endophytes with higher amounts of NDTRD compared to ODTRD. The highest concentration of the previous metabolites was measured in Dual ( $3.46 \text{ } \mu\text{g ODTRD}$  in total shoot FW) and Mix ( $11.02 \text{ } \mu\text{g NDTRD}$  in total shoot FW) inoculated plants.

Although regarded as recalcitrant in classical wastewater treatment plant processes, TRD can be removed and metabolized with a phytoremediation approach, exploiting plant-bacteria interactions to enhance/accelerate these processes through direct and/or indirect effects caused by the bacterial partners.

## Zusammenfassung

Mit dem Wachstum der Weltbevölkerung und dem Klimawandel wird der Druck auf die Süßwassernachfrage voraussichtlich erheblich zunehmen, so dass sich das Problem der Wasserknappheit vor allem in ariden und semiariden Regionen verschärfen wird. Aus diesem Grund gilt die sichere Wiederverwendung von gereinigtem Abwasser als eine der vielversprechendsten Techniken zur Überwindung der bisherigen Probleme. Eine unzureichende Abwasserbehandlung kann jedoch zu einer Verunreinigung der Wasserressourcen mit schwer abbaubaren oder rekalcitranten Verbindungen wie Arzneimitteln führen. Tramadol (TRD), eine dieser Verbindungen, wurde aufgrund des massiven Missbrauchs und der unzureichenden Entfernung durch herkömmliche Kläranlagen häufig in verschiedenen Wasserressourcen nachgewiesen. Während die Toxizität von TRD in Wasserorganismen erforscht wurde, gibt es nur wenige Untersuchungen zu seiner Präsenz und seinem Verhalten in Pflanzen. Daher haben wir in dieser Studie die Entfernung von TRD mit Gerstenkeimlingen in hydroponischen Kulturen mit umweltrelevanten TRD-Konzentrationen untersucht, seine Verteilung in Pflanzenteilen (Wurzel und Spross) analysiert und seine Auswirkungen auf ausgewählte Pflanzenenzyme und wurzelassoziierte Bakteriengemeinschaften in jungen Gerstenpflanzen bewertet. Um die mögliche Kooperation zwischen Bakterien und Pflanzen zur Verbesserung der Beseitigung von TRD aufzudecken, wurde ein hydroponisches Inokulationsexperiment mit bakteriellen Endophyten durchgeführt, die aus den Wurzeln von TRD-belasteten Pflanzen gewonnen worden waren. Im weiteren Verlauf des Experiments untersuchten wir die Metabolisierung von TRD im Pflanzengewebe und wie die Inokulation mit bakteriellen Endophyten diesen Prozess beeinflusst.

Die Ergebnisse zeigten, dass abgetrennte Wurzeln von Gersten- und Rohrkolbenpflanzen in der Lage sind, TRD in Kurzzeit-Aufnahmeexperimenten basal zu transportieren, wobei die Transportrate von TRD bis zu 5,18 bzw. 5,79  $\mu\text{g g}^{-1}$  Wurzel-Frischgewicht  $\text{Tag}^{-1}$  betrug. Darüber hinaus zeigten andere Experimente mit der gleichen Technik eine starke Hemmung des TRD-Transports, nachdem diese abgetrennten Wurzeln einer Mischung aus TRD entweder mit Venlafaxin (VEN; hat eine ähnliche chemische Struktur wie TRD) oder Chinidin (Q; wird als Inhibitor für zelluläre organische Kationentransporter verwendet) ausgesetzt wurden. Ganze Gerstenkeimlinge zeigten eine hohe Effizienz für die Aufnahme von TRD von bis zu 89.13 % innerhalb von 15 Tagen, nachdem sie umweltrelevanten Konzentrationen dieser Verbindung ausgesetzt waren. Darüber hinaus wurde TRD im Wurzel- und Sprossgewebe der Gerstensämlinge nachgewiesen, was auf eine leichte

Aufnahme von TRD in die Wurzeln der Sämlinge sowie auf die Tendenz von TRD zur Translokation in die oberirdischen Teile der Pflanze hinweist.

Ein weiterer Versuch in dieser Arbeit zeigte die Anreicherung von TRD im Laufe der Zeit (12 und 24 Tage) im gesamten Wurzel-Frischgewicht (FW) von Gerstenpflanzen. Darüber hinaus schien TRD das antioxidative Abwehrsystem von Gerste zu beeinflussen. In den Geweben junger Gerstenpflanzen wurden nach der TRD-Exposition Induktionen der Aktivitäten von Guajakolperoxidase, Katalase und Glutathion-S-Transferase festgestellt. TRD stimuliert nicht nur die Aktivität dieser Enzyme in den behandelten Pflanzen, sondern verändert auch die wurzellozierten bakteriellen Gemeinschaften. Die Behandlung von Gerstenpflanzen mit TRD führte zu einer signifikanten Auswirkung auf die Beta-Diversität der wurzellozierten Bakteriengemeinschaften. Die relativen Häufigkeiten der dominantesten Familien zeigten, dass Xanthomonadaceae die dominierende Familie in den Wurzeln der TRD-behandelten Pflanzen nach 24 Tagen war. Interessanterweise waren bestimmte Amplikon-Sequenzvarianten (ASVs) in Gerstenwurzeln, die TRD ausgesetzt waren, im Vergleich zu den Kontrollen zu beiden Zeitpunkten (12 und 24 Tage) unterschiedlich häufig vorhanden.

Darüber hinaus zeigten die endophytischen Bakterienisolate aus TRD-exponierten Rohrkolbenwurzeln positive Ergebnisse bei den In-vitro-Tests zur Förderung des Pflanzenwachstums, abgesehen von dem Potenzial einiger Isolate, TRD in Gegenwart von Glukose oder L(-)Äpfelsäure-Dinatrium (Malat) als Kohlenstoffquelle teilweise zu entfernen. Die Beimpfung von Gerstensämlingen mit einem, zwei oder einer Mischung von Bakterienisolaten verbesserte die Effizienz der Beseitigung von TRD ( $1 \text{ mg L}^{-1}$ ) in hydroponischen Kulturen im Vergleich zu nicht beimpften Pflanzen. Zweifach beimpfte Pflanzen zeigten die höchste Entfernungseffizienz (87.53 %), während die höchsten TRD-Konzentrationen im Gewebe der Keimlinge in Sprossen von Pflanzen festgestellt wurden, die mit einer Mischung ausgewählter bakterieller Endophyten beimpft waren ( $255,87 \text{ } \mu\text{g TRD}$  in der gesamten Spross-FW). Darüber hinaus wurden die Metaboliten O- und N-Desmethyltramadol (ODTRD bzw. NDTRD) in Wurzeln und Sprossen von Gerstensämlingen nachgewiesen und quantifiziert, und zwar unabhängig vom Status der Inokulation mit bakteriellen Endophyten, wobei die Mengen an NDTRD höher waren als die an ODTRD. Die höchste Konzentration der vorgenannten Metaboliten wurde in mit Dual ( $3,46 \text{ } \mu\text{g ODTRD}$  in der gesamten Spross-FW) und Mix ( $11,02 \text{ } \mu\text{g NDTRD}$  in der gesamten Spross-FW) beimpften Pflanzen gemessen.



Obwohl TRD in klassischen Kläranlagen als rekalzitranz gilt, kann es mit einem Phytosanierungskonzept entfernt und verstoffwechselt werden. Dabei werden die Wechselwirkungen zwischen Pflanzen und Bakterien genutzt, um diese Prozesse durch direkte und/oder indirekte Effekte der bakteriellen Partner zu verbessern/beschleunigen.

## I. List of Abbreviations

<i>ACC</i>	1-aminocyclopropane-1-carboxylate
<i>alkB</i>	Alkane hydroxylase gene
<i>APX</i>	Ascorbate peroxidase
<i>BCF</i>	Bioconcentration factor
<i>CAT</i>	Catalase
<i>CDNB</i>	1-chloro-2,4-dinitrobenzene
<i>CECs</i>	Contaminants of emerging concern
<i>CWs</i>	Constructed wetlands
<i>CYP</i>	Cytochrome P450
<i>EC</i>	European Commission
<i>EDTA</i>	Ethylene diaminetetraacetic acid
<i>FAO</i>	Food and Agriculture Organization
<i>FW</i>	Fresh weight
<i>GPX</i>	Guaiacol peroxidase
<i>GSH</i>	Reduced glutathione
<i>GST</i>	Glutathione S-transferase
<i>IAA</i>	Indole-3-acetic acid
<i>IS</i>	Internal standard
<i>NDTRD</i>	N-desmethyltramadol
<i>ODTRD</i>	O-desmethyltramadol
<i>PGP</i>	Plant growth promoting
<i>pNPA</i>	p-nitrophenyl acetate
<i>PPCPs</i>	Pharmaceuticals and personal care products
<i>Q</i>	Quinidine
<i>R-2A</i>	Reasoner's 2A
<i>ROS</i>	Reactive oxygen species
<i>rRNA</i>	Ribosomal ribonucleic acid
<i>SOD</i>	Superoxide dismutase
<i>TF</i>	Translocation factor
<i>TFN</i>	Triphenyl formazan
<i>TRD</i>	Tramadol
<i>TTC</i>	Triphenyltetrazolium chloride
<i>VEN</i>	Venlafaxine
<i>WHO</i>	World Health Organization
<i>WWAP</i>	World Water Assessment Programme

## **II. List of Figures**

Figure 1. Simplified diagram showing basic routes for tramadol metabolism

Figure 2. Scheme to demonstrate the different experiments conducted in this study

## **1. Introduction**

### **1.1. Climate change and water scarcity**

Climate change is a critical problem facing our world these days. Moreover, it represents one of the main drivers for water scarcity which will affect two-thirds of the world population by 2025 (FAO, 2007; Ungureanu et al., 2020). Approximately 20% of the global increase in water scarcity is predicted to be linked to climate change issues (FAO, 2007). Gerten and coauthors (2013) concluded that continuing the global warming with the current rate without solutions to abate it will significantly change the availability of freshwater as well as ecosystem properties in the future. The typical solutions for water scarcity concentrate on either improving water use efficiencies or on increasing water resources and availability (Ward et al., 2010; Wada et al., 2014). Other solutions such as reuse of treated wastewater and usage of desalinated water would offer a fast growing option to reduce scarcity of freshwater as well as minimize water pollution, but require further research (Elimelech and Phillip, 2011; Gude, 2017; Jones et al., 2019).

### **1.2. Reuse of wastewater as a solution for the water scarcity problem**

Many arid and semi-arid areas are facing big challenges in water resource management because of increased water consumption and water scarcity problems. Moreover, water scarcity can also hit the regions with abundant rainfall, as water scarcity in this case may be more linked to quality of water resources (Pereira et al., 2002). Discharging untreated sewage along with agricultural runoff and insufficient wastewater treatment have already resulted in degrading quality of water around the world. Moreover, estimates about wastewater treatment from countries depending on their income support the idea that more than 80% of wastewater is discharged into the environment without proper treatment (World Water Assessment Programme [WWAP], 2017). The main drivers to adopt advanced techniques for treating wastewater in high-income countries are based on maintaining high water quality as well as providing an alternative water source to cope with water scarcity problem. However, in developing countries, discharging wastewater without any treatment stays a common practice (WWAP, 2017), that has to be banned and replaced by more environmentally safe options.

### **1.3. Contaminants of emerging concern (CECs)**

CECs are contaminants which are not integrated in routine monitoring programmes; however, it can enter into the environment and adversely affect ecological and/or human health in high concentrations (Nawaz and Sengupta, 2019). These contaminants are not only limited to

chemical compounds but also can include other threats such as (micro)plastic, antibiotic resistance and new pathogenic organisms (Water JPI, 2019). One group of the important CECs are pharmaceuticals and personal care products (PPCPs) which comprise chemicals used in veterinary and human health care drugs as well as cosmetic products for improving the quality of daily life such as shampoos, toothpastes, deodorants, lipsticks and hair colours. CECs, in particular pharmaceuticals, are commonly detected in various water bodies such as wastewater (Schröder et al., 2016; Yang et al., 2017a), surface and ground water (Balakrishna et al., 2017), and even in our most valuable resource, drinking water (Carmona et al., 2014; Bexfield et al., 2019) due to their high consumption and their recalcitrance. These contaminants have been listed among the forty most vital issues in the US, due to their frequent detection in the environment besides their (eco-)toxicological effects (Fleishman et al., 2011). In the same direction, EU Parliament has added some pharmaceutical compounds to their watch list of emerging water pollutants (European Commission [EC], 2015). Although effects of these contaminants are not yet completely assessed and their impact on human health is in some cases unclear, adverse effects on animals and microbial populations are likely and the alteration of biochemical and physiological functions in all biota is possible.

#### **1.4. The opioid Tramadol (TRD)**

PPCPs, similar to other harmful xenobiotics, usually possess more or less the same physico-chemical properties such as persistence (to avoid the conversion to inactive forms before doing their effect), lipophilicity (to facilitate their passage through membranes) besides their usage in large quantities (like various pesticides) (Barceló and Petrovic, 2007). Tramadol (IUPAC name: 2-[(dimethylamino)methyl]-1-(3-methoxyphenyl)cyclohexan-1-ol; CAS number: 27203-92-5; Fig. 1) is an opioid analgesic which is used in moderate to severe pain treatments and commonly prescribed due to its low addiction properties as well as its high efficacy (Gong et al., 2014; Bravo et al., 2017). Recently, various studies showed the massive abuse of TRD in some African, Middle East and Asian countries (WHO, 2018). TRD has been detected in various water bodies such as surface water, influents and effluents of wastewater treatment plants (WWTPs) with high value ( $\sim 97 \mu\text{g L}^{-1}$ ) detected in the effluent of WWTP Cilfynydd (Kasprzyk-Hordern et al., 2007, 2008, 2009; Wick et al., 2009; Rúa-Gómez and Püttmann, 2012; Loos et al., 2013; Mackuľak et al., 2015; Archer et al., 2017; Malnes et al., 2022).

Mammalian TRD metabolism (Fig. 1) starts in the liver with O- and N-demethylation followed by conjugation reactions forming different sulphate and glucuronide metabolites (Wu et al., 2002; Gong et al., 2014).

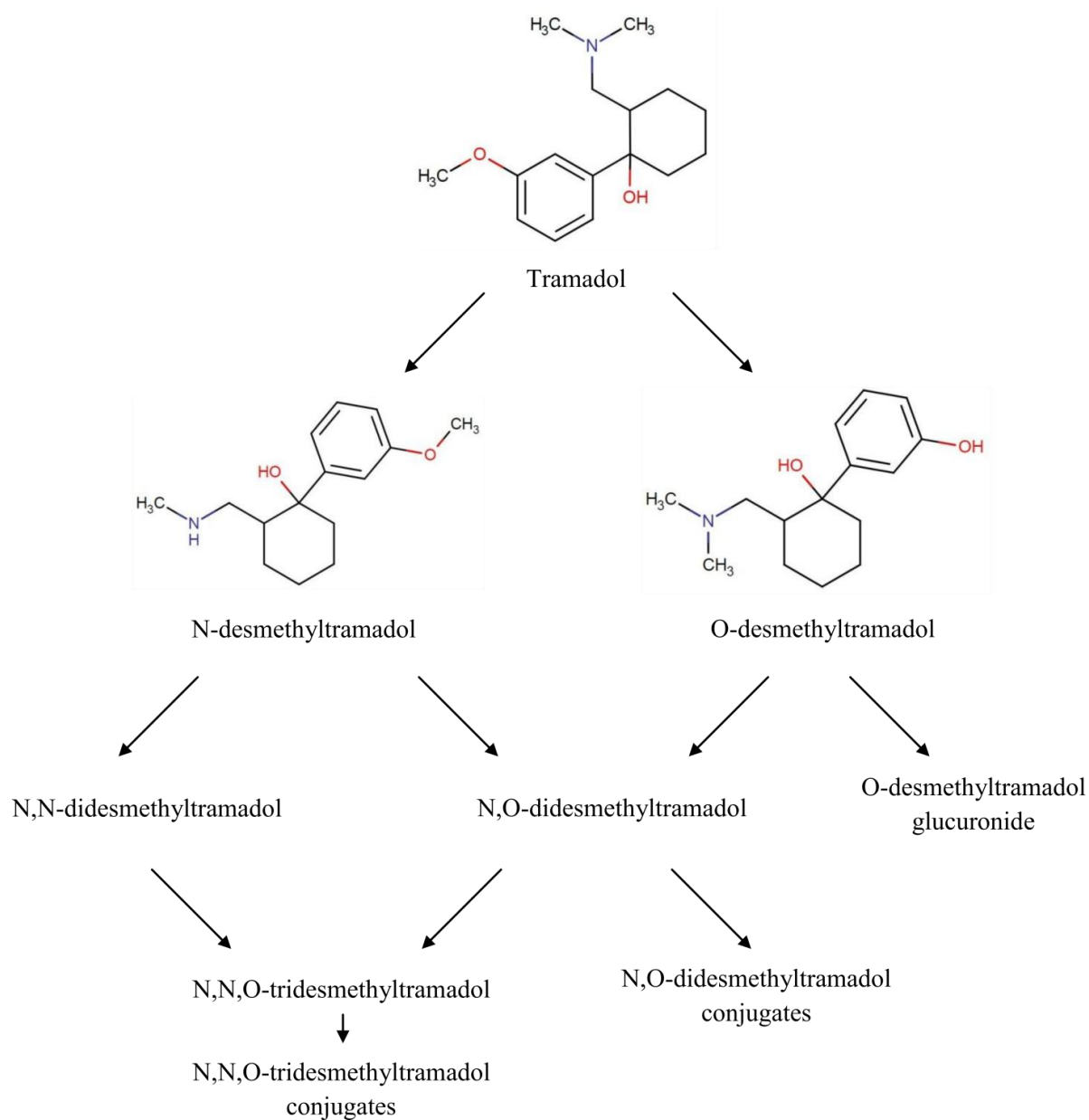


**Figure 1.** Simplified diagram showing basic routes for tramadol metabolism (modified from the online scheme at <http://www.pharmgkb.org/pathway/PA165946349>; molecules structures were taken from <https://go.drugbank.com/drugs/DB00193>)

About 30% of the administered TRD dose is excreted without change in the urine, whereas the rest are excreted as primary or secondary metabolites. In human, cytochrome P450 (CYP) 2D6 is the responsible enzyme for TRD conversion to O-desmethyltramadol (ODTRD; the pharmacologically active metabolite), while the conversion of TRD to N-desmethyltramadol (NDTRD; the pharmacologically inactive metabolite) is catalyzed by CYP2B6 and CYP3A4 (Paar et al., 1997; Subrahmanyam et al., 2001). Further degradation for ODTRD and TRD may occur resulting in the production of N,N-didesmethyltramadol, N,N, O-tridesmethyltramadol and N,O-didesmethyltramadol which can be conjugated with sulphate and glucuronic acid before excretion via urine (Lintz et al., 1981; Subrahmanyam et al., 2001). Previous studies demonstrated the occurrence of both, ODTRD and NDTRD in WWTP and surface water (de Jongh et al., 2012; Rúa-Gómez and Püttmann, 2012; Archer et al., 2017; Styszko et al., 2021). Some studies have called attention for the effects of TRD in aquatic environments. For example, Sehonova and coauthors (2016) reported that hatching in zebrafish (*Danio rerio*) was delayed after exposure to TRD (10, 50, 100 and 200  $\mu\text{g L}^{-1}$ ), while under the same conditions, the common carp (*Cyprinus carpio*) was significantly affected by TRD which appeared on hatching, morphology, early ontogeny and histopathology. Another study reported that environmentally relevant concentrations ( $\sim 1 \mu\text{g L}^{-1}$ ) of TRD may affect the behaviour of marbled crayfish (Buřič et al., 2018). Furthermore, TRD has been pointed out as one of the three substances contributing predominantly to the acute mixture toxic pressure in Swedish water system (Lindim et al., 2019).

### **1.5. Phytoremediation as a solution for PPCPs removal**

Since treatment of wastewater using traditional methods in WWTP is insufficient to completely eliminate these PPCPs (Ramirez-Morales et al., 2020; Rout et al., 2021), other techniques should urgently be adopted. Physical and chemical processes such as photolysis, ozonation and membrane filtration might be state of the art modern physico-technical solutions (Esplugas et al., 2007; Klavarioti et al., 2009; Zhang et al., 2020; Krishnan et al., 2021; Lozano et al., 2022), however, the high cost of these techniques stays as a barrier to spread them worldwide. In recent years, several reports have demonstrated that constructed wetlands (CWs) are promising eco-friendly, energy saving and cost-effective solutions to polish effluents from these contaminants, even in developing countries, as they combine a diverse set of biological, physical and chemical processes for instance microbial degradation or cometabolization, uptake and accumulation in plant tissue, volatilization as well as sorption and sedimentation (Carvalho et al., 2014; Li et al., 2014; Verlicchi & Zambello,

2014; Zhang et al., 2014; Liu et al., 2019; Nguyen et al., 2019a; Hu et al., 2021). Plants possess a set of specific mechanisms by which they can cope with and/or reduce the toxicity of foreign compounds such as xenobiotics. These mechanisms were described by Sandermann (1992; 1994) under the “Green Liver” concept and resemble those in human liver where they are found for drug detoxification. In this concept, the metabolism of xenobiotic by plants can be simply divided into three phases, (I) activation, (II) detoxification and (III) compartmentation/sequestration. Where, in phase (I) cytochrome P450 monooxygenases and peroxidases are the main enzymes for activating and preparing the xenobiotic for the next phase, whilst in phase (II) the modified xenobiotics undergo conjugation with glutathione or sugar to make the molecule less or non-toxic, a process that is mediated by glutathione- and glycosyl-transferases, respectively. Several examples have demonstrated high removal efficiencies of pharmaceutical compounds using plant based CW techniques. For instance, Dordio and coauthors (2010) showed that in microcosm CWs planted with *Typha* spp., a high removal efficiency of clofibric acid, ibuprofen and carbamazepine from wastewater by 75%, 96% and 97% was reached after 7 days under summer conditions. Another study was conducted to explore the competence of CWs in eliminating 36 PPCPs (Bayati et al., 2021). These authors found high removal efficiencies (>88%) towards azithromycin, diphenhydramine, tolfenamic acid and sertraline. Moreover, they found a high variability in removal efficiencies among the same pharmaceutical category which reflects the importance of physico-chemical properties of the compounds for the removal process; antibiotics (4.7-96.7%), nonsteroidal antiinflammatory drug (3.5-88%), antidepressant and anti-seizure drugs (5-86%),  $\beta$ -blockers (29-77%) and other types of PPCPs were used in this study (5.5-94%). Falahi and coauthors (2021) showed the ability of pilot-scale vertical subsurface flow CW planted with *Scirpus grossus* in removing up to 99.3% of ibuprofen (with hydraulic retention time of 5 days and  $2 \text{ L min}^{-1}$  aeration) from domestic wastewater after 21 days. Other studies showed high removal efficiencies in controlled hydroponic experiments. For instance, Cui and Schröder (2016) demonstrated the ability of *Typha latifolia* plants to remove metformin by and ~81% and ~74% after 28 days of exposure to this compound in concentration levels of  $50 \mu\text{mol L}^{-1}$  and  $250 \mu\text{mol L}^{-1}$ , respectively. Furthermore, *T. latifolia* plants exposed to iopromide in a concentration of  $20 \mu\text{mol L}^{-1}$  were able to remove ~87% of this compound within 28 days from exposure (Cui et al., 2017). Dordio and coauthors (2011) noticed removal efficiencies of carbamazepine from hydroponic cultures by 82% and 56% after exposing cattail plants to this compound for 21 days at concentrations  $0.5$  and  $2 \text{ mg L}^{-1}$ , respectively. Also, Zhang and coauthors (2013)



demonstrated the ability of *Scirpus validus* plants to remove naproxen and carbamazepine from hydroponic cultures amended with 0.5, 1 and 2 mg L<sup>-1</sup> of these compounds. After 21 days of exposure to the highest concentration 2.0 mg L<sup>-1</sup>, removal efficiencies for naproxen reached 98% whereas it was ~74% for carbamazepine. Furthermore, Chen and coauthors (2017) showed that *Cyperus alternifolius* plants were able to remove oxybenzone by 86.5% and 81.4% after 5 days when they were grown hydroponically on a nutrient solution amended with 5 and 25 µM, respectively, of this compound.

Concerning TRD, previous studies showed the ability of CWs to remove this compound (TRD monitored with other pharmaceuticals) with efficiencies ranged from ~16-85 % where the highest concentration of TRD which detected in the influents did not exceed 1.2 µg L<sup>-1</sup> (Rühmland et al., 2015; Chen et al., 2016; Vymazal et al., 2017). Mackul'ak and coauthors (2015), using pilot scale reactors, reported that the aquatic plants *Cabomba caroliniana*, *Limnophila sessiliflora* and *Egeria najas* have the potential to remove TRD from treated WWTP effluents (~ 710 ng L<sup>-1</sup>) by 29-59 %. The correlation between the diverse factors in CWs as well as the full mechanisms is still not fully understood. Although phytoremediation is an important and efficient tool for cleaning-up a lot of contaminants in CWs, the presence of organic compounds, including other PPCPs, in the vicinity of plant roots may cause a negative impact on plant growth and subsequently decrease the remediation efficacy.

### **1.6. Impact of PPCPs on plant health**

Previous studies investigated the effect of PPCPs on plant growth and performance. Kong and coauthors (2007) explored the uptake and toxicity of oxytetracycline towards alfalfa (*Medicago sativa*). A maximum inhibition in root and shoot fresh weights by 85% and 61%, respectively, was recorded after exposing alfalfa plants to 0.2 mM oxytetracycline for 10 days. Furthermore, Dordio and coauthors (2009) showed that *Typha* spp. were able to remove clofibric acid (20 µg L<sup>-1</sup>) from hydroponic cultures by 80% after 21 days of exposure. The same authors demonstrated that exposure to higher concentrations of clofibric acid (0.5, 1 and 2 mg L<sup>-1</sup>) did not negatively affect cattail plants and the photosynthetic pigments, however, it increased the activities of catalase (CAT), superoxide dismutase (SOD), ascorbate peroxidase (APX) and guaiacol peroxidase (GPX), indicating that clofibric acid induces antioxidative defence in roots and leaves of cattail plants. Yan and coauthors (2016) explored the ability of *Cyperus alternifolius* plants to remove and uptake sulfamethoxazole, carbamazepine, roxithromycin and ofloxacin. The same authors did not notice visual symptoms of toxicity when plants were exposed to these pharmaceuticals in a concentration range of 10-500 µg L<sup>-1</sup>.

However, they recorded an increase in activities of CAT, SOD and GPX with increasing concentrations of the pharmaceutical compounds. Michelini and coauthors (2012) showed that willow (*Salix fragilis*) and maize (*Zea mays*) grown in soil amended with high concentrations of sulfadiazine ( $200 \text{ mg kg}^{-1}$ ) had reduced C/N ratio as well as lowered total chlorophyll content in willow plants, while the maize plants died under this concentration. Ravichandran and Philip (2021) revealed that exposing *Canna indica* and *Chrysopogon zizanioides* to a mixture of carbamazepine, atenolol and diclofenac ( $1 \text{ mg L}^{-1}$  per each) caused development of yellowish patches, burnt edges and necrotic spots on their leaves. Moreover, the same authors noticed an accumulation of reactive oxygen species (ROS- $\text{H}_2\text{O}_2$ ), increasing in APX and CAT activities in roots of both species which confirms the oxidative stress symptoms. Sun and coauthors (2018) showed that a mixture of 17 PPCPs (at concentrations 5 and  $50 \text{ } \mu\text{g L}^{-1}$ ) was able to induce burning symptoms at edges of mature leaves of cucumber plants besides a decrease in photosynthesis pigments. The same authors recorded an increase in lipid peroxidation and ROS production in addition to an elevation in activities of SOD, APX, GPX and glutathione S-transferase (GST) in cucumber leaves with increasing PPCPs concentrations. Hammad and coauthors (2018) showed that two maize varieties had the ability to accumulate paracetamol in their roots as well as grains. Also, they noticed a reduction in grain yield up to 50% in one of these varieties at the highest paracetamol concentration ( $1.24 \text{ g L}^{-1}$ ); while no change in contents of grain protein was recorded. Amy-Sagers and coauthors (2017) noticed adverse effect of the antidepressant fluoxetine on root growth and asexual reproduction of *Lemna minor* after exposure to  $323 \text{ nmol L}^{-1}$  fluoxetine for 21 days. Bartha and coauthors (2010) investigated the impact of acetaminophen at 1 mM concentration on Indian mustard (*Brassica juncea*). Many visual stress symptoms appeared on the treated plants such as dot-like lesions (after 3 days) on leaf's adaxial side, necroses (after 7 days), dark brown roots (from 3 to 7 days), hindering new lateral root development and a huge decrease in photosynthetic pigments reaching 70% after 7 days of exposure to acetaminophen compared to control plants. Another study noticed a reduction in carrot growth and biomass production when plants were grown on soil amended either with metformin, ciprofloxacin or narasin (Eggen et al., 2011). D'Abrosca and coauthors (2008) showed that exposing lettuce (*Lactuca sativa*) seedlings to gemfibrozil, tamoxifen, ethinyl estradiol, atorvastatin or sildenafil either at  $1 \text{ } \mu\text{M}$  or  $1 \text{ nM}$  caused a decrement in photosynthetic pigments, sugars, fatty acids, lipids, flavonoids and phenols compared to controls.

### 1.7. Role of beneficial bacteria in enhancing phytoremediation of xenobiotics

The use of beneficial microorganisms, especially bacteria, was suggested to overcome the previous challenges on plants. Such a combination can increase the potential of phytoremediation as well as enhance removal efficiencies during remediation processes (Becerra-Castro et al. 2013; Hussain et al., 2018 a&b; Rehman et al., 2018). During this plant-microbe partnership, bacteria (either rhizospheric or endophytic) play a crucial role not only to enhance the plant growth but also to detoxify/degrade the pollutants to reduce their phytotoxic effect (Weyens et al., 2009; Khan et al., 2013). For example, inoculation of Italian ryegrass plants (tolerant to diesel contamination) with a bacterial consortium from alkane degrading strains (*Pantoea* sp. BTRH79 & ITSI10, and *Pseudomonas* sp. MixRI75) enhanced plant growth and hydrocarbon (diesel) degradation after their addition to the soil (Afzal et al., 2012). Shehzadi and coauthors (2014) showed a positive impact of two endophytic strains *Bacillus pumilus* PIRI30 and *Microbacterium arborescens* TYSI04 in promoting plant growth and enhancing remediation process of textile contaminated effluent using reactor vegetated with *Typha domingensis*. In the same line, the beneficial interaction between *Pantoea* sp. FC1 and *Brassica napus* hairy roots in enhancing the removal efficiency of phenol as well as increasing accumulation of chromium by hairy root cultures compared to non-inoculated ones was noticed (Ontañón et al., 2014). Moreover, Fatima and coauthors (2016) demonstrated the potential of two bacterial endophytic strains, i.e. *Pseudomonas aeruginosa* BRRI54 and *Acinetobacter* sp. BRSI56 (having oil degradation characteristics), in degrading crude oil (by ~78 %), producing alkane hydroxylase gene (*alkB*) as well as root colonization ability in soil contaminated with crude oil which vegetated with *Brachiaria mutica* plants. Another study also revealed that inoculating *Dracaena sanderiana* plants with the endophytic bacteria *Pantoea dispersa* boost removal efficiency of of bisphenol A from hydroponic cultures compared to non-inoculated plants (Suyamud et al., 2018). Iqbal and coauthors (2019) demonstrated positive effects of inoculating the endophytic strain *Pseudomonas* sp. J10 in remediating total petroleum hydrocarbon either in soil or hydroponically with *Arabidopsis thaliana* and two cultivars of *Lolium perenne* in addition to reducing phytotoxicity and promoting plant growth.

Despite their ability to take up, metabolize (even partially) and sequester organic pollutants depending on their enzymatic system, plants at least in part rely on their endophytic bacteria for degrading these pollutants (Van Aken et al., 2011). Endophytic bacteria can promote plant growth through several ways; phytohormones production (as auxins, gibberellins and cytokinins), nutrients availability (such as phosphate solubilisation and nitrogen fixation),

reducing stress-induced ethylene via 1-aminocyclopropane-1-carboxylate (ACC) deaminase synthesis, biological control of plant pathogens and siderophores production which facilitate iron availability to the plants and prevent phytopathogen from it (Bhattacharyya and Jha, 2012; Khan et al., 2014; Santoyo et al., 2016; Olanrewaju et al., 2017; Yadav et al., 2018). While previous studies revealed the potential of CWs in PPCPs remediation, hitherto, limited information is available concerning the role of plant-bacterial interaction in PPCPs degradation. For instance, Sauvêtre and Schröder (2015) succeeded to recover and identify 22 endophytic species from *Phragmites australis* plants exposed to 5 mg L<sup>-1</sup> carbamazepine. When these strains were tested for carbamazepine (50 µM) removal from liquid bacterial media, only few strains showed the ability to take up carbamazepine. Among these strains *Rhizobium daejeonense* and *Chryseobacterium taeanense* showed removal efficiencies for carbamazepine by 2.45% and 2.18% as well as positive results in plant growth promoting traits tests such as indole-3-acetic acid (IAA) and siderophore production and phosphate solubilization (Sauvêtre and Schröder, 2015). Furthermore, Sauvêtre and coauthors (2018) investigated the role of bacterial inoculants for eliminating carbamazepine from Murashige and Skoog medium cultivated with horseradish hairy root cultures. While the removal efficiency of the hairy root cultures alone was up to 5%, inoculation of these cultures with *Rhizobium radiobacter* and *Diaphorobacter nitroreducens* enhanced removal efficiencies to 21% and 10 % respectively (Sauvêtre et al., 2018). The same authors also detected several transformation products in cultures either inoculated or non-inoculated with bacteria, such as carbamazepine-10,11-epoxide, 10,11-dihydro-10,11-dihydroxy-carbamazepine, 10,11-dihydro-10-hydroxy-carbamazepine, 2,3-dihydro-2,3-dihydroxy-carbamazepine, 2,3-dihydroxy-carbamazepine, carbamazepine-2,3-quinone, 11-glutathionyl-carbamazepine, 10,11-dihydro-10-hydroxy-11-cysteinylglyciny-carbamazepine, 10,11-dihydro-10-hydroxy-11-cysteinyl-carbamazepine, acridine, 9-acridine carboxaldehyde, 9-OH-acridine and acridone. Another study showed the beneficial role of using *Pseudomonas fluorescens* MC46 as bioinoculant for enhancing the removal efficiency of triclocarban from soil vegetated with mung bean (*Vigna radiata*) plants, restoration of plant health as well as boosting activities of soil enzymes (Sipahutar et al., 2018). He and coauthors (2019) noticed that inoculation of *Hyphomicrobium* sp. GHH to *Lolium perenne* plants had a positive impact on the removal of 17 $\alpha$ -ethynylestradiol from the contaminated soil. Shah and coauthors (2022) reported the advantage of using a bacterial consortium from three bacterial strains either free or immobilized on Fe<sub>3</sub>O<sub>4</sub>-nanoparticles for elimination of ciprofloxacin (100 mg L<sup>-1</sup>) from water with a floating treatment wetland technique. The authors found that addition of bacterial

consortia (immobilized or free) in the floating treatment wetland enhanced the removal efficiency of ciprofloxacin, with highest removal rates of 98% which was recorded in case of bacterial cells immobilized on Fe<sub>3</sub>O<sub>4</sub>-nanoparticles.

### **1.8. Impact of PPCPs on bacterial communities associated with plant roots**

Hitherto, root-associated microbiome studies are gaining more attention in the research field because of their impact on plant health via their effects on growth, immunity and nutritional status of the host plant besides their assistance in adaptation to diverse environmental conditions (Reinhold-Hurek and Hurek, 2011; Berendsen et al., 2012; Backer et al., 2018; Matilla and Krell, 2018; Goswami and Suresh, 2020; Trivedi et al., 2020). Recent studies revealed the potential of the pharmaceutical compounds in altering the bacterial communities associated with plant roots or the ones inhabiting the soil with effect on their function as well. For example, Bigott and coauthors (2022) showed that irrigation of lettuce plants with water or wastewater spiked with a mixture of 14 PPCPs had a positive effect on the relative abundance of the *Allorhizobium-Neorhizobium-Pararhizobium-Rhizobium* clade and a negative impact on *Haliangium* when PPCPs were applied at 100 µg L<sup>-1</sup>, whereas McLain and coauthors (2022) reported a positive alteration in bacterial communities of soil cultivated with eggplants which had been irrigated with environmentally relevant concentrations of acetaminophen, by selecting bacterial members having the ability to metabolize the products (such as carboxylic acids and glycosides) resulting from breakdown of acetaminophen. In the same direction, other studies tried to demonstrate the possible correlation between plants' associated microbiome and their role in pharmaceuticals metabolization. For instance, Zhao and coauthors (2015) explored the alteration in relative abundances of Proteobacteria (beta, delta and gamma) and Sphingobacteria resulting from triclosan application in CWs, and they suggested their possible role in triclosan degradation. Li and coauthors (2016) proposed the contribution of the genus *Ignavibacterium* and family Rhodocyclaceae in Ibuprofen degradation process after their relative abundances increment in the planted bed with *Typha angustifolia* of horizontal subsurface flow CW. Another study demonstrated enrichment in the relative abundance of some genera, such as *Sphingobium* and members of the phylum Actinomycetes like *Streptomyces* after exposing *Miscanthus × giganteus* to a mixture of diclofenac and sulfamethoxazole (Sauvêtre et al., 2020). The same authors suggested the contribution of these genera in diclofenac and sulfamethoxazole degradation as well as showing the ability of some isolated strains, from exposed plants, to degrade these compounds *in vitro*. Another study revealed that exposure of lettuce plants to a mixture of 11

pharmaceutical compounds enriched the abundance of Proteobacteria especially the family Methylophilaceae (Shen et al., 2019). Moreover, Cerqueira and coauthors (2020) showed that irrigation of lettuce plants with a mixture of 3 antibiotics (ofloxacin, trimethoprim and sulfamethoxazole) adversely affect the relative abundance of members of the order Rhizobiales and positively increase Xanthomonadales in root tissues. Li and coauthors (2020) noticed changes in the rhizobacterial communities of *Typha angustifolia* in CWs treated with ibuprofen compared to controls at different developmental stages, where the phylum Actinobacteria was the most dominant bacterial group. The same authors linked these changes with the predictable functions of the 16S rRNA genes from these communities which revealed their potential in co-metabolism and metabolism of ibuprofen. Opinion papers also tried to illustrate the synergistic relation between plant and their associated bacteria for enhancing the degradation efficiency of the PPCPs in CWs (Nguyen et al., 2019a).

## 1.9. Aim of the Thesis

The current thesis aims to explore the removal, uptake and translocation of TRD, as a widely detected contaminant in treated/ non-treated wastewater, in plants. In addition to evaluate the impacts of introducing TRD via irrigation water, on plant enzymes and root-associated bacterial communities, and to demonstrate the possible role of plant-bacterial interactions in facilitating the removal of TRD from contaminated water with this recalcitrant compound as well as to provide information about the possible metabolites formed inside plant tissues under the impact of this partnership.

### Objectives

The specific objectives of the current work aimed to:

- (I) Monitor the possible uptake and transport of TRD by excised roots of two plants (barley and cattail) in short-term uptake experiments using Pitman chamber technique with reference to the possible interaction between TRD and other contaminants;
- (II) Determine the capability of plants (e.g. barley seedlings) to uptake TRD by roots as well as investigate its translocation through the aerial parts, providing a general picture of TRD removal rate from hydroponic culture over time;
- (III) Explore the effect of TRD on root-associated bacterial community composition and the antioxidative defence system of barley plants grown in hydroponic cultures;
- (IV) Screen the ability of bacterial endophytes, isolated from roots of cattail plants exposed to TRD, to remove TRD using *in vitro* experiments besides exploring their plant growth-promoting characteristics;
- (V) Assess the interaction between selected bacterial endophytes and barley plants to enhance the removal efficiency of TRD from hydroponic cultures, identifying the possible metabolites formed in barley tissues and trying to understand the fate of this compound inside plant either with or without bacterial inoculation.

## **2. Materials and methods**

### **2.1. Experimental designs**

#### **2.1.1. Removal of TRD by plants and its interaction with other contaminants (M1)**

A series of Pitman chamber experiments was done using root segments (approximately 10 cm) with intact root tips from barley (*Hordeum vulgare* L., cv. 'Salome') and cattail (*Typha angustifolia* L.) plants. Barley seeds were obtained from Nordsaat Saatzucht GmbH (Langenstein, Germany), while cattail plants were purchased from Gärtnerei Hollern (Unterschleißheim, Germany). Eight Pitman chamber sets (three chambers each), four for each plant and two per each treatment, were included in these experiments. Four treatments were set up as follows: TRD, TRD+VEN, TRD+Q and ODTRD (shown in M1 appendix, Fig.2). The second part was performed using barley seedlings cultivated in hydroponic system. The treatments set up of this part illustrated in M1 appendix, Fig.3. Briefly, barley seedlings were grown in three different treatments; TRD ( $100 \mu\text{g L}^{-1}$ ), TRD ( $100 \mu\text{g L}^{-1}$ ) + Q1 (0.5 mM) or TRD ( $100 \mu\text{g L}^{-1}$ ) + Q2 (1 mM). The experiment was done within 15 days, thereafter; roots and shoots were separated and preserved at  $-80 \text{ }^{\circ}\text{C}$  for further analysis. During the 15 days, water aliquots (0.5 mL) were taken from the hydroponic culture media at time intervals 0, 1, 3, 6, 9, 12 and 15 days, and then stored at  $-20 \text{ }^{\circ}\text{C}$  for further assessment. An abiotic control group, having the same nutrient medium and supplemented with  $100 \mu\text{g L}^{-1}$  TRD, was used to explore the abiotic degradation/adsorption of TRD in the glass pots during the experiment. Measurements were done using three biological replicates.

#### **2.1.2. Effect of TRD on plant performance and root-associated bacterial community (M2)**

To evaluate the effect of TRD on the antioxidant enzyme system and the root-associated bacterial community composition, hydroponic culture experiments were performed. Barley plants (one month old) were used in this study, the acclimatization and growth conditions for barley plants are mentioned in M2 appendix. After acclimatization, plants were divided into five groups after transferring them to 3 L glass containers depending on treatment conditions (control and treated) and collecting periods (T0, T1 and T2). Treated plants were grown on nutrient solution supplemented with  $100 \mu\text{g L}^{-1}$  TRD (only spiked at the beginning), while control plants did not receive TRD. The collecting periods were set at the beginning of the experiment (T0), after 12 days (T1) and after 24 days (T2) (showed in M2 appendix, Fig. S1). The measurements were conducted using three biological replicates, five plants for each, and the glass containers were randomly distributed in a climate chamber under the conditions



described in the M1 appendix. Collected plants from each time period were separated into roots and shoots, weighed then stored at -80 °C. Water loss resulting from transpiration was compensated during the experiment.

### **2.1.3. Plant-bacterial interaction to enhance removal and metabolization of TRD (M3-in preparation for publication)**

Two main experiments were done in this section. In the first experiment, cuttings from subcultivated cattail plants (*Typha angustifolia* L.) were washed with tap water followed by distilled (dist.) water and transferred to 3 L glass containers. Cattail plants, after an acclimatization period, were grown on full-strength nutrient solution supplemented with 5 mg L<sup>-1</sup> TRD. The plants, three biological replicates with five plants per each, were kept for approximately one month before their root systems were harvested. Separated roots from different plants were washed several times with tap water thereafter by sterile dist. water. Subsequently, under sterile conditions, the washed roots were cut into 1-2 cm pieces and then surface sterilized following the steps; ethyl alcohol (70%), NaOCl (3%), ethyl alcohol (70%), then washed with sterile dist. water for three times prior to use. After sterilization, the root segments were ground with 2 mL of sterile dist. water in a sterile mortar. Serial dilutions were made using 1 mL from the previous root extracts. Bacterial endophytes were isolated and purified, using the serial dilutions, on R-2A (Reasoner's 2A) and nutrient agar plates. Pure bacterial endophytic isolates were kept on fresh growth media and glycerol stocks.

The second main experiment was conducted using selected isolates from the above experiment together with barley seedlings. Bacterial isolates were selected depending on their results from *in vitro* experiments for TRD removal and/or PGP activities including tests for ammonia, IAA and siderophore production besides phosphate solubilization ability (in M3 appendix). Barley seedlings, following an acclimatization phase, were cultivated in a hydroponic system utilizing full-strength nutrient solutions. The plants were divided into six groups: (1) control group (seedlings receiving only nutrient solution), (2) TRD group (seedlings treated with 1 mg L<sup>-1</sup> TRD), (3) TE12 group (seedlings treated with 1 mg L<sup>-1</sup> TRD and inoculated with isolate TE12), (4) TE17 group (seedlings treated with 1 mg L<sup>-1</sup> TRD and inoculated with isolate TE17), (5) Dual group (seedlings treated with 1 mg L<sup>-1</sup> TRD and inoculated with isolates TE12+TE17) and (6) Mix group (seedlings treated with 1 mg L<sup>-1</sup> TRD and inoculated with bacterial consortium from TE12+TE17+TE2+TE3+TE6+TE20). Bacterial inocula (1 mL from OD<sub>600</sub> 2) were added twice at the first days of the experiment. A seventh group without seedlings worked as abiotic control (AB-Cont group) which

received nutrient solution amended with 1 mg L<sup>-1</sup> TRD to explore the possible degradation of TRD during the experimental time (experimental design shown in M3 appendix, Fig. S1). The experiment was performed in triplicates over a period of 24 days. Water loss was compensated with dist. H<sub>2</sub>O, while nutrients were added once during the midway point of the exposure period. Aliquots (0.5 mL) from external media were taken at different time points and stored at -20 °C for further use. Collected samples from 0, 3, 6, 10, 18, 21 and 24 days were measured to assess TRD removal. By the end of the experiment, the plants were collected, separated into roots and shoots, and then stored at -80 °C for further analysis.

## **2.2. Samples (liquid, root and shoot) preparation for injection**

Before injections, 5-sulfosalicylic acid (1.9 M) was added in a ratio 1:10 v/v to liquid samples collected from the Pitman chambers (M1) and hydroponic culture experiments [M1 and M3], mixed well and centrifuged (10 min, 4 °C, 16,100 x g). Subsequently, formic acid was added to the collected supernatants (to reach 0.1%), and the mixture was supplemented with internal standard (IS, at a final concentration of 20 µg L<sup>-1</sup>). A modified QuEChERS method (based on the European Standard method [EN 15662:2008]) was used to extract root and shoot samples (from M1, M2 and M3), followed by a clean-up step for the shoot samples. Briefly, acridine-D<sub>9</sub> (20 µL; 12.5 ppm) was added to 0.25 g from ground tissues, vortexed then mixed with 2.5 mL of acetonitrile, thereafter, vigorously shaken and vortexed. To the previous mixture, a set of salts (1 g magnesium sulphate anhydrous, 250 mg trisodium citrate anhydrous, 250 mg sodium chloride, 125 mg disodium hydrogen citrate sesquihydrate) was added, vigorously shaken and vortexed. The mixture was then centrifuged (for 10 min, 3750 rpm) and the upper liquid layer collected. The shoot samples were then incubated for 2 h at -20 °C. Then, to 1.5 mL of the latter incubated solution, a second mixture of salts (125 mg MgSO<sub>4</sub> anhydrous, 25 mg PSA, 25 mg C18, 7.5 mg activated carbon) was added, vigorously shaken, vortexed, centrifuged and then the upper liquid layer collected.

All extracts, from root and shoot samples, were passed through 0.2 µm RC filters (SPARTAN™ 13/0.2), acidified and mixed with IS, as mentioned previously. Limits of detection (LODs) and quantification (LOQs) calculations were obtained according to the formulas;  $LOD=3.3(\alpha/S)$  and  $LOQ=10(\alpha/S)$ , where  $\alpha$  refers to standard deviation slope and S refers to the average slope of calibration curves (M1 and M3). Accuracy, precision, absolute recoveries and stability were estimated using samples from roots and shoots (three for each) spiked with 10LOQ concentration and then analyzed at three subsequent days (Table S2 in M1 appendix). ICH guidelines (2005) were used for the validation procedure of the

extraction, detection and quantification method. The matrix effect (Table S2 in M1 appendix) was also checked using the same concentration as described in Cruzeiro et al. (2016):

$$\text{Matrix effect (\%)} = -[(\text{Area ratio}_{\text{standards}} - \text{Area ratio}_{\text{standards in matrix}}) / \text{Area ratio}_{\text{standards}}] * 100 \quad \text{Eq. (1)}$$

## **2.3. Plant analysis**

### **2.3.1. Evaluation of root activity (in M1 appendix)**

Barley and cattail roots were tested for their vitality using a modified protocol from Prajitha and Thoppil (2017). Briefly, three intact root tip segments (~2 cm length) were collected at different time intervals (0, 2, 6, 16, 20 and 24 hr). Thereafter, the root segments were washed with dist. water, then immersed in 0.5% triphenyl tetrazolium chloride (TTC) solution and incubated for 30 min in the dark at  $35 \pm 2$  °C. Then, The TTC-treated root tips were rinsed with dist. water, and finally the formed red-colored complex (triphenyl formazan (TFN)) in the root segments was extracted by 1 mL ethanol (95%). The extracted red-colored complex was measured spectrophotometrically at 490 nm against ethanol (95%) as a blank (Genesys 30, ThermoFisher Scientific, USA). According to Ruf and Brunner (2003), the reduction of TTC to TFN can be directly linked to the mitochondrial respiratory chain activity.

### **2.3.2. Accumulation and translocation of TRD (in M1 appendix)**

Distribution of TRD, accumulation and translocation, in root and shoot tissues of barley seedlings were calculated depending on the equation mentioned in Bigott et al. (2020) as follows:

a- Bioconcentration factor (BCF) =  $C_{\text{root}} / C_{\text{initial}}$  Eq. (2)

b- Translocation factor (TF) =  $C_{\text{shoot}} / C_{\text{root}}$  Eq. (3)

where  $C_{\text{root}}$  and  $C_{\text{shoot}}$  are the concentrations of TRD in root and shoot tissues of barley plants after 15 days, while  $C_{\text{initial}}$  is the TRD concentration in the nutrient hydroponic culture solution at the beginning of the experiment.

### **2.3.3. Extraction of crude enzymes (in M2 appendix)**

Crude enzyme extraction from barley tissues was done following the protocol described in Schröder et al. (2005); crude enzymes were extracted from barley tissues to measure GSTs, GPX and CAT activities. In brief, three grams of ground root and shoot tissues were extracted for 30 min, using a stirring ice bath, with 30 mL of 100 mM Tris/HCl buffer pH 7.8 containing; 1% PVP K90, 1% Nonidet P40, 5 mM dithioerythritol and 5 mM ethylene diaminetetraacetic acid (EDTA). The previous mixture was then centrifuged for 30 min at

20000 rpm and 4 °C. The supernatant was subjected to stepwise addition of powdered ammonium sulphate for protein precipitation. The precipitation process was done in two steps; in the first step ammonium sulphate reaches 40% saturation while in the second step it reaches 80%. Each precipitation step was followed by centrifugation for 30 and 45 min for step 1 and 2, respectively at 20000 rpm and 4 °C. In the last step, the supernatant was discarded and the pellet was collected, resuspended in 2.5 mL of 25 mM Tris/HCl buffer (pH 7.8), and then the suspension was desalted using PD 10 columns (GE Healthcare, UK). After the desalting step, elution of the crude enzymes was carried out using the latter Tris/HCl buffer, then the eluted extracts were divided into aliquots and stored for further analysis at -80 °C.

#### **2.3.4. Measured enzymes (in M2 appendix)**

Activities of enzymes under investigation were determined in a 96-well spectrophotometer (Spectra MAX 190, Molecular devices, Germany). The GSTs activity was measured using two model substrates 1-chloro-2,4-dinitrobenzene (CDNB) and p-nitrophenyl acetate (pNPA) following the protocols in Habig et al. (1974) and Schröder et al. (2008). For measurements, desalted crude enzymes were incubated with a mixture of the substrate (CDNB or pNPA), L-glutathione reduced (GSH) using 0.1 M buffer, either potassium phosphate (pH 7.0) or Tris/HCl (pH 6.4) for pNPA or CDNB, respectively. GS-conjugates were quantified at 400 nm ( $\epsilon = 8.79 \text{ mM}^{-1} \text{ cm}^{-1}$ ) for pNPA and 340 nm ( $\epsilon = 9.6 \text{ mM}^{-1} \text{ cm}^{-1}$ ) for CDNB. Activity of GPX was determined as mentioned in Bigott et al. (2021), by following guaiacol oxidation to tetraguaiacol in the presence of  $\text{H}_2\text{O}_2$  at 420 nm ( $\epsilon = 26.6 \text{ mM}^{-1} \text{ cm}^{-1}$ ). The crude enzymes were mixed in 0.05 M Tris/HCl buffer pH 6.0 with guaiacol and  $\text{H}_2\text{O}_2$ . Measurements of CAT activities were carried out by mixing the crude enzymes in potassium phosphate buffer 0.1 M (pH 7) with  $\text{H}_2\text{O}_2$ , then following the breakdown of  $\text{H}_2\text{O}_2$  at 240 nm ( $\epsilon = 0.036 \text{ mM}^{-1} \text{ cm}^{-1}$ ) (Verma and Dubey, 2003). Blank samples in each assay and measurement were included. Protein concentration was determined in the aliquot used in the enzyme measurements to calculate the specific enzyme activities using the standard technique of Bradford (1976). Bovine serum albumin was used for preparing a calibration curve to quantify the protein content. The unit of enzyme specific activity is  $\mu\text{kat mg}^{-1}$  protein.

## **2.4. Bacterial analysis**

### **2.4.1. Screening for plant growth promoting (PGP) traits (in M3 appendix)**

Twenty-three endophytic isolates were tested for their ability to produce ammonia, IAA, siderophores and solubilize phosphate. For ammonia and IAA production assays, suspensions from bacterial isolates having equal OD<sub>600</sub> were used for both tests. For the ammonia production assay, a modified method from the protocol mentioned by Ahmad et al. (2008) was used. Briefly, sterile peptone water medium (1% peptone and 0.5% NaCl; 1.2 mL in total) was inoculated with bacterial isolates suspensions (as mentioned in M3 appendix) then incubated at 28±2 °C for 72 h. Fifty microliters of Nessler's reagent were mixed with 1 mL from the supernatant of the centrifuged bacterial cultures. The produced yellow to brown colour was measured spectrophotometrically at 450 nm. Ammonia concentration was quantified using a calibration curve of ammonium sulphate with concentrations ranging from 1 to 20 µmol L<sup>-1</sup>. The production of IAA by endophytic bacterial isolates was measured following a modified protocol of Sauvêtre and Schröder (2015). Shortly, suspensions from endophytic isolates (as mentioned in M3 appendix) were used to inoculate Luria Broth (LB; 1.2 mL in total) medium amended with tryptophan (1 mg mL<sup>-1</sup>) and incubated at 28±2 °C for 72 h. After the incubation period, the cultures were centrifuged, supernatants were collected and pellets were discarded. One millilitre of the supernatant was mixed with 1 mL of Salkowski reagent, and then incubated at room temperature in dark for 25 min. The developed pink colour was spectrophotometrically measured at 530 nm. IAA concentration was calculated using a standard curve from IAA ranging from 1 to 10 µg mL<sup>-1</sup>. Concerning siderophore production, a modified protocol from previously published methods in Pérez-Miranda et al. (2007) and Loudon et al. (2011) was used. In brief, freshly subcultured bacterial endophytes were grown in nutrient agar plates for 48 h. Thereafter, ten millilitres from freshly prepared overlay mixture were poured on the top of the inoculated plates. The overlay mixture consisted of two parts which were mixed together after autoclaving; the first part (dye mixture) composed of hexadecyltrimethylammonium bromide (HDTMA), chrome azurol S (CAS) and FeCl<sub>3</sub>, while the second part contained piperazine-N,N'-bis(2-ethanesulfonic acid) (PIPES) dissolved in dist. water amended with agar (0.9%), the final pH of the second solution was 6.8. Then, the inoculated plates with the layer on top were incubated at 28±2 °C approximately for 24 h. Bacterial colonies which were able to change colour from blue to orange-yellow were considered as positive (under the colony [+]) or around it [++] for siderophore production. For qualitative detection of phosphate solubilization, freshly grown isolates were spotted on Pikovskaya's agar plates. The previous

medium composed of; glucose (10 g L<sup>-1</sup>), ammonium sulphate (0.5 g L<sup>-1</sup>), Ca<sub>3</sub>(PO<sub>4</sub>)<sub>2</sub> (5 g L<sup>-1</sup>), MgSO<sub>4</sub>·7H<sub>2</sub>O (0.1 g L<sup>-1</sup>), KCl (0.1 g L<sup>-1</sup>), yeast extract (0.5 g L<sup>-1</sup>), FeSO<sub>4</sub>·7H<sub>2</sub>O (0.0001 g L<sup>-1</sup>), MnSO<sub>4</sub>·H<sub>2</sub>O (0.0001 g L<sup>-1</sup>) and agar (15 g L<sup>-1</sup>). The inoculated plates were incubated at 28±2 °C for 5 days, then, bacterial colonies forming clear zone on the Pikovskaya's medium were considered positive (+) to the test.

#### **2.4.2. Screening for *in vitro* TRD removal (in M3 appendix)**

Bacterial endophytes were screened for their potency to remove TRD from minimal growth media. Bacterial isolates were firstly subcultured on nutrient broth medium to get proper bacterial growth. Bacteria were collected through centrifugation then washed twice by PBS (1X) then in the final step suspended in the same solution. Thereafter, 3 mL of sterile AB minimal medium, supplemented with TRD and carbon source, were inoculated with the bacterial suspensions having the same OD<sub>600</sub> to reach final value of 0.01. AB minimal medium composed of: ammonium sulphate (2 g L<sup>-1</sup>), sodium phosphate dibasic (6 g L<sup>-1</sup>), sodium chloride (3 g L<sup>-1</sup>), potassium phosphate monobasic (3 g L<sup>-1</sup>), calcium chloride dehydrate (200 µL, 0.5 M), magnesium chloride (2 mL, 1 M) and ferric chloride (300 µL, 0.01 M). The previous medium was amended with 100 µg L<sup>-1</sup> TRD and additionally supplemented with either 1 g L<sup>-1</sup> glucose or L(-)malic acid disodium (malate) used as a carbon source. Control tubes containing the same media without bacterial inoculation and same concentration of TRD were used. The experiment was done using three biological replicates. All inoculated tubes were incubated in orbital shaker (120 rpm) at 28±2 °C for 14 days. By the end of the incubation period, 0.5 mL of the bacterial growth was centrifuged for 5 min at 10000 rpm and the supernatant was used for TRD determination. Prior to injection, the collected supernatants were mixed with 5-sulfosalicylic acid (as mentioned in section 2.2) for protein precipitation. After another centrifugation, the supernatants were collected, acidified with formic acid (to reach 0.1%) then filtered via SPARTAN™ 13/0.2 RC filters with 0.2 µm pore size. Finally, the filtrates were spiked with IS (TRD-D3) to reach 20 µg L<sup>-1</sup> as a final concentration in the sample before injection.

#### **2.4.3. Molecular identification of bacterial endophytes (in M3 appendix)**

Amplification of 16S rRNA gene region was performed to cattail's bacterial root endophytes using colony PCR technique shown in Duffner et al. (2022). The specific primer pairs used in this process were 27f and 1492r. Shortly, the reaction mixture composed of (per one reaction): 5 µL PCR buffer (10X), 0.25 µL dNTPs (10 mM), 3 µL MgCl<sub>2</sub> (1.5 mM), 5 µL

BSA (30%), 1  $\mu\text{L}$  forward primer 27f (10 pmol  $\mu\text{L}^{-1}$ ), 1  $\mu\text{L}$  reverse primer 1492r (10 pmol  $\mu\text{L}^{-1}$ ), 0.5  $\mu\text{L}$  Taq DNA polymerase (5 U), 31.25  $\mu\text{L}$  MiliQ-DEPC water and 3  $\mu\text{L}$  from diluted bacterial colony. Thereafter, the amplified products were purified and subjected to Sanger sequencing. The sequenced chromatograms from all isolates were manually checked by MEGA-X software (Kumar et al., 2018), then both reads (forward and reverse) were combined using BioEdit software (to obtain assembled contig), except in case of TE2, TE10 and TE19 isolates which have only forward sequences, and compared using nucleotide BLAST search against the rRNA/ITS data in the NCBI database (NCBI: <https://blast.ncbi.nlm.nih.gov/Blast.cgi>).

#### **2.4.4. Identification of root-associated bacterial communities**

Extraction of genomic DNA was performed on 0.3 g of fine ground root tissues by using NucleoSpin® Soil Kit set (Macherey-Nagel, Düren, Germany) according to the manufacturer's instructions. Cell lysis of root-associated bacteria were done using SL1 buffer. Additional extraction controls (as negative control) were used, these controls either done by using empty extraction tubes or by the previous tubes amended with liquid nitrogen. The concentration of DNA extracts was determined by using Quant-iT™ Pico Green® dsDNA assay Kit (Thermo Fisher Scientific, Darmstadt, Germany) according to the manufacturer's instructions. DNA extracts were reserved for further steps at  $-80\text{ }^{\circ}\text{C}$ .

PCR was done on the previously extracted DNA for Illumina sequencing using NEBNext High-Fidelity Master Mix (2X) to amplify the V3-V4 regions from bacterial 16S rRNA gene. The primer set used in the previous reaction was 335F (CADACTCCTACGGGAGGC) and 769R (ATCCTGTTTGMTMCCCVCRC) which also can exclude amplification of plant chloroplast (Dorn-In et al., 2015). The reaction mixture contained 12.5  $\mu\text{L}$  of the PCR master mix, 2.5  $\mu\text{L}$  of BSA (3%), 0.5  $\mu\text{L}$  per primer (10 pmol  $\mu\text{L}^{-1}$ ), 1  $\mu\text{L}$  of DNA (5 ng  $\mu\text{L}^{-1}$ ) and 8  $\mu\text{L}$  of DEPC water. The program of amplification was started with 60 s at  $98\text{ }^{\circ}\text{C}$  as initial denaturation step, followed by 25 cycles started with 10 s at  $98\text{ }^{\circ}\text{C}$  for denaturation, 30 s at  $60\text{ }^{\circ}\text{C}$  for annealing and ended by 30 s at  $72\text{ }^{\circ}\text{C}$  for 30 s for extension, afterwards terminated with 5 min at  $72\text{ }^{\circ}\text{C}$  as final extension step. An agarose gel (2%) was used to check the quality of the PCR products. Then, purification of these products was done using Agencourt AMPure XP beads, followed by checking the quality and quantity of DNA with the Fragment Analyzer device (Agilent Technologies, Santa Clara, CA, United States). Thereafter, indexing PCR by using Nextera XT Index Kit v2 (Illumina, San Diego, CA, United States) was conducted in a final volume of 25  $\mu\text{L}$  that contains; 12.5  $\mu\text{L}$  NEBNext High-Fidelity

Master Mix (2X), 1.28  $\mu\text{L}$  of DNA ( $7.8 \text{ ng } \mu\text{L}^{-1}$ ), 2.5  $\mu\text{L}$  of each index and 6.22  $\mu\text{L}$  of DEPC water. PCR conditions were initiated at 98 °C for 30 s (initial denaturation); followed by 8 cycles started with 10 s at 98 °C, 30 s at 55 °C and ended with 30 s at 72 °C; then a final step of PCR at 72 °C for 5 min (final elongation). The indexed product from the previous PCR were again purified and quantified as previously described. Subsequently, the samples were pooled together in equimolar ratio of 4 nM. Finally, sequencing of the pooled samples was done using Illumina Miseq instrument (Illumina, San Diego, CA, United States) with Reagent Kit v3 (600 cycles).

The data produced from amplicon sequencing was 323,7 MB of raw reads. The treatment of the data started with trimming the reads by Cutadapt (ver. 4.1; Martin, 2011) to remove adapters from all reads. Subsequently, Bioconductor package dada2 (ver. 1.26; Callahan et al., 2016), in the environment of R (ver. 4.2.2; R Core Team, 2022), was used for quality filtering and denoising of reads (Specification of reads for each sample shown in Table S2; in M2 appendix), in addition to deduce amplicon sequence variants (ASVs) as well as mapping these ASVs against SILVA rRNA database (v138.1, SSU Ref NR 99; release date: 27-08-20; Quast et al., 2013). A total 529143 reads among 387 ASVs were produced after using dada2 pipeline. Rarefaction curves revealed that samples were sequenced till saturation except only one sample (Fig. S2; in M2 appendix). Chloroplast and non-bacterial ASVs (1 ASV, 32 reads) were removed, then the obtained 529111 reads (with median of 27549 per sample) with taxonomy tables (386 ASVs) were imported to phyloseq-class object using phyloseq package (ver. 1.42) (McMurdie and Holmes, 2013). Alpha diversity indices (Shannon and Simpson) were evaluated by the function "divnet" (DivNet ver. 0.40; Willis and Martin, 2022), while for beta diversity and variance of the samples, principal component analysis (PCA) was conducted based on the centred-log ratio (CLR) transformed count data using vegan package (ver. 2.6.4) (Aitchison et al., 2000). Furthermore, with using the ANCOMBC package (ver. 2.0.1), the differentially abundant ASVs through the bacterial families were identified (Lin and Peddada, 2020). The raw sequence reads which produced for the analysis were uploaded in the NCBI Sequence Read Archive database under BioProject PRJNA939407.

## **2.5. Analytical instrument setup and conditions (M1, M2 and M3)**

Samples, either from the liquid media or those extracted from root and shoot tissues, were injected through an autosampler into UHPLC (Dionex UltiMate 3000RS, Gemering, Germany) which connected to a triple quadrupole mass spectrometer (Thermo Scientific



HESI-MS/MS, TSQ Quantum Access Max, USA). For chromatographic separation, Accucore PFP column (2.6  $\mu\text{m}$  particle size, 100 mm  $\times$  2.1 mm, Thermo Scientific, USA) coupled with pre-column (Accucore PFP, 2.6  $\mu\text{m}$  particle size, 10  $\times$  2.1 mm, Thermo Scientific, USA) was used during the analysis with a flow rate 0.45 mL min<sup>-1</sup>. The mobile phases were; Mili-Q water acidified with formic acid (to a final concentration 0.1%, A) and acetonitrile acidified with formic acid (to a final concentration 0.1%, B) with a linear gradient of 0-2 min 5% B, 2-8 min 5-100% B, 8-9 min 100% B, 9-9.1 min 100-5% B and 9.1-10 min 5% B. the used method was operated in positive mode at 5000 V capillary voltage, 50 psi sheath gas pressure, 5 psi auxiliary gas pressure, 200 °C capillary temperature and 350 °C nitrogen dumping gas temperature. Samples were either analyzed in selected ion monitoring (SIM) mode (samples in M1, M2 and M3) or in tandem mass spectrometry (MSMS) mode (samples from root and shoot extracts in M3). The software Xcalibur (ver. 4.1) was used in peak identification, integration and quantification.

## 2.6. Statistical analyses

The kinetic uptake results of Pitman chamber experiments showed a change of TRD and VEN concentration during the time (24 h) of the experiment. The recorded data were fit to Boltzmann sigmoid curve, from the nonlinear regression analysis, as expressed in the following equation:

$$Y = (\text{Top} - \text{Bottom}) / (1 + \exp [(\text{V50} - X) / \text{Slope}]) \quad \text{Eq. (4)}$$

Originally, the previous equation describes voltage-dependent activation of ion channels which here is replaced by concentration. The equation represents the change in the concentration from the “bottom” to the “top” of each curve, while “V50” describes its halfway and “Slope” represents the curve’s steepness, with a larger value indicating a shallow curve. Several models were tested along with Boltzmann model which showed the best fit. The criteria used to select the good fit model were to have a relatively high coefficient of determination ( $R^2$ ) and low standard deviation of residues ( $S_{x,y}$ ). GraphPad Prism (ver. 6.00) was used for graphical analyses (Fig. 4 in M1 appendix). Differences between plant species (barley vs. cattail) or compound (TRD and VEN) and sampling time were checked using the 2-way factorial ANOVA in conjugation with the post-hoc Tukey's test. The latter statistical analysis was conducted in Statistica (ver. 7.0) and the differences were considered significant in the case of  $p \leq 0.05$ . For the data produced from the plant enzymes measurements (shown in M2 appendix), a comparison between control and TRD-treated plants for all enzymes was done and statistical differences were calculated using unpaired t-tests with the GraphPad

Prism website ([www.graphpad.com/quickcalcs/ttest1.cfm](http://www.graphpad.com/quickcalcs/ttest1.cfm)) and depicted on Fig. 1 and 2 in M2 appendix. Bacterial alpha diversity was calculated using the "divnet" function in the phyloseq package. The significance of changes in alpha diversity indices (Shannon and Simpson) between control and TRD-treated plants was deduced by using Holm's corrected *p*-values from Welch's t-test ( $\alpha = 0.05$ ), while beta diversity of the root-associated bacterial communities was visualised by using principal component analysis (PCA) based on the centred-log ratio (CLR) transformed data (Fig. 4 in M2 appendix). PERMANOVA analysis was done to confirm the results from PCA and show the significant effect of treatment, time and the interaction between both parameters (time and treatment) on beta diversity (Table 2 in M2 appendix). Differences in relative abundances of root-associated bacterial ASVs over the time and under presence or absence of TRD treatment were calculated using ANCOMBC package (Fig. 5 in M2 appendix).

### 3. Manuscript Overview

The upcoming part summarizes the manuscripts included in the Thesis and its publication status and authors contributions.

#### **I. Manuscript I (M1, first author, published)**

**Khalaf, D. M.**, Cruzeiro, C., & Schröder, P. (2022). Removal of tramadol from water using *Typha angustifolia* and *Hordeum vulgare* as biological models: Possible interaction with other pollutants in short-term uptake experiments. *Science of the Total Environment*, 809, 151164.

#### **II. Manuscript 2 (M2, first author, published)**

**Khalaf, D. M.**, Cruzeiro, C., Siani, R., Kublik, S. & Schröder, P. (2023). Resilience of barley (*Hordeum vulgare*) plants upon exposure to tramadol: Implication for the root-associated bacterial community and the antioxidative plant defence system. *Science of the Total Environment*, 164260.

#### **III. Manuscript 3 (M3, first author, in preparation for publication)**

**Khalaf, D. M.**, Cruzeiro, C., & Schröder, P. (in preparation for publication). Impact of plant-bacterial synergism on removal and metabolization of the recalcitrant tramadol (not submitted yet).

#### **Contribution to additional publications:**

Bigott, Y., **Khalaf, D.M.**, Schröder, P., Schröder, P.M. & Cruzeiro, C. (2020). Uptake and translocation of pharmaceuticals in plants: principles and data analysis. *The Handbook of Environmental Chemistry*. Springer, Berlin, Heidelberg, pp. 1-38.

**Manuscript I (M1) - Removal of tramadol from water using *Typha angustifolia* and *Hordeum vulgare* as biological models: Possible interaction with other pollutants in short-term uptake experiments**

Khalaf, D. M., Cruzeiro, C., & Schröder, P.

Published in Science of the Total Environment (2022), Volume 809,

DOI: 10.1016/j.scitotenv.2021.151164

Manuscript (M1) demonstrates the removal/root uptake rate of TRD in short-term Pitman chamber experiments with the possible interaction with other pollutants besides exploring the removal efficiency, uptake and translocation of TRD from hydroponic cultures.

The possible removal and root uptake rate of TRD either alone or in combination with other pollutants was studied in short-term Pitman chambers experiments. Also, another target for the study was to explore the accumulation and translocation of TRD inside plant tissues in hydroponic culture experiments. The rates of TRD uptake by cattail and barley excised roots were recorded as 5.79 and 5.18  $\mu\text{g g}^{-1}$  root fresh weight per day, respectively. These uptake rates for TRD were retarded or completely inhibited after competing with other pollutants such as venlafaxine (VEN; chemically analogous compound to TRD) or quinidine (Q; an organic cation transporters [OCT] inhibitor), respectively. The results showed the possibility of plants to uptake TRD and transport it through excised roots. To confirm that, hydroponic culture experiments using barley seedlings was done to explore the removal efficiency over time, uptake and accumulation of TRD in roots besides the possibility to be translocated into the shoots. The barley seedlings were incubated with TRD ( $100 \mu\text{g L}^{-1}$ ) either alone or with Q for 15 days. The barley seedlings were able to remove TRD from the nutrient medium up to 89.13 %. However, with supplementing the previous medium with Q, the removal efficiency of TRD was reduced. TRD was detected in roots and shoots of barley seedlings either exposed to TRD alone or in combination with Q. These results show the ability of barley plants to remove, uptake, accumulate and translocate TRD in their tissues.

Manuscript idea: Khalaf D.M., Schröder, P.

Experiment preparations, sampling, lab work: Khalaf D.M., Cruzeiro, C. (with analytical work)

Data interpretation and analysis: Khalaf D.M., Cruzeiro, C. (model and statistics)

Manuscript Draft: Khalaf D.M.

Final Manuscript: Khalaf D.M. & Schröder P.

**Manuscript II (M2) - Resilience of barley (*Hordeum vulgare*) plants upon exposure to tramadol: implication for the root-associated bacterial community and the antioxidative plant defence system**

Khalaf, D. M., Cruzeiro, C., Siani, R., Kublik, S. & Schröder, P.

Published in Science of the Total Environment (2023)

DOI: 10.1016/j.scitotenv.2023.164260

Manuscript (M2) highlights the impact of TRD on the community structure of root-associated bacteria in addition to evaluate its effect on some plant enzymes.

Root-associated bacterial community and selected plant enzymes (GST, GPX and CAT) were explored in this study to show their status under TRD contamination conditions in barley plants. The experiment was done using a 3 L hydroponic culture system supplemented with 100 µg L<sup>-1</sup> TRD. Barley plants (one month old) were grown on these systems and then the plants were harvested after 12 and 24 days of exposure to TRD. The results showed accumulation of TRD inside the roots of barley plants over the time. Analysis of enzymatic status in barley roots and shoots revealed a stimulation of GST (with CDNB and pNPA substrates), GPX and CAT in both roots and shoots in TRD-treated plants compared to those of control especially after exposure to TRD for 24 days. While alpha diversity indices did not record a significant change between control and TRD-treated plants, beta diversity showed a significant change due to the treatment. Furthermore, it was noticed that certain ASVs belonging to *Hydrogenophaga*, U. Xanthobacteraceae, *Pseudacidovorax*, were differentially abundant in TRD-treated plants compared to controls at both time points. These results showed the ability of TRD to cause changes in the measured enzymes as well as initiate alteration in root-associated bacterial community.

Manuscript idea: Khalaf D.M., Schröder, P.

Experiment preparations, sampling, lab work: Khalaf D.M., Cruzeiro, C., Kublik, S. (Technical Support for Amplicon Sequencing)

Data interpretation and analysis: Khalaf D.M., Cruzeiro, C., Siani, R. (Bioinformatic analysis, curation pipeline for analyzing amplicon sequence data)

Manuscript Draft: Khalaf D.M.

Final manuscript: Khalaf D.M., Cruzeiro, C. & Schröder P.

**Manuscript III (M3) - Impact of plant-bacterial synergism on removal and  
metabolization of the recalcitrant tramadol**

Khalaf, D. M., Cruzeiro, C., & Schröder, P.

*Manuscript in preparation for publication (2023)*

Manuscript (M3) describes the possible interaction between isolated root endophytic bacteria and the plant to enhance the removal of TRD and how this affects TRD metabolism.

During this study, cultivable root bacterial endophytes were recovered from cattail plants exposed to 5 mg L<sup>-1</sup> TRD for one month. Twenty-three isolates were tested *in vitro* to explore their PGP characteristics; IAA, ammonia and siderophore production as well as phosphate solubilization. Moreover, they were tested to evaluate their potential to remove TRD (100 µg L<sup>-1</sup>) from AB minimal media which was supplemented either with glucose or malate. Most of the bacterial endophytes showed positive results for PGP activities besides their potential to partially remove TRD from AB minimal media. From the previous results, six isolates were used for conducting an inoculation experiment. In this experiment, barley seedlings were cultivated on a nutrient medium containing 1 mg L<sup>-1</sup> TRD and either inoculated or non-inoculated with bacteria. Bacterial inoculation was done using Single (TE12 or TE17), Dual (TE12+TE17) or Mix (bacterial consortium) bacterial inocula. Dual-inoculated plants recorded the highest removal potential with 87.53 % after 24 days of exposure to TRD. Moreover, barley seedlings inoculated with bacteria recorded higher concentration of TRD in their tissues compared to non-inoculated plants. In barley seedlings, TRD metabolized through O- and N-demethylation pathways, resulting in the first main metabolites ODTRD and NDTRD which were found and quantified in roots and shoots of all treatments. This study revealed that using bacterial inoculants, especially the dual inoculation, can boost the plant performance in eliminating TRD from liquid cultures besides quantifying two confirmed (ODTRD and NDTRD) metabolites inside plant tissues.

Manuscript idea: Khalaf D.M., Schröder, P.

Experiment preparations, sampling, lab work: Khalaf D.M., Cruzeiro, C.,

Data interpretation and analysis: Khalaf D.M., Cruzeiro, C.,

Manuscript Draft: Khalaf D.M.

#### 4. General Discussion

The studies (M1, M2 & M3) included in this Thesis, aim to provide a general view of the possible biological eco-friendly and cheaper ways to remove one of the emerging persistent contaminants, the pharmaceutical Tramadol, from water treatment systems by using either plant alone or in combination with bacteria (M1 and M3) besides trying to explore the metabolites which can be formed inside plant tissues with/without bacterial inoculation (M3). It also elucidates the potential effect of TRD on the root-associated bacterial community composition and the antioxidative defence system in plants (M2). Four main questions were formulated and thoroughly discussed in this Thesis. The first was whether TRD can be taken up by plant roots and how the uptake rate when this compound is introduced to the plant/root system, either alone or together with other contaminants. The second was whether plants can be used as a tool for TRD removal from water-based systems, and how it distributes inside plant parts. The third was to explore the accumulation of TRD in the root system over time and to elucidate whether this has an effect on root-associated bacterial community composition as well as plant antioxidative defence system or not. And the fourth question was whether cultivable bacterial root endophytes, isolated from TRD-exposed plants, when inoculated with plants can improve the removal process of TRD and have an impact on the metabolism of TRD or not.

Figure (2) illustrates the main steps included in this thesis to understand the possible use and role of plant and/or bacterial inoculation in TRD removal process as well as its metabolization.

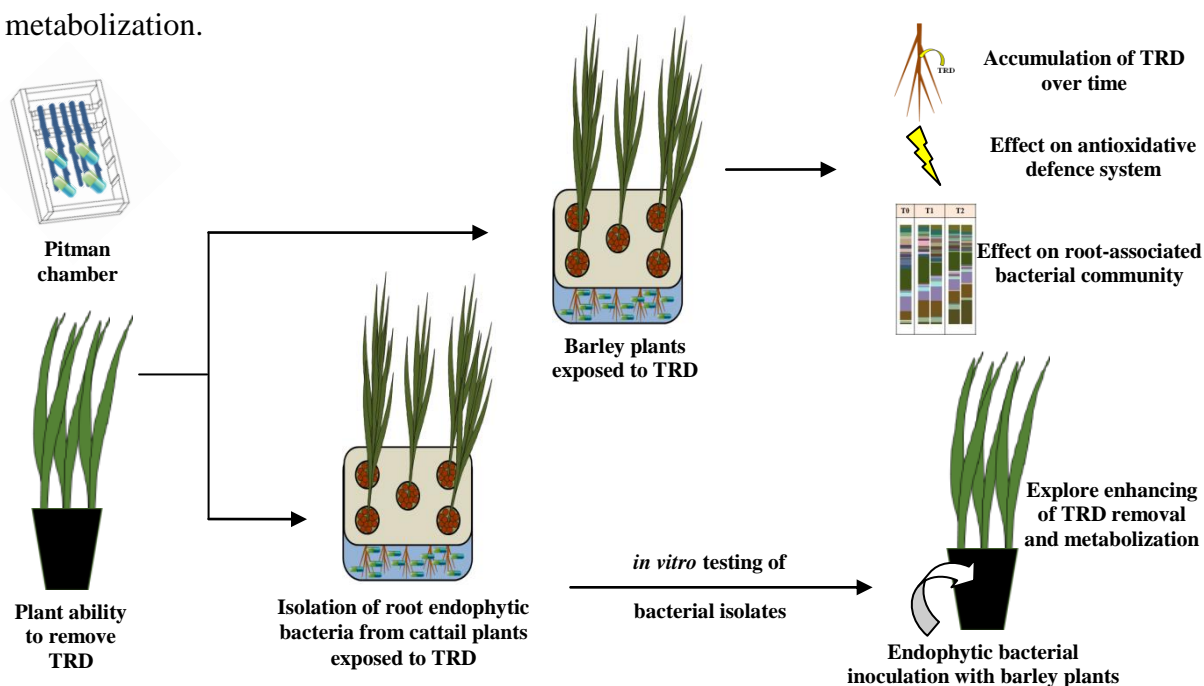


**Figure 2.** Scheme to demonstrate the different experiments conducted in this study

#### 4.1. TRD uptake/removal in short-term and hydroponic experiments

Short-term uptake experiments have been formerly done using Pitman chambers to evaluate the uptake rate of pharmaceutical compounds as well as the transfer of glutathione-xenobiotics conjugates in plant roots (Schröder et al., 2007; Cui et al., 2015). This technique was used in our study to explore the removal/uptake rate of TRD either alone or in combination with other pharmaceuticals by plant roots. Regardless of the reduction in the activity during the 24 h, the root tips showed vitality which allowed the usage of the excised cattail and barley roots in Pitman chambers experiments (M1). TRD was shown to be readily taken up and transported by excised roots of barley and cattail with similar rates in both species. These results emphasise the easy entrance of TRD into the root cells besides the movement of this compound via root cells and possible transport to other plant parts. It is known that water and small-sized solutes with molecular mass  $\leq 500$  can enter the plant root via the roots tips' epidermis (Miller et al., 2016). Moreover, Chuang and coauthors (2019) reported that pharmaceuticals having small size ( $MW < 300 \text{ g mol}^{-1}$ ) can easily enter roots of lettuce plants with water flow following the symplastic route in which ionic pharmaceuticals might enter root cells via transport proteins. This can be the same in the case of TRD which has a small size (i.e., molecular weight  $263.37 \text{ g mol}^{-1}$ ) as well as a cationic moiety. Thus, this can facilitate the uptake of this compound through the root tips of barley and cattail plants besides being determinant for its movement via root cells.

The uptake of TRD was retarded after exposing barley and cattail roots to TRD+VEN mixture, with the ability of both plants' roots to transport VEN (M1). As both compounds are chemically analogous, competition on the routes of uptake/transport is likely which in turn ultimately affects TRD uptake as well as its transport rate. In accordance with our results, Szkutnik-Fiedler and coauthors (2017), found that TRD concentration decreased in plasma of one rabbits group after exposing to TRD+VEN mixture in comparison to the control group exposed only to TRD.

In the case of using Q in a mixture with TRD, a complete inhibition in TRD transport was recorded in Pitman chamber experiments with both plants' roots. This shows that OCT might be involved in TRD uptake/transport process, as Q is a well-known OCT inhibitor. In the same line with our results, Kitamura and coauthors (2014) showed that the usage of Q (1 mM) as an OCT inhibitor causes a high decrease in the uptake of TRD (close to 84%) by human cells. Moreover, Cui and coauthors (2015), using the same Pitman chamber technique



in short-term uptake experiments, showed that metformin transport by cattail roots was inhibited significantly after using Q (0.5 mM) in a mixture with metformin.

The previous experiments from Pitman chambers showed the ability of plant roots to uptake and transport TRD. Subsequently, a hydroponic experiment using barley seedlings was conducted to explore and track the efficiency of plants to remove TRD from water systems over time. The results from the hydroponic experiment revealed that the removal of TRD ( $100 \mu\text{g L}^{-1}$ ) reached 89.13% after 15 days of incubation with barley seedlings. This value was reduced to 48.58% and 28.65% when TRD was co-administrated to barley seedlings with 0.5 mM and 1 mM Q, respectively (M1). The high removal efficiency in plants exposed to TRD alone confirms the easy access and uptake TRD by barley roots from water systems. In addition to that, abiotic controls showed the stability of TRD concentration during the experiment, revealing that neither degradation nor adsorption of this compound occurred during the experiment. Suno and coauthors (2015) demonstrated the stability of TRD in an aqueous solution towards sunlight or diffused light in a controlled room (Suno et al., 2015), while another study recorded its low biotic degradation characteristics (Rúa-Gómez and Püttmann, 2013). Due to the frequent detection of TRD in water systems besides its low removal efficiency by conventional WWTPs (Kasprzyk-Hordern et al., 2009), previous studies were conducted to explore the potential of CWs for eliminating TRD from treated/untreated wastewater. Rühmland and coauthors (2015), after monitoring the removal of 29 pharmaceuticals using CWs or ponds (with/without floating plants), demonstrated that subsurface flow CWs recorded the highest removal efficiency by 80% in summer while in winter the same CWs recorded lower removal efficiency reaching 16%. The previous CWs were inhabited by *P. australis*, *Lemna* and floating algae. Another study showed the seasonal removal efficiency of three horizontal subsurface flow CWs, inhabited either by *P. australis* or *Phalaris arundinacea*, towards selected types of PPCPs, where TRD recorded an elimination range 54-85% (Chen et al., 2016). Moreover, Vymazal and coauthors (2017) explored the usage of four horizontal subsurface flow CWs, inhabited either with *P. australis* alone or *P. australis*+*P. arundinacea*, and showed removal efficiency of TRD, as one of the monitored PPCPs in this study, varied between 29% to 69%. These studies strengthen our results which showed the ability of barley seedlings to remove TRD. However, in CWs several processes are participating in PPCPs elimination, while our study illustrated the actual efficiency of the plant in removing TRD from hydroponic cultures.

In addition, other advanced techniques such as oxidation with ferrate and ozone, photocatalysis in aqueous titanium dioxide ( $\text{TiO}_2$ ), UV-based advanced oxidation processes,

electro-Fenton method using boron doped diamond (BDD) anode, biological activated carbon biofilters, coupling gamma irradiation (advanced oxidation technique) with nanofiltration showed high removal/degradation performance (more than 95% to complete removal) towards TRD (Zimmermann et al., 2012; Antonopoulou and Konstantinou, 2016; Miklos et al., 2019; Monteil et al., 2020; Zhiteneva et al., 2021; Ghazouani et al., 2022; ). The latter techniques showed the efforts which have been done to search for a suitable method to deal with TRD contamination problem, however, these techniques are advanced and it may be too costly to implement them into existing or projected WWTP systems. According to M1 results, plants can be considered as a promising tool to clean up TRD from contaminated water due to their easy and wide usage, ecofriendly, sustainable and cost-effective characteristics.

From the previous hydroponic experiment, the TRD concentration was determined in the tissues of barley seedlings. Fifteen days of exposure to TRD was enough for barley seedlings to take up and accumulate TRD in their roots and shoots, as shown in M1. In all three treatment groups (TRD, TRQ1 and TRQ2), it was noticed that TRD concentration in shoots was higher than in roots (M1). Moreover, barley seedlings exposed to TRD alone showed BCF and TF values close to 9 and 1. Few studies showed the ability of plants (such as, common reed, spinach and lettuce) to accumulate TRD in their tissues (Petrie et al., 2017; Kodešová et al., 2019; Mercl et al., 2020). TRD has some physico-chemical characteristics facilitating its easy passage through the plant roots such as small MW 263.37, low number of H-bonds (acceptors = 3, donors = 1) as well as  $\log K_{ow}$  2.45. The previous characteristics are matching with the “Rule of 3” suggested by Kumar and Gupta (2016). According to this prediction theory, the physico-chemical properties of trace organic compounds limit their uptake by the plants; compounds with MW < 300, H-bond acceptors and donors < 6 and < 3, respectively and with  $\log K_{ow}$  < 3 are likely to have higher absorption and greater permeability. In the same line, it was reported that basic compounds have a tendency to move through the xylem and are easily translocated to the aerial parts via transpiration flow when their  $\log K_{ow}$  is in a range of 0 to 4 (Miller et al., 2016). Furthermore, it was stated that ionic small-sized pharmaceuticals with MW < 300 g mol<sup>-1</sup> might pass through roots with the water stream following symplastic pathway (Chuang et al., 2019). Consequently, these compounds could reach the xylem after passing through the endodermis and would subsequently be translocated to the shoot system by transpiration force. These studies strengthen our findings which showed that TRD has the tendency to be translocated in the aerial parts of the plant.

#### 4.2. Effect of TRD on GPX, CAT and GST plant enzymes

After exploring the ability of barley seedlings to uptake and translocate TRD in their roots and shoots (M1), it was worthy to evaluate its effects on selected plant enzymes. Activities of GPX, CAT and GST were scrutinized after exposing barley plants (one month old) to TRD ( $100 \mu\text{g L}^{-1}$ ). These measurements were done at the beginning (T0) and after TRD exposure by 12 (T1) and 24 (T2) days. In addition, TRD concentrations were determined in the roots of barley plants and the results showed the ability of root tissues to accumulate TRD over time (M2). For enzymes, significant differences were recorded in GPX activities between TRD-treated plants and the controls at both time points. These results can be linked to the accumulation of TRD in plant tissues as shown in M1 and M2. GPX plays a role in plant protection against oxidative stress through the utilization of  $\text{H}_2\text{O}_2$ , either in normal metabolism conditions or under stress, for oxidation of aromatic electron donor compounds such as guaiacol and pyrogallol (Sharma et al., 2012; Das and Roychoudhury, 2014). The heme-containing enzyme GPX is localized in the vacuole, cytosol as well as in the cell wall (Das and Roychoudhury, 2014). Induction of GPX has been demonstrated under different stressful environmental conditions such as drought, salinity,  $\gamma$ -radiation, or heavy metal contamination (Shah et al., 2001; Verma and Dubey, 2003; Sharma and Dubey, 2005; Mishra et al., 2013; Nahar et al., 2018). Previous studies demonstrated the change in GPX activity after exposing plants to pharmaceuticals. Yan and coauthors (2016) recorded stimulation in GPX activity in leaves of *Cyperus alternifolius* plants upto to 183.6% and 218.2% of the control after 23 days of exposure to a mixture of pharmaceuticals (sulfamethoxazole, carbamazepine, roxithromycin and ofloxacin) at concentration levels  $100$  and  $500 \mu\text{g L}^{-1}$ , respectively. Noticeable increases in GPX activities either in leaves or in both roots and leaves of cattail plants were recorded after treatment with carbamazepine and clofibric acid, respectively, after 21 days of exposure (Dordio et al., 2009 & 2011). Bartha and coauthors (2014) also found a higher GPX activity in cattail roots exposed to diclofenac (up to 250%) compared to controls. In lettuce plants, the increase in GPX activities was pronounced in the roots of plants exposed to  $1 \text{ mg L}^{-1}$  acetaminophen after 8 and 15 days (Leitão et al., 2021). Ryzdyński and coauthors (2017), recorded a 3-fold increase in GPX activities in shoots of yellow lupin seedlings (*Lupinus luteus*) grown in soil supplemented with tetracycline ( $90 \text{ mg kg}^{-1}$ ). Another study highlighted the importance of plant peroxidases in the oxidation process of diclofenac which helps in activating this compound for further conjugation (Huber et al., 2016).

Concerning CAT activities, the results from the barley experiment did not show significant differences between control and treated plants after 12 days of exposure to TRD. However, this changed after 24 days of TRD treatment recording induction in CAT activities in TRD-treated plants compared to control in roots and shoots. CAT is an antioxidant enzyme which localized mainly in peroxisomes (as it's the major spot for H<sub>2</sub>O<sub>2</sub> production), cytosol and mitochondria and catalyses the dismutation of two H<sub>2</sub>O<sub>2</sub> molecules into oxygen and water (Willekens et al., 1995; Mittler, 2002; Sharma et al., 2012). CAT possesses high specificity towards H<sub>2</sub>O<sub>2</sub> with a fast turnover rate (6×10<sup>6</sup> of H<sub>2</sub>O<sub>2</sub> molecules into water and oxygen per min; Sharma et al., 2012; Das and Roychoudhury, 2014). Previous studies explored the effect of pharmaceuticals on the activities of CAT. Chen and coauthors (2017) observed a strong enhancement in CAT activities of *Cyperus alternifolius* (umbrella papyrus) roots after 3 days of exposure to 25 µM (5.7 mg L<sup>-1</sup>) oxybenzone, which then decreased after 5 days. Moreover, it has been reported that treatment of lettuce and cattail plants with acetaminophen and clofibrac acid, respectively, induces CAT activities in the leaves of these plants (Dordio et al., 2009; Leitão et al., 2021). Another study showed an increase in CAT activities in leaves of *Cyperus alternifolius* plants after exposure to a pharmaceutical cocktail (sulfamethoxazole, carbamazepine, roxithromycin and ofloxacin) at different concentration levels 10, 30, 100 and 500 µg L<sup>-1</sup> for 23 days (Yan et al., 2016). Rydzyński and coauthors (2017), showed a high increase of CAT activities in yellow lupin seedlings grown in contaminated soil with ciprofloxacin and tetracycline (90 mg kg<sup>-1</sup>) for 10 days by 1560% and 650%, respectively, over the control plants. Another study recorded a linkage between pharmaceutical concentration (0.032 µg L<sup>-1</sup> chlorpromazine, 25 µg L<sup>-1</sup> acetaminophen and 100 µg L<sup>-1</sup> diclofenac) and the highest CAT activities were recorded in *Lemna minor* compared to the controls (Alkimi et al., 2019). The findings in our study along with the results from other studies strengthen the idea that both GPX and CAT play a crucial role in equilibrating H<sub>2</sub>O<sub>2</sub> levels in plants exposed to pharmaceutical compounds or in the case of GPX may contribute to the oxidation of pharmaceuticals/their metabolites and preparing it for the conjugation step as in case of diclofenac mentioned above.

In the current study, GST activities, towards two substrates (CDNB and pNPA), recorded significant changes at both time points as well as in roots and shoots of barley plants exposed to TRD in comparison with those of controls (M2). These differences in GST activities between TRD-treated plants and controls, match with what was expected as GSTs are important enzymes contributing to “Green Liver” theory and their induction can be linked to TRD conjugation/metabolism processes. GSTs are common enzymes in plants, which have a

crucial role either in metabolism processes or in stress detoxification cycles. It has been intensively studied in terms of xenobiotic detoxification reactions (Cummins et al., 2011) with a special focus on herbicides. Biotic and abiotic stressors, such as extreme temperatures, drought, and pathogen attacks can induce the activities of GSTs (Mauch and Dudler, 1993; Anderson and Davis, 2004; Gallé et al., 2009). However, beyond their well-established role in xenobiotic detoxification, GSTs have been found to play significant roles in diverse processes. Notably, studies have demonstrated their involvement in various pathways, including tyrosine degradation, biosynthesis of essential plant hormones, peroxide cleavage, stress signaling molecules, and even the proper functioning of root nodules (Loyall et al., 2000; Mueller et al., 2000; Dalton et al., 2009; Oakley, 2011). The induction in GST activity towards two substrates, CDNB and pNPA used in the current study, might point to plant reaction against TRD accumulation as well as its metabolites in the treated plants. Previous studies demonstrated that oxidative stress works as an inducer for GSTs and their contribution to detoxification processes via conjugating evolved metabolites are likely (Edwards et al., 2000; Schröder, 2001; Sappl et al., 2009; Lee et al., 2014). Bartha and coauthors (2014) noticed an increase in GST activities in both roots and shoots, towards CDNB and pNPA, after exposing cattail plants to 1 mg L<sup>-1</sup> diclofenac. Pierattini and coauthors (2018), after exposing poplar plants to 1 mg L<sup>-1</sup> diclofenac, recorded an induction in GST activity, after 28 days of treatments, towards CDNB and fluorodifen in roots, when diclofenac and its metabolite 4-OH-diclofenac was detected, while in the stem, only an increase of GST-CDNB activity was noticed and no change in activity towards fluorodifen was noticed after 28 days of exposure, when they could not detect diclofenac or its metabolite in the aerial parts. Similarly, Sun and coauthors (2018) recorded an enhancement in GST activity towards CDNB after exposing cucumber (*Cucumis sativus*) seedlings to a cocktail from 17 pharmaceuticals and personal care products at different concentrations (0, 0.5, 5 and 50 µg L<sup>-1</sup>) for 7 days. Moreover, it was reported that exposing cucumber seedlings to 5 mg L<sup>-1</sup> acetaminophen causes an increase in GST-CDNB activities in both roots and leaves by 1.30-1.60 and 1.07-1.94 folds, respectively, compared to control plants (Sun et al., 2019). Sousa and coauthors (2021), recorded an enhancement in GST-CDNB activities with increasing diclofenac concentration (0.5 and 5 mg L<sup>-1</sup>) treatment to tomato (*Solanum lycopersicum*) plants compared to controls, but this pattern was only recorded in roots. The previous studies in addition to our results reveal the crucial role that GPX and GST may play in transforming and conjugating pharmaceutical compounds inside plant tissues.

### 4.3. TRD effect on root-associated bacterial community

Plants are good hosts harbouring a huge diversity of microbes either inside roots and shoots (endophytes) or around it, in the rhizobiome. For both compartments, the plant microbiome plays a crucial role in determining plant health status besides adaptation towards different environmental conditions. As results from (M1) showed accumulation of TRD in barley roots, it was worthy to explore its effect on the root-associated bacterial communities in (M2). In this study, no statistical differences in alpha diversity indices (Shannon and Simpson) were recorded between control and TRD-treated plants' root-associated bacterial communities at both time points (T1 and T2). However, small differences in alpha diversity indices were noticed, especially at T1, suggesting the possible effect of TRD on the root-associated bacterial community through the direct response of some bacterial taxa towards TRD and/or changes in secondary metabolites root exudation patterns of the barley plants under TRD treatment. Previous studies postulated the active role of plants in recruiting soil microbes that are beneficial to their growth and health by releasing different compounds in the root vicinity which stimulate these targeted microorganisms in the rhizosphere (Reinhold-Hurek et al., 2015; Sasse et al., 2018; Pascale et al., 2020). Visualizing beta diversity using PCA analysis showed a clear separation of TRD-treated plants from the controls as well as separating the barley plant groups according to the harvesting time (M2). PERMANOVA analysis for the previous results showed that time and TRD treatment affected the root-associated bacterial community (M2). In line with these findings, other studies showed how time and pharmaceutical compounds can cause alteration of bacterial community structure. Dombrowski and coauthors (2017), after monitoring the microbiota profile of *Arabidopsis thaliana* for 7 months, noticed that all tested taxonomic ranks were dramatically altered, owing to the residence time of plants in soil instead of either plant stature or plant developmental stages, while Xiong and coauthors (2021) demonstrated that microbial diversity and composition in plant compartments were strongly affected by plant developmental stages. Moreover, these authors suggested that the ecological role of bacterial and fungal microbiomes significantly shifted along with maize growth stages. In the same direction, it was reported that spike formation is a key stage during wheat growth, influencing either root-associated or rhizospheric bacterial community compositions (Usyskin-Tonne et al., 2021). Also, Yang and coauthors (2017b) recorded noticeable changes in the composition of bacterial communities at different growth stages of barley plants (seedling and booting stages). Cerqueira and coauthors (2020) concluded that exposure of lettuce plants to 20 or 100  $\mu\text{g L}^{-1}$  mixtures of antibiotics (trimethoprim, ofloxacin, sulfamethoxazole) caused only a mild shift in the root

microbiome. Also, Bigott and coauthors (2022) showed that irrigation practices with treated wastewater and two different concentrations from a pharmaceutical cocktail (14 compounds) affected the community structure of root-associated bacteria in lettuce plants. Relative abundances data from root-associated bacterial communities showed that barley roots, considering all hydroponic cultures, were dominated by 16 major families over the duration of the experiment (M2). Xanthomonadaceae was the dominating family at T2 and was noticed to be slightly enriched in TRD-treated plants compared to controls. Furthermore, the relative abundance of the most dominating families revealed that Methylophilaceae was presented in TRD-treated plants at T1. A previous study showed enrichment in relative abundance of Xanthomonadaceae, besides other families, in sediment microcosms amended with ibuprofen compared to the non-amended controls (Rutere et al., 2020). Syranidou and coauthors (2018) reported that after exposing *Juncus acutus* plants to high concentration levels of heavy metals (Ni, Zn, Cd) and emerging contaminants (ciprofloxacin, sulfamethoxazole, bisphenol-A), Sphingomonadaceae was the highest relatively abundant family in the root endophytic communities besides Methylophilaceae, Xanthobacteraceae and Burkholderiaceae families. Wang and coauthors (2018), according to relative abundances results from biodegradation microcosm experiments, reported that Methylophilaceae and Rhizobiaceae were from the predominant candidatus families in the biodegradation of methamphetamine and ketamine. Kalyuhznaya and coauthors (2009) demonstrated the direct linkage between Methylophilaceae and degradation of methanol. As Gong and coauthors (2014) showed that O- and N-demethylation are the main routes in TRD metabolism, this might give an explanation for the presence of Methylophilaceae, as one of the most dominant families, in TRD-treated barley roots at T1.

Further analysis using the ANCOMBC algorithm was used to figure out the differential abundance between bacterial ASVs in TRD-treated and controls over time (T1 and T2). Several ASVs were differentially abundant in the roots of TRD-treated plants compared to controls especially at T2 compared to T1 (M2). The differentially abundant ASVs, in TRD-treated plants compared to controls at both time points, belong to Xanthobacteraceae, Spirosomaceae, *Pantoea*, Comamonadaceae, *Pseudacidovorax*, *Hydrogenophaga*, *Pseudoxanthomonas*, *Sphingomonas*, *Sphingopyxis*, Pseudomonadaceae, Hyphomonadaceae, Chitinophagaceae, Comamonadaceae and Bacillaceae (ANCOMBC, Holm-adjusted  $p$ -values  $\leq 0.05$ ). It was recorded that certain ASVs belonging to Xanthobacteraceae, *Hydrogenophaga* and *Pseudacidovorax* were differentially abundant at T1 and T2 in roots of TRD-treated plants compared to controls, which might reflect the importance of these taxa in

removal/metabolization processes related to TRD contamination. Few data are available in the literature expressing the behaviour of bacterial communities after exposure only to TRD. Kostanjevecki and coauthors (2019) noticed after following the aerobic degradation of TRD, using one year-TRD-acclimatized sludge culture and without glucose supplementation, enrichment in the relative abundances of the genera *Xanthobacter* (Xanthobacteraceae), *Bacillus* (Bacillaceae), *Methylobacillus* (Methylophilaceae) and *Sphingobacterium* (Sphingobacteriaceae). Furthermore, the same authors postulated that using a consortium from *Xanthobacter*, *Bacillus*, *Methylobacillus*, *Sphingobacterium* and *Enterobacter* might help in TRD removal. The previous observations are in accordance with results from the relative abundance of the most dominant families which showed the representation of Methylophilaceae, as one of the dominating families, in roots of TRD-treated plants at T1 besides the enrichment of ASVs assigned to Bacillaceae (at T2) and Xanthobacteraceae (at both time points) families in roots of TRD-treated plants (M2). To the best of our knowledge, information about effects of TRD on rhizospheric or root-associated bacterial communities is still lacking. Bigott and coauthors (2022), showed that the relative abundance of *Hydrogenophaga* significantly increased in lettuce roots irrigated with treated wastewater compared to those irrigated with water, while irrigation with water or treated wastewater amended with mixture from 14 PPCPs (at  $100 \mu\text{g L}^{-1}$ ) caused an enrichment in the relative abundance of clade *Allorhizobium-Neorhizobium-Pararhizobium-Rhizobium* in roots of lettuce plants. Yi and coauthors (2022) recorded the degradation ability of *Hydrogenophaga* sp. YM1 towards atenolol in actual wastewater. Nguyen and coauthors (2019b), suggested the possible contribution of *Pseudacidovorax*, *Asticcacaulis* and *Nitratireductor* in the diclofenac biodegradation process after their proliferation in the fed-batch bioreactors which had been inoculated with activated sludge and amended with 50, 500, 5000  $\mu\text{g L}^{-1}$  diclofenac. Murdoch and Hay (2005) reported the ability of *Sphingomonas* sp. strain Ibu-2 to degrade ibuprofen by eliminating the acidic side chain from this compound. Another study revealed that specific phylotypes including *Sphingomonas*, *Methylophilus*, unknown Cytophagaceae and *Beijerinckia* may contribute to PPCPs biodegradation (Kim et al., 2017). The same authors demonstrated the importance of the microbial community structure, besides the source of this community, in determining the efficiency and the rate of PPCPs transformation. Lu and coauthors (2019), recorded the degradation ability of *Pseudoxanthomonas* sp. strain DIN-3 towards ibuprofen, diclofenac and naproxen ( $50 \mu\text{g L}^{-1}$ ) by 41, 23 and 39%, respectively after incubation for 14 days. Aguilar-Romero and coauthors (2021) reported that *Sphingopyxis granuli* RW412, isolated from river sediment, was able to



eliminate ibuprofen from a biopurification system. These findings strengthen our results, which demonstrated that certain ASVs belonging to *Sphingomonas*, *Pseudacidovorax*, *Hydrogenophaga*, *Pseudoxanthomonas* and *Sphingopyxis* were differentially abundant in roots of TRD-treated plants compared to controls after 24 days from exposure to TRD. Consequently, this reflects the potential of TRD in causing changes in root-associated bacterial communities and may reveal the possible role of these genera in TRD metabolization/degradation process inside the plant.

#### **4.4. Isolation of endophytic bacteria from TRD-exposed plants and their PGP characteristics**

Data shown in M1 and M2 reveal the ability of plants to uptake and accumulate TRD in their roots. Consequently, the effect of TRD on root endophytic bacteria is worth to be explored. Twenty-three endophytic bacterial isolates were recovered from cattail plants exposed to TRD (5 mg L<sup>-1</sup>) for one month, and only twenty-two isolates showed closest similarities of more than 98% after comparison with rRNA/ITS databases from NCBI (<https://blast.ncbi.nlm.nih.gov/Blast.cgi>). These twenty-two isolates were clustered into 12 bacterial families; Alcaligenaceae, Azospirillaceae, Bacillaceae, Burkholderiaceae, Comamonadaceae, Microbacteriaceae, Mycobacteriaceae, Nocardiaceae, Oxalobacteraceae, Paenibacillaceae, Rhodanobacteraceae and Sphingomonadaceae (M3). Previous results in M2 showed that certain bacterial ASVs were differentially abundant in the roots of barley plants after exposure to 100 µg L<sup>-1</sup> TRD compared to control plants (M2). Some of these ASVs belong to Bacillaceae, Comamonadaceae and Sphingomonadaceae families either represented by classified or unclassified bacterial genera. These families were represented in the obtained endophytic bacteria which were isolated from cattail plants exposed to 5 mg L<sup>-1</sup> TRD. Both findings suggest the possible contribution of these families in TRD removal/metabolization process. Several studies demonstrated the ability of Bacilli members to degrade various xenobiotic compounds such as pharmaceutical compounds, herbicides, pesticides, explosives, dyes and aromatic hydrocarbons (Bisht et al., 2014; Arora et al., 2016; Birolli et al., 2016; Singh and Singh, 2016; Górný et al., 2019; Arora, 2020). Chen and Rosazza (1994) reported that *Nocardia* sp. from family Nocardiaceae was able to degrade ibuprofen. Furthermore, previous studies showed that members from Comamonadaceae and Sphingomonadaceae can degrade aromatic compounds including herbicides (Müller et al., 2001&2004; Liu et al., 2011; Dallinger and Horn, 2014). The previous studies strengthen our results which suggest

the possible contribution of members from these families to xenobiotic degradation processes.

All isolates showed positive responses for PGP traits, especially the production of IAA, ammonia and siderophores, while only sixteen isolates recorded positive results for solubilizing the inorganic phosphate (M3). Bacterial isolate TE3 (closely related to *Azospirillum palustre*) recorded the highest values to produce IAA from tryptophan. This genus is well-known for its ability to be used in biofertilization process and known to enhance plant productivity, has the potential to remediate hydrocarbons, possess heavy metals tolerance and play a role in mitigating osmotic stress in plants (Cassán et al., 2009; Cassán and Diaz-Zorita, 2016; Cruz-Hernández et al., 2022). Tikhonova and coauthors (2019) showed the potential of *A. palustre* to produce IAA, whereas other studies demonstrated the ability of other *Azospirillum* strains to solubilize inorganic phosphate, produce siderophores in addition to IAA production (Saxena et al., 1986; Naqqash et al., 2022). Bacterial isolate TE20 (closely related to *Duganella aceris*) showed the highest value for producing ammonia after growing on peptone water medium. Jeon and coauthors (2021) succeeded to isolate and identify this bacterium from *Acer pictum* tree's sap. Hitherto, this bacterium is scantily investigated in the literature, however, other species from the same genus showed their possible contribution to the plant growth promotion process. Zhang and coauthors (2016) revealed the positive potential of *D. ginsengisoli* for the production of IAA and siderophore. Whereas, Fang and coauthors (2019) demonstrated the ability of *Duganella* isolates to produce IAA as well as positively affecting the root growth in *Ageratina adenophora* seedlings. Moreover, it was noticed that *D. callida* possesses several genes correlated to plant growth promotion (Raths et al., 2021). The previous observations strengthen our results showing that the obtained isolates possess PGP properties depending on their performance on the *in vitro* tests.

#### **4.5. *In vitro* and *in vivo* removal of TRD using endophytic bacterial isolates**

Bacterial isolates recovered from cattail plants were grown for 14 days on AB minimal medium containing TRD (100 µg L<sup>-1</sup>), with using glucose or malate as a carbon source, to test their TRD removal ability. The highest *in vitro* removal efficiency, recorded in AB minimal medium, either with glucose or malate, was around 18 % in case of using single isolates. Bacterial isolates with close similarity to *Microbacterium azadirachtae* (TE12), *Bacillus toyonensis* (TE8) and *Rhodanobacter xiangquanii* (TE6) accounted for the highest TRD removal efficiencies using glucose as an amendment, whereas using malate as carbon

source showed best removal efficiencies for bacterial isolates with close similarity to *Paenibacillus curdlanolyticus* (TE16), *B. toyonensis* (TE17) and *Nocardia coeliaca* (TE2) (M3). The previous results revealed the degree of hardness for complete TRD removal as well as the role which may be played by these genera in TRD removal process. This is in accordance with the findings of Kostanjevecki and coauthors (2019) which demonstrated the incapability of TRD removal from biodegradation medium, supplemented with 20 mg L<sup>-1</sup> TRD, using an original culture from activated sludge, while the same authors showed the ability of the same culture after seven months of adaptation to remove 30% of TRD, whereas using a one-year optimized culture succeeded to remove TRD by ~82% after using glucose as additional carbon source during 14 days of incubation. Moreover, the community structure of the previously activated sludge culture revealed that *Bacillus* genus comprised 30 % of the total bacterial community after using glucose in the biodegradation medium. Kim and coauthors (2011) demonstrated the ability of *Microbacterium* sp. strain 4N2-2 to degrade the fluoroquinolone antibiotic norfloxacin and produce four metabolites. The same authors stated the presence of similarities by 99.70% between this strain and the PGP *M. azadirachtae* AI-S262T strain. *R. xiangquanii* BJQ-6<sup>T</sup>, as mentioned in the previous section, can degrade the herbicide anilofos (Zhang et al., 2011). Moreover, the ability of bacterial strain CCH1, similar to uncultured *Rhodanobacter* sp. by 98 %, to degrade azoxystrobin fungicide was reported (Howell et al., 2014). Taylor and Wain (1962) showed the ability of *N. coeliaca* to degrade  $\omega$ -phenoxyalkanecarboxylic via  $\beta$ -oxidation of the side-chains (up to nine methylene groups) located on this compound. Another species, from the *Nocardia* family, *N. soli* Y48 was able to degrade alkane fractions from the crude oil in addition to harbour some genes accounting for long-chain alkanes degradation (Yang et al., 2019). Concerning *P. curdlanolyticus* (formely *B. curdlanolyticus*), a previous study demonstrated the degradation characteristics of this strain towards the recalcitrant polysaccharides curdlan, pullulan and pustulan (Kanzawa et al., 1995). Another study highlighted the ability of *P. curdlanolyticus* strain B-6, after aerobically grown on xylan-containing medium, to produce several xylanolytic-cellulolytic such as xylanase, acetyl esterase, carboxymethyl cellulose, arabinofuranosidase, avicelase, cellobiohydrolase, mannanase,  $\beta$ -xylosidase, amylase, chitinase and  $\beta$ -glucosidase (Pason et al., 2006). Relating to *B. toyonensis*, Meda and coauthors (2020) explored the degradation ability of this species towards high melting explosives (HMX; octahydro-1,3,5,7-tetranitro-1,3,5,7-tetrazocine). These findings strengthen our observations and reveal the possible contribution of these bacterial genera in the removal/degradation processes of various xenobiotics.

According to results from the previous *in vitro* experiments, six isolates were selected to study their ability to enhance TRD removal process with barley seedlings. These isolates are TE12 (closely related to *M. azadirachtae*), TE17 (closely related to *B. toyonensis*), TE2 (closely related to *N. coeliaca*), TE3 (closely related to *A. palustre*), TE6 (closely related to *R. xiangquanii*) and TE20 (closely related to *D. aceris*). The inoculation of barley seedlings was done with single isolates (TE12 or TE17), Dual (TE12+TE17) or Mix (consortium from TE12+TE17+TE2+TE3+TE6+TE20) as shown in M3. Dual inoculation resulted in the highest removal efficiency for TRD compared to the non-inoculated plants (M3). Barley seedlings proved their ability to uptake and remove TRD from hydroponic cultures reaching 89.13 % after 15 days when the hydroponic cultures were supplemented with 100  $\mu\text{g L}^{-1}$  TRD (M1). Although the concentration of TRD used in the inoculation experiments was 10 times higher than in the M1 experiments, barley seedlings without bacterial inoculation recorded 77.69 % TRD removal efficiency after 24 days of exposure to this compound. As is shown in section 4.1, the physico-chemical properties of TRD play a crucial role in facilitating the uptake and removal of this compound from the external medium into plant roots. Inoculation treatments with bacteria revealed an enhancement in TRD removal compared to the non-inoculated plants (M3). This can be through the direct effect on the removal/metabolization processes of TRD from the external medium or indirect action via enhancing plant growth especially increasing root biomass which in turn increases the TRD uptake rate (M3). Previous *in vivo* studies showed the ability of the bacterial taxa, which is used in the current inoculation experiment, to promote plant growth at various stressed conditions. Rojas-Solis and coauthors (2020) demonstrated the active role of *B. toyonensis* COPE52 towards tomato plants grown under 0 and 100 mM NaCl via increasing the chlorophyll content besides root and shoot biomass in inoculated plants compared to controls, whereas inoculating maize plants grown under aluminium (Al) stress conditions with *B. toyonensis* Bt04 resulted in enhancing root development and promotion of maize growth (Zerrouk et al., 2020). Perazzoli and coauthors (2022) revealed that an endophytic *Duganella* sp. strain S1.OA.B\_B10 was able to colonize tomato seedlings tissue in addition to its contribution in enhancing tomato growth under low-temperature conditions ( $15 \pm 1$  °C). *Nocardia* sp. WB46 enhanced root and shoot lengths of canola plants grown on a 3% n-hexadecane containing medium compared to controls with the same conditions but without inoculation (Alotaibi et al., 2022). Previous studies showed that inoculation of plants such as wheat and sugarcane with *Azospirillum* sp. can ameliorate drought stress and promote plant growth as well as yield (Moutia et al., 2010; Arzanesh et al., 2011). These findings along with our observations

revealed the beneficial use of the mentioned bacterial genera with plants grown under stress/contamination conditions to enhance their performance.

#### **4.6. Quantification of TRD and its O- and N-demethylated metabolites in barley tissues**

TRD, ODTRD and NDTRD were quantified in the roots and shoots of all plants exposed to 1 mg L<sup>-1</sup> TRD with/without bacterial inoculation (M3). The highest concentrations of TRD and its metabolites were detected in shoots of Dual or Mix inoculated barley seedlings. This suggests the importance of bacterial inoculation in facilitating the uptake/removal process of TRD besides their possible effect on the metabolization of TRD to its main metabolites ODTRD and NDTRD. Hitherto, no information available concerns the effect of bacterial inoculation on the metabolization of TRD inside plant tissue. However, previous studies showed the possible routes for TRD metabolization in mammals. Gong and coauthors (2014), mentioned that O- and N-demethylations are the main routes for TRD metabolization followed by either other demethylation steps or conjugation with sulphates or glucuronides. It was reported that CYP2D6 catalyzes O-demethylation of TRD to ODTRD its main active metabolite (Paar et al., 1997), whereas, CYP3A4 and CYP2B6 mediate the N-demethylation of TRD to the pharmacologically inactive metabolite NDTRD (Subrahmanyam et al., 2001). These findings along with the current results demonstrated the huge similarities between the mammalian and the plant/bacterial systems toward TRD metabolization. Moreover, it's worth mentioning that concentrations of NDTRD in roots and shoots of barley seedlings with all treatments were higher than ODTRD (M3); which reveals the tendency of bacterial inoculated or non-inoculated plants either to metabolize TRD through N-demethylation pathway or to actively metabolize/conjugate the formed ODTRD in roots and shoots to a different metabolite. In accordance with our observations, Kostanjevecki and coauthors (2019) recorded the formation of NDTRD after following *in vitro* degradation of TRD especially in the absence of glucose in the degradation medium. The previous authors suggested that N-demethylation is considered as one of the important mechanisms during microbial degradation of TRD. Moreover, Giorgi and coauthors (2009) found that NDTRD concentrations in dogs' plasma as well as urine were higher than ODTRD after oral administration of TRD in immediate-release capsules to these dogs. TRD metabolization in plants can follow the "green liver" theory as described in M2, in which important group of enzymes such as CYP450 monooxygenases, oxidation/reduction or hydrolysis reactions enzymes and glutathione S-transferases can take place (Sandermann, 1994; Schröder, 1997). It was reported that the conversion of nicotine to nornicotine in tobacco plants followed N-

demethylation route with an active role of the CYP450 monooxygenase member “CYP82E4” in this process (Siminszky et al., 2005). Another study showed that sorghum shoots’ microsomes can metabolize metolachlor (herbicide) via O-demethylation pathway (Moreland et al., 1990). Moreover, the same authors showed that using inhibitors for CYP450 monooxygenases can prevent the formation of the previous metabolite, whereas, in the case of bacterial taxa, previous studies showed the essential role of CYP450 monooxygenases in different strains of *Sphingobium* sp. for bisphenol A degradation (Sasaki et al., 2005a&b; Jia et al., 2020). Furthermore, another *in vitro* study reported that CYP107E4, a CYP450 enzyme isolated from *Actinoplanes* sp., was able to bind diclofenac and produce the 4'-hydroxydiclofenac metabolite (Prior et al., 2010). Other studies showed the important role of CYP450 in *B. subtilis* and strain LYK-6 (identified as a member of *Pseudomonas* genus) in degradation processes of diclofenac and carbamazepine (via oxidation reactions), respectively (Chen et al., 2020; Zhou et al., 2022). The previous findings demonstrate that bacterial CYP450 can play a role in the metabolism/degradation of pharmaceuticals.

## 5. Conclusion and Recommendations

Information about the impact of pharmaceutical compounds on plant health as well as their associated microbiome is still limited. Moreover, the use of bacterial-plant-based systems to improve removal efficiency of these compounds from raw/treated wastewater is scantily discussed. Thus, the current Thesis is devoted to provide a general picture of the possible usage of plants either alone or in combination with bacterial endophytes as an eco-friendly method to remediate problematic compounds like the pharmaceutical TRD from contaminated aquatic systems. In addition, it explores the possible effects of TRD on some plant enzymes and the bacterial community associated with their roots. Based on the findings obtained in the current thesis, we derived the following:

- TRD is taken up and transported through roots of cattail and barley plants;
- Coadministration of TRD with other pollutants adversely affects the uptake rate of TRD through cattail and barley roots;
- Barley plants can effectively remove TRD from hydroponic cultures, accumulate it in their roots as well as translocate it into the aerial parts;
- TRD triggers alterations in root-associated bacterial communities, and differential abundance results showed representation of certain ASVs in TRD-treated plants over time;
- Exposure to TRD stimulates CAT, GPX and GST activities in plant tissues;
- PGP bacterial inoculation enhanced barley root growth under TRD contamination;
- Bacterial inoculation leads to fortified plants and supports phytoremediation of TRD;
- TRD metabolization inside barley tissues proceeds via both O- and N-demethylation, with higher accumulating concentrations of NDTRD compared to ODTRD;
- Bacterial-inoculated plants revealed a trend of accumulating more TRD and its main metabolites in their tissues than non-inoculated controls.

These findings confirm the high potential of phytoremediation, as an eco-friendly, sustainable, widely applicable and cost-effective solution, in solving TRD contamination problem through the fast uptake, accumulation and translocation of TRD in plant tissues. Taking into consideration the actual scenario in WWTPs, the competition of TRD with other pharmaceutical pollutants can retard the uptake/transport rate of TRD by plants. Therefore, bacterial inoculation, using TRD-adapted inocula, can overcome this problem as it showed the potential to boost TRD removal efficiency from water-based systems. In addition to that,

the detection and quantification of NDTRD and ODTRD inside plant tissues give an important vision for the fate of TRD in plants.

Thus, not only due to the massive abuse of this medicament and its frequent detection in different water resources (such as WWTPs' influents and effluents) but also its possible accumulation and translocation in different plant parts, we recommend carefully monitoring this compound in treated wastewater before its usage for agricultural purposes to prevent its entrance to the human food chain either through the accumulation inside the edible parts of crops or by using TRD-contaminated fodder for livestock animals which in turn may cause risk to human health after their consumption. We further recommend the use of TRD-adapted bacterial consortia that possess PGP traits as a plant-bacterial inoculation strategy in the CWs, to boost the removal of TRD or its residues prior to the discharge into fresh water sources or be used to irrigate agricultural lands.



### III. References

- Afzal, M., Yousaf, S., Reichenauer, T. G., & Sessitsch, A. (2012). The inoculation method affects colonization and performance of bacterial inoculant strains in the phytoremediation of soil contaminated with diesel oil. *International Journal of Phytoremediation*, 14, 35-47. <https://doi.org/10.1080/15226514.2011.552928>
- Aguilar-Romero, I., De la Torre-Zúñiga, J., Quesada, J. M., Haïdour, A., O'Connell, G., McAmmond, B. M., Van Hamme, J. D., Romero, E., Wittich, R. M., & Van Dillewijn, P. (2021). Effluent decontamination by the ibuprofen-mineralizing strain, *Sphingopyxis granulii* RW412: Metabolic processes. *Environmental Pollution*, 274, 116536. <https://doi.org/10.1016/j.envpol.2021.116536>
- Ahmad, F., Ahmad, I., & Khan, M. S. (2008). Screening of free-living rhizospheric bacteria for their multiple plant growth promoting activities. *Microbiological Research*, 163, 173-181. <https://doi.org/10.1016/j.micres.2006.04.001>
- Aitchison, J., Barceló-Vidal, C., Martín-Fernández, J. A., & Pawlowsky-Glahn, V. (2000). Logratio analysis and compositional distance. *Mathematical Geology*, 32, 271-275. <https://doi.org/10.1023/A:1007529726302>
- Alkimin, G. D., Daniel, D., Frankenbach, S., Serôdio, J., Soares, A. M., Barata, C., & Nunes, B. (2019). Evaluation of pharmaceutical toxic effects of non-standard endpoints on the macrophyte species *Lemna minor* and *Lemna gibba*. *Science of the Total Environment*, 657, 926-937. <https://doi.org/10.1016/j.scitotenv.2018.12.002>
- Alotaibi, F., St-Arnaud, M., & Hijri, M. (2022). In-Depth characterization of plant growth promotion potentials of selected alkanes-degrading plant growth-promoting bacterial isolates. *Frontiers in Microbiology*, 13. <https://doi.org/10.3389/fmicb.2022.863702>
- Amy-Sagers, C., Reinhardt, K., & Larson, D. M. (2017). Ecotoxicological assessments show sucralose and fluoxetine affect the aquatic plant, *Lemna minor*. *Aquatic Toxicology*, 185, 76-85. <https://doi.org/10.1016/j.aquatox.2017.01.008>
- Anderson, J. V., & Davis, D. G. (2004). Abiotic stress alters transcript profiles and activity of glutathione S-transferase, glutathione peroxidase, and glutathione reductase in *Euphorbia esula*. *Physiologia Plantarum*, 120, 421-433. <https://doi.org/10.1111/j.0031-9317.2004.00249.x>
- Antonopoulou, M., & Konstantinou, I. (2016). Photocatalytic degradation and mineralization of tramadol pharmaceutical in aqueous TiO<sub>2</sub> suspensions: evaluation of kinetics, mechanisms and ecotoxicity. *Applied Catalysis A: General*, 515, 136-143.

<https://doi.org/10.1016/j.apcata.2016.02.005>

- Archer, E., Petrie, B., Kasprzyk-Hordern, B., & Wolfaardt, G. M. (2017). The fate of pharmaceuticals and personal care products (PPCPs), endocrine disrupting contaminants (EDCs), metabolites and illicit drugs in a WWTW and environmental waters. *Chemosphere*, 174, 437-446. <https://doi.org/10.1016/j.chemosphere.2017.01.101>
- Arora, P. K. (2020). Bacilli-mediated degradation of xenobiotic compounds and heavy metals. *Frontiers in Bioengineering and Biotechnology*, 8, 570307. <https://doi.org/10.3389/fbioe.2020.570307>
- Arora, P. K., Srivastava, A., & Singh, V. P. (2016). Diversity of 4-chloro-2-nitrophenol-degrading bacteria in a waste water sample. *Journal of Chemistry*, 2016. <https://doi.org/10.1155/2016/7589068>
- Arzanesh, M. H., Alikhani, H. A., Khavazi, K., Rahimian, H. A., & Miransari, M. (2011). Wheat (*Triticum aestivum* L.) growth enhancement by *Azospirillum* sp. under drought stress. *World Journal of Microbiology and Biotechnology*, 27, 197-205. <https://doi.org/10.1007/s11274-010-0444-1>
- Backer, R., Rokem, J. S., Ilangumaran, G., Lamont, J., Praslickova, D., Ricci, E., Subramanian, S., & Smith, D. L. (2018). Plant growth-promoting rhizobacteria: context, mechanisms of action, and roadmap to commercialization of biostimulants for sustainable agriculture. *Frontiers in Plant Science*, 9, 1473. <https://doi.org/10.3389/fpls.2018.01473>
- Balakrishna, K., Rath, A., Praveenkumarreddy, Y., Guruge, K. S., & Subedi, B. (2017). A review of the occurrence of pharmaceuticals and personal care products in Indian water bodies. *Ecotoxicology and Environmental Safety*, 137, 113-120. <https://doi.org/10.1016/j.ecoenv.2016.11.014>
- Barceló, D., & Petrovic, M. (2007). Pharmaceuticals and personal care products (PPCPs) in the environment. *Analytical and Bioanalytical Chemistry*, 387, 1141-1142. <https://doi.org/10.1007/s00216-006-1012-2>
- Bartha, B., Huber, C., & Schröder, P. (2014). Uptake and metabolism of diclofenac in *Typha latifolia*—how plants cope with human pharmaceutical pollution. *Plant Science*, 227, 12-20. <https://doi.org/10.1016/j.plantsci.2014.06.001>
- Bartha, B., Huber, C., Harpaintner, R., & Schröder, P. (2010). Effects of acetaminophen in *Brassica juncea* L. Czern.: investigation of uptake, translocation, detoxification, and the induced defense pathways. *Environmental Science and Pollution Research*, 17, 1553-1562. <https://doi.org/10.1007/s11356-010-0342-y>

- Bayati, M., Ho, T. L., Vu, D. C., Wang, F., Rogers, E., Cuvelier, C., Huebotter, S., Inniss, E. C., Udawatta, R., Jose, S. & Lin, C. H. (2021). Assessing the efficiency of constructed wetlands in removing PPCPs from treated wastewater and mitigating the ecotoxicological impacts. *International Journal of Hygiene and Environmental Health*, 231, 113664. <https://doi.org/10.1016/j.ijheh.2020.113664>
- Becerra-Castro, C., Kidd, P. S., Rodríguez-Garrido, B., Monterroso, C., Santos-Ucha, P., & Prieto-Fernández, Á. (2013). Phytoremediation of hexachlorocyclohexane (HCH)-contaminated soils using *Cytisus striatus* and bacterial inoculants in soils with distinct organic matter content. *Environmental Pollution*, 178, 202-210. <https://doi.org/10.1016/j.envpol.2013.03.027>
- Berendsen, R. L., Pieterse, C. M., & Bakker, P. A. (2012). The rhizosphere microbiome and plant health. *Trends in Plant Science*, 17, 478-486. <https://doi.org/10.1016/j.tplants.2012.04.001>
- Bexfield, L. M., Toccalino, P. L., Belitz, K., Foreman, W. T., & Furlong, E. T. (2019). Hormones and pharmaceuticals in groundwater used as a source of drinking water across the United States. *Environmental Science & Technology*, 53, 2950-2960. <https://doi.org/10.1021/acs.est.8b05592>
- Bhattacharyya, P. N., & Jha, D. K. (2012). Plant growth-promoting rhizobacteria (PGPR): emergence in agriculture. *World Journal of Microbiology and Biotechnology*, 28, 1327-1350. <https://doi.org/10.1007/s11274-011-0979-9>
- Bigott, Y., Chowdhury, S. P., Pérez, S., Montemurro, N., Manasfi, R., & Schröder, P. (2021). Effect of the pharmaceuticals diclofenac and lamotrigine on stress responses and stress gene expression in lettuce (*Lactuca sativa*) at environmentally relevant concentrations. *Journal of Hazardous Materials*, 403, 123881. <https://doi.org/10.1016/j.jhazmat.2020.123881>
- Bigott, Y., Gallego, S., Montemurro, N., Breuil, M. C., Pérez, S., Michas, A., Martin-Laurent, F., & Schröder, P. (2022). Fate and impact of wastewater-borne micropollutants in lettuce and the root-associated bacteria. *Science of the Total Environment*, 831, 154674. <https://doi.org/10.1016/j.scitotenv.2022.154674>
- Bigott, Y., Khalaf, D.M., Schröder, P., Schröder, P.M., Cruzeiro, C., 2020. Uptake and translocation of pharmaceuticals in plants: principles and data analysis. *The Handbook of Environmental Chemistry*. Springer, Berlin, Heidelberg, pp. 1-38.
- Birolli, W. G., Borges, E. M., Nitschke, M., Romão, L. P., & Porto, A. L. (2016). Biodegradation pathway of the pyrethroid pesticide esfenvalerate by bacteria from

- different biomes. *Water, Air, & Soil Pollution*, 227, 1-11. <https://doi.org/10.1007/s11270-016-2968-y>
- Bisht, S., Pandey, P., Kaur, G., Aggarwal, H., Sood, A., Sharma, S., Kumar, V., & Bisht, N. S. (2014). Utilization of endophytic strain *Bacillus* sp. SBER3 for biodegradation of polyaromatic hydrocarbons (PAH) in soil model system. *European Journal of Soil Biology*, 60, 67-76. <https://doi.org/10.1016/j.ejsobi.2013.10.009>
- Bradford, M. M. (1976). A rapid and sensitive method for the quantitation of microgram quantities of protein utilizing the principle of protein-dye binding. *Analytical Biochemistry*, 72, 248-254. [https://doi.org/10.1016/0003-2697\(76\)90527-3](https://doi.org/10.1016/0003-2697(76)90527-3)
- Bravo, L., Mico, J. A., & Berrocoso, E. (2017). Discovery and development of tramadol for the treatment of pain. *Expert Opinion on Drug Discovery*, 12, 1281-1291. <https://doi.org/10.1080/17460441.2017.1377697>
- Buřič, M., Grabicová, K., Kubec, J., Kouba, A., Kuklina, I., Kozák, P., Grabic, R. & Randák, T. (2018). Environmentally relevant concentrations of tramadol and citalopram alter behaviour of an aquatic invertebrate. *Aquatic Toxicology*, 200, 226-232. <https://doi.org/10.1016/j.aquatox.2018.05.008>
- Callahan, B. J., McMurdie, P. J., Rosen, M. J., Han, A. W., Johnson, A. J. A., & Holmes, S. P. (2016). DADA2: High-resolution sample inference from Illumina amplicon data. *Nature Methods*, 13, 581-583. <https://doi.org/10.1038/nmeth.3869>
- Carmona, E., Andreu, V., & Picó, Y. (2014). Occurrence of acidic pharmaceuticals and personal care products in Turia River Basin: from waste to drinking water. *Science of the Total Environment*, 484, 53-63. <https://doi.org/10.1016/j.scitotenv.2014.02.085>
- Carvalho, P. N., Basto, M. C. P., Almeida, C. M. R., & Brix, H. (2014). A review of plant-pharmaceutical interactions: from uptake and effects in crop plants to phytoremediation in constructed wetlands. *Environmental Science and Pollution Research*, 21, 11729-11763. <https://doi.org/10.1007/s11356-014-2550-3>
- Cassán, F., & Diaz-Zorita, M. (2016). *Azospirillum* sp. in current agriculture: From the laboratory to the field. *Soil Biology and Biochemistry*, 103, 117-130. <https://doi.org/10.1016/j.soilbio.2016.08.020>
- Cassán, F., Maiale, S., Masciarelli, O., Vidal, A., Luna, V., & Ruiz, O. (2009). Cadaverine production by *Azospirillum brasilense* and its possible role in plant growth promotion and osmotic stress mitigation. *European Journal of Soil Biology*, 45, 12-19. <https://doi.org/10.1016/j.ejsobi.2008.08.003>
- Cerqueira, F., Christou, A., Fatta-Kassinos, D., Vila-Costa, M., Bayona, J. M., & Pina, B.

- (2020). Effects of prescription antibiotics on soil-and root-associated microbiomes and resistomes in an agricultural context. *Journal of Hazardous Materials*, 400, 123208. <https://doi.org/10.1016/j.jhazmat.2020.123208>
- Chen, F., Huber, C., & Schröder, P. (2017). Fate of the sunscreen compound oxybenzone in *Cyperus alternifolius* based hydroponic culture: Uptake, biotransformation and phytotoxicity. *Chemosphere*, 182, 638-646. <https://doi.org/10.1016/j.chemosphere.2017.05.072>
- Chen, L., Li, Y., Lin, L., Tian, X., Cui, H., & Zhao, F. (2020). Degradation of diclofenac by *B. subtilis* through a cytochrome P450-dependent pathway. *Environmental Technology & Innovation*, 20, 101160. <https://doi.org/10.1016/j.eti.2020.101160>
- Chen, Y., & Rosazza, J. P. (1994). Microbial transformation of ibuprofen by a *Nocardia* species. *Applied and Environmental Microbiology*, 60, 1292-1296. <https://doi.org/10.1128/aem.60.4.1292-1296.1994>
- Chen, Y., Vymazal, J., Březinová, T., Koželuh, M., Kule, L., Huang, J., & Chen, Z. (2016). Occurrence, removal and environmental risk assessment of pharmaceuticals and personal care products in rural wastewater treatment wetlands. *Science of the Total Environment*, 566, 1660-1669. <https://doi.org/10.1016/j.scitotenv.2016.06.069>
- Chuang, Y. H., Liu, C. H., Sallach, J. B., Hammerschmidt, R., Zhang, W., Boyd, S. A., & Li, H. (2019). Mechanistic study on uptake and transport of pharmaceuticals in lettuce from water. *Environment International*, 131, 104976. <https://doi.org/10.1016/j.envint.2019.104976>
- Cruz-Hernández, M. A., Mendoza-Herrera, A., Bocanegra-García, V., & Rivera, G. (2022). *Azospirillum* spp. from plant growth-promoting bacteria to their use in bioremediation. *Microorganisms*, 10, 1057. <https://doi.org/10.3390/microorganisms10051057>
- Cruzeiro, C., Rodrigues-Oliveira, N., Velhote, S., Pardal, M. Â., Rocha, E., & Rocha, M. J. (2016). Development and application of a QuEChERS-based extraction method for the analysis of 55 pesticides in the bivalve *Scrobicularia plana* by GC-MS/MS. *Analytical and Bioanalytical Chemistry*, 408, 3681-3698. <https://doi.org/10.1007/s00216-016-9440-0>
- Cui, H., & Schröder, P. (2016). Uptake, translocation and possible biodegradation of the antidiabetic agent metformin by hydroponically grown *Typha latifolia*. *Journal of Hazardous Materials*, 308, 355-361. <https://doi.org/10.1016/j.jhazmat.2016.01.054>
- Cui, H., Hrabec de Angelis, M., & Schröder, P. (2017). Iopromide exposure in *Typha latifolia* L.: Evaluation of uptake, translocation and different transformation mechanisms in

- planta. Water Research, 122, 290-298. <https://doi.org/10.1016/j.watres.2017.06.004>
- Cui, H., Hense, B. A., Müller, J., & Schröder, P. (2015). Short term uptake and transport process for metformin in roots of *Phragmites australis* and *Typha latifolia*. Chemosphere, 134, 307-312. <https://doi.org/10.1016/j.chemosphere.2015.04.072>
- Cummins, I., Dixon, D. P., Freitag-Pohl, S., Skipsey, M., & Edwards, R. (2011). Multiple roles for plant glutathione transferases in xenobiotic detoxification. Drug Metabolism Reviews, 43, 266-280. <https://doi.org/10.3109/03602532.2011.552910>
- D'Abrosca, B., Fiorentino, A., Izzo, A., Cefarelli, G., Pascarella, M. T., Uzzo, P., & Monaco, P. (2008). Phytotoxicity evaluation of five pharmaceutical pollutants detected in surface water on germination and growth of cultivated and spontaneous plants. Journal of Environmental Science and Health, Part A, 43, 285-294. <https://doi.org/10.1080/10934520701792803>
- Dallinger, A., & Horn, M. A. (2014). Agricultural soil and drilosphere as reservoirs of new and unusual assimilators of 2, 4-dichlorophenol carbon. Environmental Microbiology, 16, 84-100. <https://doi.org/10.1111/1462-2920.12209>
- Dalton, D. A., Boniface, C., Turner, Z., Lindahl, A., Kim, H. J., Jelinek, L., Govindarajulu, M., Finger, R. E., & Taylor, C. G. (2009). Physiological roles of glutathione S-transferases in soybean root nodules. Plant Physiology, 150, 521-530. <https://doi.org/10.1104/pp.109.136630>
- Das, K., & Roychoudhury, A. (2014). Reactive oxygen species (ROS) and response of antioxidants as ROS-scavengers during environmental stress in plants. Frontiers in Environmental Science, 2, 53. <https://doi.org/10.3389/fenvs.2014.00053>
- de Jongh, C. M., Kooij, P. J., de Voogt, P., & ter Laak, T. L. (2012). Screening and human health risk assessment of pharmaceuticals and their transformation products in Dutch surface waters and drinking water. Science of the Total Environment, 427, 70-77. <https://doi.org/10.1016/j.scitotenv.2012.04.010>
- Dombrowski, N., Schlaeppli, K., Agler, M. T., Hacquard, S., Kemen, E., Garrido-Oter, R., Wunder, J., Coupland, G., & Schulze-Lefert, P. (2017). Root microbiota dynamics of perennial *Arabidopsis alpina* are dependent on soil residence time but independent of flowering time. The ISME Journal, 11, 43-55. <https://doi.org/10.1038/ismej.2016.109>
- Dordio, A. V., Belo, M., Teixeira, D. M., Carvalho, A. P., Dias, C. M. B., Picó, Y., & Pinto, A. P. (2011). Evaluation of carbamazepine uptake and metabolization by *Typha* spp., a plant with potential use in phytotreatment. Bioresource Technology, 102, 7827-7834. <https://doi.org/10.1016/j.biortech.2011.06.050>



- Dordio, A. V., Duarte, C., Barreiros, M., Carvalho, A. P., Pinto, A. P., & da Costa, C. T. (2009). Toxicity and removal efficiency of pharmaceutical metabolite clofibric acid by *Typha* spp.-potential use for phytoremediation?. *Bioresource Technology*, 100, 1156-1161. <https://doi.org/10.1016/j.biortech.2008.08.034>
- Dordio, A., Carvalho, A. P., Teixeira, D. M., Dias, C. B., & Pinto, A. P. (2010). Removal of pharmaceuticals in microcosm constructed wetlands using *Typha* spp. and LECA. *Bioresource Technology*, 101, 886-892. <https://doi.org/10.1016/j.biortech.2009.09.001>
- Dorn-In, S., Bassitta, R., Schwaiger, K., Bauer, J., & Hölzel, C. S. (2015). Specific amplification of bacterial DNA by optimized so-called universal bacterial primers in samples rich of plant DNA. *Journal of Microbiological Methods*, 113, 50-56. <https://doi.org/10.1016/j.mimet.2015.04.001>
- Duffner, C., Kublik, S., Fösel, B., Frostegård, Å., Schloter, M., Bakken, L., & Schulz, S. (2022). Genotypic and phenotypic characterization of hydrogenotrophic denitrifiers. *Environmental Microbiology*, 24, 1887-1901. <https://doi.org/10.1111/1462-2920.15921>
- Edwards, R., Dixon, D. P., & Walbot, V. (2000). Plant glutathione S-transferases: enzymes with multiple functions in sickness and in health. *Trends in Plant Science*, 5, 193-198. [https://doi.org/10.1016/S1360-1385\(00\)01601-0](https://doi.org/10.1016/S1360-1385(00)01601-0)
- Eggen, T., Asp, T. N., Grave, K., & Hormazabal, V. (2011). Uptake and translocation of metformin, ciprofloxacin and narasin in forage-and crop plants. *Chemosphere*, 85, 26-33. <https://doi.org/10.1016/j.chemosphere.2011.06.041>
- Elimelech, M., & Phillip, W. A. (2011). The future of seawater desalination: energy, technology, and the environment. *Science*, 333, 712-717. <https://doi.org/10.1126/science.1200488>
- EN 15662, 2008. Foods of plant origin - Determination of pesticide residues using GC-MS and/or LC-MS/MS following acetonitrile extraction/partitioning and clean-up by dispersive SPE - QuEChERS method. BSI British Standard.
- Esplugas, S., Bila, D. M., Krause, L. G. T., & Dezotti, M. (2007). Ozonation and advanced oxidation technologies to remove endocrine disrupting chemicals (EDCs) and pharmaceuticals and personal care products (PPCPs) in water effluents. *Journal of Hazardous Materials*, 149, 631-642. <https://doi.org/10.1016/j.jhazmat.2007.07.073>
- European Commission (2015). Commission Implementing Decision (EU) 2015/495 of 20 march 2015. Establishing a watch list of substances for union-wide monitoring in the field of water policy pursuant to Directive 2008/105/EC of the European Parliament and of the Council. *Official Journal of the European Union*, 78(C (2015) 1756), 20-30.

- Falahi, O. A. A., Abdullah, S. R. S., Hasan, H. A., Othman, A. R., Ewadh, H. M., Al-Baldawi, I. A., Kurniawan, S. B., Imron, M. F. & Ismail, N. I. (2021). Simultaneous removal of ibuprofen, organic material, and nutrients from domestic wastewater through a pilot-scale vertical sub-surface flow constructed wetland with aeration system. *Journal of Water Process Engineering*, 43, 102214. <https://doi.org/10.1016/j.jwpe.2021.102214>
- Fang, K., Chen, L., Zhou, J., Yang, Z. P., Dong, X. F., & Zhang, H. B. (2019). Growth-promoting characteristics of potential nitrogen-fixing bacteria in the root of an invasive plant *Ageratina adenophora*. *PeerJ*, 7, e7099. <https://doi.org/10.7717/peerj.7099>
- FAO. (2007). *Coping with water scarcity: challenge of the twenty-first century*. UN Food and Agriculture Organization, Rome.
- Fatima, K., Imran, A., Amin, I., Khan, Q. M., & Afzal, M. (2016). Plant species affect colonization patterns and metabolic activity of associated endophytes during phytoremediation of crude oil-contaminated soil. *Environmental Science and Pollution Research*, 23, 6188-6196. <https://doi.org/10.1007/s11356-015-5845-0>
- Fleishman, E., Blockstein, D. E., Hall, J. A., Mascia, M. B., Rudd, M. A., Scott, J. M., Sutherland, W. J., Bartuska, A. M., Brown, A. G., Christen, C. A., Clement, J. P., Dellasala, D., Duke, C. S., Eaton, M., Fiske, S. J., Gosnell, H., Haney, J. C., Hutchins, M., Klein, M. L., Marqusee, J., Noon, B. R., Nordgren, J. R., Orbach, P. M., Powell, J., Quarles, S. P., Saterson, K. A., Savitt, C. C., Stein, B. A., Webster, M. S., & Vedder, A. (2011). Top 40 priorities for science to inform US conservation and management policy. *BioScience*, 61, 290-300. <https://doi.org/10.1525/bio.2011.61.4.9>
- Gallé, Á., Csiszár, J., Secenji, M., Guóth, A., Cseuz, L., Tari, I., Györgyey, J., & Erdei, L. (2009). Glutathione transferase activity and expression patterns during grain filling in flag leaves of wheat genotypes differing in drought tolerance: response to water deficit. *Journal of Plant Physiology*, 166, 1878-1891. <https://doi.org/10.1016/j.jplph.2009.05.016>
- Gerten, D., Lucht, W., Ostberg, S., Heinke, J., Kowarsch, M., Kreft, H., Kundzewicz, Z. W., Rastgooy, J., Warren, R., & Schellnhuber, H. J. (2013). Asynchronous exposure to global warming: freshwater resources and terrestrial ecosystems. *Environmental Research Letters*, 8, 034032. <https://doi.org/10.1088/1748-9326/8/3/034032>
- Ghazouani, S., Boujelbane, F., Ennigrou, D. J., Van der Bruggen, B., & Mzoughi, N. (2022). Removal of tramadol hydrochloride, an emerging pollutant, from aqueous solution using gamma irradiation combined by nanofiltration. *Process Safety and Environmental Protection*, 159, 442-451. <https://doi.org/10.1016/j.psep.2022.01.005>



- Giorgi, M., Del Carlo, S., Saccomanni, G., Łebkowska-Wieruszewska, B., & Kowalski, C. J. (2009). Pharmacokinetic and urine profile of tramadol and its major metabolites following oral immediate release capsules administration in dogs. *Veterinary Research Communications*, 33, 875-885. <https://doi.org/10.1007/s11259-009-9236-1>
- Gong, L., Stamer, U. M., Tzvetkov, M. V., Altman, R. B., & Klein, T. E. (2014). PharmGKB summary: tramadol pathway. *Pharmacogenetics and Genomics*, 24, 374-380. doi: 10.1097/FPC.0000000000000057
- Górny, D., Guzik, U., Hupert-Kocurek, K., & Wojcieszńska, D. (2019). A new pathway for naproxen utilisation by *Bacillus thuringiensis* B1 (2015b) and its decomposition in the presence of organic and inorganic contaminants. *Journal of Environmental Management*, 239, 1-7. <https://doi.org/10.1016/j.jenvman.2019.03.034>
- Goswami, M., & Suresh, D. E. K. A. (2020). Plant growth-promoting rhizobacteria-alleviators of abiotic stresses in soil: a review. *Pedosphere*, 30, 40-61. [https://doi.org/10.1016/S1002-0160\(19\)60839-8](https://doi.org/10.1016/S1002-0160(19)60839-8)
- Gude, V. G. (2017). Desalination and water reuse to address global water scarcity. *Reviews in Environmental Science and Bio/Technology*, 16, 591-609. <https://doi.org/10.1007/s11157-017-9449-7>
- Habig, W. H., Pabst, M. J., & Jakoby, W. B. (1974). Glutathione S-transferases: the first enzymatic step in mercapturic acid formation. *Journal of Biological Chemistry*, 249, 7130-7139. [https://doi.org/10.1016/S0021-9258\(19\)42083-8](https://doi.org/10.1016/S0021-9258(19)42083-8)
- Hammad, H. M., Zia, F., Bakhat, H. F., Fahad, S., Ashraf, M. R., Wilkerson, C. J., Shah G. M., Nasim, W., Khosa, I. & Shahid, M. (2018). Uptake and toxicological effects of pharmaceutical active compounds on maize. *Agriculture, Ecosystems & Environment*, 258, 143-148. <https://doi.org/10.1016/j.agee.2018.02.022>
- He, S., Guo, H., He, Z., Yang, C., Yu, T., Chai, Q., & Lu, L. (2019). Interaction of *Lolium perenne* and *Hyphomicrobium* sp. GHH enhances the removal of 17 $\alpha$ -ethinyestradiol (EE2) from soil. *Journal of Soils and Sediments*, 19, 1297-1305. <https://doi.org/10.1007/s11368-018-2116-y>
- Howell, C. C., Semple, K. T., & Bending, G. D. (2014). Isolation and characterisation of azoxystrobin degrading bacteria from soil. *Chemosphere*, 95, 370-378. <https://doi.org/10.1016/j.chemosphere.2013.09.048>
- Hu, X., Xie, H., Zhuang, L., Zhang, J., Hu, Z., Liang, S., & Feng, K. (2021). A review on the role of plant in pharmaceuticals and personal care products (PPCPs) removal in constructed wetlands. *Science of the Total Environment*, 780, 146637.

<https://doi.org/10.1016/j.scitotenv.2021.146637>

- Huber, C., Preis, M., Harvey, P. J., Grosse, S., Letzel, T., & Schröder, P. (2016). Emerging pollutants and plants—metabolic activation of diclofenac by peroxidases. *Chemosphere*, 146, 435-441. <https://doi.org/10.1016/j.chemosphere.2015.12.059>
- Hussain, Z., Arslan, M., Malik, M. H., Mohsin, M., Iqbal, S., & Afzal, M. (2018a). Integrated perspectives on the use of bacterial endophytes in horizontal flow constructed wetlands for the treatment of liquid textile effluent: phytoremediation advances in the field. *Journal of Environmental Management*, 224, 387-395. <https://doi.org/10.1016/j.jenvman.2018.07.057>
- Hussain, Z., Arslan, M., Malik, M. H., Mohsin, M., Iqbal, S., & Afzal, M. (2018b). Treatment of the textile industry effluent in a pilot-scale vertical flow constructed wetland system augmented with bacterial endophytes. *Science of the Total Environment*, 645, 966-973. <https://doi.org/10.1016/j.scitotenv.2018.07.163>
- ICH, 2005. ICH harmonized tripartite guideline: validation of analytical procedures: text and methodology Q2(R1). International Conference of harmonization of technical requirements for registration of pharmaceuticals for human use, pp. 1–13.
- Iqbal, A., Mukherjee, M., Rashid, J., Khan, S. A., Ali, M. A., & Arshad, M. (2019). Development of plant-microbe phytoremediation system for petroleum hydrocarbon degradation: an insight from *alkb* gene expression and phytotoxicity analysis. *Science of the Total Environment*, 671, 696-704. <https://doi.org/10.1016/j.scitotenv.2019.03.331>
- Jeon, D., Kim, I. S., Choe, H., Kim, J. S., & Lee, S. D. (2021). *Duganella aceris* sp. nov., isolated from tree sap and proposal to transfer of *Rugamonas aquatica* and *Rugamonas rivuli* to the genus *Duganella* as *Duganella aquatica* comb. nov., with the emended description of the genus *Rugamonas*. *Archives of Microbiology*, 203, 2843-2852. <https://doi.org/10.1007/s00203-021-02191-z>
- Jia, Y., Eltoukhy, A., Wang, J., Li, X., Hlaing, T. S., Aung, M. M., Nwe, M. T., Lamraoui, I., & Yan, Y. (2020). Biodegradation of bisphenol A by *Sphingobium* sp. YC-JY1 and the essential role of cytochrome P450 monooxygenase. *International Journal of Molecular Sciences*, 21, 3588. <https://doi.org/10.3390/ijms21103588>
- Jones, E., Qadir, M., van Vliet, M. T., Smakhtin, V., & Kang, S. M. (2019). The state of desalination and brine production: A global outlook. *Science of the Total Environment*, 657, 1343-1356. <https://doi.org/10.1016/j.scitotenv.2018.12.076>
- Kalyuhznaya, M. G., Martens-Habbena, W., Wang, T., Hackett, M., Stolyar, S. M., Stahl, D. A., Lidstrom, M. E., & Chistoserdova, L. (2009). Methylophilaceae link methanol

- oxidation to denitrification in freshwater lake sediment as suggested by stable isotope probing and pure culture analysis. *Environmental Microbiology Reports*, 1, 385-392. <https://doi.org/10.1111/j.1758-2229.2009.00046.x>
- Kanzawa, Y., Harada, A., Takeuchi, M., Yokota, A., & Harada, T. (1995). *Bacillus curdlanolyticus* sp. nov. and *Bacillus kobensis* sp. nov., which hydrolyze resistant curdlan. *International Journal of Systematic Bacteriology*, 45, 515-521. <https://doi.org/10.1099/00207713-45-3-515>
- Kasprzyk-Hordern, B., Dinsdale, R. M., & Guwy, A. J. (2007). Multi-residue method for the determination of basic/neutral pharmaceuticals and illicit drugs in surface water by solid-phase extraction and ultra performance liquid chromatography-positive electrospray ionisation tandem mass spectrometry. *Journal of Chromatography A*, 1161, 132-145. <https://doi.org/10.1016/j.chroma.2007.05.074>
- Kasprzyk-Hordern, B., Dinsdale, R. M., & Guwy, A. J. (2008). The occurrence of pharmaceuticals, personal care products, endocrine disruptors and illicit drugs in surface water in South Wales, UK. *Water Research*, 42, 3498-3518. <https://doi.org/10.1016/j.watres.2008.04.026>
- Kasprzyk-Hordern, B., Dinsdale, R. M., & Guwy, A. J. (2009). The removal of pharmaceuticals, personal care products, endocrine disruptors and illicit drugs during wastewater treatment and its impact on the quality of receiving waters. *Water Research*, 43, 363-380. <https://doi.org/10.1016/j.watres.2008.10.047>
- Khan, A. L., Waqas, M., Kang, S. M., Al-Harrasi, A., Hussain, J., Al-Rawahi, A., Al-Khiziri, S., Ullah, I., Ali, L., Jung, H. Y., & Lee, I. J. (2014). Bacterial endophyte *Sphingomonas* sp. LK11 produces gibberellins and IAA and promotes tomato plant growth. *Journal of Microbiology*, 52, 689-695. <https://doi.org/10.1007/s12275-014-4002-7>
- Khan, S., Afzal, M., Iqbal, S., & Khan, Q. M. (2013). Plant-bacteria partnerships for the remediation of hydrocarbon contaminated soils. *Chemosphere*, 90, 1317-1332. <https://doi.org/10.1016/j.chemosphere.2012.09.045>
- Kim, D. W., Heinze, T. M., Kim, B. S., Schnackenberg, L. K., Woodling, K. A., & Sutherland, J. B. (2011). Modification of norfloxacin by a *Microbacterium* sp. strain isolated from a wastewater treatment plant. *Applied and Environmental Microbiology*, 77, 6100-6108. <https://doi.org/10.1128/AEM.00545-11>
- Kim, S., Rossmassler, K., Broeckling, C. D., Galloway, S., Prenni, J., & De Long, S. K. (2017). Impact of inoculum sources on biotransformation of pharmaceuticals and personal care products. *Water Research*, 125, 227-236.

<https://doi.org/10.1016/j.watres.2017.08.041>

- Kitamura, A., Higuchi, K., Okura, T., & Deguchi, Y. (2014). Transport characteristics of tramadol in the blood-brain barrier. *Journal of Pharmaceutical Sciences*, 103, 3335-3341. <https://doi.org/10.1002/jps.24129>
- Klavarioti, M., Mantzavinos, D., & Kassinos, D. (2009). Removal of residual pharmaceuticals from aqueous systems by advanced oxidation processes. *Environment International*, 35, 402-417. <https://doi.org/10.1016/j.envint.2008.07.009>
- Kodešová, R., Klement, A., Golovko, O., Fér, M., Kočárek, M., Nikodem, A., & Grabic, R. (2019). Soil influences on uptake and transfer of pharmaceuticals from sewage sludge amended soils to spinach. *Journal of Environmental Management*, 250, 109407. <https://doi.org/10.1016/j.jenvman.2019.109407>
- Kong, W. D., Zhu, Y. G., Liang, Y. C., Zhang, J., Smith, F. A., & Yang, M. (2007). Uptake of oxytetracycline and its phytotoxicity to alfalfa (*Medicago sativa* L.). *Environmental Pollution*, 147, 187-193. <https://doi.org/10.1016/j.envpol.2006.08.016>
- Kostanjevecki, P., Petric, I., Loncar, J., Smital, T., Ahel, M., & Terzic, S. (2019). Aerobic biodegradation of tramadol by pre-adapted activated sludge culture: Cometabolic transformations and bacterial community changes during enrichment. *Science of the Total Environment*, 687, 858-866. <https://doi.org/10.1016/j.scitotenv.2019.06.118>
- Krishnan, R. Y., Manikandan, S., Subbaiya, R., Biruntha, M., Govarthanam, M., & Karmegam, N. (2021). Removal of emerging micropollutants originating from pharmaceuticals and personal care products (PPCPs) in water and wastewater by advanced oxidation processes: A review. *Environmental Technology & Innovation*, 23, 101757. <https://doi.org/10.1016/j.eti.2021.101757>
- Kumar, K., & Gupta, S. C. (2016). A framework to predict uptake of trace organic compounds by plants. *Journal of Environmental Quality*, 45, 555-564. <https://doi.org/10.2134/jeq2015.06.0261>
- Kumar, S., Stecher, G., Li, M., Knyaz, C., & Tamura, K. (2018). MEGA X: molecular evolutionary genetics analysis across computing platforms. *Molecular Biology and Evolution*, 35, 1547. <https://doi.org/10.1093/molbev/msy096>
- Lee, S. H., Li, C. W., Koh, K. W., Chuang, H. Y., Chen, Y. R., Lin, C. S., & Chan, M. T. (2014). MSRB7 reverses oxidation of GSTF2/3 to confer tolerance of *Arabidopsis thaliana* to oxidative stress. *Journal of Experimental Botany*, 65, 5049-5062. <https://doi.org/10.1093/jxb/eru270>
- Leitão, I., Martins, L. L., Carvalho, L., Oliveira, M. C., Marques, M. M., & Mourato, M. P.

- (2021). Acetaminophen induces an antioxidative response in lettuce plants. *Plants*, 10, 1152. <https://doi.org/10.3390/plants10061152>
- Li, Y., Lian, J., Wu, B., Zou, H., & Tan, S. K. (2020). Phytoremediation of pharmaceutical-contaminated wastewater: Insights into rhizobacterial dynamics related to pollutant degradation mechanisms during plant life cycle. *Chemosphere*, 253, 126681. <https://doi.org/10.1016/j.chemosphere.2020.126681>
- Li, Y., Wu, B., Zhu, G., Liu, Y., Ng, W. J., Appan, A., & Tan, S. K. (2016). High-throughput pyrosequencing analysis of bacteria relevant to cometabolic and metabolic degradation of ibuprofen in horizontal subsurface flow constructed wetlands. *Science of the Total Environment*, 562, 604-613. <https://doi.org/10.1016/j.scitotenv.2016.04.020>
- Li, Y., Zhu, G., Ng, W. J., & Tan, S. K. (2014). A review on removing pharmaceutical contaminants from wastewater by constructed wetlands: design, performance and mechanism. *Science of the Total Environment*, 468, 908-932. <https://doi.org/10.1016/j.scitotenv.2013.09.018>
- Lin, H., & Peddada, S. D. (2020). Analysis of compositions of microbiomes with bias correction. *Nature Communications*, 11, 1-11. <https://doi.org/10.1038/s41467-020-17041-7>
- Lindim, C., de Zwart, D., Cousins, I. T., Kutsarova, S., Kühne, R., & Schüürmann, G. (2019). Exposure and ecotoxicological risk assessment of mixtures of top prescribed pharmaceuticals in Swedish freshwaters. *Chemosphere*, 220, 344-352. <https://doi.org/10.1016/j.chemosphere.2018.12.118>
- Lintz, W., Erlacin, S., Frankus, E., & Uragg, H. (1981). Biotransformation of tramadol in man and animal (author's transl). *Arzneimittel-Forschung*, 31, 1932-1943.
- Liu, X., Guo, X., Liu, Y., Lu, S., Xi, B., Zhang, J., Wang, Z. & Bi, B. (2019). A review on removing antibiotics and antibiotic resistance genes from wastewater by constructed wetlands: performance and microbial response. *Environmental Pollution*, 254, 112996. <https://doi.org/10.1016/j.envpol.2019.112996>
- Liu, Y. J., Liu, S. J., Drake, H. L., & Horn, M. A. (2011). Alphaproteobacteria dominate active 2-methyl-4-chlorophenoxyacetic acid herbicide degraders in agricultural soil and drilosphere. *Environmental Microbiology*, 13, 991-1009. <https://doi.org/10.1111/j.1462-2920.2010.02405.x>
- Loos, R., Carvalho, R., António, D. C., Comero, S., Locoro, G., Tavazzi, S., Paracchini, B., Ghiani, M., Lettieri, T., Blaha, L., Jarosova, B., Voorspoels, S., Servaes, K., Haglund, P., Fick, J., Lindberg, R. H., Schwesig, D. & Gawlik, B. M. (2013). EU-wide monitoring

- survey on emerging polar organic contaminants in wastewater treatment plant effluents. *Water Research*, 47, 6475-6487. <https://doi.org/10.1016/j.watres.2013.08.024>
- Louden, B. C., Haarmann, D., & Lynne, A. M. (2011). Use of blue agar CAS assay for siderophore detection. *Journal of Microbiology & Biology Education*, 12, 51-53. <https://doi.org/10.1128/jmbe.v12i1.249>
- Loyall, L., Uchida, K., Braun, S., Furuya, M., & Frohnmeier, H. (2000). Glutathione and a UV light-induced glutathione S-transferase are involved in signaling to chalcone synthase in cell cultures. *The Plant Cell*, 12, 1939-1950. <https://doi.org/10.1105/tpc.12.10.1939>
- Lozano, I., Pérez-Guzmán, C. J., Mora, A., Mahlknecht, J., Aguilar, C. L., & Cervantes-Avilés, P. (2022). Pharmaceuticals and personal care products in water streams: Occurrence, detection, and removal by electrochemical advanced oxidation processes. *Science of the Total Environment*, 154348. <https://doi.org/10.1016/j.scitotenv.2022.154348>
- Lu, Z., Sun, W., Li, C., Ao, X., Yang, C., & Li, S. (2019). Bioremoval of non-steroidal anti-inflammatory drugs by *Pseudoxanthomonas* sp. DIN-3 isolated from biological activated carbon process. *Water Research*, 161, 459-472. <https://doi.org/10.1016/j.watres.2019.05.065>
- Mackul'ak, T., Mosný, M., Škubák, J., Grabic, R., & Birošová, L. (2015). Fate of psychoactive compounds in wastewater treatment plant and the possibility of their degradation using aquatic plants. *Environmental Toxicology and Pharmacology*, 39, 969-973. <https://doi.org/10.1016/j.etap.2015.02.018>
- Malnes, D., Ahrens, L., Köhler, S., Forsberg, M., & Golovko, O. (2022). Occurrence and mass flows of contaminants of emerging concern (CECs) in Sweden's three largest lakes and associated rivers. *Chemosphere*, 294, 133825. <https://doi.org/10.1016/j.chemosphere.2022.133825>
- Martin, M. (2011). Cutadapt removes adapter sequences from high-throughput sequencing reads. *EMBnet.journal*, 17, 10-12. <https://doi.org/10.14806/ej.17.1.200>
- Matilla, M.A., Krell, T. (2018). Plant growth promotion and biocontrol mediated by plant-associated bacteria. In: Egamberdieva, D., Ahmad, P. (eds) *Plant Microbiome: Stress Response. Microorganisms for Sustainability*, vol 5. Springer, Singapore, 45-80. [https://doi.org/10.1007/978-981-10-5514-0\\_3](https://doi.org/10.1007/978-981-10-5514-0_3)
- Mauch, F., & Dudler, R. (1993). Differential induction of distinct glutathione-S-transferases of wheat by xenobiotics and by pathogen attack. *Plant Physiology*, 102, 1193-1201.



<https://doi.org/10.1104/pp.102.4.1193>

- McLain, N. K., Gomez, M. Y., & Gachomo, E. W. (2022). Acetaminophen levels found in recycled wastewater alter soil microbial community structure and functional diversity. *Microbial Ecology*, 1-15. <https://doi.org/10.1007/s00248-022-02022-8>
- McMurdie, P. J., & Holmes, S. (2013). phyloseq: an R package for reproducible interactive analysis and graphics of microbiome census data. *PloS one*, 8, e61217. <https://doi.org/10.1371/journal.pone.0061217>
- Meda, A., Sangwan, P., & Bala, K. (2020). Optimization of process parameters for degradation of HMX with *Bacillus toyonensis* using response surface methodology. *International Journal of Environmental Science and Technology*, 17, 4601-4610. <https://doi.org/10.1007/s13762-020-02783-0>
- Mercl, F., Košnář, Z., Maršík, P., Vojtíšek, M., Dušek, J., Száková, J., & Tlustoš, P. (2021). Pyrolysis of biosolids as an effective tool to reduce the uptake of pharmaceuticals by plants. *Journal of Hazardous Materials*, 405, 124278. <https://doi.org/10.1016/j.jhazmat.2020.124278>
- Michellini, L. R. R. W., Reichel, R., Werner, W., Ghisi, R., & Thiele-Bruhn, S. (2012). Sulfadiazine uptake and effects on *Salix fragilis* L. and *Zea mays* L. plants. *Water, Air, and Soil Pollution*, 223, 5243-5257. <https://doi.org/10.1007/s11270-012-1275-5>
- Miklos, D. B., Wang, W. L., Linden, K. G., Drewes, J. E., & Hübner, U. (2019). Comparison of UV-AOPs (UV/H<sub>2</sub>O<sub>2</sub>, UV/PDS and UV/Chlorine) for TOrC removal from municipal wastewater effluent and optical surrogate model evaluation. *Chemical Engineering Journal*, 362, 537-547. <https://doi.org/10.1016/j.cej.2019.01.041>
- Miller, E. L., Nason, S. L., Karthikeyan, K. G., & Pedersen, J. A. (2016). Root uptake of pharmaceuticals and personal care product ingredients. *Environmental Science and Technology*, 50, 525-541. <https://doi.org/10.1021/acs.est.5b01546>
- Mishra, P., Bhoomika, K., & Dubey, R. S. (2013). Differential responses of antioxidative defense system to prolonged salinity stress in salt-tolerant and salt-sensitive Indica rice (*Oryza sativa* L.) seedlings. *Protoplasma*, 250, 3-19. <https://doi.org/10.1007/s00709-011-0365-3>
- Mittler, R. (2002). Oxidative stress, antioxidants and stress tolerance. *Trends in Plant Science*, 7, 405-410. [https://doi.org/10.1016/S1360-1385\(02\)02312-9](https://doi.org/10.1016/S1360-1385(02)02312-9)
- Monteil, H., Oturan, N., Péchaud, Y., & Oturan, M. A. (2020). Electro-Fenton treatment of the analgesic tramadol: Kinetics, mechanism and energetic evaluation. *Chemosphere*, 247, 125939. <https://doi.org/10.1016/j.chemosphere.2020.125939>

- Moreland, D. E., Corbin, F. T., Novitzky, W. P., Parker, C. E., & Tomer, K. B. (1990). Metabolism of metolachlor by a microsomal fraction isolated from grain sorghum (*Sorghum bicolor*) shoots. *Zeitschrift für Naturforschung C*, 45, 558-564. <https://doi.org/10.1515/znc-1990-0544>
- Moutia, J. F. Y., Saumtally, S., Spaepen, S., & Vanderleyden, J. (2010). Plant growth promotion by *Azospirillum* sp. in sugarcane is influenced by genotype and drought stress. *Plant and Soil*, 337, 233-242. <https://doi.org/10.1007/s11104-010-0519-7>
- Mueller, L. A., Goodman, C. D., Silady, R. A., & Walbot, V. (2000). AN9, a petunia glutathione S-transferase required for anthocyanin sequestration, is a flavonoid-binding protein. *Plant Physiology*, 123, 1561-1570. <https://doi.org/10.1104/pp.123.4.1561>
- Müller, R. H., Kleinstüber, S., & Babel, W. (2001). Physiological and genetic characteristics of two bacterial strains utilizing phenoxypropionate and phenoxyacetate herbicides. *Microbiological Research*, 156, 121-131. <https://doi.org/10.1078/0944-5013-00089>
- Müller, T. A., Byrde, S. M., Werlen, C., Van Der Meer, J. R., & Kohler, H. P. E. (2004). Genetic analysis of phenoxyalkanoic acid degradation in *Sphingomonas herbicidovorans* MH. *Applied and Environmental Microbiology*, 70, 6066-6075. <https://doi.org/10.1128/AEM.70.10.6066-6075.2004>
- Murdoch, R. W., & Hay, A. G. (2005). Formation of catechols via removal of acid side chains from ibuprofen and related aromatic acids. *Applied and Environmental Microbiology*, 71, 6121-6125. <https://doi.org/10.1128/AEM.71.10.6121-6125.2005>
- Nahar, S., Vemireddy, L. R., Sahoo, L., & Tanti, B. (2018). Antioxidant protection mechanisms reveal significant response in drought-induced oxidative stress in some traditional rice of Assam, India. *Rice Science*, 25, 185-196. <https://doi.org/10.1016/j.rsci.2018.06.002>
- Naqqash, T., Malik, K. A., Imran, A., Hameed, S., Shahid, M., Hanif, M. K., Majeed, A., Iqbal, M. J., Qaisrani, M. M., & Van Elsas, J. D. (2022). Inoculation with *Azospirillum* spp. acts as the liming source for improving growth and nitrogen use efficiency of potato. *Frontiers in Plant Science*, 13. <https://doi.org/10.3389/fpls.2022.929114>
- Nawaz, T., & Sengupta, S. (2019). Contaminants of emerging concern: occurrence, fate, and remediation. In: *Advances in water purification techniques: Meeting the Needs of Developed and Developing Countries*; Ahuja, S., Ed.; Elsevier: Amsterdam, The Netherlands, 2019; pp. 67–114. <https://doi.org/10.1016/B978-0-12-814790-0.00004-1>
- Nguyen, L. N., Nghiem, L. D., Pramanik, B. K., & Oh, S. (2019b). Cometabolic biotransformation and impacts of the anti-inflammatory drug diclofenac on activated



- sludge microbial communities. *Science of the Total Environment*, 657, 739-745. <https://doi.org/10.1016/j.scitotenv.2018.12.094>
- Nguyen, P. M., Afzal, M., Ullah, I., Shahid, N., Baqar, M., & Arslan, M. (2019a). Removal of pharmaceuticals and personal care products using constructed wetlands: effective plant-bacteria synergism may enhance degradation efficiency. *Environmental Science and Pollution Research*, 26, 21109-21126. <https://doi.org/10.1007/s11356-019-05320-w>
- Oakley, A. (2011). Glutathione transferases: a structural perspective. *Drug Metabolism Reviews*, 43, 138-151. <https://doi.org/10.3109/03602532.2011.558093>
- Olanrewaju, O. S., Glick, B. R., & Babalola, O. O. (2017). Mechanisms of action of plant growth promoting bacteria. *World Journal of Microbiology and Biotechnology*, 33, 1-16. <https://doi.org/10.1007/s11274-017-2364-9>
- Ontañón, O. M., González, P. S., Ambrosio, L. F., Paisio, C. E., & Agostini, E. (2014). Rhizoremediation of phenol and chromium by the synergistic combination of a native bacterial strain and *Brassica napus* hairy roots. *International Biodeterioration & Biodegradation*, 88, 192-198. <https://doi.org/10.1016/j.ibiod.2013.10.017>
- Paar, W. D., Poche, S., Gerloff, J., & Dengler, H. J. (1997). Polymorphic CYP2D6 mediates O-demethylation of the opioid analgesic tramadol. *European Journal of Clinical Pharmacology*, 53, 235-239. <https://doi.org/10.1007/s002280050368>
- Pascale, A., Proietti, S., Pantelides, I. S., & Stringlis, I. A. (2020). Modulation of the root microbiome by plant molecules: the basis for targeted disease suppression and plant growth promotion. *Frontiers in Plant Science*, 10, 1741. <https://doi.org/10.3389/fpls.2019.01741>
- Pason, P., Kyu, K. L., & Ratanakhanokchai, K. (2006). *Paenibacillus curdlanolyticus* strain B-6 xylanolytic-cellulolytic enzyme system that degrades insoluble polysaccharides. *Applied and Environmental Microbiology*, 72, 2483-2490. <https://doi.org/10.1128/AEM.72.4.2483-2490.2006>
- Perazzolli, M., Vicelli, B., Antonielli, L., Longa, C. M., Bozza, E., Bertini, L., Caruso, C., & Pertot, I. (2022). Simulated global warming affects endophytic bacterial and fungal communities of Antarctic pearlwort leaves and some bacterial isolates support plant growth at low temperatures. *Scientific Reports*, 12, 18839. <https://doi.org/10.1038/s41598-022-23582-2>
- Pereira, L. S., Oweis, T., & Zairi, A. (2002). Irrigation management under water scarcity. *Agricultural Water Management*, 57, 175-206. [https://doi.org/10.1016/S0378-3774\(02\)00075-6](https://doi.org/10.1016/S0378-3774(02)00075-6)

- Pérez-Miranda, S., Cabirol, N., George-Téllez, R., Zamudio-Rivera, L. S., & Fernández, F. J. (2007). O-CAS, a fast and universal method for siderophore detection. *Journal of Microbiological Methods*, 70, 127-131. <https://doi.org/10.1016/j.mimet.2007.03.023>
- Petrie, B., Smith, B. D., Youdan, J., Barden, R., & Kasprzyk-Hordern, B. (2017). Multi-residue determination of micropollutants in *Phragmites australis* from constructed wetlands using microwave assisted extraction and ultra-high-performance liquid chromatography tandem mass spectrometry. *Analytica Chimica Acta*, 959, 91-101. <https://doi.org/10.1016/j.aca.2016.12.042>
- Pierattini, E. C., Francini, A., Huber, C., Sebastiani, L., & Schröder, P. (2018). Poplar and diclofenac pollution: a focus on physiology, oxidative stress and uptake in plant organs. *Science of the Total Environment*, 636, 944-952. <https://doi.org/10.1016/j.scitotenv.2018.04.355>
- Prajitha, V., & Thoppil, J. E. (2017). Cytotoxic and apoptotic activities of extract of *Amaranthus spinosus* L. in *Allium cepa* and human erythrocytes. *Cytotechnology*, 69, 123-133. <https://doi.org/10.1007/s10616-016-0044-5>
- Prior, J. E., Shokati, T., Christians, U., & Gill, R. T. (2010). Identification and characterization of a bacterial cytochrome P450 for the metabolism of diclofenac. *Applied Microbiology and Biotechnology*, 85, 625-633. <https://doi.org/10.1007/s00253-009-2135-0>
- Quast, C., Pruesse, E., Yilmaz, P., Gerken, J., Schweer, T., Yarza, P., Peplies, J., & Glöckner, F. O. (2012). The SILVA ribosomal RNA gene database project: improved data processing and web-based tools. *Nucleic Acids Research*, 41, D590-D596. <https://doi.org/10.1093/nar/gks1219>
- R Core Team, 2022. R: A language and environment for statistical computing. R Foundation for Statistical Computing, Vienna, Austria. URL <https://www.R-project.org/>
- Ramírez-Morales, D., Masís-Mora, M., Montiel-Mora, J. R., Cambroner-Heinrichs, J. C., Briceño-Guevara, S., Rojas-Sánchez, C. E., Méndez-Rivera, M., Arias-Mora, V., Tormo-Budowski, R., Brenes-Alfaro, L., & Rodríguez-Rodríguez, C. E. (2020). Occurrence of pharmaceuticals, hazard assessment and ecotoxicological evaluation of wastewater treatment plants in Costa Rica. *Science of the Total Environment*, 746, 141200. <https://doi.org/10.1016/j.scitotenv.2020.141200>
- Raths, R., Peta, V., & Bücking, H. (2021). *Duganella callida* sp. nov., a novel addition to the *Duganella* genus, isolated from the soil of a cultivated maize field. *International Journal of Systematic and Evolutionary Microbiology*, 71, 004599.

<https://doi.org/10.1099/ijsem.0.004599>

- Ravichandran, M. K., & Philip, L. (2021). Insight into the uptake, fate and toxic effects of pharmaceutical compounds in two wetland plant species through hydroponics studies. *Chemical Engineering Journal*, 426, 131078. <https://doi.org/10.1016/j.cej.2021.131078>
- Rehman, K., Imran, A., Amin, I., & Afzal, M. (2018). Inoculation with bacteria in floating treatment wetlands positively modulates the phytoremediation of oil field wastewater. *Journal of Hazardous Materials*, 349, 242-251. <https://doi.org/10.1016/j.jhazmat.2018.02.013>
- Reinhold-Hurek, B., & Hurek, T. (2011). Living inside plants: bacterial endophytes. *Current Opinion in Plant Biology*, 14, 435-443. <https://doi.org/10.1016/j.pbi.2011.04.004>
- Reinhold-Hurek, B., Bünger, W., Burbano, C. S., Sabale, M., & Hurek, T. (2015). Roots shaping their microbiome: global hotspots for microbial activity. *Annual Review of Phytopathology*, 53, 403-424. <https://doi.org/10.1146/annurev-phyto-082712-102342>
- Rojas-Solis, D., Vences-Guzmán, M. A., Sohlenkamp, C., & Santoyo, G. (2020). *Bacillus toyonensis* COPE52 modifies lipid and fatty acid composition, exhibits antifungal activity, and stimulates growth of tomato plants under saline conditions. *Current Microbiology*, 77, 2735-2744. <https://doi.org/10.1007/s00284-020-02069-1>
- Rout, P. R., Zhang, T. C., Bhunia, P., & Surampalli, R. Y. (2021). Treatment technologies for emerging contaminants in wastewater treatment plants: A review. *Science of the Total Environment*, 753, 141990. <https://doi.org/10.1016/j.scitotenv.2020.141990>
- Rúa-Gómez, P. C., & Püttmann, W. (2012). Impact of wastewater treatment plant discharge of lidocaine, tramadol, venlafaxine and their metabolites on the quality of surface waters and groundwater. *Journal of Environmental Monitoring*, 14, 1391-1399. <https://doi.org/10.1039/C2EM10950F>
- Rúa-Gómez, P. C., & Püttmann, W. (2013). Degradation of lidocaine, tramadol, venlafaxine and the metabolites O-desmethyltramadol and O-desmethylvenlafaxine in surface waters. *Chemosphere*, 90, 1952-1959. <https://doi.org/10.1016/j.chemosphere.2012.10.039>
- Ruf, M., & Brunner, I. (2003). Vitality of tree fine roots: reevaluation of the tetrazolium test. *Tree Physiology*, 23, 257-263. <https://doi.org/10.1093/treephys/23.4.257>
- Rühmland, S., Wick, A., Ternes, T. A., & Barjenbruch, M. (2015). Fate of pharmaceuticals in a subsurface flow constructed wetland and two ponds. *Ecological Engineering*, 80, 125-139. <https://doi.org/10.1016/j.ecoleng.2015.01.036>
- Rutere, C., Knoop, K., Posselt, M., Ho, A., & Horn, M. A. (2020). Ibuprofen degradation and

- associated bacterial communities in hyporheic zone sediments. *Microorganisms*, 8, 1245. <https://doi.org/10.3390/microorganisms8081245>
- Rydzynski, D., Piotrowicz-Cieślak, A. I., Grajek, H., & Michalczyk, D. J. (2017). Instability of chlorophyll in yellow lupin seedlings grown in soil contaminated with ciprofloxacin and tetracycline. *Chemosphere*, 184, 62-73. <https://doi.org/10.1016/j.chemosphere.2017.05.147>
- Sandermann Jr, H. (1992). Plant metabolism of xenobiotics. *Trends in Biochemical Sciences*, 17, 82-84. [https://doi.org/10.1016/0968-0004\(92\)90507-6](https://doi.org/10.1016/0968-0004(92)90507-6)
- Sandermann Jr, H. (1994). Higher plant metabolism of xenobiotics: the 'green liver' concept. *Pharmacogenetics*, 4, 225-241. <https://doi.org/10.1097/00008571-199410000-00001>
- Santoyo, G., Moreno-Hagelsieb, G., del Carmen Orozco-Mosqueda, M., & Glick, B. R. (2016). Plant growth-promoting bacterial endophytes. *Microbiological Research*, 183, 92-99. <https://doi.org/10.1016/j.micres.2015.11.008>
- Sappl, P. G., Carroll, A. J., Clifton, R., Lister, R., Whelan, J., Harvey Millar, A., & Singh, K. B. (2009). The *Arabidopsis* glutathione transferase gene family displays complex stress regulation and co-silencing multiple genes results in altered metabolic sensitivity to oxidative stress. *The Plant Journal*, 58, 53-68. <https://doi.org/10.1111/j.1365-313X.2008.03761.x>
- Sasaki, M., Akahira, A., Oshiman, K. I., Tsuchido, T., & Matsumura, Y. (2005a). Purification of cytochrome P450 and ferredoxin, involved in bisphenol A degradation, from *Sphingomonas* sp. strain AO1. *Applied and Environmental Microbiology*, 71, 8024-8030. <https://doi.org/10.1128/AEM.71.12.8024-8030.2005>
- Sasaki, M., Maki, J. I., Oshiman, K. I., Matsumura, Y., & Tsuchido, T. (2005b). Biodegradation of bisphenol A by cells and cell lysate from *Sphingomonas* sp. strain AO1. *Biodegradation*, 16, 449-459. <https://doi.org/10.1007/s10532-004-5023-4>
- Sasse, J., Martinoia, E., & Northen, T. (2018). Feed your friends: do plant exudates shape the root microbiome?. *Trends in Plant Science*, 23, 25-41. <https://doi.org/10.1016/j.tplants.2017.09.003>
- Sauvêtre, A., & Schröder, P. (2015). Uptake of carbamazepine by rhizomes and endophytic bacteria of *Phragmites australis*. *Frontiers in Plant Science*, 6, 83. <https://doi.org/10.3389/fpls.2015.00083>
- Sauvêtre, A., May, R., Harpaintner, R., Poschenrieder, C., & Schröder, P. (2018). Metabolism of carbamazepine in plant roots and endophytic rhizobacteria isolated from *Phragmites australis*. *Journal of Hazardous Materials*, 342, 85-95.

<https://doi.org/10.1016/j.jhazmat.2017.08.006>

- Sauvêtre, A., Węgrzyn, A., Yang, L., Vestergaard, G., Miksch, K., Schröder, P., & Radl, V. (2020). Enrichment of endophytic Actinobacteria in roots and rhizomes of *Miscanthus× giganteus* plants exposed to diclofenac and sulfamethoxazole. *Environmental Science and Pollution Research*, 27, 11892-11904. <https://doi.org/10.1007/s11356-020-07609-7>
- Saxena, B., Modi, M., & Modi, V. V. (1986). Isolation and characterization of siderophores from *Azospirillum lipoferum* D-2. *Microbiology*, 132, 2219-2224. <https://doi.org/10.1099/00221287-132-8-2219>
- Schröder, P. (1997). Fate of glutathione S-conjugates in plants: Cleavage of the glutathione moiety. In: Hatzios KK (ed), Regulation of enzymatic systems detoxifying xenobiotics in plants. NATO ASI Series Vol. 37, Kluwer Academic Publishers, The Netherlands, pp 233–244.
- Schröder, P. (2001). The role of glutathione and glutathione S-transferases in plant reaction and adaptation to xenobiotics. In: Grill, D., Tausz, M. and DeKok, L.J. (Ed.) Significance of glutathione in plant adaptation to the environment. Handbook Series of Plant Ecophysiology. Kluwer Acad. Publ., Boston, Dordrecht, London, pp. 157-182. [https://doi.org/10.1007/0-306-47644-4\\_7](https://doi.org/10.1007/0-306-47644-4_7)
- Schröder, P., Daubner, D., Maier, H., Neustifter, J., & Debus, R. (2008). Phytoremediation of organic xenobiotics-Glutathione dependent detoxification in *Phragmites* plants from European treatment sites. *Bioresource Technology*, 99, 7183-7191. <https://doi.org/10.1016/j.biortech.2007.12.081>
- Schröder, P., Helmreich, B., Škrbić, B., Carballa, M., Papa, M., Pastore, C., Emre, Z., Oehmen, A., Langenhoff, A., Molinos, M., Dvarioniene, J., Huber, C., Tsagarakis, K. P., Martinez-Lopez, E., Meric Pagano, S., Vogelsang, C., & Mascolo, G. (2016). Status of hormones and painkillers in wastewater effluents across several European states-considerations for the EU watch list concerning estradiols and diclofenac. *Environmental Science and Pollution Research*, 23, 12835-12866. <https://doi.org/10.1007/s11356-016-6503-x>
- Schröder, P., Maier, H., & Debus, R. (2005). Detoxification of herbicides in *Phragmites australis*. *Zeitschrift für Naturforschung C*, 60, 317-324. <https://doi.org/10.1515/znc-2005-3-417>
- Schröder, P., Scheer, C. E., Diekmann, F., & Stampfl, A. (2007). How plants cope with

- foreign compounds. Translocation of xenobiotic glutathione conjugates in roots of barley (*Hordeum vulgare*). *Environmental Science and Pollution Research-International*, 14, 114-122. <https://doi.org/10.1065/espr2006.10.352>
- Sehonova, P., Plhalova, L., Blahova, J., Berankova, P., Doubkova, V., Prokes, M., Tichy, F., Vecerek, V. & Svobodova, Z. (2016). The effect of tramadol hydrochloride on early life stages of fish. *Environmental Toxicology and Pharmacology*, 44, 151-157. <https://doi.org/10.1016/j.etap.2016.05.006>
- Shah, K., Kumar, R. G., Verma, S., & Dubey, R. S. (2001). Effect of cadmium on lipid peroxidation, superoxide anion generation and activities of antioxidant enzymes in growing rice seedlings. *Plant Science*, 161, 1135-1144. [https://doi.org/10.1016/S0168-9452\(01\)00517-9](https://doi.org/10.1016/S0168-9452(01)00517-9)
- Shah, S. W. A., Rehman, M. U., Hayat, A., Tahseen, R., Bajwa, S., Islam, E., Naqvi, S. N. H., Shabir, G., Iqbal, S., Afzal, M. & Niazi, N. K. (2022). Enhanced degradation of ciprofloxacin in floating treatment wetlands augmented with bacterial cells immobilized on iron oxide nanoparticles. *Sustainability*, 14, 14997. <https://doi.org/10.3390/su142214997>
- Sharma, P., & Dubey, R. S. (2005). Drought induces oxidative stress and enhances the activities of antioxidant enzymes in growing rice seedlings. *Plant Growth Regulation*, 46, 209-221. <https://doi.org/10.1007/s10725-005-0002-2>
- Sharma, P., Jha, A. B., Dubey, R. S., & Pessarakli, M. (2012). Reactive oxygen species, oxidative damage, and antioxidative defense mechanism in plants under stressful conditions. *Journal of Botany*, 2012. <https://doi.org/10.1155/2012/217037>
- Shehzadi, M., Afzal, M., Khan, M. U., Islam, E., Mobin, A., Anwar, S., & Khan, Q. M. (2014). Enhanced degradation of textile effluent in constructed wetland system using *Typha domingensis* and textile effluent-degrading endophytic bacteria. *Water Research*, 58, 152-159. <https://doi.org/10.1016/j.watres.2014.03.064>
- Shen, Y., Stedtfeld, R. D., Guo, X., Bhalsod, G. D., Jeon, S., Tiedje, J. M., Li, H., & Zhang, W. (2019). Pharmaceutical exposure changed antibiotic resistance genes and bacterial communities in soil-surface-and overhead-irrigated greenhouse lettuce. *Environment International*, 131, 105031. <https://doi.org/10.1016/j.envint.2019.105031>
- Siminszky, B., Gavilano, L., Bowen, S. W., & Dewey, R. E. (2005). Conversion of nicotine to nornicotine in *Nicotiana tabacum* is mediated by CYP82E4, a cytochrome P450 monooxygenase. *Proceedings of the National Academy of Sciences*, 102, 14919-14924. <https://doi.org/10.1073/pnas.0506581102>



- Singh, B., & Singh, K. (2016). *Bacillus*: As bioremediator agent of major environmental pollutants. In: Islam, M., Rahman, M., Pandey, P., Jha, C., Aeron, A. (eds) *Bacilli and Agrobiotechnology*. Springer, Cham. [https://doi.org/10.1007/978-3-319-44409-3\\_2](https://doi.org/10.1007/978-3-319-44409-3_2)
- Sipahutar, M. K., Piapukiew, J., & Vangnai, A. S. (2018). Efficiency of the formulated plant-growth promoting *Pseudomonas fluorescens* MC46 inoculant on triclocarban treatment in soil and its effect on *Vigna radiata* growth and soil enzyme activities. *Journal of Hazardous Materials*, 344, 883-892. <https://doi.org/10.1016/j.jhazmat.2017.11.046>
- Sousa, B., Lopes, J., Leal, A., Martins, M., Soares, C., Azenha, M., Fidalgo, F., & Teixeira, J. (2021). Specific glutathione-S-transferases ensure an efficient detoxification of diclofenac in *Solanum lycopersicum* L. plants. *Plant Physiology and Biochemistry*, 168, 263-271. <https://doi.org/10.1016/j.plaphy.2021.10.019>
- Styszko, K., Proctor, K., Castrignanò, E., & Kasprzyk-Hordern, B. (2021). Occurrence of pharmaceutical residues, personal care products, lifestyle chemicals, illicit drugs and metabolites in wastewater and receiving surface waters of Krakow agglomeration in South Poland. *Science of the Total Environment*, 768, 144360. <https://doi.org/10.1016/j.scitotenv.2020.144360>
- Subrahmanyam, V., Renwick, A. B., Walters, D. G., Young, P. J., Price, R. J., Tonelli, A. P., & Lake, B. G. (2001). Identification of cytochrome P-450 isoforms responsible for cis-tramadol metabolism in human liver microsomes. *Drug Metabolism and Disposition*, 29, 1146-1155.
- Sun, C., Dudley, S., McGinnis, M., Trumble, J., & Gan, J. (2019). Acetaminophen detoxification in cucumber plants via induction of glutathione S-transferases. *Science of the Total Environment*, 649, 431-439. <https://doi.org/10.1016/j.scitotenv.2018.08.346>
- Sun, C., Dudley, S., Trumble, J., & Gan, J. (2018). Pharmaceutical and personal care products-induced stress symptoms and detoxification mechanisms in cucumber plants. *Environmental Pollution*, 234, 39-47. <https://doi.org/10.1016/j.envpol.2017.11.041>
- Suno, M., Ichihara, H., Ishino, T., Yamamoto, K., & Yoshizaki, Y. (2015). Photostability studies on (±)-tramadol in a liquid formulation. *Journal of Pharmaceutical Health Care and Sciences*, 1, 1-6. <https://doi.org/10.1186/s40780-014-0003-2>
- Suyamud, B., Thiravetyan, P., Panyapinyopol, B., & Inthorn, D. (2018). *Dracaena sanderiana* endophytic bacteria interactions: effect of endophyte inoculation on bisphenol A removal. *Ecotoxicology and Environmental Safety*, 157, 318-326. <https://doi.org/10.1016/j.ecoenv.2018.03.066>
- Syranidou, E., Thijs, S., Avramidou, M., Weyens, N., Venieri, D., Pintelon, I., Vangronsveld,

- J., & Kalogerakis, N. (2018). Responses of the endophytic bacterial communities of *Juncus acutus* to pollution with metals, emerging organic pollutants and to bioaugmentation with indigenous strains. *Frontiers in Plant Science*, 9, 1526. <https://doi.org/10.3389/fpls.2018.01526>
- Szkutnik-Fiedler, D., Grabowski, T., Balcerkiewicz, M., Michalak, M., Pilipczuk, I., Wyrowski, L., Urjasz, H., & Grześkowiak, E. (2017). The influence of a single and chronic administration of venlafaxine on tramadol pharmacokinetics in a rabbit model. *Pharmacological Reports*, 69, 555-559. <https://doi.org/10.1016/j.pharep.2017.01.027>
- Taylor, H. F., & Wain, R. L. (1962). Side-chain degradation of certain  $\omega$ -phenoxyalkanecarboxylic acids by *Nocardia coeliaca* and other micro-organisms isolated from soil. *Proceedings of the Royal Society of London. Series B. Biological Sciences*, 156, 172-186. <https://doi.org/10.1098/rspb.1962.0038>
- Tikhonova, E. N., Grouzdev, D. S., & Kravchenko, I. K. (2019). *Azospirillum palustre* sp. nov., a methylotrophic nitrogen-fixing species isolated from raised bog. *International Journal of Systematic and Evolutionary Microbiology*, 69, 2787-2793. <https://doi.org/10.1099/ijsem.0.003560>
- Trivedi, P., Leach, J. E., Tringe, S. G., Sa, T., & Singh, B. K. (2020). Plant-microbiome interactions: from community assembly to plant health. *Nature Reviews Microbiology*, 18, 607-621. <https://doi.org/10.1038/s41579-020-0412-1>
- Ungureanu, N., Vlăduț, V., & Voicu, G. (2020). Water scarcity and wastewater reuse in crop irrigation. *Sustainability*, 12, 9055. <https://doi.org/10.3390/su12219055>
- Usyskin-Tonne, A., Hadar, Y., & Minz, D. (2021). Spike formation is a turning point determining wheat root microbiome abundance, structures and functions. *International Journal of Molecular Sciences*, 22, 11948. <https://doi.org/10.3390/ijms222111948>
- Van Aken, B., Tehrani, R., & Schnoor, J. L. (2011). Endophyte-assisted phytoremediation of explosives in poplar trees by *Methylobacterium populi* BJ001 T. *Endophytes of Forest Trees: Biology and Applications*, 217-234. [https://doi.org/10.1007/978-94-007-1599-8\\_14](https://doi.org/10.1007/978-94-007-1599-8_14)
- Verlicchi, P., & Zambello, E. (2014). How efficient are constructed wetlands in removing pharmaceuticals from untreated and treated urban wastewaters? A review. *Science of the Total Environment*, 470, 1281-1306. <https://doi.org/10.1016/j.scitotenv.2013.10.085>
- Verma, S., & Dubey, R. S. (2003). Lead toxicity induces lipid peroxidation and alters the activities of antioxidant enzymes in growing rice plants. *Plant Science*, 164, 645-655. [https://doi.org/10.1016/S0168-9452\(03\)00022-0](https://doi.org/10.1016/S0168-9452(03)00022-0)



- Vymazal, J., Březinová, T. D., Koželuh, M., & Kule, L. (2017). Occurrence and removal of pharmaceuticals in four full-scale constructed wetlands in the Czech Republic—the first year of monitoring. *Ecological Engineering*, 98, 354-364. <https://doi.org/10.1016/j.ecoleng.2016.08.010>
- Wada, Y., Gleeson, T., & Esnault, L. (2014). Wedge approach to water stress. *Nature Geoscience*, 7, 615-617. <https://doi.org/10.1038/ngeo2241>
- Wang, Z., Xu, Z., & Li, X. (2018). Biodegradation of methamphetamine and ketamine in aquatic ecosystem and associated shift in bacterial community. *Journal of Hazardous Materials*, 359, 356-364. <https://doi.org/10.1016/j.jhazmat.2018.07.039>
- Ward, P. J., Strzepek, K. M., Pauw, W. P., Brander, L. M., Hughes, G. A., & Aerts, J. C. (2010). Partial costs of global climate change adaptation for the supply of raw industrial and municipal water: a methodology and application. *Environmental Research Letters*, 5, 044011. <https://doi.org/10.1088/1748-9326/5/4/044011>
- Water JPI Knowledge Hub on CECs Policy Brief “Contaminants of Emerging Concern - an emerging risk in our waters” - June 2019.
- Weyens, N., van der Lelie, D., Taghavi, S., & Vangronsveld, J. (2009). Phytoremediation: plant–endophyte partnerships take the challenge. *Current Opinion in Biotechnology*, 20, 248-254. <https://doi.org/10.1016/j.copbio.2009.02.012>
- WHO (2018). WHO Expert Committee on Drug Dependence, thirty-ninth report. Geneva: World Health Organization; 2018 (WHO Technical Report Series, No. 1009). Licence: CC BY-NC-SA 3.0 IGO.
- Wick, A., Fink, G., Joss, A., Siegrist, H., & Ternes, T. A. (2009). Fate of beta blockers and psycho-active drugs in conventional wastewater treatment. *Water Research*, 43, 1060-1074. <https://doi.org/10.1016/j.watres.2008.11.031>
- Willekens, H., Inzé, D., Van Montagu, M., & Van Camp, W. (1995). Catalases in plants. *Molecular Breeding*, 1, 207-228. <https://doi.org/10.1007/BF02277422>
- Willis, A. D., & Martin, B. D. (2022). Estimating diversity in networked ecological communities. *Biostatistics*, 23, 207-222. <https://doi.org/10.1093/biostatistics/kxaa015>
- Wu, W. N., McKown, L. A., & Liao, S. (2002). Metabolism of the analgesic drug ULTRAM®(tramadol hydrochloride) in humans: API-MS and MS/MS characterization of metabolites. *Xenobiotica*, 32, 411-425. <https://doi.org/10.1080/00498250110113230>
- WWAP (United Nations World Water Assessment Programme) (2017). The United Nations World Water Development Report 2017. Wastewater: The Untapped Resource. Paris, UNESCO.

- Xiong, C., Singh, B. K., He, J. Z., Han, Y. L., Li, P. P., Wan, L. H., Meng, G. Z., Liu, S. Y., Wang, J. T., Wu, C. F., Ge, A. H., & Zhang, L. M. (2021). Plant developmental stage drives the differentiation in ecological role of the maize microbiome. *Microbiome*, 9, 1-15. <https://doi.org/10.1186/s40168-021-01118-6>
- Yadav, A. N., Kumar, V., Dhaliwal, H. S., Prasad, R., & Saxena, A. K. (2018). Microbiome in crops: diversity, distribution, and potential role in crop improvement. In *Crop improvement through microbial biotechnology* (pp. 305-332). Elsevier. <https://doi.org/10.1016/B978-0-444-63987-5.00015-3>
- Yan, Q., Feng, G., Gao, X., Sun, C., Guo, J. S., & Zhu, Z. (2016). Removal of pharmaceutically active compounds (PhACs) and toxicological response of *Cyperus alternifolius* exposed to PhACs in microcosm constructed wetlands. *Journal of Hazardous Materials*, 301, 566-575. <https://doi.org/10.1016/j.jhazmat.2015.08.057>
- Yang, L., Danzberger, J., Schöler, A., Schröder, P., Schloter, M., & Radl, V. (2017b). Dominant groups of potentially active bacteria shared by barley seeds become less abundant in root associated microbiome. *Frontiers in Plant Science*, 8, 1005. <https://doi.org/10.3389/fpls.2017.01005>
- Yang, R., Liu, G., Chen, T., Li, S., An, L., Zhang, G., Li, G., Chang, S., Zhang, W., Chen, X., Wu, X., & Zhang, B. (2019). Characterization of the genome of a *Nocardia* strain isolated from soils in the Qinghai-Tibetan Plateau that specifically degrades crude oil and of this biodegradation. *Genomics*, 111, 356-366. <https://doi.org/10.1016/j.ygeno.2018.02.010>
- Yang, Y., Ok, Y. S., Kim, K. H., Kwon, E. E., & Tsang, Y. F. (2017a). Occurrences and removal of pharmaceuticals and personal care products (PPCPs) in drinking water and water/sewage treatment plants: A review. *Science of the Total Environment*, 596, 303-320. <https://doi.org/10.1016/j.scitotenv.2017.04.102>
- Yi, M., Sheng, Q., Lv, Z., & Lu, H. (2022). Novel pathway and acetate-facilitated complete atenolol degradation by *Hydrogenophaga* sp. YM1 isolated from activated sludge. *Science of the Total Environment*, 810, 152218. <https://doi.org/10.1016/j.scitotenv.2021.152218>
- Zerrouk, I. Z., Rahmoune, B., Auer, S., Rößler, S., Lin, T., Baluska, F., Dobrev, P. I., Motyka, V., & Ludwig-Müller, J. (2020). Growth and aluminum tolerance of maize roots mediated by auxin-and cytokinin-producing *Bacillus toyonensis* requires polar auxin transport. *Environmental and Experimental Botany*, 176, 104064. <https://doi.org/10.1016/j.envexpbot.2020.104064>

- Zhang, D. Q., Hua, T., Gersberg, R. M., Zhu, J., Ng, W. J., & Tan, S. K. (2013). Carbamazepine and naproxen: fate in wetland mesocosms planted with *Scirpus validus*. *Chemosphere*, 91, 14-21. <https://doi.org/10.1016/j.chemosphere.2012.11.018>
- Zhang, D., Gersberg, R. M., Ng, W. J., & Tan, S. K. (2014). Removal of pharmaceuticals and personal care products in aquatic plant-based systems: a review. *Environmental Pollution*, 184, 620-639. <https://doi.org/10.1016/j.envpol.2013.09.009>
- Zhang, J., Kim, Y. J., Hoang, V. A., Nguyen, N. L., Wang, C., Kang, J. P., Wang, D., & Yang, D. C. (2016). *Duganella ginsengisoli* sp. nov., isolated from ginseng soil. *International Journal of Systematic and Evolutionary Microbiology*, 66, 56-61. <https://doi.org/10.1099/ijsem.0.000669>
- Zhang, J., Zheng, J. W., Hang, B. J., Ni, Y. Y., He, J., & Li, S. P. (2011). *Rhodanobacter xiangquanii* sp. nov., a novel anilofos-degrading bacterium isolated from a wastewater treating system. *Current Microbiology*, 62, 645-649. <https://doi.org/10.1007/s00284-010-9757-4>
- Zhang, K., Zhang, Z. H., Wang, H., Wang, X. M., Zhang, X. H., & Xie, Y. F. (2020). Synergistic effects of combining ozonation, ceramic membrane filtration and biologically active carbon filtration for wastewater reclamation. *Journal of Hazardous Materials*, 382, 121091. <https://doi.org/10.1016/j.jhazmat.2019.121091>
- Zhao, C., Xie, H., Xu, J., Xu, X., Zhang, J., Hu, Z., Liu, C., Liang, S., Wang, Q., & Wang, J. (2015). Bacterial community variation and microbial mechanism of triclosan (TCS) removal by constructed wetlands with different types of plants. *Science of the Total Environment*, 505, 633-639. <https://doi.org/10.1016/j.scitotenv.2014.10.053>
- Zhiteneva, V., Drewes, J. E., & Hübner, U. (2020). Removal of trace organic chemicals during long-term biofilter operation. *ACS ES&T Water*, 1, 300-308. <https://doi.org/10.1021/acsestwater.0c00072>
- Zhou, Z., Wu, Y., Xu, Y., Wang, Z., Fu, H., & Zheng, Y. (2022). Carbamazepine degradation and genome sequencing of a novel exoelectrogen isolated from microbial fuel cells. *Science of the Total Environment*, 838, 156161. <https://doi.org/10.1016/j.scitotenv.2022.156161>
- Zimmermann, S. G., Schmukat, A., Schulz, M., Benner, J., Gunten, U. V., & Ternes, T. A. (2012). Kinetic and mechanistic investigations of the oxidation of tramadol by ferrate and ozone. *Environmental Science and Technology*, 46, 876-884. <https://doi.org/10.1021/es203348q>

#### **IV. Acknowledgement**

I extend my heartfelt gratitude to my supervisor, Prof. Peter Schröder, for providing me the opportunity to work under his guidance. His support and the congenial scientific atmosphere during the setup of the experiments for this Thesis have been invaluable.

I would like to express my gratitude to the Catholic Academic Exchange Service (KAAD) for their financial support. I am also thankful to the Helmholtz Munich Institute (HMGU) and the Technical University of Munich (TUM) for affording me the opportunity to pursue my PhD studies in Germany. Deep appreciation goes to Dr. Catarina Cruzeiro, Yvonne Bigott, and Roberto Siani for their unwavering support. The enriching scientific environment of our lab, the time devoted to fruitful discussions, collaborative efforts in the laboratory, and data analysis have been truly indispensable.

Furthermore, I am profoundly thankful to the entire COMI Team at HMGU. A special note of appreciation goes to Akane, Alexandra, Andrés, Antonios, Benoit, Clara, Diana, Fatma, Franz, Gudrun, Juliette, Lisa, Martha, Michi, Miljenka, Sarah, Seun, Stephanie, Viviane and Zhongjie. The multicultural conversations, mutual assistance, and the camaraderie we shared not only made our time in the lab productive but also provided unwavering support in overcoming challenges.

Lastly, this work is dedicated to the memory of my father, who passed away at the onset of the COVID-19 pandemic.

Also, I extend my heartfelt thanks to my wife and daughter, my mother, my brothers, and the members of my wife's family for their prayers, unwavering support, and the positivity they infused into my journey, especially during the more demanding phases.

## **V. Appendix**

### **i. Appendix M1 (Manuscript I)**

This article was published in “Khalaf, D. M., Cruzeiro, C., & Schröder, P. (2022). Removal of tramadol from water using *Typha angustifolia* and *Hordeum vulgare* as biological models: Possible interaction with other pollutants in short-term uptake experiments. Science of the Total Environment, 809, 151164”, Copyright Elsevier (2022).



# Removal of tramadol from water using *Typha angustifolia* and *Hordeum vulgare* as biological models: Possible interaction with other pollutants in short-term uptake experiments



David Mamdouh Khalaf<sup>a,b</sup>, Catarina Cruzeiro<sup>a</sup>, Peter Schröder<sup>a,\*</sup>

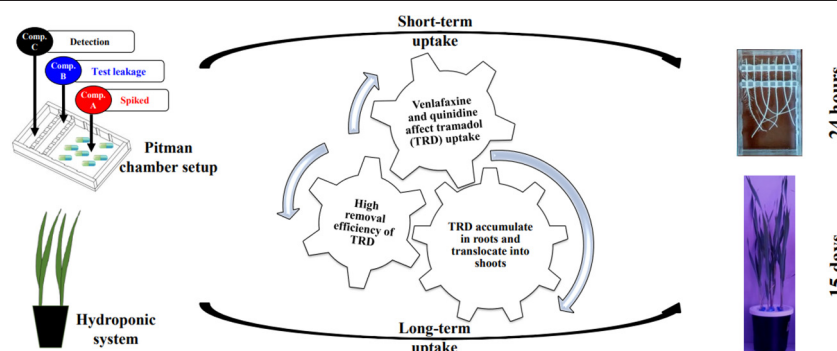
<sup>a</sup> Research Unit Comparative Microbiome Analysis, Helmholtz Zentrum München GmbH, German Research Center for Environmental Health, Ingolstädter Landstr. 1, 85764 Neuherberg, Germany

<sup>b</sup> Botany and Microbiology Department, Faculty of Science, Assiut University, 71516 Assiut, Egypt

## HIGHLIGHTS

- Barley seedlings have the ability to take up TRD.
- Venlafaxine delays the transport rate of tramadol (TRD).
- TRD can be easily translocated to aerial parts.
- TRD uptake is strongly inhibited after co-exposing plant roots with quinidine.
- Organic cation transporters may be involved in the uptake of TRD by plants.

## GRAPHICAL ABSTRACT



## ARTICLE INFO

### Article history:

Received 29 August 2021

Received in revised form 18 October 2021

Accepted 18 October 2021

Available online 22 October 2021

Editor: Damià Barceló

### Keywords:

Pharmaceutical pollution

Barley

Cattail

Bioconcentration factor

Hydroponic system

Translocation factor

## ABSTRACT

Tramadol (TRD) is widely detected in aquatic ecosystems as a result of massive abuse and insufficient removal from wastewater facilities. As a result, TRD can contaminate groundwater sources and/or agricultural soils. While TRD toxicity has been reported from aquatic biota, data about TRD detection in plants are scarce. Moreover, information regarding plant capability for TRD removal is lacking. To understand the fate of this opioid, we have investigated the uptake, translocation and removal capacity of TRD by plants, addressing short-term and long-term uptake. The uptake rates of TRD, in excised barley and cattail roots, were 5.18 and 5.79  $\mu\text{g g}^{-1}$  root fresh weight day<sup>-1</sup>, respectively. However, TRD uptake was strongly inhibited after co-exposing these roots either with the drug venlafaxine (similar molecular structure as TRD) or with quinidine (an inhibitor of cellular organic cation transporters). When barley seedlings were exposed to TRD in a hydroponic experiment a removal efficiency up to 90% (within 15 days) was obtained, with bioconcentration and translocation factors close to 9 and 1, respectively. The combination of results from both plants and the inhibition observed after treatment with quinidine revealed that organic cation transporters may be involved in the uptake of TRD by plants.

© 2021 Elsevier B.V. All rights reserved.

## 1. Introduction

Contaminants of emerging concern, particularly pharmaceutical compounds, are frequently detected in wastewater (Schröder et al., 2016; Yang et al., 2017), ground and surface water (Balakrishna et al., 2017), and even in drinking water (Carmona et al., 2014; Bexfield

\* Corresponding author.

E-mail address: [peter.schroeder@helmholtz-muenchen.de](mailto:peter.schroeder@helmholtz-muenchen.de) (P. Schröder).

et al., 2019). The frequent detection of these compounds, besides their (eco-) toxicological effects, made them one of the 40 most important issues in the US (Fleishman et al., 2011), and the EU Parliament has added several pharmaceuticals to their watch list of water pollutants (EC, 2015). Previous studies conducted on plants explored adverse effects caused by some of these contaminants such as ibuprofen, carbamazepine, diclofenac and paracetamol on plant performance (i.e., total biomass, pigments, oxidative stress disorders) (An et al., 2009; Kummerová et al., 2016; García-Medina et al., 2020; Wijaya et al., 2020; Leitão et al., 2021).

Among these compounds, we highlight the opioid tramadol (TRD), which is not fully studied but widely used to treat moderate to severe pain and frequently prescribed due to its high efficiency and low addiction properties (Bravo et al., 2017). Indeed, in recent years, several studies reported an increase of abusive usage of TRD in some African, Asian and Middle East countries (WHO, 2018b). In 2018, the Egyptian Ministry of Social Solidarity reported that TRD poses the second rank of the abused substances after cannabis, while in Iran, several cases of TRD abuse, seizures and numerous TRD-related deaths were reported in last years (Rostam-Abadi et al., 2020). Due to this abusive usage, TRD has been detected in various water resources with highest values in surface water ( $8 \mu\text{g L}^{-1}$ ), wastewater treatment plant (WWTP) influent ( $87 \mu\text{g L}^{-1}$ ) and WWTP effluent ( $55 \mu\text{g L}^{-1}$ ) because of inefficient wastewater treatment and/or misuse (Kasprzyk-Hordern et al., 2008, 2009). Tramadol has many characteristics in common with the antidepressant venlafaxine (Fig. 1). Both drugs are structurally similar, share both serotonergic and noradrenergic properties, and undergo similar metabolic fate.

Venlafaxine reduces re-uptake of serotonin and noradrenaline into presynaptic vesicles of certain synapses in the brain. Resulting is an increased supply of these neurotransmitters in the synaptic gap, which alleviates depressive symptoms. Tramadol acts as agonist of opioid receptors in the nervous tissue. Its affinity is low and not particularly specific for individual opioid receptors. Attenuation of pain perception seems to be mediated by inhibiting the re-uptake of norepinephrine into neurons.

In humans, approximately 30% of TRD dosage is excreted in the urine without any change, while 60% is converted to metabolites (WHO, 2018a), via two pathways: N- and O-demethylation reactions (phase-I) and conjugation processes (phase-II), where O-desmethyltramadol (ODTRD) is the main pharmacologically active metabolite (WHO, 2018a). Previous studies detected the presence of TRD metabolites, especially those produced from phase-I, in surface water and WWTP (de Jongh et al., 2012; Archer et al., 2017; Styszko et al., 2021). Moreover, the metabolite ODTRD was quantified in higher amounts (1-fold) than TRD in the upstream ( $98 \text{ ng L}^{-1}$ ) and downstream ( $300 \text{ ng L}^{-1}$ ) of WWTP located in the Gauteng Province of South Africa (Archer et al., 2017).

Since traditional wastewater treatment is insufficient to remove compounds like TRD, constructed wetlands (CWs) can become a valid option for effluent polishing since they combine a diverse set of chemical, physical and biological processes such as sorption and sedimentation, volatilization, microbial degradation as well as plant uptake and

accumulation (Zhang et al., 2014). Among these processes, phytoremediation is considered as a promising tool for the removal of contaminants from wastewater, especially those which are recalcitrant to biodegradation (e.g., clofibrac acid) or possess high polarity/solubility (e.g., caffeine). CWs are considered as a robust and cost-effective technology which can be used to treat wastewater even in developing countries (Zhang et al., 2014). In the last decade, several studies were conducted to elucidate the role of plants in uptake and removal of pharmaceutical compounds (Sauvêtre and Schröder, 2015; Chen et al., 2017; Cui et al., 2017; He et al., 2017; Bigott et al., 2021). In this context, the use of model plants or cell cultures was highlighted, since they facilitate the separate investigation of processes like uptake, translocation and metabolism during phytoremediation. Seedlings, hairy root cultures, and excised roots have been used successfully (Schröder et al., 2007; Macherius et al., 2014).

Information regarding TRD uptake by plants, either alone or in combination with other pollutants is scarce. Only few studies tried to explore the ability of different plant species such as spinach and lettuce to accumulate TRD in roots and/or to translocate TRD into aerial parts of the plant (Kodešová et al., 2019; Mercl et al., 2020). To the best of our knowledge, there is no information available about plant removal efficiency of TRD from water bodies.

Since TRD and compounds with similar chemical structure (i.e., venlafaxine) and its main metabolite are cationic compounds, it is assumed that root uptake is apoplastic while translocation into the shoot follows symplastic pathways, in which integral transport proteins play a main role (Chuang et al., 2019). Theoretical approaches can be used to predict the potential uptake and translocation of xenobiotic molecules in plants. For example, Kumar and Gupta (2016) developed a theory that predicts the uptake of trace organic compounds in plants, called "Rule of 3" based on physicochemical properties of the compounds. According to this rule, trace organic compounds having MW  $< 300$ ,  $\log K_{ow} < 3$ , H-bond acceptors are  $< 6$  and H-bond donors  $< 3$ , possess higher absorption and permeability in plants. According to that, we hypothesized (H1) that TRD and VEN can be easily taken up by plants, with a high tendency to be translocated to the aerial part as both compounds possess chemical and molecular structures within the range mentioned above.

It is worthwhile to mention that some studies already showed the importance of organic cation transporters (OCTs) in the uptake, distribution and excretion of organic cations, especially of cationic drugs (Koepsell et al., 2007). In plants, six members of this group (OCT1-OCT6) are known, with different localization in the plant tissue (Lelandais-Brière et al., 2007; Küfner and Koch, 2008). Cui et al. (2015) demonstrated the involvement of OCTs in the uptake of the cationic pharmaceutical metformin into plant roots, through the selective usage of the inhibitor, quinidine. Therefore, we hypothesized (H2) that OCT may also be involved in uptake and translocation of TRD inside plant tissues, influencing the removal efficiency from the external medium.

Hence, the aims of the present investigation were to (1) explore the short-term uptake of TRD (either alone or in mixture with venlafaxine) and its active metabolite (ODTRD) into roots of different plant species

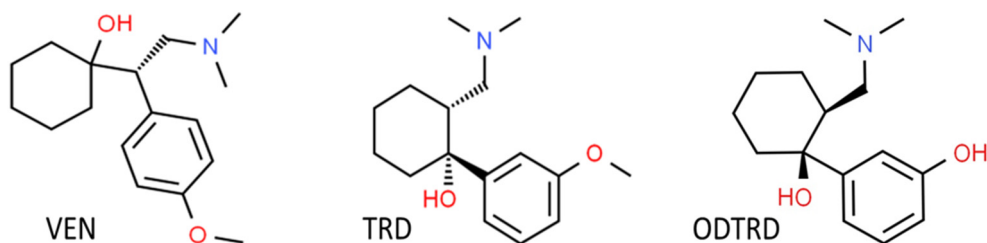


Fig. 1. Structural similarities between the antidepressant venlafaxine, VEN, (left) and the pain-killer tramadol, TRD, (middle), and the primary TRD metabolite, O-desmethyltramadol, ODTRD, (right).



(cattail, barley), (2) assess the removal efficiency of TRD by plant seedlings (barley), as a long-term exposure situation and (3) elucidate the process of uptake and translocation of TRD in plant tissue in the presence or absence of inhibitors for OCTs, such as quinidine (barley seedlings).

## 2. Materials and methods

### 2.1. Chemicals

Tramadol HCl (TRD, 99%), cis-Tramadol- $^{13}\text{C}$ , D<sub>3</sub> HCl solution (TRD-D<sub>3</sub>, 100  $\mu\text{g mL}^{-1}$  in methanol) and venlafaxine HCl (VEN, 99%) were purchased from Sigma–Aldrich (Germany), *O*-desmethyltramadol HCl (ODTRD, 98%) from Focus Biomolecules (BIOZOL Diagnostica Vertrieb GmbH, Germany), quinidine (Q, 98%) from Alfa Aesar (Karlsruhe, Germany), acetonitrile and formic acid, both HPLC-grade, were obtained from Roth (Carl Roth, Karlsruhe, Germany) and Merck (Darmstadt, Germany), respectively. All other chemicals used were analytical grade. The structures and physicochemical characteristics of compounds are provided in Fig. 1 and Table S1.

### 2.2. Plant propagation and growth conditions

Cattail plants (*Typha angustifolia* L.) were ordered from Gärtnerei Hollern (Unterschleißheim, Germany), while barley seeds (*Hordeum vulgare* L., cv. 'Salome') were provided by Nordsaat Saatzeit GmbH (Langenstein, Germany). A hydroponic cultivation system (3L glass container) was used to grow both, cattail and barley plants either from plant cuttings or from seeds, respectively. Cattail plants were washed several times with tap water to eliminate soil particles. Then, the connected rhizomes were separated into individuals and washed with distilled (dist.) water before transferring them to the hydroponic system. Barley seeds were surface sterilized using ethanol (70%; 1 min), NaOCl (5%; 3 min) and washed 5 times with sterilized dist. water, then sown in black plastic pots containing autoclaved perlite for germination before finally transferring them to the hydroponic system. Both, cattail and barley plants were maintained in full-strength modified Hoagland's solution (pH 5.8) after a period of acclimatization (10 days) from a lower concentration (Taiz and Zeiger, 2010). Plants were kept in a growth chamber at 50% humidity under long-day conditions with daily cycles of 16 h of light at 20 °C and 8 h of dark at 15 °C. LED lamps (model LX601G; Heliospectra, Sweden) were used as light source. During experimentation, the nutrient solution was changed twice a week by transferring the plants into new glass containers with

fresh medium. The plants were kept in these growth conditions for one month prior to their use in the experiments. Three independent replicates (with five plants, each) were randomly placed under the same light, temperature and humidity conditions as mentioned above.

### 2.3. Short-term uptake experiment using Pitman chamber setup

In order to follow the uptake of TRD in plant roots and the subsequent acropetal transport, three incubating chambers for both plant species were used; the design of these chambers followed previous studies (Pitman, 1971; Schröder et al., 2007; Cui et al., 2015). Each chamber was divided into three compartments (A, B and C) using vertical baffles, as shown in Fig. 2A, and separately filled with water. Per chamber, seven roots were cut (ca. 10 cm length), washed with tap water, then with dist. water and carefully fixed horizontally in the apparatus using KWS-grease from Roth (Carl Roth, Karlsruhe, Germany). The same grease was also used to tightly seal all spaces to prevent leaking of solutions from one compartment to another. Prior to their use, roots were thoroughly checked for intact root tips. For each plant species, two experimental sets (each in triplicate) were established; the first one to explore the uptake and transport of TRD, while the second one was used to assess the correlation between the inhibition of OCTs and the transport of TRD (Fig. 2B). Based on the maximum concentration of TRD detected in water bodies, 100  $\mu\text{g L}^{-1}$  were set as target initial concentration (Kasprzyk-Hordern et al., 2009). In both experiments, compartment A was spiked with TRD to a final concentration (concentration) of 100  $\mu\text{g L}^{-1}$ , while in the second one the same chamber was extra supplemented with quinidine (as OCTs inhibitor) at a concentration of 0.5 mM.

In order to assess the interaction between TRD and the chemical homologous compound VEN, another set of six Pitman chambers was prepared (in triplicate for each plant species) where compartment A was supplemented with VEN + TRD at concentration 100  $\mu\text{g L}^{-1}$  for each one (Fig. 2B). To explore the uptake of the metabolite ODTRD, a third set was prepared, however here, compartment A was only spiked with ODTRD at final concentration 100  $\mu\text{g L}^{-1}$  (Fig. 2B).

From every Pitman chamber, water samples were collected out of each of the three compartments at time zero, whereas aliquots from compartment C were taken at different time intervals (after 2, 4, 6, 16, 18, 20, 22 and 24 h). At the end of the experiment, a final water sample from compartment A was taken to inspect the possible presence of TRD by leakage. Results from leaky chambers were discarded. At the end of the transport studies the fresh weight of the roots from each chamber was recorded. All samples were stored at  $-20\text{ °C}$  until further analysis.

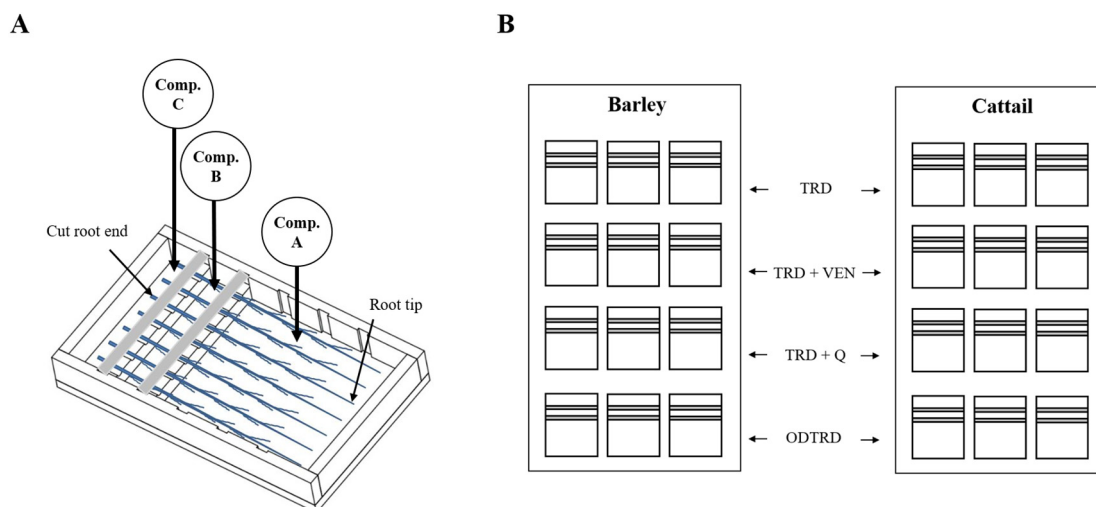


Fig. 2. Pitman chamber setup (A) and the experimental design (B).



#### 2.4. Evaluation of root metabolic activity

To assess the vitality of roots throughout the experiment, cattail and barley roots were used for that, by applying the protocol discussed in [Prajitha and Thoppil \(2017\)](#) but with some modifications; three root tips of 2 cm length were collected at several time points of exposure (0, 2, 6, 16, 20, 24 h). The excised root tips were immediately rinsed with dist. water twice, then immersed in 2, 3, 5-triphenyl tetrazolium chloride (TTC) solution (0.5%) and incubated at  $35 \pm 2^\circ\text{C}$  in the dark for 30 min. Subsequently, the root tips were washed with dist. water. As last step, the red-colored complex (triphenyl formazan [TF]) was extracted from the tissue using 1 mL ethanol (95%). The absorbance of the extracts was measured against blanks consisting of ethanol (95%) at 490 nm with a spectrophotometer (Genesys 30, Thermo Fisher Scientific, USA). The principle of the TTC assay depends on the reduction of TTC to the red-colored insoluble TF, which is directly related to the activity of the mitochondrial respiratory chain ([Ruf and Brunner, 2003](#)).

#### 2.5. Removal of TRD in early seedling stage of barley plants

To evaluate the ability of barley seedlings to remove TRD, hydroponic experiments were performed. Surface sterilized barley seeds were grown on sterilized perlite for four days, then transferred into the hydroponic system (250 mL glass pots). They were initially maintained in dist. water for three days, and then kept on half-strength nutrient solution for one additional week. Then, the seedlings were transferred to full-strength nutrient solution and divided into three groups as follows: TRD group (the medium contains  $100 \mu\text{g L}^{-1}$  TRD), TRQ1 group (the medium supplemented with  $100 \mu\text{g L}^{-1}$  TRD + 0.5 mM Q) and TRQ2 group (the medium received  $100 \mu\text{g L}^{-1}$  TRD + 1 mM Q). Each group consisted of three replicates and each replicate had seven seedlings. A fourth group was prepared as an abiotic control (AB group) receiving the full strength nutrient solution and TRD ( $100 \mu\text{g L}^{-1}$ ) without seedlings to evaluate the abiotic degradation of TRD during the experiment ([Fig. 3](#)).

Aliquots (0.5 mL) from the media of all groups were taken at 0, 3, 6, 9, 12 and 15 days and frozen at  $-20^\circ\text{C}$  until further analysis. At the end of the experiment (15 days), seedlings were separated in roots and shoots, roots were washed four times with dist. water, and then both roots and shoots were weighted, and frozen at  $-80^\circ\text{C}$  until further analysis. Transpiration rate was determined during the experiment, via weighing method, and the water loss was compensated before collecting the aliquots.

#### 2.6. Sample preparation for pharmaceutical quantification

Prior to injection, water samples were mixed with 5-sulfosalicylic acid (10:1 v/v, 1.9 M in water) and centrifuged at  $16,100 \times g$  for 10 min at  $4^\circ\text{C}$ , for protein precipitation. Then, supernatants were collected, acidified with formic acid (final concentration 0.1%) and spiked with the internal standard (IS; TRD-D3) to a final concentration of  $20 \mu\text{g L}^{-1}$ . Root and shoot samples were ground and homogenized

under liquid nitrogen. A modified QuEChERS methodology (based on the European Standard method [[EN 15662:2008](#)]) was used for extraction and clean up. In short, 0.25 g of previously homogenized tissue was spiked with  $20 \mu\text{L}$  of acridine D9 (ACR-D9; 12.5 ppm, to reach a final concentration  $200 \mu\text{g L}^{-1}$ ), vortexed for 5 s followed by addition of acetonitrile (2.5 mL), shaken vigorously and vortexed for 10 s. A mixture of salts (1 g  $\text{MgSO}_4$  anhydrous, 250 mg NaCl, 250 mg trisodium citrate anhydrous, 125 mg disodium hydrogen citrate sesquihydrate) was then added, shaken and vortexed for 10–20 s. Thereafter, the mixture was centrifuged at 3750 rpm for 10 min before the upper phase was collected. For shoot samples, the collected upper phase was incubated at  $-20^\circ\text{C}$  for 2 h. Then, 1.5 mL was collected (upper phase), mixed with 125 mg  $\text{MgSO}_4$  anhydrous, 25 mg C18, 25 mg PSA, 7.5 mg activated carbon, shaken vigorously and vortexed for 10 s prior to centrifugation (12,000 rpm for 10 min). Subsequently, the collected upper phase was passed through  $0.2 \mu\text{m}$  filter (SPARTAN™ 13/0.2 RC) and the filtrate was supplemented with formic acid and spiked with IS as mentioned above for the water samples.

#### 2.7. Analytical instrument setup and conditions

Samples were injected (at least  $3 \times 10 \mu\text{L}$ ) via an autosampler (Dionex UltiMate 3000TRS, Gering, Germany) into an UHPLC (Dionex UltiMate 3000RS, Gering, Germany) coupled to a triple quadrupole mass spectrometer (Thermo Scientific HESI-MS/MS, TSQ Quantum Access Max, San Jose, USA). An Accucore PFP column ( $100 \text{ mm} \times 2.1 \text{ mm}$ ,  $2.6 \mu\text{m}$  particle size, Thermo Scientific, San Jose, USA) with an Accucore PFP pre-column ( $10 \times 2.1 \text{ mm}$ ,  $2.6 \mu\text{m}$  particle size, Thermo Scientific, San Jose, USA) at a flow rate of  $0.45 \text{ mL min}^{-1}$  was applied for chromatographic separation. The mobile phases 0.1% formic acid in Mili-Q water (A) and 0.1% formic acid in acetonitrile (B) were used to apply a linear gradient of 0–2 min 5% buffer B, 2–8 min 5–100% B, 8–9 min 100% B, 9–9.1 min 100–5% B, 9.1–10 min 5% B.

The mass spectrometer was operated in positive HESI mode at a capillary voltage of 5000 V; nitrogen dumping gas temperature of  $350^\circ\text{C}$ ; sheath gas pressure 50 psi, auxiliary gas pressure 5 psi, capillary temperature  $200^\circ\text{C}$ , skimmer offset of 6 and tube lenses of 106.37 V. Sample analysis was in selected ion monitoring (SIM) mode, with TRD 263.24  $m/z$  (+1), OTRD 250.16 (+1), ACR-D9 189.27 (+1), VEN 278.2 (+1) and TRD-D3 (IS) 267.97  $m/z$  (+1). After integration, samples were mathematically quantified against a calibration curve (linear model with zero included) with six nominal concentrations from  $3.75$  to  $120 \mu\text{g L}^{-1}$ , where the IS was used at a final concentration of  $20 \mu\text{g L}^{-1}$ . Xcalibur software (ver. 4.1) was used for peak identification and quantification.

#### 2.8. Quality assurance and quality control procedures

The performance of the equipment was checked daily, using blanks (solvent controls), fortified samples spiked with internal standard (quality controls, QCs =  $30 \mu\text{g L}^{-1}$ ) and new calibration curves for

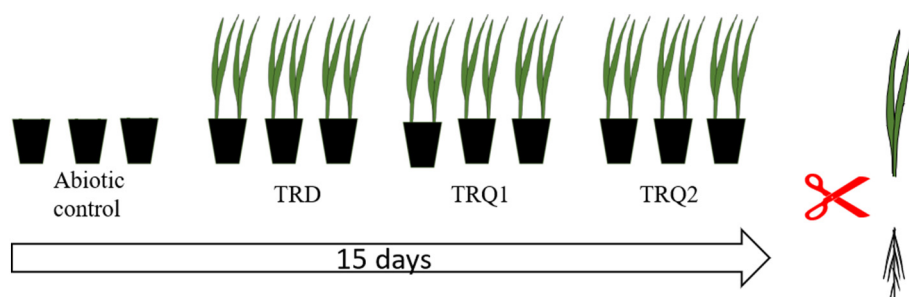


**Fig. 3.** Workflow of a hydroponic experiment; abiotic control was used to assess the adsorption or degradation of TRD during the time of the experiment (15 days).

each Pitman setup and seedling experiment. The limits of detection (LODs) and quantification (LOQs) for each pharmaceutical were defined as  $LOD = 3.3(\alpha/S)$  and  $LOQ = 10(\alpha/S)$ ; with  $\alpha$ , the standard deviation slope and  $S$ , the average slope of the calibration curves. To evaluate precision, accuracy, absolute recoveries and stability, three independent samples (of roots and shoots) were spiked with one concentration (10LOQ) and analyzed at three subsequent days following the criteria established by the ICH (2005). The same concentration was used to check the matrix effect following Eq. (1), as described in Cruzeiro et al. (2016):

$$\text{Matrix effect (\%)} = - \left[ \frac{\text{Area ratio}_{\text{standards}} - \text{Area ratio}_{\text{standards in matrix}}}{\text{Area ratio}_{\text{standards}}} \right] * 100 \quad (1)$$

The results from this part can be found in supplementary materials (Table S2).

## 2.9. Data analysis and statistics

Uptake kinetics of the cattail and barley roots were expressed in terms of TRD and VEN change of concentration over time (24 h). The data obtained per unit of time (hours) followed the nonlinear regression analysis, Boltzmann sigmoid curve, as Eq. (2):

$$Y = \text{Bottom} + \frac{(\text{Top} - \text{Bottom})}{1 + \exp\left(\frac{V_{50} - X}{\text{slope}}\right)} \quad (2)$$

This equation originally describes voltage dependent activation of ion channels that in this case translated as concentration; the concentration

varies from “bottom” and “top” of the curve, where the “V50” represents its halfway. “Slope” describes the steepness of the curve, with a larger value denoting a shallow curve.

While several other models (Plateau followed by one phase association, Allosteric sigmoidal, Sigmoidal dose-response, Asymmetric 5PL and Sigmoidal 4PL) were tested, Boltzmann was the one presenting the best fit. A relatively high coefficient of determination ( $R^2$ ) and low standard deviation of residues ( $S_{x,y}$ ) were used as criteria for good fit.

For each case (Fig. 4A-D), the fitting was tested using the mean of concentrations (in triplicate) at each time-point studied (9 time points within 24 h). The graphical analyses were performed using GraphPad Prism (ver. 6.00).

The bioconcentration factor (BCF) was calculated as Eq. (3)

$$\text{BCF} = \frac{C_{\text{root}}}{C_{\text{initial}}} \quad (3)$$

where  $C_{\text{root}}$  is the final concentration of TRD in the root tissue after 15 days of incubation and  $C_{\text{initial}}$  is the concentration of TRD in the media at the beginning of the experiment.

The mobilization of TRD from root to shoot was calculated using translocation factor (TF) which is indicated by Eq. (4)

$$\text{TF} = \frac{C_{\text{shoot}}}{C_{\text{root}}} \quad (4)$$

where  $C_{\text{shoot}}$  and  $C_{\text{root}}$  are the concentration of TRD in shoot and root after 15 days of incubation, respectively (Bigott et al., 2020, 2021).

To infer differences between treatments and sampling times, all data were initially checked for normality (Shapiro-Wilk test) and homogeneity of variances (Levene's test). In order to determine differences

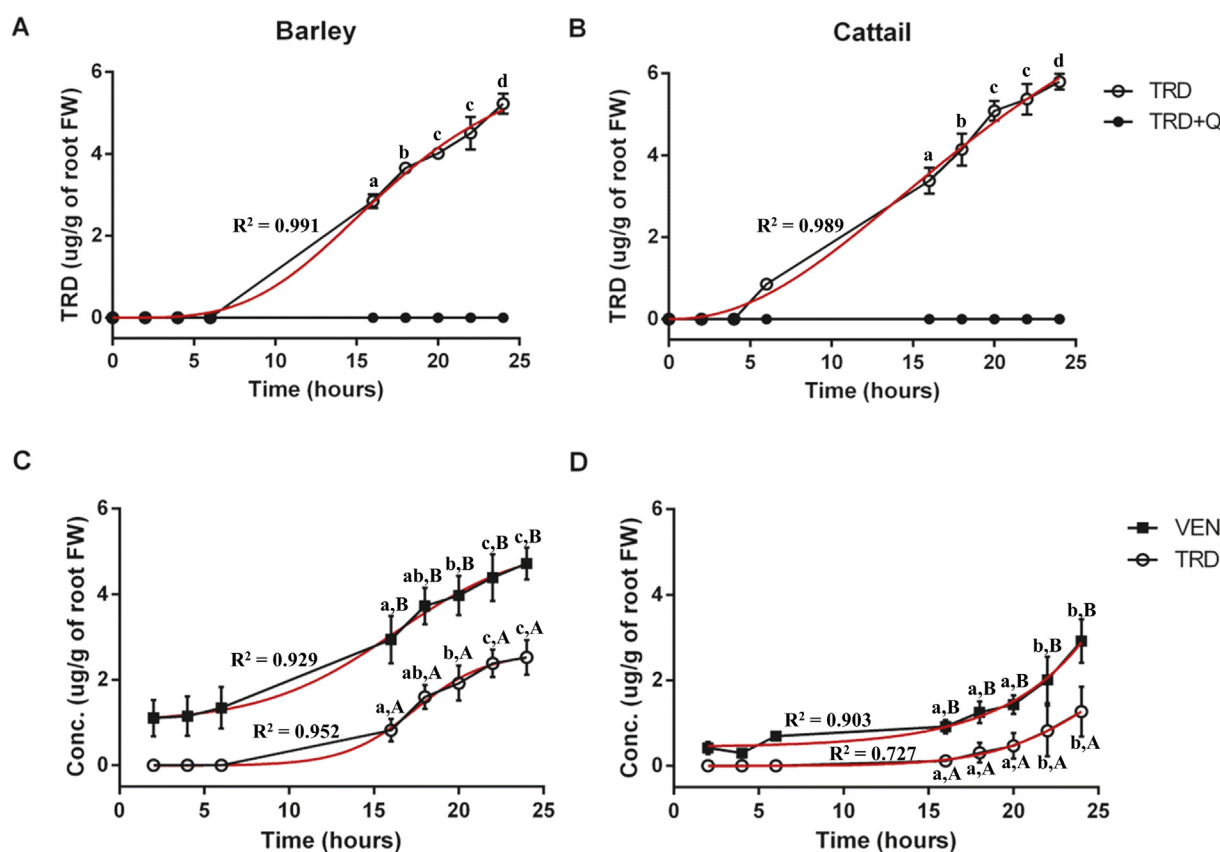


**Fig. 4.** Tramadol (TRD) concentration in compartment C using barley (A, C) and cattail (B, D) roots. (A, B) show the effect of Q on TRD transport while (C, D) reveals the effect of VEN on the transport; each value is as the mean of three independent replicates  $\pm$  SD; small superscript letters mean differences among sampling times and capital superscript letters mean differences between compounds (TRD + VEN). The red curves represent Boltzmann sigmoid curves calculated on the base of nonlinear regression analysis.

between sampling times and plant species (barley vs cattail) or compound (TRD and VEN), a 2-way factorial ANOVA was performed, followed by the post-hoc Tukey's test. Data was ranked when necessary to fit the assumptions for analysis. Differences were considered significant for  $p \leq 0.05$ . All statistical analyses were performed in Statistica 7.0.

### 3. Results and discussion

#### 3.1. Root metabolic activity

Root vitality testing was performed using the TCC staining technique. Our results showed that cattail and barley roots stayed viable during the 24 h, which permits the use of these roots in short-term uptake experiments (Fig. 5). After 24 h, a 31.7% and 23.9% reduction in the activity was observed for excised barley and cattail roots, respectively, indicating that other approaches, e.g. using whole plants, should be used for controlled uptake experiments longer than 24 h.

#### 3.2. Short-term uptake using Pitman chambers

Pitman chambers had been previously used to explore transport of xenobiotic glutathione conjugates and uptake of pharmaceuticals during short-term experiments (Schröder et al., 2007; Cui et al., 2015). In the current study, we determined the uptake and transport of TRD (alone or in mixture with VEN) and its active metabolite ODTRD using roots of barley and cattail plants. In the chambers spiked with TRD alone, transport rates of up to 5.18 and 5.79  $\mu\text{g g}^{-1}$  root FW day<sup>-1</sup> were recorded for barley and cattail roots, respectively (Fig. 4A & B, Table S3). The slightly higher rate in cattail roots was confirmed by the Boltzmann model (see Table 1), which showed that the slope of the curve in the cattail experiment (5.013) was higher than that in the barley root experiment (3.659). While exposing roots to TRD + VEN retarded transport rates of TRD to 2.53 and 1.27  $\mu\text{g g}^{-1}$  root FW day<sup>-1</sup> for barley and cattail, respectively. It is clear (Table 1) that slopes from curves obtained from co-spiked TRD + VEN solution (Fig. 4C & D and Tables S4 & S5) were lower for both barley and cattail (2.095 and 3.043, respectively) than in chambers spiked with TRD alone (Fig. 4A & B). These results are in line with H1 that postulates an easy uptake and transport of TRD by plant roots due to the cationic moiety and the small size of the compound (MW 263.37) allowing the electrostatic

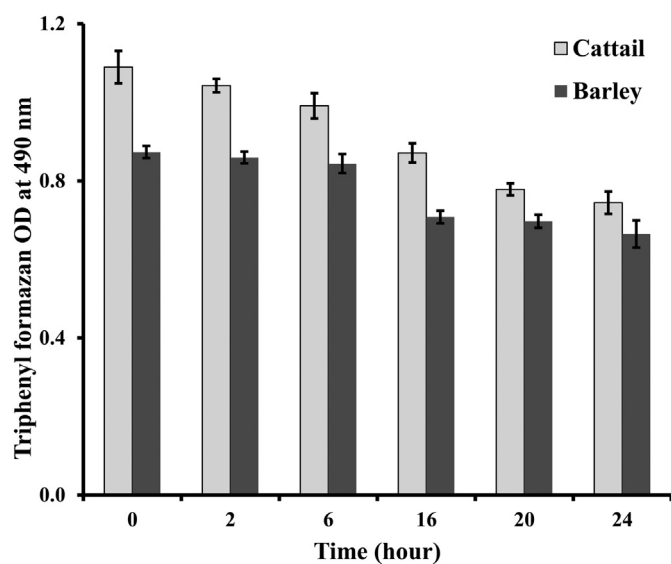


Fig. 5. Effect of incubation time on root cell viability of cattail and barley. Cell vitality was visualized by formation of triphenylformazan (TF) red-colored complex using TTC staining technique; values are represented as mean of three replicates  $\pm$  SD.

Table 1

Estimated uptake kinetics of barley (A, C) and cattail (B, D) roots using the non-linear regression analysis model, Boltzmann sigmoidal curve, in case of Pitman chambers spiked either with TRD in (A, B) or TRD + VEN in (C, D). Slope describes the steepness of the curves presented in Fig. 4, bottom and top of the curve represent the variation in TRD concentration and V50 is the halfway of the curve.  $R^2$  and  $S_{y,x}$  were used as criteria for good fit, as  $R^2$  is the coefficient of determination and  $S_{y,x}$  is the standard deviation of residues.

Boltzmann sigmoidal	A		B		C		D	
	TRD	TRD	TRD	VEN	TRD	VEN	TRD	VEN
Bottom	-0.187	-0.411	-0.008	1.007	-0.005	0.432		
Top	5.591	6.981	2.625	5.203	3.101	~2037		
V50	15.840	15.450	17.430	16.250	25.120	~56.84		
Slope	3.659	5.013	2.095	3.912	3.043	~4.886		
$R^2$	0.991	0.989	0.952	0.929	0.727	0.903		
$S_{y,x}$	0.214	0.273	0.249	0.428	0.290	0.292		

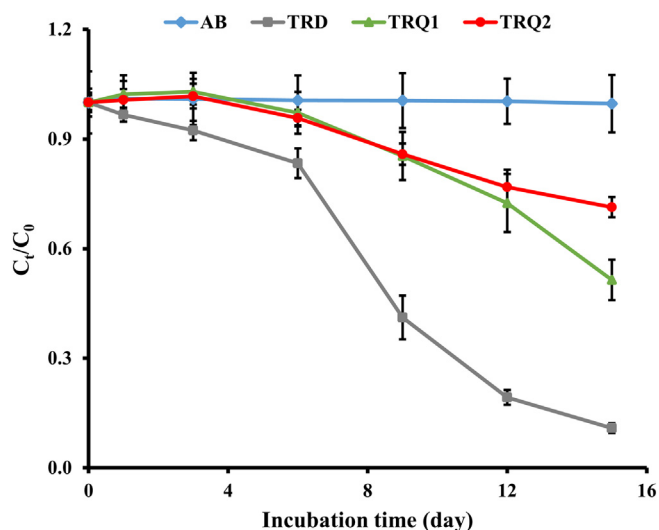
attraction to root cell (Miller et al., 2016; Li et al., 2019). Furthermore, both plant roots exposed to TRD + VEN showed the ability to transport VEN with a higher rate in barley 4.72  $\mu\text{g g}^{-1}$  root FW day<sup>-1</sup> than in cattail 2.92  $\mu\text{g g}^{-1}$  root FW day<sup>-1</sup> (Fig. 4C & D and Table S4 & S5).

Fig. 4 and Table S3 illustrates that apparently no TRD transport was measurable within the first 4 to 6 h, neither through cattail nor barley roots, respectively. Indeed, this time-lag was even longer in both plant species, when Pitman chambers were spiked with TRD + VEN mixtures. Thermodynamically, the energy required for transporting a solute across a membrane is zero as a diffusion gradient will flow from high concentration (compartment A) to a low concentration (compartment C). Parallel to that and resembling to a chemical reaction, minimum activation energy should be exceeded before transport occurs (Dettenmaier, 2008). This might explain the time-lag before TRD passes from compartment A to compartment C crossing through the root symplast. Competing with analogous compounds prolongs this time period, which means that VEN can eventually affect the uptake and transport of TRD. In accordance with this, Szkutnik-Fiedler et al. (2017) recorded a decrement (~27%) of TRD concentration in rabbit plasma after administration of TRD + VEN to one group of rabbit compared to the control group (received TRD alone).

To evaluate the involvement of OCT in the transport of TRD, an inhibitor study with quinidine (Q) was performed. The transport of TRD was completely inhibited in both barley and cattail roots when Pitman chambers were spiked with TRD + Q solution (Fig. 4A & B), indicating that in both species, OCT are involved in the TRD translocation, as postulated above (H2). Our findings are in accordance with previous studies reporting a decreased in TRD uptake by human cells up to 84% after using Q (1 mM) as an inhibitor (Kitamura et al., 2014) and significant inhibition of metformin transport in cattail roots after addition of Q (0.5 mM) (Cui et al., 2015). These data also strengthen our hypothesis (H2) considering OCTs as one of the major routes controlling the transport of TRD. Concerning ODTRD, all results were below the LOQ (0.654  $\mu\text{g L}^{-1}$ ). These results can be related to its lower lipophilicity ( $\log K_{ow}$  1.72), which may reduce the passive diffusion process across cell membranes (Miller et al., 2016). Moreover, Tzvetkov et al. (2011) reported that ODTRD is a carrier-dependent compound that can be transported actively only through OCT1; so, this can also influence the velocity of the transport.

#### 3.3. Removal of TRD from a hydroponic system using barley seedlings

The decrement of TRD from the external medium was determined during 15 days of exposure to barley seedlings. Within 8 days, a sharp decrease of TRD concentration alone or after addition of Q (Fig. 6) occurred, while the abiotic control group (AB group) showed constant concentration proving that neither adsorption on the glass surface nor photodegradation of TRD occurred during the experiment. This was in accordance with previous studies that reported high stability of TRD in aqueous solution subjected either to sunlight or diffuse light in a



**Fig. 6.** Removal kinetics of tramadol ( $100 \mu\text{g L}^{-1}$ ) during 15 days of incubation with *H. vulgare* seedlings in controlled hydroponic culture conditions. The graph shows four different groups: the abiotic control (AB group), barley seedlings exposed only to tramadol (TRD group), barley seedlings co-exposed to TRD + 0.5 mM quinidine (TRQ1 group) and the last group exposed to TRD + 1 mM quinidine (TRQ2 group).  $C_0$  represents the initial concentration of TRD at the beginning of experiment in the medium, while  $C_t$  refers to the concentration of the residual TRD in the medium at the given time (day); each incubation time is represented by the average of three independent replicates  $\pm$  SD.

controlled room, and low rates of biotic degradation ( $\leq 0.00029 \text{ h}^{-1}$ ) in surface water (Rúa-Gómez and Püttmann, 2013; Suno et al., 2015). Other studies reported that after treatment in some WWTPs, no or low removal efficiency of TRD (<40%) was detected (Kasprzyk-Hordern et al., 2009). This stresses the recalcitrant properties of this molecule (high photo-stability and low volatility).

In TRD group, a slight decrease was observed with a removal efficiency  $3.37 \pm 1.93\%$  after the first day, while no removal was observed in TRQ1 and TRQ2 groups within this period (Fig. 6 and Table S6); the latter findings are in line with results obtained from our experiments (Fig. 3B), where a complete inhibition of TRD transport after Q addition was observed. The first significant diminishment of TRD in media was achieved after 6 days in TRQ1 and TRQ2 groups; this may be due to the uptake and translocation of large amounts of Q by barley roots during this period. Consequently, TRD could be available for uptake through the rest of the incubation time. Indeed, a rapid decrease of TRD was achieved after 6 days leading to a removal efficiency of  $89.13 \pm 1.34\%$  after 15 days of incubation (Fig. 6 and S1). The same pattern was observed in TRQ1 and TRQ2 groups but with lower removal efficiencies, i.e.,  $48.58 \pm 5.54\%$  and  $28.65 \pm 2.75\%$ , respectively (Fig. 6 and S1), which is in compliance with both hypotheses (H1&H2) that shows the importance of OCTs in the uptake and transport of cationic compounds like TRD. From the results obtained by our experiments, it was anticipated that the absolute value of transported TRD would be  $\sim 78 \mu\text{g}$  after 15 days. This expected value was close to the quantity of TRD ( $\sim 89 \mu\text{g}$ ) removed from the hydroponic medium after incubation with barley seedlings for 15 days.

### 3.4. Uptake and translocation of TRD into barley seedlings tissues

In order to explore its fate and distribution inside plants, we determined the bioaccumulation pattern of TRD in barley seedlings exposed to different treatments (Table 2). The highest BCF value ( $9.08 \pm 0.53$ ) was calculated for TRD group followed by TRQ1 group, while the lowest value ( $2.24 \pm 0.53$ ) was recorded in TRQ2 group. In contrary to BCF, the TF values followed a reverse pattern. The highest TF was detected in TRQ2 group ( $15.52 \pm 3.97$ ), while the lowest was in TRD group ( $1.18 \pm 0.14$ ).

**Table 2**

Concentration of TRD ( $\mu\text{g g}^{-1}$  root FW) detected in both roots and shoots together with the BCF and TF calculated for barley seedlings grown in different treatments; each value represents the mean of three independent replicates  $\pm$  SD.

Treatment groups	TRD ( $\mu\text{g g}^{-1}$ root FW)		BCF	TF
	Root	Shoot		
TRD	$4.56 \pm 0.32$	$5.41 \pm 1.00$	$9.08 \pm 0.53$	$1.18 \pm 0.14$
TRQ1	$0.72 \pm 0.08$	$8.14 \pm 1.55$	$4.49 \pm 0.53$	$11.49 \pm 3.43$
TRQ2	$0.24 \pm 0.02$	$3.69 \pm 0.56$	$2.24 \pm 0.53$	$15.52 \pm 3.97$

TRD ( $100 \mu\text{g L}^{-1}$  TRD), TRQ1 ( $100 \mu\text{g L}^{-1}$  TRD + 0.5 mM Q), TRQ2 ( $100 \mu\text{g L}^{-1}$  TRD + 1 mM Q).

The easy access and uptake of TRD (removal efficiency  $\sim 90\%$ ) is due to the chemical characteristics of the molecule:  $\log K_{ow}$  (2.45) and MW (263.37) as well as the lower number of H-bonds (donors = 1, acceptors = 3), which are in accordance to the values mentioned by Kumar and Gupta (2016) in their prediction rule; the same idea is supported by Limmer and Burken (2014). Moreover, Miller et al. (2016) showed that bases with  $\log K_{ow}$  ranging from 0 to 4 tend to move via xylem and as a result, they can be translocated in the aerial parts through the transpiration stream. Also, Chuang et al. (2019) reported that ionic pharmaceuticals with small size (MW < 300) may enter plant roots symplastically with water flow and under control of integral transport proteins. Consequently, these small sized compounds could pass via the endodermis into xylem elements followed by upward translocation to shoots driven by transpiration. This supports our results (TFs > BCFs), and our hypothesis (H1) indicating that TRD is preferably translocated to shoots and not accumulated in roots.

## 4. Conclusion

The current study evaluates the use of two monocot plant species for the uptake and translocation of pharmaceutical compounds. Results indicate that TRD and related cationic compounds, like VEN, can be easily taken up and transported into plant roots with the aid of integral transport proteins (like OCTs). Both pharmaceuticals had a high tendency to translocate to plant aerial parts, which may be facilitated by carrying these molecules via water flow in the symplastic pathway. While this is desirable for plants used in phytoremediation, TRD could also be easily accumulated, within a short-time, in crop plants if it was present in irrigation water. Therefore, it is important to avoid introducing TRD or its metabolites in water used for irrigation to prevent its accumulation in food or fodder crops, through proper removal during water treatment. Based on our results, we postulate that VEN can interfere with the bioavailability of TRD in plants, e.g., by competing for the same transmembrane transporter. With our experimental approach we were able to identify the transport of organic compounds in short-time period that can be essential to identify target compounds for more elaborated experiments.

## Credit authorship contribution statement

**David M. Khalaf:** Conceptualization, Methodology, Analytical validation, Formal analysis, Investigation, Writing - Original Draft, Writing & Editing, Visualization. **Catarina Cruzeiro:** Analytical validation, Software analysis, Formal analysis, Writing - Review & Editing. **Peter Schröder:** Conceptualization, Writing - Review & Editing, Supervision, Funding acquisition.

## Declaration of competing interest

The authors declare that they have no known competing financial interests or personal relationships that could have appeared to influence the work reported in this paper.



## Acknowledgments

The authors would like to thank Katholischer Akademischer Ausländer-Dienst (KAAD) for financial support of David M. Khalaf. C. Cruzeiro was funded by the Water Joint Programming Initiative (WATER 21015 JPI) through the European research project IDOUM - Innovative Decentralized and low-cost treatment systems for Optimal Urban wastewater Management, financed by the German BMBF.

## Appendix A. Supplementary data

Supplementary data to this article can be found online at <https://doi.org/10.1016/j.scitotenv.2021.151164>.

## References

- An, J., Zhou, Q., Sun, F., Zhang, L., 2009. Ecotoxicological effects of paracetamol on seed germination and seedling development of wheat (*Triticum aestivum* L.). *J. Hazard. Mater.* 169, 751–757. <https://doi.org/10.1016/j.jhazmat.2009.04.011>.
- Archer, E., Petrie, B., Kasprzyk-Hordern, B., Wolfaardt, G.M., 2017. The fate of pharmaceuticals and personal care products (PPCPs), endocrine disrupting contaminants (EDCs), metabolites and illicit drugs in a WWTW and environmental waters. *Chemosphere* 174, 437–446. <https://doi.org/10.1016/j.chemosphere.2017.01.101>.
- Balakrishna, K., Rath, A., Praveenkumarreddy, Y., Guruge, K.S., Subedi, B., 2017. A review of the occurrence of pharmaceuticals and personal care products in Indian water bodies. *Ecotoxicol. Environ. Saf.* 137, 113–120. <https://doi.org/10.1016/j.ecoenv.2016.11.014>.
- Bexfield, L.M., Toccalino, P.L., Belitz, K., Foreman, W.T., Furlong, E.T., 2019. Hormones and pharmaceuticals in groundwater used as a source of drinking water across the United States. *Environ. Sci. Technol.* 53, 2950–2960. <https://doi.org/10.1021/acs.est.8b05592>.
- Bigott, Y., Chowdhury, S.P., Pérez, S., Montemurro, N., Manasfi, R., Schröder, P., 2021. Effect of the pharmaceuticals diclofenac and lamotrigine on stress responses and stress gene expression in lettuce (*Lactuca sativa*) at environmentally relevant concentrations. *J. Hazard. Mater.* 403, 123881. <https://doi.org/10.1016/j.jhazmat.2020.123881>.
- Bigott, Y., Khalaf, D.M., Schröder, P., Schröder, P.M., Cruzeiro, C., 2020. Uptake and translocation of pharmaceuticals in plants: principles and data analysis. *The Handbook of Environmental Chemistry*. Springer, Berlin, Heidelberg, pp. 1–38.
- Bravo, L., Mico, J.A., Berrocoso, E., 2017. Discovery and development of tramadol for the treatment of pain. *Expert. Opin. Drug. Discov.* 12, 1281–1291. <https://doi.org/10.1080/17460441.2017.1377697>.
- Carmona, E., Andreu, V., Picó, Y., 2014. Occurrence of acidic pharmaceuticals and personal care products in Turia River basin: from waste to drinking water. *Sci. Total Environ.* 484, 53–63. <https://doi.org/10.1016/j.scitotenv.2014.02.085>.
- Chen, F., Huber, C., Schröder, P., 2017. Fate of the sunscreen compound oxybenzone in *Cyperus alternifolius* based hydroponic culture: uptake, biotransformation and phytotoxicity. *Chemosphere* 182, 638–646. <https://doi.org/10.1016/j.chemosphere.2017.05.072>.
- Chuang, Y.H., Liu, C.H., Sallach, J.B., Hammerschmidt, R., Zhang, W., Boyd, S.A., Li, H., 2019. Mechanistic study on uptake and transport of pharmaceuticals in lettuce from water. *Environ. Int.* 131, 104976. <https://doi.org/10.1016/j.envint.2019.104976>.
- Cruzeiro, C., Rodrigues-Oliveira, N., Velhote, S., Pardo, M.A., Rocha, E., Rocha, M.J., 2016. Development and application of a QuEChERS-based extraction method for the analysis of 55 pesticides in the bivalve *Scrobicularia plana* by GC-MS/MS. *Anal. Bioanal. Chem.* 408, 3681–3698. <https://doi.org/10.1007/s00216-016-9440-0>.
- Cui, H., Hense, B.A., Müller, J., Schröder, P., 2015. Short term uptake and transport process for metformin in roots of *Phragmites australis* and *Typha latifolia*. *Chemosphere* 134, 307–312. <https://doi.org/10.1016/j.chemosphere.2015.04.072>.
- Cui, H., Hrabec de Angelis, M., Schröder, P., 2017. Iopromide exposure in *Typha latifolia* L.: evaluation of uptake, translocation and different transformation mechanisms in planta. *Water Res.* 122, 290–298. <https://doi.org/10.1016/j.watres.2017.06.004>.
- Dettenmaier, E., 2008. Measuring and modeling of plant root uptake of organic chemicals. Utah State University, Logan, UT, USA Doctoral dissertation.
- EC, 2015. Commission implementing decision (EU) 2015/495 of 20 March 2015 establishing a watch list of substances for union-wide monitoring in the field of water policy pursuant to directive 2008/105/EC of the European Parliament and of the council (notified under document C(2015) 1756). *O.J.E.U. L* 78, 40–42.
- EN 15662, 2008. Foods of plant origin - Determination of pesticide residues using GC-MS and/or LC-MS/MS following acetonitrile extraction/partitioning and clean-up by dispersive SPE - QuEChERS method. BSI British Standard.
- Fleishman, E., Blockstein, D.E., Hall, J.A., Mascia, M.B., Rudd, M.A., Scott, J.M., Sutherland, W.J., Bartuska, A.M., Brown, A.G., Christen, C.A., Clement, J.P., Dellasala, D., Duke, C.S., Eaton, M., Fiske, S.J., Gosnell, H., Haney, J.C., Hutchins, M., Klein, M.L., Marqusee, J., Noon, B.R., Nordgren, J.R., Orbuch, P.M., Powell, J., Quarles, S.P., Saterson, K.A., Savitt, C.C., Stein, B.A., Webster, M.S., Vedder, A., 2011. Top 40 priorities for science to inform US conservation and management policy. *Bioscience* 61, 290–300.
- García-Medina, S., Galar-Martínez, M., Gómez-Oliván, L.M., del Consuelo Torres-Bezaury, R.M., Islas-Flores, H., Gasca-Pérez, E., 2020. The relationship between cytogenotoxic damage and oxidative stress produced by emerging pollutants on a bioindicator organism (*Allium cepa*): the carbamazepine case. *Chemosphere* 253, 126675. <https://doi.org/10.1016/j.chemosphere.2020.126675>.
- He, Y., Langenhoff, A.A., Sutton, N.B., Rijnaarts, H.H., Blokland, M.H., Chen, F., Huber, C., Schröder, P., 2017. Metabolism of ibuprofen by *Phragmites australis*: uptake and phytodegradation. *Environ. Sci. Technol.* 51, 4576–4584. <https://doi.org/10.1021/acs.est.7b00458>.
- ICH, 2005. ICH harmonized tripartite guideline: validation of analytical procedures: text and methodology Q2(R1). International Conference of harmonization of technical requirements for registration of pharmaceuticals for human use, pp. 1–13.
- de Jongh, C.M., Kooij, P.J., de Voogt, P., ter Laak, T.L., 2012. Screening and human health risk assessment of pharmaceuticals and their transformation products in Dutch surface waters and drinking water. *Sci. Total Environ.* 427, 70–77. <https://doi.org/10.1016/j.scitotenv.2012.04.010>.
- Kasprzyk-Hordern, B., Dinsdale, R.M., Guwy, A.J., 2008. The occurrence of pharmaceuticals, personal care products, endocrine disruptors and illicit drugs in surface water in South Wales UK. 42, 3498–3518. <https://doi.org/10.1016/j.watres.2008.04.026>.
- Kasprzyk-Hordern, B., Dinsdale, R.M., Guwy, A.J., 2009. The removal of pharmaceuticals, personal care products, endocrine disruptors and illicit drugs during wastewater treatment and its impact on the quality of receiving waters. *Water Res.* 43, 363–380. <https://doi.org/10.1016/j.watres.2008.10.047>.
- Kitamura, A., Higuchi, K., Okura, T., Deguchi, Y., 2014. Transport characteristics of tramadol in the blood-brain barrier. *J. Pharm. Sci.* 103, 3335–3341. <https://doi.org/10.1002/jps.24129>.
- Kodešová, R., Klement, A., Golovko, O., Fér, M., Kočárek, M., Nikodem, A., Grabic, R., 2019. Soil influences on uptake and transfer of pharmaceuticals from sewage sludge amended soils to spinach. *J. Environ. Manag.* 250, 109407. <https://doi.org/10.1016/j.jenvman.2019.109407>.
- Koepsell, H., Lips, K., Volk, C., 2007. Polyspecific organic cation transporters: structure, function, physiological roles, and biopharmaceutical implications. *Pharm. Res.* 24, 1227–1251. <https://doi.org/10.1007/s11095-007-9254-z>.
- Küfner, I., Koch, W., 2008. Stress regulated members of the plant organic cation transporter family are localized to the vacuolar membrane. *BMC Res. Notes* 1, 1–10. <https://doi.org/10.1186/1756-0500-1-43>.
- Kumar, K., Gupta, S.C., 2016. A framework to predict uptake of trace organic compounds by plants. *J. Environ. Qual.* 45, 555–564. <https://doi.org/10.2134/jeq2015.06.0261>.
- Kummerová, M., Zezulka, Š., Babula, P., Tříška, J., 2016. Possible ecological risk of two pharmaceuticals diclofenac and paracetamol demonstrated on a model plant *Lemma minor*. *J. Hazard. Mater.* 302, 351–361. <https://doi.org/10.1016/j.jhazmat.2015.09.057>.
- Leitão, I., Mourato, M.P., Carvalho, L., Oliveira, M.C., Marques, M.M., Martins, L.L., 2021. Antioxidative response of lettuce (*Lactuca sativa*) to carbamazepine-induced stress. *Environ. Sci. Pollut. Res.* 1–13. <https://doi.org/10.1007/s11356-021-13979-3>.
- Lelandais-Brière, C., Jovanovic, M., Torres, G.A., Perrin, Y., Lemoine, R., Corre-Menguy, F., Hartmann, C., 2007. Disruption of AtOCT1, an organic cation transporter gene, affects root development and carnitine-related responses in arabidopsis. *Plant J.* 51, 154–164. <https://doi.org/10.1111/j.1365-3113.2007.03131.x>.
- Li, Y., Sallach, J.B., Zhang, W., Boyd, S.A., Li, H., 2019. Insight into the distribution of pharmaceuticals in soil-water-plant systems. *Water Res.* 152, 38–46. <https://doi.org/10.1016/j.watres.2018.12.039>.
- Limmer, M.A., Burken, J.G., 2014. Plant translocation of organic compounds: molecular and physicochemical predictors. *Environ. Sci. Technol. Lett.* 1, 156–161. <https://doi.org/10.1021/ez400214q>.
- Macherius, A., Seiwert, B., Schröder, P., Huber, C., Lorenz, W., Reemtsma, T., 2014. Triclosan in horseradish - Identification of plant metabolites of environmental contaminants by UPLC-QTOF-MS. *J. Agric. Food Chem.* 62 (5), 1001–1009. <https://doi.org/10.1021/jf404784q>.
- Merci, F., Košnář, Z., Maršík, P., Vojtíšek, M., Dušek, J., Száková, J., Tlustoš, P., 2020. Pyrolysis of biosolids as an effective tool to reduce the uptake of pharmaceuticals by plants. *J. Hazard. Mater.* 124278. <https://doi.org/10.1016/j.jhazmat.2020.124278>.
- Miller, E.L., Nason, S.L., Karthikeyan, K.G., Pedersen, J.A., 2016. Root uptake of pharmaceuticals and personal care product ingredients. *Environ. Sci. Technol.* 50, 525–541. <https://doi.org/10.1021/acs.est.5b01546>.
- Pitman, M., 1971. Uptake and transport of ions in barley seedlings I. Estimation of chloride fluxes in cells of excised roots. *Aust. J. Biol. Sci.* 24, 407–422. <https://doi.org/10.1071/B19710407>.
- Prajitha, V., Thoppil, J.E., 2017. Cytotoxic and apoptotic activities of extract of *Amaranthus spinosus* L. in *Allium cepa* and human erythrocytes. *Cytotechnology* 69, 123–133. <https://doi.org/10.1007/s10616-016-0044-5>.
- Rostam-Abadi, Y., Gholami, J., Amin-Esmaili, M., Safarcherati, A., Mojtabai, R., Ghadirzadeh, M.R., Rahimi, H., Rahimi-Movaghar, A., 2020. Tramadol use and public health consequences in Iran: a systematic review and meta-analysis. *Addiction* 115, 2213–2242. <https://doi.org/10.1111/add.15059>.
- Rúa-Gómez, P.C., Püttmann, W., 2013. Degradation of lidocaine, tramadol, venlafaxine and the metabolites O-desmethyltramadol and O-desmethylvenlafaxine in surface waters. *Chemosphere* 90, 1952–1959. <https://doi.org/10.1016/j.chemosphere.2012.10.039>.
- Ruf, M., Brunner, I., 2003. Vitality of tree fine roots: reevaluation of the tetrazolium test. *Tree Physiol.* 23, 257–263. <https://doi.org/10.1093/treephys/23.4.257>.
- Sauvêtre, A., Schröder, P., 2015. Uptake of carbamazepine by rhizomes and endophytic bacteria of *Phragmites australis*. *Front. Plant Sci.* 6, 83. <https://doi.org/10.3389/fpls.2015.00083>.
- Schröder, P., Scheer, C.E., Diekmann, F., Stampfl, A., 2007. How plants cope with foreign compounds. Translocation of xenobiotic glutathione conjugates in roots of barley (*Hordeum vulgare*). *Environ. Sci. Pollut. Res.* 14, 114–122. <https://doi.org/10.1065/espr2006.10.352>.
- Schröder, P., Helmreich, B., Škrbič, B., Carballa, M., Papa, M., Pastore, C., Emre, Z., Oehmen, A., Langenhoff, A., Molinos, M., Dvarioniene, J., Huber, C., Tsagarakis, K.P., Martínez-Lopez, E., Meric Pagano, S., Vogelsang, C., Mascolo, G., 2016. Status of hormones and painkillers in wastewater effluents across several European states—considerations for the EU watch list concerning estradiols and diclofenac. *Environ. Sci. Pollut. Res.* 23, 12835–12866. <https://doi.org/10.1007/s11356-016-6503-x>.

- Styszko, K., Proctor, K., Castrignanò, E., Kasprzyk-Hordern, B., 2021. Occurrence of pharmaceutical residues, personal care products, lifestyle chemicals, illicit drugs and metabolites in wastewater and receiving surface waters of Krakow agglomeration in South Poland. *Sci. Total Environ.* 768, 144360. <https://doi.org/10.1016/j.scitotenv.2020.144360>.
- Suno, M., Ichihara, H., Ishino, T., Yamamoto, K., Yoshizaki, Y., 2015. Photostability studies on ( $\pm$ )-tramadol in a liquid formulation. *J. Pharm. Health Care Sci.* 1, 5. <https://doi.org/10.1186/s40780-014-0003-2>.
- Szkutnik-Fiedler, D., Grabowski, T., Balcerkiewicz, M., Michalak, M., Pilipczuk, I., Wyrowski, Ł., Urjasz, H., Grzeškowiak, E., 2017. The influence of a single and chronic administration of venlafaxine on tramadol pharmacokinetics in a rabbit model. *Pharmacol. Rep.* 69, 555–559. <https://doi.org/10.1016/j.pharep.2017.01.027>.
- Taiz, L., Zeiger, E., 2010. *Plant Physiology*, 5th ed. Sinauer Associates, Sunderland, MA, p. 464.
- Tzvetkov, M.V., Saadatmand, A.R., Lötsch, J., Tegeder, I., Stingl, J.C., Brockmöller, J., 2011. Genetically polymorphic OCT1: another piece in the puzzle of the variable pharmacokinetics and pharmacodynamics of the opioidergic drug tramadol. *Clin. Pharm. Therap.* 90, 143–150. <https://doi.org/10.1038/clpt.2011.56>.
- WHO, 2018a. World Health Organization (WHO) Critical review report: Tramadol. Forty-first Meeting. Expert Committee on Drug Dependence.
- WHO, 2018b. World Health Organization (WHO) WHO Expert Committee on Drug Dependence, Thirty-ninth Report. WHO Technical Report Series, No. 1009 License: CC BY-NC-SA 3.0 IGO.
- Wijaya, L., Alyemeni, M., Ahmad, P., Alfarhan, A., Barcelo, D., El-Sheikh, M.A., Pico, Y., 2020. Ecotoxicological effects of ibuprofen on plant growth of *Vigna unguiculata* L. *Plants* 9, 1473. <https://doi.org/10.3390/plants9111473>.
- Yang, Y., Ok, Y.S., Kim, K.H., Kwon, E.E., Tsang, Y.F., 2017. Occurrences and removal of pharmaceuticals and personal care products (PPCPs) in drinking water and water/sewage treatment plants: a review. *Sci. Total Environ.* 596, 303–320. <https://doi.org/10.1016/j.scitotenv.2017.04.102>.
- Zhang, D., Gersberg, R.M., Ng, W.J., Tan, S.K., 2014. Removal of pharmaceuticals and personal care products in aquatic plant-based systems: a review. *Environ. Pollut.* 184, 620–639. <https://doi.org/10.1016/j.envpol.2013.09.009>.

## **Appendix M1 (Supplements I)**

This article was published in “Khalaf, D. M., Cruzeiro, C., & Schröder, P. (2022). Removal of tramadol from water using *Typha angustifolia* and *Hordeum vulgare* as biological models: Possible interaction with other pollutants in short-term uptake experiments. *Science of the Total Environment*, 809, 151164”, Copyright Elsevier (2022).

**Supplementary material-**

**Removal of the opioid, Tramadol, from water using a phytoremediation approach: Possible interaction with other pollutants in short-term uptake experiments**

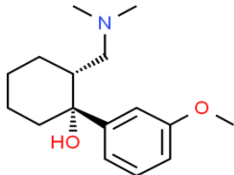
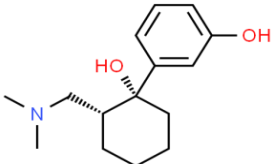
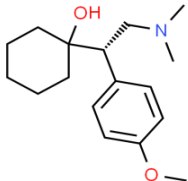
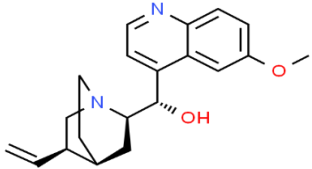
**David Mamdouh Khalaf<sup>1,2</sup>, Catarina Cruzeiro<sup>1</sup>, Peter Schröder\*<sup>1</sup>**

<sup>1</sup>Research Unit Comparative Microbiome Analysis, Helmholtz Zentrum München German Research Center for Environmental Health, Ingolstädter Landstr. 1, 85764 Neuherberg, Germany

<sup>2</sup>Botany and Microbiology Department, Faculty of Science, Assiut University, 71516 Assiut, Egypt



**Table S1.** Structures and physicochemical characteristics of compounds

Compound	Drug class	Molecular structure <sup>a</sup>	Molecular weight <sup>a</sup> (g mol <sup>-1</sup> )	log <i>k<sub>ow</sub></i> <sup>b</sup>	p <i>k<sub>a</sub></i> (basic, acidic) <sup>b</sup>	H-bonds (acceptors, donors) <sup>b</sup>
Tramadol	Analgesics		263.375	2.45	9.23, 13.8	3, 1
O-desmethyltramadol	Analgesics (metabolite)		249.3486	1.72	8.97, 9.62	3, 2
Venlafaxine	Antidepressants		277.4	2.74	8.91, 14.42	3, 1
Quinidine	Antiarrhythmic		324.4168	2.51	9.05, 13.89	4, 1

<sup>a</sup>source: [www.chemspider.com](http://www.chemspider.com)<sup>b</sup>source: <https://go.drugbank.com/>

### Analytical methods

Retention times and mass spectra were similar between standards and fortified matrices (average RSD<20%), proving that the chromatographic procedures were selective for the quantification of TRD. Calibration curves proved to have good fits ( $r^2 = 0.98 \pm 0.01$ ) as a linear regression model and very low LOD and LOQ (see Table S2) showed that equipment and methods were sensitive enough for the target quantifications.

**Table S2.** Calibration parameters of the extraction methods, including the limit of detection (LOD), limit of quantification (LOQ), precision (%), accuracy (%), absolute recoveries (%) and matrix effect (%).

	TRD alone	TRD+VEN		TRD in root	TRD in Shoot	ODTRD
		TRD	VEN			
<b>LOD</b>	0.066 $\mu\text{g L}^{-1}$	0.022 $\mu\text{g L}^{-1}$	0.056 $\mu\text{g L}^{-1}$	0.147 $\mu\text{g g}^{-1}$	0.073 $\mu\text{g g}^{-1}$	0.216 $\mu\text{g L}^{-1}$
<b>LOQ</b>	0.199 $\mu\text{g L}^{-1}$	0.066 $\mu\text{g L}^{-1}$	0.170 $\mu\text{g L}^{-1}$	0.446 $\mu\text{g g}^{-1}$	0.220 $\mu\text{g g}^{-1}$	0.654 $\mu\text{g L}^{-1}$
<b>Precision (<math>\pm</math> %)</b>	0.019	nc	nc	0.033	0.123	nc
<b>Accuracy (%)</b>	105.89	nc	nc	112.47	113.24	nc
<b>Absolute recoveries (%)</b>	93.08	nc	nc	91.03	94.33	nc
<b>Matrix effect (%)</b>	3.88	nc	nc	3.37	-2.89	nc

*nc = not calculated*

The applied extraction methods guaranteed absolute recoveries of more than 90% of TRD from media, root and shoot samples. Besides, values are in accordance with the recoveries range (70-120%) established by the ICH guidelines; in the same way, precision (<0.5%) and accuracy (between 60-120%) also fulfilled the established criteria of ICH (2005).

Interestingly, a lower matrix effect was observed for the three matrices (<|4%|), showing that the applied extraction procedures were ideal.

At last, the stability was evaluated after a period of 7, 14 and 21 days, with extracts stored at -20°C. In average, for root and shoot matrices, we obtained  $\sim 100 \pm 2.7\%$ . Although all injections were done within 72 hours, these results indicate high stability over longer periods.

**Table S3-S5.** Concentration of tramadol (TRD) and venlafaxine (VEN) in  $\mu\text{g g}^{-1}$  root FW  $\text{day}^{-1}$  detected in compartment C of Pitman chambers spiked either with TRD alone or TRD+VEN, using barley and cattail roots; each value is represented as mean of three independent replicates  $\pm$  SD; small superscript letters mean differences among sampling times and capital superscript letters mean differences between plant species (in the TRD alone) or between compounds (TRD+VEN); statistical table are embedded.

<b>Table S3</b>			<b>Pitman chambers exposed to TRD alone</b>		
Time (hr)	Barley	Cattail			
0	<LOQ	<LOQ			
2	<LOQ	<LOQ			
4	<LOQ	<LOQ			
6	<LOQ	0.85 $\pm$ 0.10			
16	2.84 $\pm$ 0.17 <sup>a,A</sup>	3.38 $\pm$ 0.29 <sup>a,B</sup>			
18	3.65 $\pm$ 0.14 <sup>b,A</sup>	4.16 $\pm$ 0.38 <sup>b,B</sup>			
20	4.01 $\pm$ 0.13 <sup>c,A</sup>	5.10 $\pm$ 0.29 <sup>c,B</sup>			
22	4.50 $\pm$ 0.35 <sup>c,A</sup>	5.37 $\pm$ 0.33 <sup>c,B</sup>			
24	5.18 $\pm$ 0.31 <sup>d,A</sup>	5.79 $\pm$ 0.22 <sup>d,B</sup>			

<LOQ means below limit of quantification

	SS	Degr. of freedom	MS	F	P
<b>Intercept</b>	580.5487	1	580.5487	6864.653	<0.00001
<b>time</b>	20.4078	4	5.1019	60.328	<0.00001
<b>plant</b>	3.9078	1	3.9078	46.207	<0.00001
<b>time x plant</b>	0.3793	4	0.0948	1.121	>0.05
<b>error</b>	1.6914	20	0.0846		

where SS refers to sum of squares, MS to mean square, F to F-statistic and

Table S4	Pitman chambers exposed to TRD+VEN			
	Barley		Cattail	
Time (hr)	TRD	VEN	TRD	VEN
0	<LOQ	<LOQ	<LOQ	<LOQ
2	<LOQ	1.10±0.38	<LOQ	0.42±0.13
4	<LOQ	1.15±0.39	<LOQ	0.30±0.04
6	<LOQ	1.35±0.42	<LOQ	0.70±0.06
16	0.82±0.24 <sup>a,A</sup>	2.94±0.50 <sup>a,B</sup>	0.11±0.03 <sup>a,A</sup>	0.92±0.14 <sup>a,B</sup>
18	1.60±0.26 <sup>ab,A</sup>	3.73±0.37 <sup>ab,B</sup>	0.31±0.20 <sup>a,A</sup>	1.26±0.23 <sup>a,B</sup>
20	1.92±0.37 <sup>b,A</sup>	3.97±0.40 <sup>b,B</sup>	0.47±0.26 <sup>a,A</sup>	1.43±0.19 <sup>a,B</sup>
22	2.39±0.29 <sup>c,A</sup>	4.39±0.47 <sup>c,B</sup>	0.82±0.51 <sup>b,A</sup>	2.01±0.46 <sup>b,B</sup>
24	2.53±0.35 <sup>c,A</sup>	4.72±0.34 <sup>c,B</sup>	1.27±0.51 <sup>b,A</sup>	2.92±0.44 <sup>b,B</sup>

<LOQ means bellow limit of quantification

*For barely*

	SS	Degr. of freedom	MS	F	P
Intercept	11456.48	1	11456.48	721.2111	<0.00001
time	968.43	4	242.11	15.2412	<0.00001
compound	2976.48	1	2976.48	187.3761	<0.00001
time x compound	14.55	4	3.64	0.2290	>0.05
error	460.67	29	15.89		

where SS refers to sum of squares, MS to mean square, F to F-statistic and

*For cattail*

	SS	Degr. of freedom	MS	F	P
Intercept	10706.13	1	10706.13	455.4685	<0.00001
time	1967.14	4	491.78	20.9219	<0.00001
compound	1924.01	1	1924.01	81.8527	<0.00001
time x compound	15.26	4	3.81	0.1623	>0.05
error	681.67	29	23.51		

where SS refers to sum of squares, MS to mean square, F to F-statistic and

Table S5 Pitman chambers exposed to TRD+VEN				
	TRD		VEN	
Time (hr)	Barley	Cattail	Barley	Cattail
0	<LOQ	<LOQ	<LOQ	<LOQ
2	<LOQ	<LOQ	1.10±0.38 <sup>a,A</sup>	0.42±0.13 <sup>a,B</sup>
4	<LOQ	<LOQ	1.15±0.39 <sup>a,A</sup>	0.30±0.04 <sup>a,B</sup>
6	<LOQ	<LOQ	1.35±0.42 <sup>a,A</sup>	0.70±0.06 <sup>a,B</sup>
16	0.82±0.24 <sup>a,A</sup>	0.11±0.03 <sup>a,B</sup>	2.94±0.50 <sup>b,A</sup>	0.92±0.14 <sup>b,B</sup>
18	1.60±0.26 <sup>ab,A</sup>	0.31±0.20 <sup>ab,B</sup>	3.73±0.37 <sup>bc,A</sup>	1.26±0.23 <sup>bc,B</sup>
20	1.92±0.37 <sup>bc,A</sup>	0.47±0.26 <sup>bc,B</sup>	3.97±0.40 <sup>bcd,A</sup>	1.43±0.19 <sup>bcd,B</sup>
22	2.39±0.29 <sup>cd,A</sup>	0.82±0.51 <sup>cd,B</sup>	4.39±0.47 <sup>cd,A</sup>	2.01±0.46 <sup>cd,B</sup>
24	2.53±0.35 <sup>d,A</sup>	1.27±0.51 <sup>d,B</sup>	4.72±0.34 <sup>d,A</sup>	2.92±0.44 <sup>d,B</sup>

<LOQ means below limit of quantification

**For TRD**

	SS	Degr. of freedom	MS	F	P
Intercept	7207.500	1	7207.500	550.8917	<0.00001
plant	1190.700	1	1190.700	91.0089	<0.00001
time	765.750	4	191.438	14.6322	<0.00001
plant x time	28.883	4	7.221	0.5519	>0.05
error	261.667	20	13.083		

where SS refers to sum of squares, MS to mean square, F to F-statistic and

**For VEN**

	SS	Degr. of freedom	MS	F	P
Intercept	28812.00	1	28812.00	1583.258	<0.00001
plant	5565.08	7	795.01	43.687	<0.00001
time	2976.75	1	2976.75	163.576	<0.00001
plant x time	87.33	7	12.48	0.686	>0.05
error	582.33	32	18.20		

where SS refers to sum of squares, MS to mean square and F to F-statistic and

**Table S6.** Concentration of TRD ( $\mu\text{g L}^{-1}$ ) in the hydroponic culture during the period of exposure time (15 days) with barley seedlings. The data shows four different groups: the abiotic control (AB group), barley seedlings exposed to tramadol alone (TRD group), barley seedlings co-exposed to TRD+0.5 mM quinidine (TRQ1 group) and the last group exposed to TRD+1mM quinidine (TRQ2 group); each value represents the average of three independent replicates  $\pm$  SD.

<b>Incubation time (days)</b>	<b>TRD group</b>	<b>TRQ1 group</b>	<b>TRQ2 group</b>	<b>AB group</b>
<b>0</b>	100.24 $\pm$ 2.02	103.15 $\pm$ 3.95	97.49 $\pm$ 2.61	114.95 $\pm$ 9.77
<b>1</b>	96.86 $\pm$ 1.94	105.48 $\pm$ 3.77	98.21 $\pm$ 2.85	116.22 $\pm$ 7.29
<b>3</b>	92.56 $\pm$ 2.68	106.21 $\pm$ 3.67	99.20 $\pm$ 3.33	116.09 $\pm$ 8.20
<b>6</b>	83.56 $\pm$ 4.09	100.23 $\pm$ 5.91	93.35 $\pm$ 2.22	115.62 $\pm$ 7.86
<b>9</b>	41.23 $\pm$ 6.01	88.03 $\pm$ 6.81	83.71 $\pm$ 2.84	115.57 $\pm$ 8.65
<b>12</b>	19.28 $\pm$ 2.04	74.75 $\pm$ 8.19	74.93 $\pm$ 4.63	115.32 $\pm$ 7.14
<b>15</b>	10.89 $\pm$ 1.34	53.05 $\pm$ 5.71	69.56 $\pm$ 2.68	114.58 $\pm$ 9.04

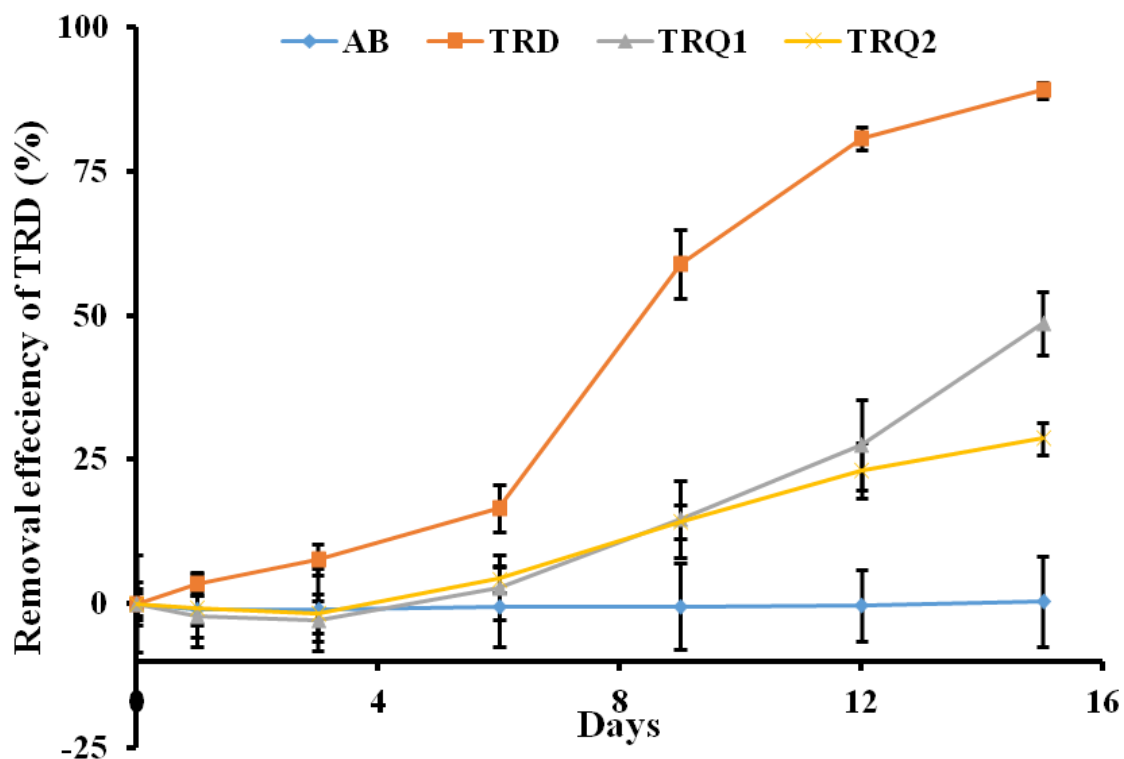


**Fig. S1.** Removal of TRD ( $100 \mu\text{g L}^{-1}$ ) from the hydroponic culture medium by barely seedlings during exposure time. Removal efficiency of TRD (%) =  $(C_0 - C_t) / C_0 \times 100$ , where  $C_0$  represents the initial concentration of TRD at the beginning of experiment in the medium,  $C_t$  refers to the concentration of the residual TRD in the medium at the given time (day). The graph shows four different groups: the abiotic control (AB group), barley seedlings exposed only to tramadol (TRD group), barley seedlings co-exposed to TRD+0.5 mM quinidine (TRQ1 group) and the last group exposed to TRD+1mM quinidine (TRQ2 group); each value represents the average of three independent replicates  $\pm$  SD.

## **ii. Appendix M2 (Manuscript II)**

This article was published in “Khalaf, D. M., Cruzeiro, C., Siani, R., Kublik, S. & Schröder, P. (2023). Resilience of barley (*Hordeum vulgare*) plants upon exposure to tramadol: Implication for the root-associated bacterial community and the antioxidative plant defence system. Science of the Total Environment, 164260”, Copyright Elsevier (2023).





# Resilience of barley (*Hordeum vulgare*) plants upon exposure to tramadol: Implication for the root-associated bacterial community and the antioxidative plant defence system



David Mamdouh Khalaf<sup>a,b</sup>, Catarina Cruzeiro<sup>a,\*</sup>, Roberto Siani<sup>a,2</sup>, Susanne Kublik<sup>a</sup>, Peter Schröder<sup>a,1</sup>

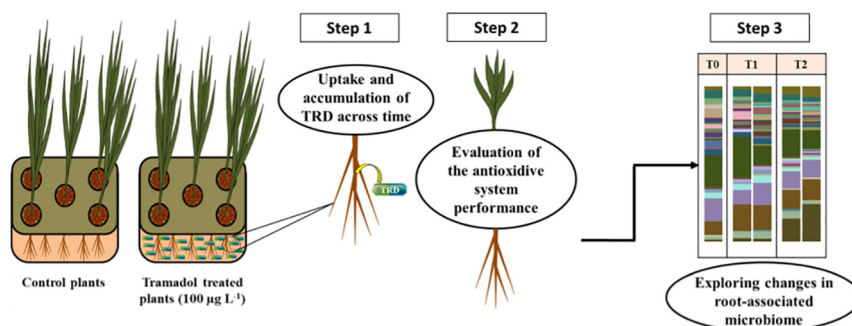
<sup>a</sup> Research Unit Comparative Microbiome Analysis, Helmholtz Zentrum München GmbH, German Research Center for Environmental Health, Ingolstädter Landstr. 1, 85764 Neuherberg, Germany

<sup>b</sup> Botany and Microbiology Department, Faculty of Science, Assiut University, 71516 Assiut, Egypt

## HIGHLIGHTS

- Barley plants can take up and accumulate tramadol (TRD) over time.
- Enzyme activities revealed a defence reaction in TRD roots + shoots after 24 days.
- Guaiacol peroxidase was 5.47-fold in TRD-treated root compared to control (24 days).
- Exposure to TRD induces alterations in the root-associated bacterial community.
- Specific genera were persistent in TRD-treated plants at both time points.

## GRAPHICAL ABSTRACT



## ARTICLE INFO

Editor: Yolanda Picó

### Keywords:

Amplicon 16S  
Bacterial microbiome  
Oxidative stress  
Pharmaceutical contamination  
Root uptake

## ABSTRACT

Insufficiently treated reclaimed water can act as a source of contamination by introducing recalcitrant contaminants (e.g., pharmaceutical compounds) to various water bodies and/or agricultural soils after irrigation. Tramadol (TRD) is one of these pharmaceuticals that can be detected in influents and effluents of wastewater treatment plants, at discharge points as well as in surface waters in Europe. While the uptake of TRD by plants through irrigation water has been shown, plant responses towards this compound are still unclear. Therefore, this study aims to evaluate the effects of TRD on selected plant enzymes as well as on the root bacterial community structure. A hydroponic experiment was conducted to test the effects of TRD (100 µg L<sup>-1</sup> TRD) on barley plants, at two harvesting time points after treatment. Accumulation of TRD in root tissues over time was observed reaching concentrations of 111.74 and 138.39 µg g<sup>-1</sup> in total root FW after 12 and 24 days of exposure, respectively. Furthermore, noticeable inductions in guaiacol peroxidase (5.47-fold), catalase (1.83-fold) and glutathione S-transferase (3.23- and 2.09-fold) were recorded in roots of TRD-treated plants compared to controls after 24 days. A significant alteration in the beta diversity of root-associated bacteria due to TRD treatment was observed. Three amplicon sequence variants assigned to *Hydrogenophaga*, *U. Xanthobacteraceae* and *Pseudacidovorax* were differentially abundant in TRD-treated compared to control plants at both harvesting time points. This study reveals the resilience of plants through the induction of the antioxidative system and changes in the root-associated bacterial community to cope with the TRD metabolism/detoxification process.

\* Corresponding author.

E-mail address: [catarina.cruzeiro@helmholtz-muenchen.de](mailto:catarina.cruzeiro@helmholtz-muenchen.de) (C. Cruzeiro).

<sup>1</sup> Present address: Unit Environmental Simulation, Helmholtz Zentrum München GmbH, German Research Center for Environmental Health, Ingolstädter Landstr. 1, 85764 Neuherberg, Germany.

<sup>2</sup> Both authors contributed equally to this work; joint authors.

## 1. Introduction

During the last decades, great attention has been paid to aquatic ecosystem contamination by pharmaceutical compounds. The uncontrolled disposal of expired or unused pharmaceuticals, as well as the improper removal of compounds and/or their metabolites during the conventional water treatment process, may lead to excessive accumulation of unwanted chemicals in our aquatic environment (Bound and Voulvoulis, 2005; Carmona et al., 2014; Schröder et al., 2016; Balakrishna et al., 2017; Yang et al., 2017a; Bexfield et al., 2019). Due to their biological activity, these compounds might have an impact on the aquatic animals, even at lowest concentrations ranging from ng to  $\mu\text{g}$  (Fabbri and Franzellitti, 2016). In 2020, the United Nations Educational, Scientific and Cultural Organization (UNESCO) reported that 40 % of the world's inhabitants will be subjected to severe water scarcity problems by 2050 (UNESCO, UN-Water, 2020). Hence, the reuse of treated wastewater for agricultural irrigation is a growing practice in a wide range of areas, especially in the Middle East (Tran et al., 2018; Carter et al., 2019; Mordechay et al., 2021). However, it is challenging to eliminate the contamination of various pollutants (including pharmaceuticals and personal care products, PPCPs) in treated wastewater. Recent studies showed that after irrigation with treated wastewater, these compounds can end up in crops (Wu et al., 2015; Mordechay et al., 2021) and subsequently can be detected in human urine after crop consumption (Paltiel et al., 2016; Schapira et al., 2020). The opioid tramadol (TRD) is one of these micropollutants that has been detected (from  $\text{ng L}^{-1}$  to  $\mu\text{g L}^{-1}$ ) in different aquatic systems, such as surface water (river Ely, 731–7731  $\text{ng L}^{-1}$ ), wastewater treatment plants (WWTPs) as in Cilfynydd WWTP influents (8505–89026  $\text{ng L}^{-1}$ ) and effluents (24132–97616  $\text{ng L}^{-1}$ ) (Kasprzyk-Hordern et al., 2008, 2009). Despite its relevance, only few studies have so far addressed plant uptake and accumulation capacity of TRD in different plant organs (Kodešová et al., 2019; Mercl et al., 2020; Khalaf et al., 2022). Moreover, to the best of our knowledge, there is neither information available about TRD effects on plant performance (antioxidative defence system) nor about its influence on the root-associated bacterial community.

Micropollutants, after their uptake by plants, undergo metabolization during which they are (in)activated, detoxified and frequently sequestered (Schröder et al., 2007; Bartha et al., 2014). During the detoxification/metabolization of micropollutants/xenobiotics, the formation of reactive oxygen species (ROS) can occur, which is followed by activation of plant antioxidative enzymes such as catalase (CAT), peroxidase (POX) or superoxide dismutase (SOD) to prevent harmful effects (Mittler, 2002; Dordio et al., 2011; Chen et al., 2018). Moreover, these pollutants undergo metabolization inside the plant following the “Green Liver” concept, described by Sandermann Jr (1992, 1994). This concept comprises three phases in which key plant enzymes such as cytochrome P450 monooxygenases, peroxidases, glutathione S-transferases (GSTs), and glycosyltransferases are involved. GSTs are well-known enzymes in plants, which are inducible by different biotic and abiotic stresses such as drought, extreme temperatures, pathogen attack and xenobiotics (Mauch and Dudler, 1993; Anderson and Davis, 2004; Smith et al., 2004; Gallé et al., 2009). GSTs play a crucial role in facilitating conjugation reactions between glutathione and various xenobiotics that possess electrophilic centers. These conjugation reactions lead to the formation of conjugates, which can then be efficiently sequestered within the central vacuole (Martinoia et al., 1993; Schröder et al., 2007). In addition to the protective effect of the previously mentioned enzymes, the products from their reactions may have an impact on the root-associated bacterial communities. Therefore, we hypothesized that TRD can affect the activities of the antioxidant enzyme system. Until now, the study of root-associated bacteria gained more attraction by the scientific community due to their crucial role in the nutritional, immunity and growth status of the host plant (Reinhold-Hurek and Hurek, 2011; Berendsen et al., 2012; Backer et al., 2018). Moreover, previous studies demonstrated that irrigation with water containing pharmaceutical compounds can affect both, the root-associated bacteria community as well as the structure of the soil microbial community and

their functional diversity (Bigott et al., 2022; McLain et al., 2022). Further studies attempted to explore the possible connection between plant microbiome communities and degradation/metabolization of these pharmaceuticals (Zhao et al., 2015; Li et al., 2016, 2020; Nguyen et al., 2019a; Sauvêtre et al., 2020). Considering these facts, we hypothesized that TRD might have an impact on the diversity of the root-associated bacterial community. In the current study, barley (model plant) was used as it is considered a resilient crop which is cultivated in productive agricultural systems as well as in marginal environments. Furthermore, it has significant economical importance as it is used in animal feed, beer production and as food in human diet (Newton et al., 2011).

Therefore, this work aimed to (1) detect the accumulation of TRD in root tissue over time and explore its effects on the activity of antioxidative defence system (Guaiacol peroxidase (GPX), CAT and GSTs) of barley plants grown under hydroponic culture conditions; (2) evaluate the impact of TRD on root-associated bacterial community composition through detecting changes in biodiversity indices (alpha and beta) and relative abundances criteria. The results will provide, for the first time, an understanding of the bacterial groups which might interfere with the process of TRD removal and degradation, as well as illustrate the defence mechanistic system of plants towards this opioid.

## 2. Materials and methods

### 2.1. Chemicals

Tramadol HCl (TRD, 99 %), cis-Tramadol- $^{13}\text{C}$ , D<sub>3</sub>-hydrochlorid solution (TRD-D<sub>3</sub>, 100  $\mu\text{g mL}^{-1}$  in methanol), 1-chloro-2,4-dinitrobenzene (CDNB), *p*-nitrophenyl acetate (pNPA), disodium hydrogen citrate sesquihydrate, trisodium citrate anhydrous, ethylenediaminetetraacetic acid (EDTA), hydrogen peroxide (H<sub>2</sub>O<sub>2</sub>, 35 %) and bovine serum albumin (BSA) were purchased from Sigma-Aldrich (Germany), acetonitrile HPLC-grade, polyvinylpyrrolidone K90 (PVP K90), hydrochloric acid (HCl, 32 %), ammonium sulphate, and 1,4 dithioerythritol were acquired from Carl Roth® GmbH + Co. KG (Karlsruhe, Germany), magnesium sulphate anhydrous from Chemsolute® (Renningen, Germany), sodium chloride (NaCl) and formic acid (HPLC-grade) from Merck (Darmstadt, Germany), L-glutathione reduced (GSH) and guaiacol were obtained from Fluka and acridine-D<sub>9</sub> was obtained from LGC Labor GmbH (Augsburg, Germany).

### 2.2. Plant acclimatization and growth conditions

Barley seeds (*Hordeum vulgare* L., cv. ‘Salome’; provided by Nordsaat Saatzeit GmbH [Langenstein, Germany]) were surface sterilized, propagated on sterilized perlite for 3–5 days and then moved to a hydroponic growth system in a growth chamber. The system consisted of four plastic trays with a 10 L capacity, each harbouring 24 seedlings. The seedlings were kept in distilled (dist.) water for three days, transferred then to half-strength (50 %) of modified Hoagland's solution for seven days, and finally maintained at full-strength (100 %) modified Hoagland's (Table S1) solution (pH 5.8; Taiz and Zeiger, 2010) for one month; the nutrient solution was renewed once a week. The plants were kept in controlled environmental conditions as mentioned by Khalaf et al. (2022).

### 2.3. Experimental design and sampling procedures

After the one-month acclimatization period, barley plants were transferred into a hydroponic system consisting of 3 L glass containers randomly divided into five groups depending on harvesting time (T<sub>0</sub>, T<sub>1</sub> & T<sub>2</sub>) and treatment status (control & treated). Three independent replicates (with five plants, each) were used and containers were distributed randomly in the growth chamber under the conditions previously specified by Khalaf et al. (2022). In this experiment, controls represent plants growing only on the nutrient solution, while the treated ones were additionally supplemented with 100  $\mu\text{g L}^{-1}$  TRD, only at the beginning of the experiment, which is close to the highest concentration detected in WWTP effluents

(Kasprzyk-Hordern et al., 2009). T0 plants were collected at the beginning of the experiment, while T1 plants were collected after 12 days and T2 after 24 days (Fig. S1). At each time point, the collected plants were divided into roots and shoots; roots were then washed with dist. water (4 times), and then weighed and frozen at  $-80^{\circ}\text{C}$  until further analysis. During the experimental period, water loss due to transpiration was compensated.

#### 2.4. Sample treatment and instrument analyses

To prepare samples for TRD quantification, roots were ground and homogenized under liquid nitrogen. A modified QuEChERS methodology, as previously described by Khalaf et al. (2022), was used for TRD extraction. Briefly, 0.25 g of homogenized root tissue was spiked with 20  $\mu\text{L}$  of the surrogate acridine- $\text{D}_9$  (ACR- $\text{D}_9$ ; 12.5 ppm), vortexed and mixed with 2.5 mL of acetonitrile, then vigorously shaken and vortexed. Thereafter, salts mixture (1 g  $\text{MgSO}_4$  anhydrous, 250 mg trisodium citrate anhydrous, 250 mg NaCl, 125 mg disodium hydrogen citrate sesquihydrate) was added to the previous mixture then vigorously shaken, vortexed and subsequently centrifuged (Allegra X-12 centrifuge, Beckman Coulter) for 10 min at  $3273 \times g$  (3750 rpm). The upper phase was then collected and filtered via 0.2  $\mu\text{m}$  SPARTAN™ 13/0.2 RC filter (Whatman™; GE Healthcare Life Sciences, Little Chalfont, Germany). Prior injection, the filtrates were supplemented with formic acid (final concentration 0.1 %) and spiked with internal standard TRD- $\text{D}_3$  (20  $\mu\text{g L}^{-1}$ ). Samples were then injected ( $3 \times 10 \mu\text{L}$ ) via an autosampler (Dionex UltiMate 3000TRS, Gering, Germany) into an UHPLC (Dionex UltiMate 3000RS, Gering, Germany) coupled to a triple quadrupole mass spectrometer (Thermo Scientific HESI-MS/MS, TSQ Quantum Access Max, San Jose, USA), following the analytical setup described in Khalaf et al. (2022). Samples were quantified against a six point-calibration curve (in matrix, ranging from 3.75 to 120  $\mu\text{g L}^{-1}$ ) after integration using the Xcalibur software (ver. 4.1). The performance of the method was checked using method blanks (solvent and biological controls), a quality control (30  $\mu\text{g L}^{-1}$ ), and weekly, new calibration curves.

#### 2.5. Crude enzyme extraction

The activity of GSTs and other antioxidant enzymes was determined in crude enzyme extracts as described by Schröder et al. (2005). Briefly, three grams of ground sample were extracted at  $4^{\circ}\text{C}$  using a stirring ice bath for 30 min in 10 fold (w/v) 100 mM Tris/HCl buffer pH 7.8 that contain 1 % Nonidet P40, 1 % PVP K90, 5 mM ethylenediaminetetraacetic acid (EDTA) and 5 mM dithioerythritol. Then, the extract mixture was centrifuged (Avanti™ J-25 centrifuge, Beckman Coulter) at  $4^{\circ}\text{C}$  and  $47,808 \times g$  (20,000 rpm) for 30 mins. Proteins were precipitated from the supernatant by stepwise addition of ammonium sulphate (grounded to powder) to reach 40 % (step 1) and 80 % (step 2) saturation, respectively. By the end of each step, extracts were centrifuged (Avanti™ J-25 centrifuge, Beckman Coulter) at  $4^{\circ}\text{C}$  and  $47,808 \times g$  (20,000 rpm) for 30 and 45 mins, respectively. After the last centrifugation step, the collected pellets were resuspended in 2.5 mL of 25 mM Tris/HCl buffer pH 7.8 and subsequently desalted using PD 10 columns (GE Healthcare, UK). The desalted crude enzyme extracts were eluted using Tris/HCl buffer (25 mM, pH 7.8) then divided into several aliquots and stored at  $-80^{\circ}\text{C}$  until further analysis.

#### 2.6. Spectrophotometric enzyme assays

All enzyme activities were quantified using a 96-well spectrophotometer (Spectra MAX 190, Molecular devices, Germany). Guaiacol peroxidase (GPX) activity was measured at 420 nm by following the oxidation of guaiacol in presence of  $\text{H}_2\text{O}_2$  to tetraguaiacol ( $\epsilon = 26.6 \text{ mM}^{-1} \text{ cm}^{-1}$ ) (Bigott et al., 2021). The crude enzymes were added to a mixture of guaiacol and  $\text{H}_2\text{O}_2$  in 50 mM Tris/HCl buffer (pH 6.0). CAT activity was determined by tracking the decomposition of  $\text{H}_2\text{O}_2$  at 240 nm ( $\epsilon = 0.036 \text{ mM}^{-1} \text{ cm}^{-1}$ ) (Verma and Dubey, 2003). The reaction was started by mixing the enzyme extracts with  $\text{H}_2\text{O}_2$  in potassium phosphate buffer 100 mM (pH 7). For GST, two model substrates were used to determine

its activity; 1-chloro-2,4-dinitrobenzene (CDNB), and *p*-nitrophenyl acetate (pNPA) (Habig et al., 1974; Schröder et al., 2008). For the assay, desalted aliquots of crude enzyme extract were incubated with each substrate, L-glutathione reduced (GSH) and 100 mM buffer either Tris/HCl pH 6.4 or potassium phosphate pH 7.0 in case of CDNB and pNPA, respectively. The formation of the respective GS-conjugates was followed at 340 nm ( $\epsilon = 9.6 \text{ mM}^{-1} \text{ cm}^{-1}$ ) for CDNB and at 400 nm ( $\epsilon = 8.79 \text{ mM}^{-1} \text{ cm}^{-1}$ ) for pNPA, where  $\epsilon$  refers to the extinction coefficient for each substrate. Blank samples, using the elution buffer instead of enzyme extract in the reaction mixture, were included for each assay. For specific enzyme activity calculations, protein contents were measured in the same aliquots used for enzyme assay following the standard method of Bradford (1976) and using a bovine serum albumin calibration curve. Enzyme activity is expressed as units of  $\mu\text{kat mg}^{-1}$  protein, where 1 kat (katal) is defined as the formation of 1 mol product per second in the specific enzyme assay. Statistical analyses for enzyme measurements were evaluated by unpaired *t*-tests using the GraphPad Prism website ([www.graphpad.com/quickcalcs/ttest1.cfm](http://www.graphpad.com/quickcalcs/ttest1.cfm)).

#### 2.7. Nucleic acid extraction

Total DNA was extracted from 0.3 g of previously ground root material using NucleoSpin® Soil Kit (Macherey-Nagel, Düren, Germany), following the manufacturer's instructions. SL1 buffer was used for cell lysis of root-associated bacteria. Negative extraction controls were included using extraction tubes either empty or supplemented with liquid nitrogen. The concentration of extracted DNA was quantified using Quant-iT™ Pico Green® dsDNA assay Kit (Thermo Fisher Scientific, Darmstadt, Germany) following the manufacturer's instructions. DNA extracts were stored at  $-80^{\circ}\text{C}$  for further steps.

#### 2.8. Library preparation and sequencing

Polymerase chain reaction (PCR) was performed using the NEBNext High-Fidelity 2 × PCR Master Mix (New England Biolabs, Frankfurt am Main, Germany) and the primer set 335F (CADACTCCTACGGGAGGC)/769R (ATCCTGTTTGMCCCVCR), which targets the V3-V4 regions of the bacterial 16S rRNA gene while inhibiting chloroplast amplification (Dorn-In et al., 2015). The reaction mixture consisted of 12.5  $\mu\text{L}$  of the PCR master mix, 0.5  $\mu\text{L}$  from each primer (10 pmol  $\mu\text{L}^{-1}$ ), 2.5  $\mu\text{L}$  of 3 % BSA, 8  $\mu\text{L}$  of DEPC water and 1  $\mu\text{L}$  of DNA template (5 ng  $\mu\text{L}^{-1}$ ). PCR conditions were: initial denaturation step for 60 s at  $98^{\circ}\text{C}$ , followed by 25 cycles starting at  $98^{\circ}\text{C}$  for 10 s (denaturation), 30 s at  $60^{\circ}\text{C}$  (annealing) and ended at  $72^{\circ}\text{C}$  for 30 s (extension); then, a final extension step at  $72^{\circ}\text{C}$  for 5 min. DEPC water was used as non-target control. The quality of PCR products was checked on 2 % agarose gel. PCR products were purified using Agencourt AMPure XP beads (Beckman Coulter, United States). DNA quantity and quality were checked using the Fragment Analyzer device (Agilent Technologies, Santa Clara, CA, United States). Indexing PCR using Nextera XT Index Kit v2 (Illumina, San Diego, CA, United States) was performed in a total volume of 25  $\mu\text{L}$ : 12.5  $\mu\text{L}$  NEBNext High-Fidelity 2 × PCR Master Mix, 2.5  $\mu\text{L}$  of each index, 6.22  $\mu\text{L}$  of DEPC water and 1.28  $\mu\text{L}$  of DNA template (7.8 ng  $\mu\text{L}^{-1}$ ). PCR started with initial denaturation for 30 s at  $98^{\circ}\text{C}$ ; then 8 cycles of 10 s at  $98^{\circ}\text{C}$ , 30 s at  $55^{\circ}\text{C}$  and 30 s at  $72^{\circ}\text{C}$ ; and ended with a final elongation step at  $72^{\circ}\text{C}$  for 5 min. Indexed PCR products were purified and then quantified as mentioned above and thereafter all samples were pooled in an equimolar ratio of 4 nM. Subsequently, pooled samples were sequenced with Illumina Miseq platform (Illumina, San Diego, CA, United States) using Reagent Kit v3 (600 cycles).

#### 2.9. Data processing and analyses

The amplicon sequencing generated 323,7 MB of raw reads. Firstly, the reads were trimmed using Cutadapt (v4.1; Martin, 2011). In the R environment (v4.2.2; R Core Team, 2022), the Bioconductor package dada2 (v1.26; Callahan et al., 2016) was firstly used for quality filtering and

**Table 1**

Root fresh weights (g), concentration of TRD ( $\mu\text{g g}^{-1}$  in total root FW) detected in roots and final pH values in the external medium at both time points T1 and T2; each value represents the mean of three independent replicates  $\pm$  SD.

	T1		T2	
	Control	TRD	Control	TRD
Root FW(g)	48.56 $\pm$ 3.72	50.30 $\pm$ 6.76	61.60 $\pm$ 6.36	64.97 $\pm$ 7.43
TRD conc. ( $\mu\text{g g}^{-1}$ in total root FW)	ND	111.74 $\pm$ 8.62	ND	138.39* $\pm$ 14.02
Final pH in medium	6.31 $\pm$ 0.20	6.40 $\pm$ 0.27	6.93 $\pm$ 0.17	7.03 $\pm$ 0.25

ND: not determined; symbol(\*) means significant differences ( $p$ -value  $\leq$  0.05) between T2 and T1.

denoising (full specification about the reads per each sample presented in Table S2), then to infer amplicon sequence variants (ASVs) and to map ASVs against SILVA rRNA database (v138.1, SSU Ref NR 99; release date: 27-08-20; Quast et al., 2013). The dada2 pipeline produced a total of 529,143 reads among 387 ASVs. Rarefaction curves showed that all samples were sequenced almost at saturation except for a single sample which was subject to a higher sequencing intensity (Fig. S2). Scripts used for the analyses are available in a public repository ([https://github.com/rsiani/tramadol\\_barley\\_2021](https://github.com/rsiani/tramadol_barley_2021)). After filtering out non-bacterial and chloroplast ASVs (1 ASV, 32 reads), 529,111 reads remained, with a median of 27,549 per sample. Count and taxonomy tables (386 ASVs) were imported in a phyloseq-class object (v1.42; McMurdie and Holmes, 2013). Shannon entropy and Simpson diversity indices were estimated using the function “divnet” (DivNet v0.40; Willis and Martin, 2022) as metrics of alpha diversity. A principal component analysis (PCA) was performed on the centred-log ratio (CLR) transformed count data to visualize beta diversity (Aitchison et al., 2000) and variance of the samples (vegan, v2.6.4). Differentially abundant ASVs across the classes were identified using

the “ancombe” function (ANCOMBC, v2.0.1; Lin and Peddada, 2020). All the raw sequence reads produced in the study have been deposited under the BioProject PRJNA939407 in the NCBI Sequence Read Archive database (<https://www.ncbi.nlm.nih.gov/sra>).

### 3. Results and discussion

#### 3.1. Uptake of TRD by barley roots

TRD concentration in roots increased significantly throughout the exposure time, reaching the highest levels (138.39  $\mu\text{g g}^{-1}$  in total root FW) in root tissues after 24 days (T2) of the experiment (Table 1). This result revealed the easy uptake of TRD by barley roots, which may be due to physico-chemical properties such as molecular weight (MW, 263.37),  $\log K_{ow}$  (2.45) and number of H-bonds (acceptors = 3, donors = 1) (Limmer and Burken, 2014; Kumar and Gupta, 2016). Moreover, the cationic nature of TRD, as well as its small size may induce its attraction to plant roots by electrostatic force (Miller et al., 2016; Li et al., 2019), and allow for symplastic entry with the water flow (Chuang et al., 2019; Bigott et al., 2020). Indeed, in our previous study (Khalaf et al., 2022), we showed short-term uptake of TRD by excised roots from cattail and barley plants using the Pitman-chamber technique. Furthermore, we quantified the uptake of TRD by barely seedling roots besides its transport to the aerial parts.

#### 3.2. Effect of TRD on GPX and CAT activities

GPX activities increased in both shoots and roots over time in treated plants, while these activities were more stable in shoots of control plants (Fig. 1 A&B). In addition, GPX activities were 1.8-fold (T1) and 5.47-fold (T2) higher ( $p$ -value  $\leq$  0.05) in treated plant roots when compared to control ones. These results reflect the predicted response of GPX towards TRD

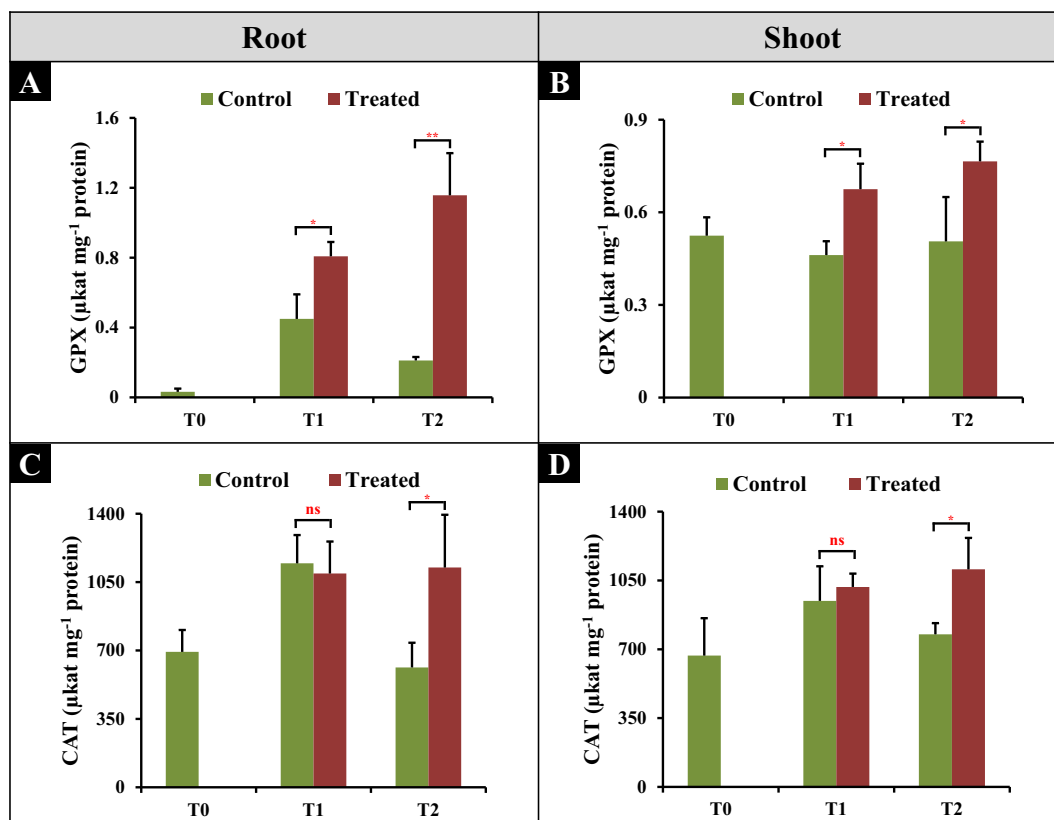


**Fig. 1.** Effect of 100  $\mu\text{g L}^{-1}$  TRD treatment on GPX (A&B) and CAT (C&D) activities in barley roots (A&C) and shoots (B&D) over time. Data are represented as mean of three replicates  $\pm$  SD. Significant differences between treated and control plants are indicated according to unpaired  $t$ -test as “ns” for  $p$ -value  $>$  0.05, “\*” for  $p$ -value  $\leq$  0.05, “\*\*” for  $p$ -value  $\leq$  0.01, “\*\*\*” for  $p$ -value  $\leq$  0.001 and “\*\*\*\*” for  $p$ -value  $\leq$  0.0001.



inside barley tissues and their behaviour after accumulation of TRD within barley roots across time. GPX is a heme-containing enzyme group with high specificity for phenolic substrates. GPXs are located intra- (cytosol and vacuole), and extracellularly (cell wall) and play a crucial role in protecting the plant against oxidative stress through consumption of  $H_2O_2$  released either during normal metabolism or in stress conditions (Das and Roychoudhury, 2014). Stimulation of GPX activity has been shown under various environmental stressors such as salinity,  $\gamma$ -radiation, drought, and heavy metal contamination (Shah et al., 2001; Verma and Dubey, 2003; Sharma and Dubey, 2005; Mishra et al., 2013; Nahar et al., 2018). In accordance with our results, previous studies recorded a significant increase of GPX activities in different plants such as cattail, yellow lupin and lettuce when they were treated with pharmaceutical compounds such as carbamazepine, clofibrac acid, diclofenac or tetracycline (Dordio et al., 2009, 2011; Bartha et al., 2014; Rydzynski et al., 2017; Leitão et al., 2021b). These increments were recorded after exposing plants to higher pharmaceutical concentrations, at least 5 times more than the concentration used in the current study ( $100 \mu\text{g L}^{-1}$  of TRD), which reflects the ability of TRD, even in low concentrations, to induce GPX activity. Huber et al. (2016) showed the ability of plant peroxidases in diclofenac oxidation to activate it for further conjugation. Thus, the current induction in GPX activities can be explained as an antioxidative reaction due to the accumulation of TRD in roots as well as its translocation to the shoot parts or it might be due to active contribution in oxidizing and transforming TRD for subsequent conjugation steps in the TRD detoxification/metabolization cycle.

CAT activities in the roots and shoots of control and treated plants were similar after T1 (Fig. 1 C&D). However, CAT activities at T2 increased by 1.83-fold and 1.43-fold in roots and shoots, respectively, of TRD-treated plants compared to controls. Different to GPX, CAT enzymes are localized in peroxisomes (main  $H_2O_2$  production spot), cytosol and mitochondria where they convert  $H_2O_2$  into  $H_2O$  and  $O_2$  (Willekens et al., 1995; Mittler, 2002; Das and Roychoudhury, 2014). Alteration in CAT activity

has been explained as an adaptive mechanism to regulate  $H_2O_2$  levels in the plant cells. Previous studies conducted on umbrella papyrus (*Cyperus alternifolius*) plants or yellow lupin (*Lupinus luteus*) seedlings showed increased CAT activity, in short time periods, after exposure to oxybenzone ( $25 \mu\text{M}$ ,  $5.7 \text{ mg L}^{-1}$ ) for 3 days and to ciprofloxacin or tetracycline ( $90 \text{ mg kg}^{-1}$ ) for 10 days, respectively (Chen et al., 2017; Rydzynski et al., 2017). Other studies recorded elevated CAT activities in leaves after exposing lettuce and cattail plants to acetaminophen (0.1, 1 and  $2 \text{ mg L}^{-1}$ ) and clofibrac acid (0.5, 1 and  $2 \text{ mg L}^{-1}$ ), respectively (Dordio et al., 2009; Leitão et al., 2021a). Alkmin et al. (2019), noticed that the highest increments of CAT activities depend on the concentration of the pharmaceutical ( $0.032 \mu\text{g L}^{-1}$  chlorpromazine,  $25 \mu\text{g L}^{-1}$  acetaminophen,  $100 \mu\text{g L}^{-1}$  diclofenac, respectively) applied to *Lemna minor* compared to the controls. Thus, the elevated CAT activities, in conjunction with GPX, indicate that both enzymes function together in preserving the equilibrium of  $H_2O_2$  content inside TRD-treated plants, which in turn suggests that both enzymes gave a positive antioxidant response to quench ROS in both root and shoot cells. Moreover, GPX and CAT could be considered as biomarkers of TRD effects on plants.

### 3.3. Effect of TRD on GST activity

GST activity was determined spectrophotometrically, following the conjugation of GSH with CDNB or pNPA using root and shoot crude enzyme extracts (Fig. 2). GST measurements showed more or less stable activities in the roots and shoots of control plants with both substrates (except for the decrement of GST-CDNB activity in the roots at T2). GST activities significantly increased ( $p$ -value  $\leq 0.05$ ) by 3.23-fold and 2.09-fold towards CDNB and pNPA, respectively, in roots of treated plants, compared to controls at T2 (Fig. 2 A&C), indicating a plant reaction due to the accumulation of TRD in root tissues at T2 as shown in Table 1. In barley shoots, GST activities increased significantly ( $p$ -value  $\leq 0.05$ ) upon TRD-treatment at

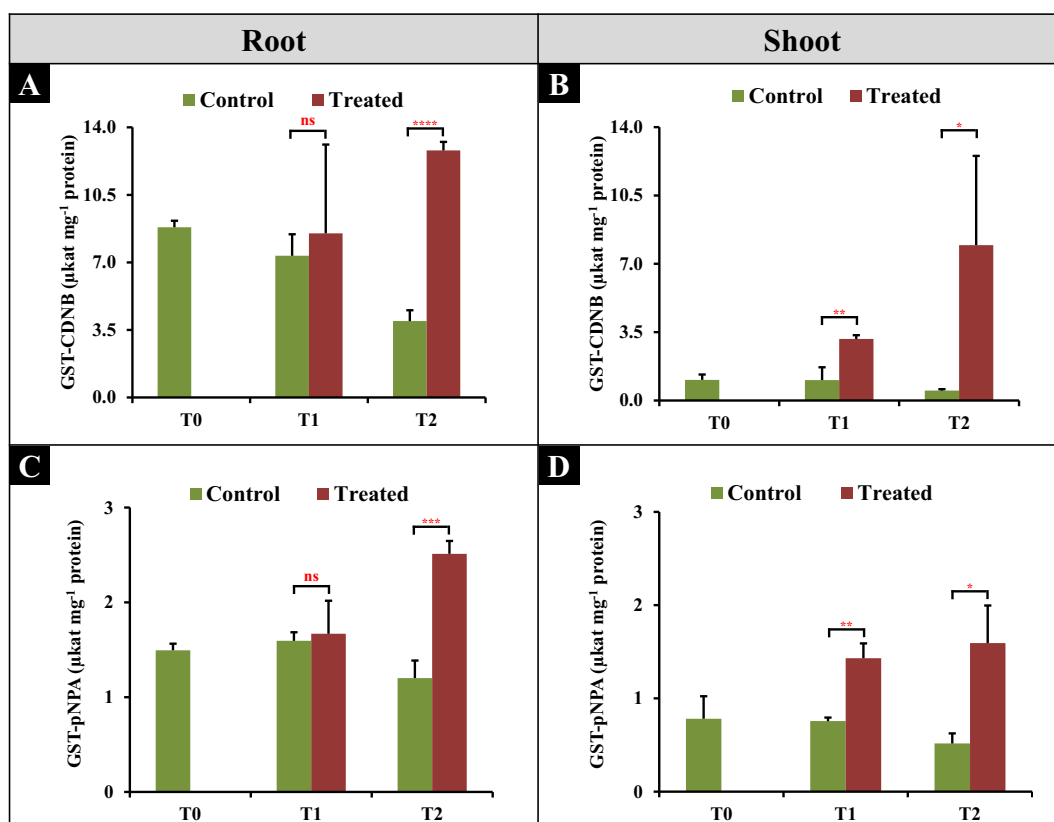


Fig. 2. Effect of  $100 \mu\text{g L}^{-1}$  TRD treatment on GSTs activities in barley roots and shoots over time. Measurement of GSTs activity was based on GSH-CDNB (in root A, shoot B) and GSH-pNPA (in root C, shoot D) conjugation. Data are represented as the mean of three replicates  $\pm$  SD. Significant differences between treated and control plants are indicated according to unpaired t-test as “ns” for  $p$ -value  $> 0.05$ , “\*” for  $p$ -value  $\leq 0.05$ , “\*\*” for  $p$ -value  $\leq 0.01$ , “\*\*\*” for  $p$ -value  $\leq 0.001$  and “\*\*\*\*\*” for  $p$ -value  $\leq 0.0001$ .

both time points (T1 and T2) with CDNB and pNPA substrates (Fig. 2 B&D). Moreover, GST activities towards both substrates in roots reached higher values compared to those in the shoots. Changes in GST activities for both substrates in TRD-treated plants, over time, strengthen the idea that this increment can be related to TRD conjugation/metabolism processes as the GSTs considered one of the key enzymes in the “Green Liver” theory for xenobiotic metabolism. Furthermore, this induction could be due to oxidative burst caused by TRD as normal behaviour for plants towards foreign compounds. This can be supported by the significant increase in TRD concentrations in barley roots over the time (Table 1). Cummins et al. (2011) illustrated the different roles of plant GSTs in xenobiotic detoxification. Additional studies reported that oxidative stress is a common inducer of GSTs and they can be involved in the detoxification processes through conjugating metabolites evolving from oxidative damage (Edwards et al., 2000; Schröder, 2001; Sappl et al., 2009; Lee et al., 2014). In line with our observations, Bartha et al. (2014), recorded higher activities of GST towards CDNB and pNPA in roots ( $\sim 1 \mu\text{kat mg}^{-1}$  protein for CDNB and  $\sim 2.5 \mu\text{kat mg}^{-1}$  protein for pNPA) compared to those in shoots ( $\sim 0.25 \mu\text{kat mg}^{-1}$  protein for CDNB and  $\sim 0.9 \mu\text{kat mg}^{-1}$  protein for pNPA) of cattail plants exposed to diclofenac ( $1 \text{ mg L}^{-1}$ ) for 7 days. Also, Sun et al. (2018), showed the induction of GST-CDNB activities in cucumber seedlings exposed to PPCPs cocktail (17 compounds, at 0, 0.5, 5 and  $50 \mu\text{g L}^{-1}$ ) for 7 days. Furthermore, Sun et al. (2019) showed that acetaminophen ( $5 \text{ mg L}^{-1}$ ) increased GST activity towards CDNB in roots (by 1.30- to 1.60-fold) and leaves (1.07- to 1.94-fold) in treated cucumber seedlings compared to those of controls. The previous results along with our findings revealed the induction in GSTs activities in response to pharmaceutical exposure trying either to conjugate and detoxify these compounds

or to eliminate the oxidative burst resulting from their presence as foreign compounds inside plant tissues.

### 3.4. Impact of TRD treatment on bacterial diversity and community composition

The microbiome is considered as one of the key players in determining overall plant health as well as adaptability to diverse environmental conditions (Berendsen et al., 2012; Trivedi et al., 2020). In the current study, we assessed differences in alpha diversity of the root-associated bacterial community with Shannon and Simpson indices. For both metrics, we did not find statistically significant differences (Holm's corrected Welch's t-test,  $\alpha = 0.05$ ) between control and treated plants (Fig. 3). Despite being small in magnitude, the observed trends in alpha diversity metrics indicate that the treatment has a discernible impact on the root-associated community. This could be explained by a direct response to the TRD treatment and/or to changes in exudation patterns, metabolism and/or immunity system of the host plants (Rohrbacher and St-Arnaud, 2016; Thijs et al., 2016; Rolfe et al., 2019). This is also supported by the work of Li et al. (2020), who noticed distinct rhizospheric bacterial communities at different developmental stages of cattail (*Typha angustifolia*) plants in the wetlands treated with ibuprofen compared to controls and attributed that to modifications in root exudation which caused by ibuprofen. At T2, both communities converge to middle values which points to the transitory nature of the suggested effects. Effects of the treatment, in particular on the community structure, can be still appreciated at T2.

The PCA was carried out to visualize the changes in the bacterial communities in TRD-treated and non-treated plant groups over time (Fig. 4). The PCA separates those barley plants which were treated with TRD from

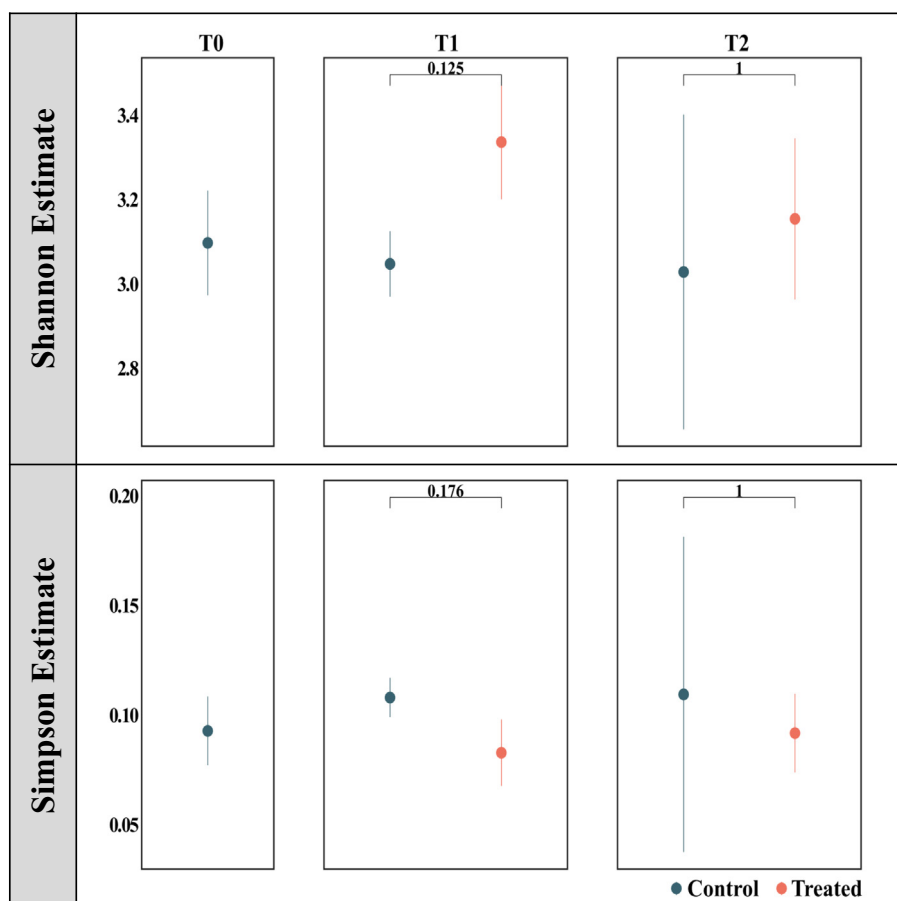


Fig. 3. Variability of the Shannon and Simpson alpha diversity indices between control and treated roots. Control: growing on the nutrient solution, Treated: growing on nutrient solution supplemented with  $100 \mu\text{g L}^{-1}$  TRD; T0, T1 and T2 refer to harvesting points at 0, 12 and 24 days from the beginning of the experiment. The Holm's corrected  $p$ -values from Welch's t-test ( $\alpha = 0.05$ ) between control and treated plants are shown for T1 and T2.

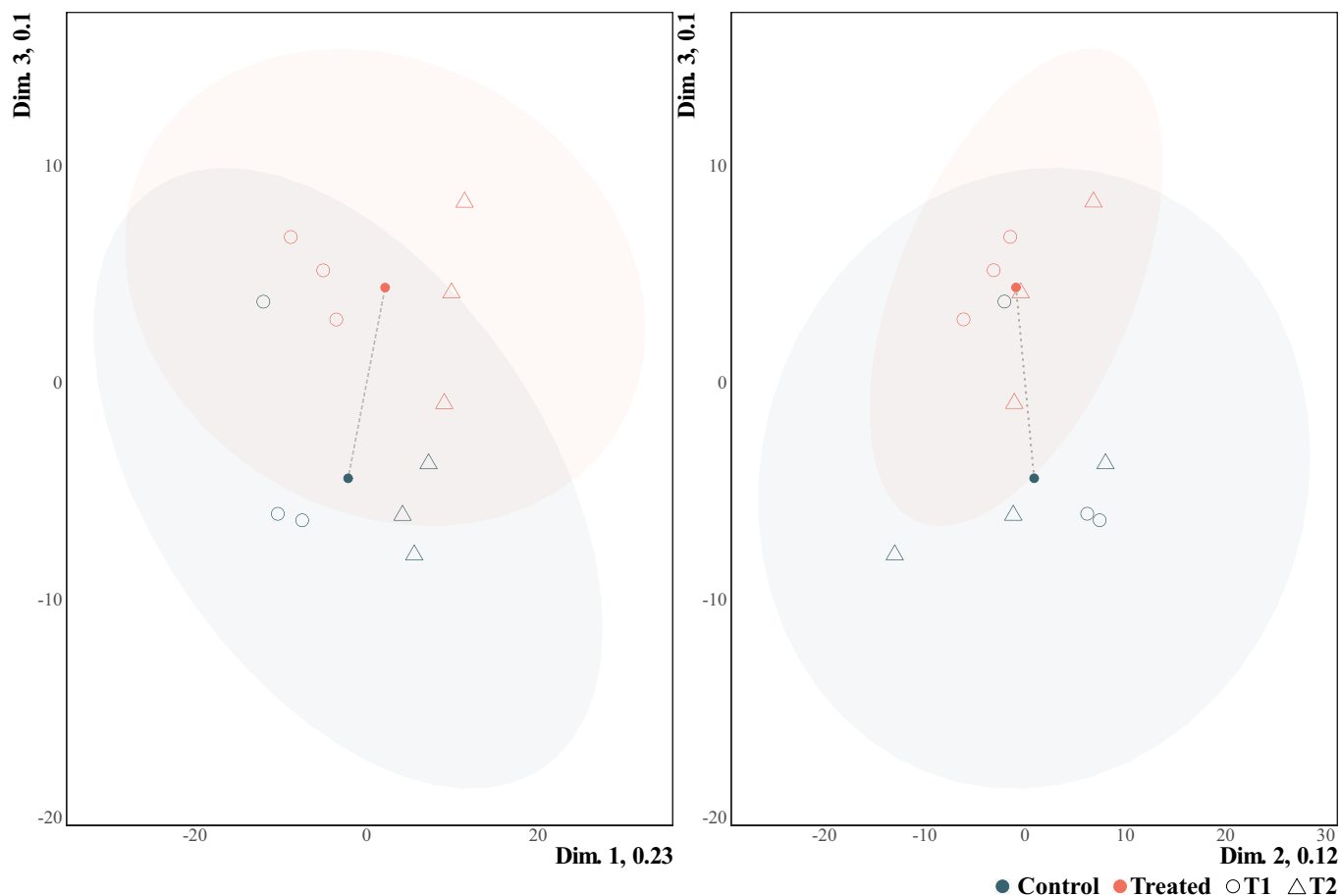


Fig. 4. PCA of CLR-transformed ASVs observed count abundances of root-associated bacteria from control plants and those treated with  $100 \mu\text{g L}^{-1}$  TRD at two different time points; T1 (12 days) and T2 (24 days).

the control ones over the 3rd component (accounting for 10 % of the variance). The first component (23 % of the variance) positively correlates with sampling time. PERMANOVA analysis showed that both time and treatment have a significant effect on the bacterial community composition (Table 2). Moreover, there was no interaction between time and treatment in the bacterial communities. Whilst alpha diversity indices converge to a similar level at T2, the community compositions remain altered throughout the experiment. Possibly, after the initial application of a disturbance, the communities reach two alternative stable states. In the absence of the following time points, no conclusions can be drawn on whether the two configurations would ultimately coalesce, after any residual effect of the treatment is eliminated, or if stochastic processes would lead the communities further astray.

Several studies showed that time and plant developmental stages, such as seedling, booting and spike formation stages, cause a noticeable shift in microbial diversity and community composition (Dombrowski et al., 2017; Yang et al., 2017b; Ussyskin-Tonne et al., 2021; Xiong et al., 2021).

**Table 2**

Test statistics from PERMANOVA reporting the effect of time, treatment and the interaction of time and treatment on beta diversity. Significant differences are designated as “ns” for  $p$ -value  $> 0.05$ , “\*” for  $p$ -value  $\leq 0.05$ , “\*\*” for  $p$ -value  $\leq 0.01$ , “\*\*\*” for  $p$ -value  $\leq 0.001$  and “\*\*\*\*” for  $p$ -value  $\leq 0.0001$ .

	Df	R <sup>2</sup>	F	p-Value
Time	1	0.239	4.644	0.0001****
Treatment	1	0.111	2.153	0.023*
Time: Treatment	1	0.083	1.620	0.074 <sup>ns</sup>
Residual	11	0.567	NA	NA
Total	14	1.000	NA	NA

Moreover, other studies showed that exposing lettuce plants to a mixture of pharmaceuticals with different concentrations caused changes in the community structure of root-associated bacteria (Cerqueira et al., 2020; Bigott et al., 2022). These studies are in accordance with our findings, indicating that both time and TRD treatment had an effect on root-associated bacterial community in barley (Table 2).

We further analysed the active bacterial groups associated with barley roots growing in hydroponic culture either supplemented with or without TRD (Fig. S3). The relative abundance data revealed that root-associated bacterial communities of barley plants were dominated by 16 major families at all time points (for all the treatments). According to the relative abundance values, at the beginning of the experiment (T0), the family Rhizobiaceae (10.02 %) followed by Comamonadaceae (6.76 %) were the most prominent families while Methylophilaceae (0.94 %), Weeksellaceae (0.94 %) and Azospirillaceae (0.93 %) comprised families with lowest abundance. However, over time, a noticeable change in the relative abundance of Xanthomonadaceae was detected. It's worthwhile to mention that this family was more pronounced (10.35 %) in the TRD-treated group compared to control ones (7.17 %) at T2 and comprised the dominating family at this time-period. Moreover, the relative abundances of Rhizobiaceae (at T1 and T2), Rhodanobacteraceae (at T1) and Rhodocyclaceae (at T2) were slightly enriched in barley plants exposed to TRD compared to controls (Fig. S3). Also, relative abundance values revealed that Methylophilaceae was only represented in TRD-treated group while Pseudomonadaceae and Enterobacteriaceae appeared only in control plants at T1.

In agreement with our results, Rutere et al. (2020), recorded enrichment in the relative abundance of Xanthomonadaceae in sediment microcosms supplemented with ibuprofen. Wang et al. (2018), showed

that Methylophilaceae and Rhizobiaceae, with few other families, were the predominant candidates in ketamine and methamphetamine biodegradation. Methylophilaceae were originally linked to methanol degradation (Kalyuhznaya et al., 2009). Since the metabolism of TRD goes firstly through O- and N-demethylation (Gong et al., 2014), this may explain the relative enrichment of Methylophilaceae at T1 only in the TRD-treated group. Li et al. (2016), suggested the possibility of Rhodocyclaceae and the genus *Ignavibacterium* in ibuprofen degradation after their obvious increase in the wetland bed planted with *Typha angustifolia*. The previous findings, along with our observations, indicate a potential positive contribution of the mentioned families in the biodegradation/metabolization process of pharmaceutical compounds.

When the ANCOMBC method was used to isolate differentially abundant bacterial ASVs between treated and non-treated plants for both time points (Fig. 5), a marked enrichment of multiple ASVs at T1 and T2 were observed, with more differentially abundant ones at T2 compared to T1 in TRD-treated plants, which may be due to increasing of TRD concentration over time inside root tissues (a heatmap visualizing the log-transformed relative abundance of the most differentially abundant taxa in control and treated plants is available as a supplementary figure, Fig. S4). ASVs belonging to Xanthobacteraceae, *Pantoea*, Spirosomaceae, Comamonadaceae, *Hydrogenophaga*, and *Pseudacidovorax* were significantly and differentially abundant at T1 in TRD-treated plants compared to non-treated ones (ANCOMBC, Holm-adjusted  $p$ -values  $\leq 0.05$ ). ASVs belonging to *Pseudoxanthomonas*, *Sphingopyxis*, *Sphingomonas*, Xanthobacteraceae, Pseudomonadaceae, Chitinophagaceae, Hyphomonadaceae, Comamonadaceae, *Pseudacidovorax*, *Hydrogenophaga*, and Bacillaceae were significantly differentially abundant at T2 in barley

roots exposed to TRD (ANCOMBC, Holm-adjusted  $p$ -values  $\leq 0.05$ ). It is noteworthy that the ASVs belonging to *Hydrogenophaga*, U. Xanthobacteraceae and *Pseudacidovorax* were significantly and differentially abundant at both time points (T1 and T2) after exposing barley plants to TRD, which might indicate their detoxification/metabolization role in processes linked to TRD contamination.

Studies demonstrating the effect of TRD on bacterial community composition are scarce. Kostanjevecki et al. (2019), followed the aerobic degradation of TRD using one year-TRD-acclimatized sludge culture and noticed the proliferation of *Xanthobacter* (Xanthobacteraceae), *Methylobacillus* (Methylophilaceae), *Sphingobacterium* (Sphingobacteriaceae) and *Bacillus* (Bacillaceae) genera (without glucose supplementation) in the sludge community. Moreover, the same authors hypothesized that a consortium of *Bacillus*, *Methylobacillus*, *Enterobacter*, *Xanthobacter* and *Sphingobacterium* might play a role in the TRD removal process. The previous findings are in line with our observations, as we noticed the enrichment of Methylophilaceae at T1 only in TRD-treated plants (Fig. S3), in addition to the proliferation of ASVs belonging to Bacillaceae (at T2) and Xanthobacteraceae (at both time points) in TRD-treated plants (Fig. 5). To the best of our knowledge, there is no information available illustrating TRD effect on the rhizospheric or root-associated microbiome structure. However, in line with our observations, Bigott et al. (2022), recorded a significant increase in the relative abundance of the genus *Hydrogenophaga* in lettuce roots by 5-folds after irrigating these plants with wastewater, whereas the same authors noticed an increase in the relative abundance of the clade *Allorhizobium-Neorhizobium-Pararhizobium-Rhizobium* in lettuce roots after irrigation with water or wastewater supplemented with a mixture from 14 PPCPs. Liu et al. (2022) reported an increase in the relative

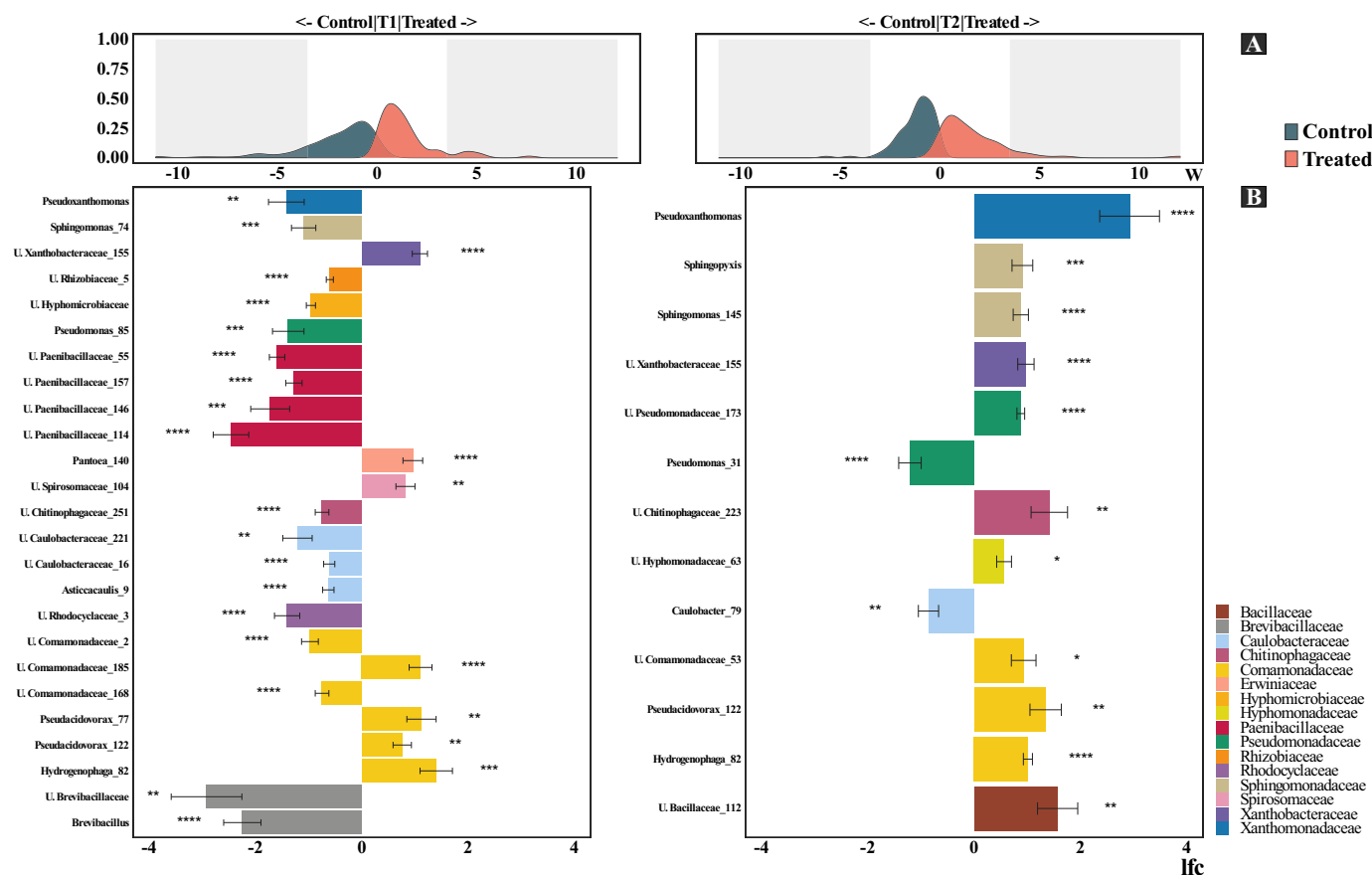


Fig. 5. Differentially abundant ASVs changes over time under TRD treatment. Density curves of the W statistic (ANCOM-BC) for all ASVs are reported as a measure of the treatment effect size (A). The log fold change (lfc), with error bars, of significantly enriched ASVs is displayed in the barplot and each ASV is coloured according to the taxonomic family (B). Level of significance reported by ANCOM-BC is summarized using the convention “\*” for  $p$ -value  $\leq 0.05$ , “\*\*\*” for  $p$ -value  $\leq 0.01$ , “\*\*\*\*” for  $p$ -value  $\leq 0.001$  and “\*\*\*\*\*” for  $p$ -value  $\leq 0.0001$ .



abundances of *Hydrogenophaga*, *Bradyrhizobium* and *Arthrobacter* in both bulk and rhizosphere soil after exposing *Arabidopsis* plants to poly(butylene adipate-co-terephthalate) microplastics. In agreement with our findings, other in vitro studies showed the potential contribution of certain bacterial taxa on pharmaceutical degradation processes. Yi et al. (2022) demonstrated the ability of *Hydrogenophaga* sp. YM1 to degrade atenolol in actual wastewater. Nguyen et al. (2019b) suggested that OTUs closely related to *Pseudacidovorax*, *Nitratireductor* and *Asticcacaulis* might play a role in diclofenac biodegradation after their enrichment in fed-batch bioreactors, inoculated with activated sludge, exposed to diclofenac (50, 500, 5000  $\mu\text{g L}^{-1}$ ). Also, it was demonstrated that *Sphingomonas* sp. strain Ibu-2 can degrade ibuprofen through the removal of the acidic side chain present in this compound (Murdoch and Hay, 2005). Kim et al. (2017) demonstrated the possible contribution of specific phylotypes including *Sphingomonas*, *Beijerinckia*, unknown Cytophagaceae and *Methylophilus* in PPCPs biodegradation. Also, the same authors concluded the huge impact of microbial community structure, or the source of this community, on efficiencies and rates of PPCPs transformation. Moreover, other *Sphingomonas* isolates showed the ability to degrade other contaminants such as dicamba (herbicide), nicotine and phenanthrene (Pinyakong et al., 2000; Yao et al., 2016; Wang et al., 2017), which reflects the active contribution of this genus in degradation/detoxification of trace organic contaminants. Lu et al. (2019) showed the ability of *Pseudoxanthomonas* sp. strain DIN-3 to degrade diclofenac, naproxen and ibuprofen (50  $\mu\text{g L}^{-1}$ ) by 23, 39 and 41 % after 14 days incubation time. Aguilar-Romero et al. (2021) showed the ability of *Sphingopyxis granuli* RW412, recovered from river sediment, to remove ibuprofen (2 mM) from a biopurification system. The previous findings strengthen our results, which showed that ASVs assigned to *Hydrogenophaga*, *Pseudacidovorax*, *Sphingomonas*, *Sphingopyxis* and *Pseudoxanthomonas* were differentially abundant in TRD-treated plants compared to controls at T2. This suggests the possible contribution of the relatively abundant ASVs, from both time points, in the metabolization/detoxification of TRD inside the plant. Moreover, several studies showed the positive impact of these taxa, as plant growth promoters (Dias et al., 2009; de Souza et al., 2013; Asaf et al., 2020; Boss et al., 2022; Ilangumaran et al., 2022; Umapathi et al., 2022), which in our case, can aid the barley plants to adapt/overcome the TRD-contamination condition.

#### 4. Conclusion

The current work demonstrates the effect of TRD on plant performance as well as its repercussion on the root-associated bacteria community, after 12 and 24 days of exposure. Results showed that TRD accumulated in barley roots over time revealing an easy uptake of this cationic compound. The accumulation of TRD in barley roots is concomitant with an oxidative burst accompanied by increasing activities of GPX and CAT. Furthermore, noticeable inductions in GST activities, in both root and shoot tissues, were recorded which might influence stress detoxification cycles as well as the TRD metabolization process. Previous findings comply with our hypothesis that TRD affects the plant antioxidant system. The exposure of barley plants to TRD leads to alterations in the root-associated bacterial community composition with a persistent representation of ASVs belonging to certain bacteria (*Hydrogenophaga*, U. Xanthobacteraceae and *Pseudacidovorax*) over time. The former conclusion is in accordance with our second hypothesis postulating the impact of TRD on the bacterial community structure of plant roots. Thus, irrigation of crop plants with TRD-containing water for longer periods might cause a higher accumulation of this compound inside the plant root which in turn might drive drastic changes in both the antioxidant system and the root-associated bacterial community. Studies using plants until the harvesting stage have to be done to confirm the achieved effects on plant performance, as well as crop production quality over a longer time scale. Additionally, further studies should be done to distinguish whether the microbiome changes are due to the direct (linked to TRD metabolization) or indirect (linked to plant physiological changes) effects of TRD. The current study reflects 1) the capacity of barley plants in coping with TRD pollution via antioxidative defence system activation, to protect

themselves against any damage and/or contribute to the metabolization/sequestration processes; 2) the shifting in the root-associated bacterial community to conserve the normal plant health status under TRD pressure, as well as their possible contribution to the TRD metabolization/detoxification processes.

#### CRedit authorship contribution statement

**David M. Khalaf:** Conceptualization, Methodology, Analytical Validation, Data Curation; Formal Analysis, Investigation, Writing - Original Draft, Writing & Editing. **Catarina Cruzeiro:** Analytical Validation, Data Curation; Review & Editing. **Roberto Siani:** Bioinformatic Analysis, Curation Pipeline for Analyzing Amplicon Sequence Data. **Susanne Kublik:** Technical Support for Amplicon Sequencing. **Peter Schröder:** Conceptualization, Writing - Review & Editing, Supervision, Funding acquisition.

#### Data availability

Data will be made available on request.

#### Declaration of competing interest

The authors declare that they have no known competing financial interests or personal relationships that could have appeared to influence the work reported in this paper.

#### Acknowledgements

The authors would like to thank Catholic Academic Exchange Service (KAAD) for the financial support of David M. Khalaf. C. Cruzeiro was funded by the Water Joint Programming Initiative (WATER 21015 JPI) through the European research project IDOUM- Innovative Decentralized and low-cost treatment systems for Optimal Urban wastewater Management, financed by the German Federal Ministry of Education and Research (BMBF). Roberto Siani was supported by a grant provided by German Research Foundation (DFG); SCHL446/38-1 from the Deutsche Forschungsgemeinschaft in the frame of the SPP2125 'Deconstruction and reconstruction of the plant microbiota [DECrypT]'. Additionally, the authors would like to thank Prof. Dr. Michael Schloter for his feedback and valuable input to the article.

#### Appendix A. Supplementary data

Supplementary data to this article can be found online at <https://doi.org/10.1016/j.scitotenv.2023.164260>.

#### References

- Aguilar-Romero, I., De la Torre-Zúñiga, J., Quesada, J.M., Haïdour, A., O'Connell, G., McAmmond, B.M., Van Hamme, J.D., Romero, E., Wittich, R.M., Van Dillewijn, P., 2021. Effluent decontamination by the ibuprofen-mineralizing strain, *Sphingopyxis granuli* RW412: metabolic processes. *Environ. Pollut.* 274, 116536. <https://doi.org/10.1016/j.envpol.2021.116536>.
- Aitchison, J., Barceló-Vidal, C., Martín-Fernández, J.A., Pawłowsky-Glahn, V., 2000. Logratio analysis and compositional distance. *Math. Geol.* 32, 271–275. <https://doi.org/10.1023/A:1007529726302>.
- Alkimi, G.D., Daniel, D., Frankenbach, S., Seródio, J., Soares, A.M., Barata, C., Nunes, B., 2019. Evaluation of pharmaceutical toxic effects of non-standard endpoints on the macrophyte species *Lemna minor* and *Lemna gibba*. *Sci. Total Environ.* 657, 926–937. <https://doi.org/10.1016/j.scitotenv.2018.12.002>.
- Anderson, J.V., Davis, D.G., 2004. Abiotic stress alters transcript profiles and activity of glutathione S-transferase, glutathione peroxidase, and glutathione reductase in *Euphorbia esula*. *Physiol. Plant.* 120, 421–433. <https://doi.org/10.1111/j.0031-9317.2004.00249.x>.
- Asaf, S., Numan, M., Khan, A.L., Al-Harrasi, A., 2020. *Sphingomonas*: from diversity and genomics to functional role in environmental remediation and plant growth. *Crit. Rev. Biotechnol.* 40, 138–152. <https://doi.org/10.1080/07388551.2019.1709793>.
- Backer, R., Rokem, J.S., Ilangumaran, G., Lamont, J., Praslickova, D., Ricci, E., Subramanian, S., Smith, D.L., 2018. Plant growth-promoting rhizobacteria: context, mechanisms of action, and roadmap to commercialization of biostimulants for sustainable agriculture. *Front. Plant Sci.* 9, 1473. <https://doi.org/10.3389/fpls.2018.01473>.







- treatment plants: a review. *Sci. Total Environ.* 596, 303–320. <https://doi.org/10.1016/j.scitotenv.2017.04.102>.
- Yang, L., Danzberger, J., Schöler, A., Schröder, P., Schloter, M., Radl, V., 2017b. Dominant groups of potentially active bacteria shared by barley seeds become less abundant in root associated microbiome. *Front. Plant Sci.* 8, 1005. <https://doi.org/10.3389/fpls.2017.01005>.
- Yao, L., Yu, L.L., Zhang, J.J., Xie, X.T., Tao, Q., Yan, X., Hong, Q., Qiu, J.G., He, J., Ding, D.R., 2016. A tetrahydrofolate-dependent methyltransferase catalyzing the demethylation of dicamba in *Sphingomonas* sp. strain Ndbn-20. *Appl. Environ. Microbiol.* 82, 5621–5630. <https://doi.org/10.1128/AEM.01201-16>.
- Yi, M., Sheng, Q., Lv, Z., Lu, H., 2022. Novel pathway and acetate-facilitated complete atenolol degradation by *Hydrogenophaga* sp. YM1 isolated from activated sludge. *Sci. Total Environ.* 810, 152218. <https://doi.org/10.1016/j.scitotenv.2021.152218>.
- Zhao, C., Xie, H., Xu, J., Xu, X., Zhang, J., Hu, Z., Liu, C., Liang, S., Wang, Q., Wang, J., 2015. Bacterial community variation and microbial mechanism of triclosan (TCS) removal by constructed wetlands with different types of plants. *Sci. Total Environ.* 505, 633–639. <https://doi.org/10.1016/j.scitotenv.2014.10.053>.

## **Appendix M2 (Supplements II)**

This article was published in “Khalaf, D. M., Cruzeiro, C., Siani, R., Kublik, S. & Schröder, P. (2023). Resilience of barley (*Hordeum vulgare*) plants upon exposure to tramadol: Implication for the root-associated bacterial community and the antioxidative plant defence system. Science of the Total Environment, 164260”, Copyright Elsevier (2023).

- Supplementary Material-

**Resilience of barley (*Hordeum vulgare*) plants upon exposure to tramadol: implication for the root-associated bacterial community and the antioxidative plant defence system**

**David Mamdouh Khalaf<sup>a,b</sup>, Catarina Cruzeiro<sup>a,c,1,\*</sup>, Roberto Siani<sup>a,1</sup>, Susanne Kublik<sup>a</sup>, Peter Schröder<sup>a,c</sup>**

<sup>a</sup>Research Unit Comparative Microbiome Analysis, Helmholtz Zentrum München GmbH, German Research Center for Environmental Health, Ingolstädter Landstr. 1, 85764 Neuherberg, Germany

<sup>b</sup>Botany and Microbiology Department, Faculty of Science, Assiut University, 71516 Assiut, Egypt

<sup>c</sup>Present address: Unit Environmental Simulation, Helmholtz Zentrum München GmbH, German Research Center for Environmental Health, Ingolstädter Landstr. 1, 85764 Neuherberg, Germany

<sup>1</sup>Both authors contributed equally to this work; joint authors

\*Corresponding author: [catarina.cruzeiro@helmholtz-muenchen.de](mailto:catarina.cruzeiro@helmholtz-muenchen.de)

- Supplementary Material-

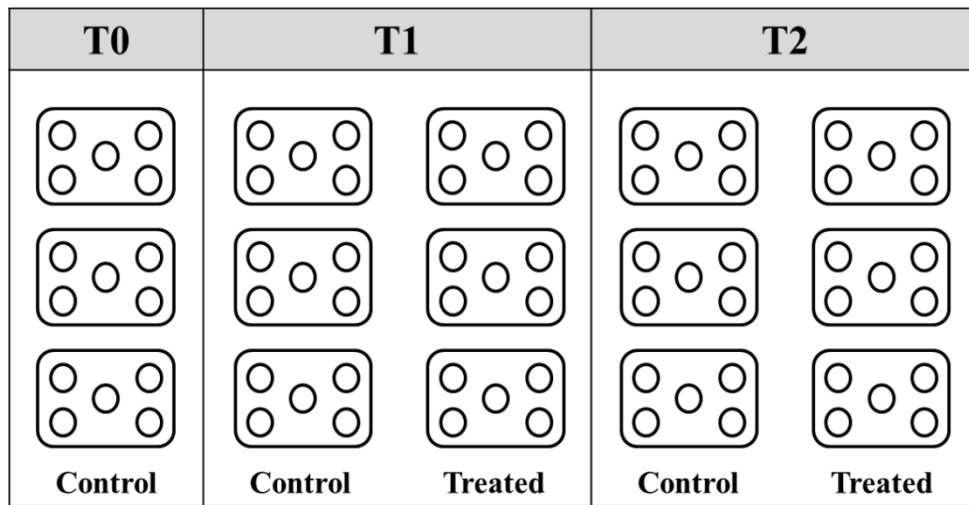


**Fig. S1.** Schematic figure illustrating the experimental design; Control: growing on nutrient solution, Treated: growing on nutrient solution supplemented with  $100 \mu\text{g L}^{-1}$  TRD; T0, T1 and T2 refer to harvesting points at: 0, 12 and 24 days from the beginning of the experiment; each time point has 3 biological replicates with 5 plants each.

- Supplementary Material-

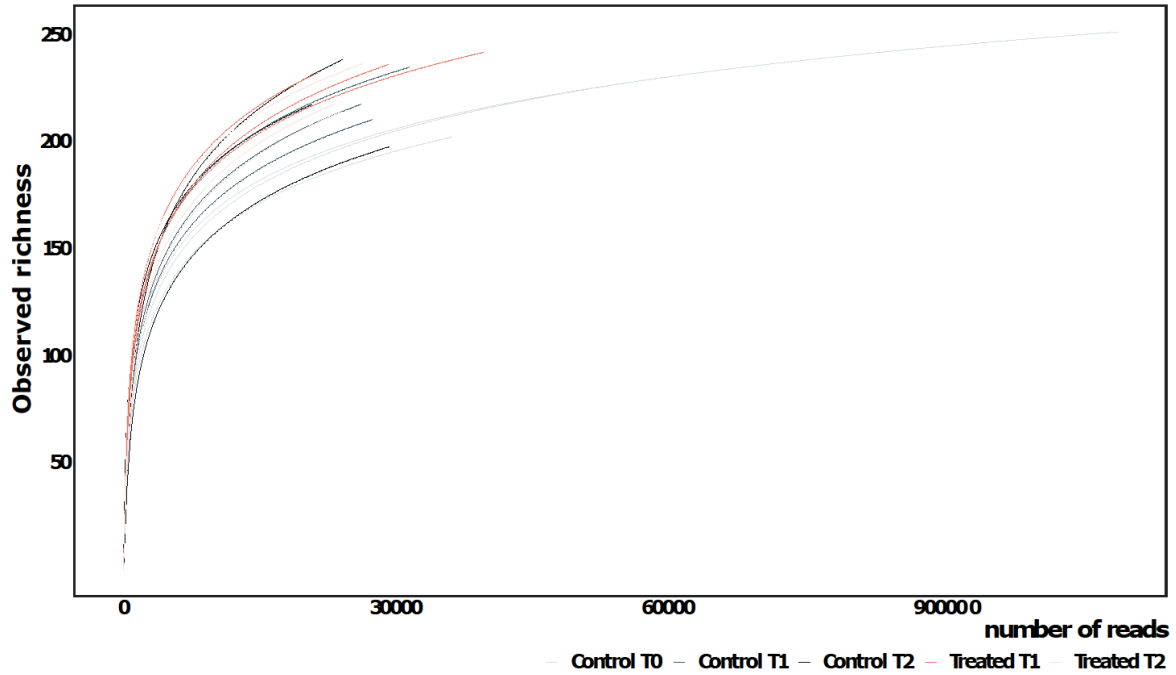


**Fig. S2.** Rarefaction curves (number of reads vs. observed richness) for control (light to dark blue curves) and TRD-treated ( $100 \mu\text{g L}^{-1}$  TRD, light to dark red curves) plants at different time points: T0 (0 days), T1 (12 days) and T2 (24 days).



- Supplementary Material-

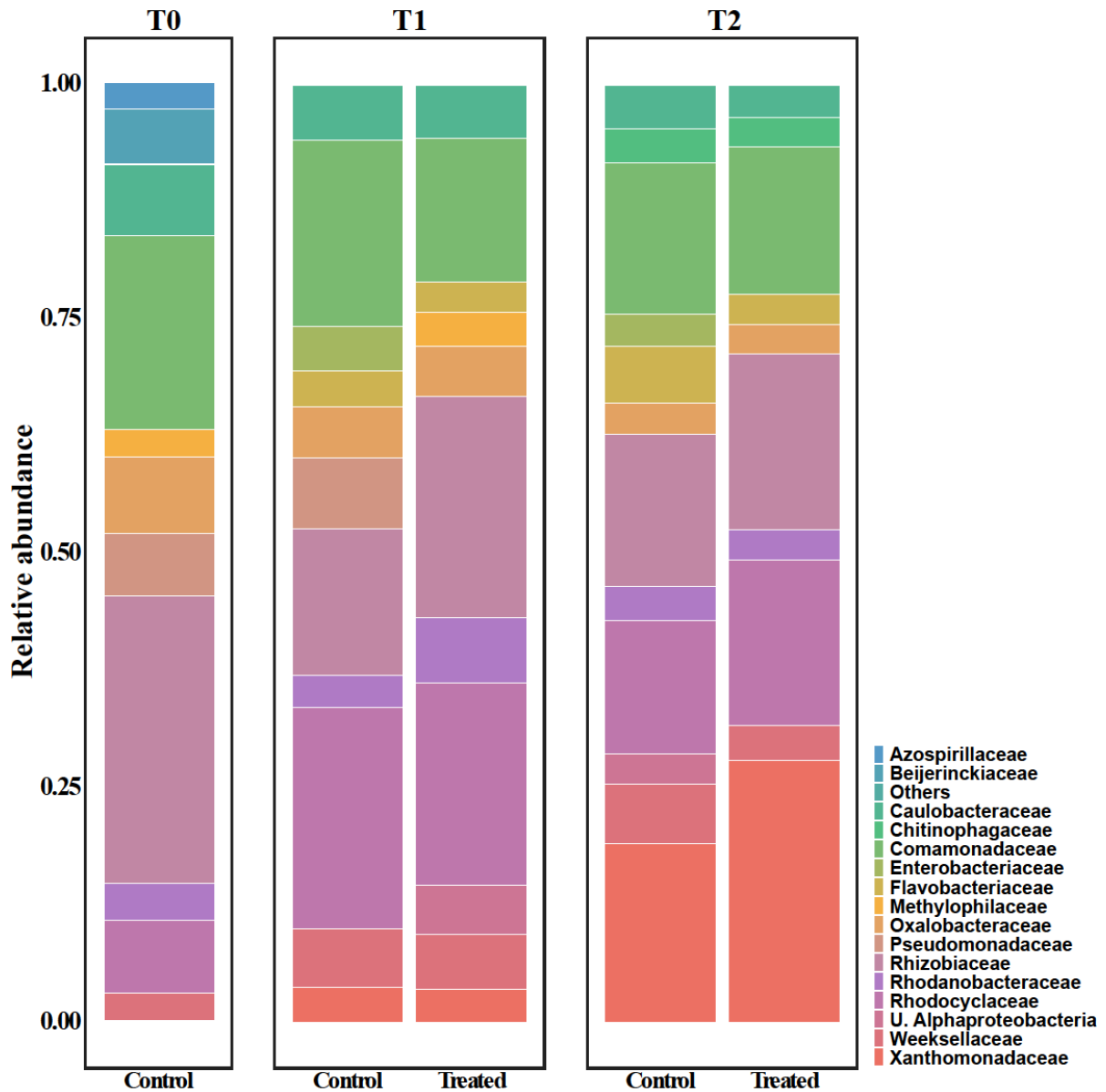


**Fig. S3.** Relative abundance of the most dominant (5%) families of root associated bacteria from control plants and those treated with  $100 \mu\text{g L}^{-1}$  TRD at three different time points; T0 (0 days), T1 (12 days) and T2 (24 days).

- Supplementary Material-

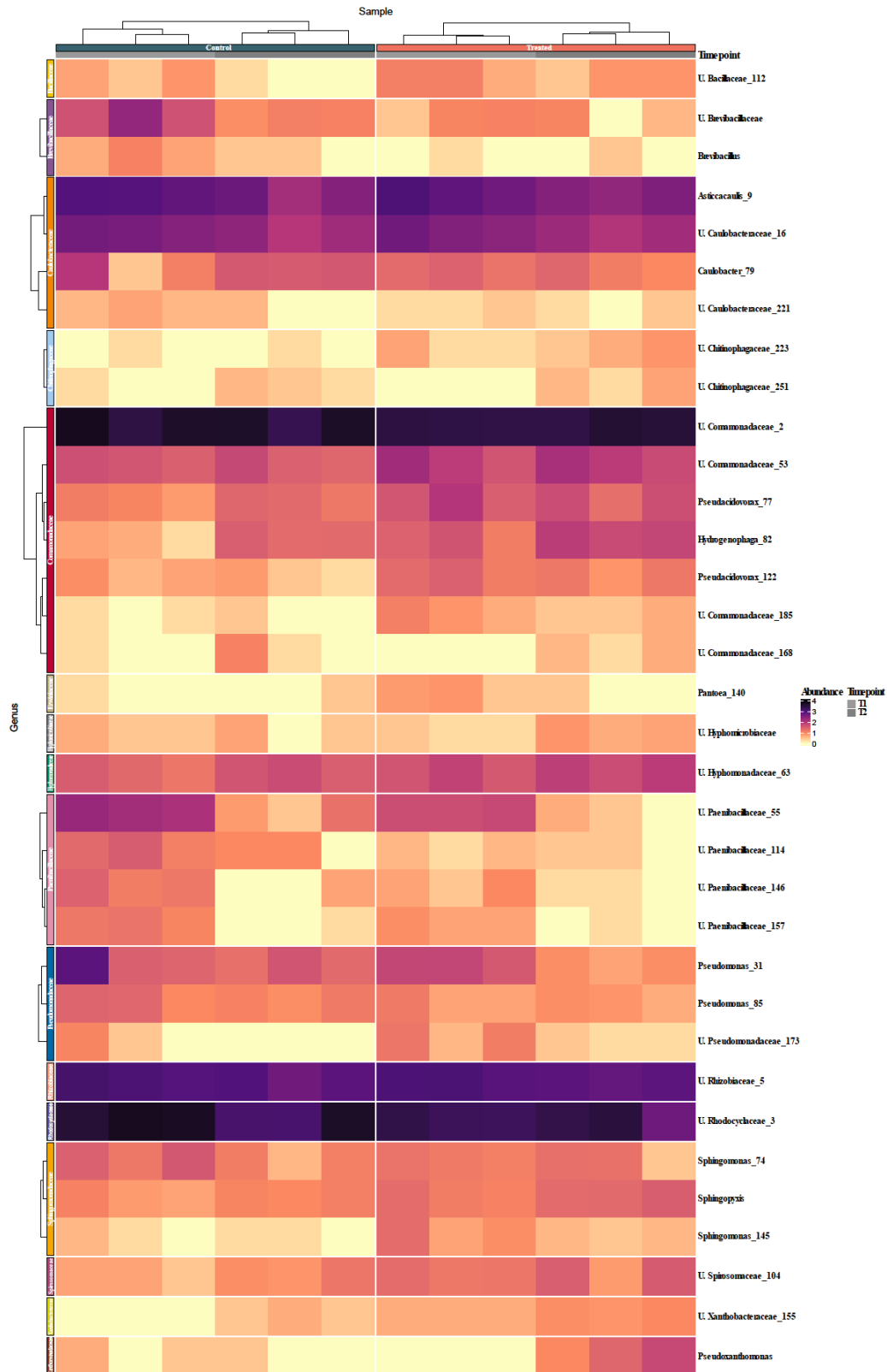


**Fig. S4.** Heatmap showing the log-transformed relative abundance of the most differentially abundant taxa in control and treated plants.

**- Supplementary Material-**

**Table S1.** Composition of the modified Hoagland's nutrient solution used for growing barley plants.

	<b>Molecular weight</b>	<b>Stock soln. (g L<sup>-1</sup>)</b>	<b>Volume taken from the stock soln. per L</b>
<b><u>Macronutrients</u></b>			
KNO <sub>3</sub> <sup>a</sup>	101.11	303.30	2
Ca(NO <sub>3</sub> ) <sub>2</sub> ·4H <sub>2</sub> O <sup>b</sup>	236.15	472.32	2
NH <sub>4</sub> H <sub>2</sub> PO <sub>4</sub> <sup>a</sup>	115.03	230.06	1
MgSO <sub>4</sub> ·7H <sub>2</sub> O <sup>c</sup>	246.48	246.48	1
<b><u>Micronutrients</u></b>			
KCl <sup>c</sup>	74.55	3.728	}
H <sub>3</sub> BO <sub>3</sub> <sup>a</sup>	61.84	1.546	
MnSO <sub>4</sub> ·H <sub>2</sub> O <sup>d</sup>	169.02	0.338	
Zn SO <sub>4</sub> ·7H <sub>2</sub> O <sup>e</sup>	287.5	0.576	
Cu SO <sub>4</sub> ·5H <sub>2</sub> O <sup>f</sup>	249.69	0.124	
(NH <sub>4</sub> ) <sub>6</sub> Mo <sub>7</sub> O <sub>24</sub> ·4H <sub>2</sub> O <sup>e</sup>	1235.86	0.084	
<b><u>Iron soln.</u></b>			
Iron ammonium citrate <sup>d</sup>	265	5	1

<sup>a</sup>(Carl Roth® GmbH+Co. KG, Karlsruhe, Germany)

<sup>b</sup>(Acros Organics, New Jersey, USA)

<sup>c</sup>(Merck, Darmstadt, Germany)

<sup>d</sup>(Sigma-Aldrich, Germany)

<sup>e</sup>(Fluka)

<sup>f</sup>(Honeywell Riedel-de Haën)

- Supplementary Material-

**Table S2.** Number of reads per sample at each processing step. Last column shows the ratio of reads passing the filters.

ID	raw	trimmed	filtered	derep	denoised	merged	non-chimera	passed
Cont-T0-1	50392	50392	40545	40545	40439	39888	36238	0.719122
Cont-T0-2	81502	81502	66271	66271	66090	65127	59401	0.728829
Cont-T0-3	150442	150442	122802	122802	122463	120588	109637	0.728766
Cont-T1-1	39999	39999	30768	30768	30627	30098	26260	0.656516
Cont-T1-2	45358	45358	36345	36345	36211	35440	31580	0.696239
Cont-T1-3	39438	39438	31567	31567	31432	30801	27459	0.696257
Cont-T2-1	33975	33975	27539	27539	27430	26914	24199	0.712259
Cont-T2-2	42344	42344	34095	34095	33945	33293	29339	0.692873
Cont-T2-3	29876	29876	23674	23674	23559	23029	20858	0.698152
TRD-T1-1	55308	55308	44836	44836	44644	43779	39718	0.718124
TRD-T1-2	41404	41404	33312	33312	33161	32329	29255	0.706574
TRD-T1-3	30157	30157	24380	24380	24280	23825	21416	0.71015
TRD-T2-1	33794	33794	27124	27124	27034	26631	24142	0.714387
TRD-T2-2	36814	36814	29784	29784	29654	29111	26448	0.718422
TRD-T2-3	32831	32831	26521	26521	26416	25733	23193	0.706436

### **iii. Appendix M3 (Manuscript III)**

Khalaf, D. M., Cruzeiro, C., & Schröder, P. (in preparation for publication). Impact of plant-bacterial synergism on removal and metabolization of the recalcitrant tramadol (not submitted yet).

1 **Impact of plant-bacterial synergism on removal and metabolization of the recalcitrant**  
2 **tramadol**

3

4

5 **David Mamdouh Khalaf<sup>a,b</sup>, Catarina Cruzeiro<sup>a,c</sup>, Peter Schröder<sup>a,c</sup>**

6 <sup>a</sup>Research Unit Comparative Microbiome Analysis, Helmholtz Zentrum München GmbH,  
7 German Research Center for Environmental Health, Ingolstädter Landstr. 1, 85764 Neuherberg,  
8 Germany

9 <sup>b</sup>Botany and Microbiology Department, Faculty of Science, Assiut University, 71516 Assiut,  
10 Egypt

11 <sup>c</sup>Present address: Unit Environmental Simulation, Helmholtz Zentrum München GmbH, German  
12 Research Center for Environmental Health, Ingolstädter Landstr. 1, 85764 Neuherberg, Germany

13

14

15

16

17

18

19

20

21

22

23

24

25

26

27

28

29 **Abstract**

30 Tramadol (TRD) has been considered a recalcitrant emerging contaminant since it has been  
31 detected in various water resources. As an increasing problem of public concern, the  
32 metabolization and complete bioconversion pathway for a huge number of these emerging  
33 contaminants in plants has been scantily investigated. To increase awareness about this opioid  
34 and explore its fate in the plant-bacterial environment, e.g., of arable crops or in  
35 phytoremediation, we have investigated the role of cultivable root endophytes with barley  
36 seedlings in TRD removal and metabolization. Twenty-three endophytic bacteria isolates were  
37 obtained from cattail plants exposed to TRD ( $5 \text{ mg L}^{-1}$ ), screened for plant growth promotion  
38 activities and for their individual ability to remove TRD ( $100 \text{ } \mu\text{g L}^{-1}$ ) *in vitro* from growth media  
39 either supplemented with glucose or malate. Thereafter, selected isolates were used for  
40 inoculation experiments with barley seedlings to explore their role in enhancing TRD removal  
41 and metabolism as well. Barley plants grown in hydroponic culture were supplemented with  
42 TRD ( $1 \text{ mg L}^{-1}$ ) and either inoculated with different bacterial sets (Single, Dual, Mix) or not  
43 inoculated. The highest removal efficiency for TRD was detected in Dual group, while the  
44 highest concentration of TRD was found in shoots ( $255.87 \text{ } \mu\text{g}$  in total shoot FW) of Mix  
45 inoculated plants. To demonstrate the fate of TRD inside plant tissues and the role of plant-  
46 bacterial synergism in this process, two main metabolites, O- and N-desmethyltramadol, from  
47 TRD were detected in root and shoot tissues. The highest concentration of these metabolites  
48 accounted for N-desmethyltramadol ( $11.02 \text{ } \mu\text{g}$  in total shoot FW) which was detected in Mix  
49 inoculated plants. Our study shows that inoculation of plants with endophytic bacteria improves  
50 the TRD removal process from hydroponic cultures, especially in dual inoculated plants, besides  
51 providing a vision of the metabolization pathway of TRD inside plants tissues.

52  
53  
54  
55  
56  
57  
58  
59

60 **Introduction:**

61 Over the years, pharmaceuticals and personal care products (PPCPs) have received significant  
62 attention due to their increasing presence in the environment (Kümmerer, 2009). With the  
63 growing global population and increased consumption of PPCPs, there is a continuous release of  
64 these compounds into the environment. The concentration of PPCPs in surface water ranges from  
65 ng to  $\mu\text{g L}^{-1}$  (Kasprzyk-Hordern et al., 2007&2008&2009; Carmona et al., 2014; Balakrishna et  
66 al., 2017; Quesada et al., 2019), and their continuous introduction can have adverse effects on  
67 aquatic ecosystems, water quality, and human health. PPCPs pose a risk similar to that of  
68 persistent organic contaminants (Sirés and Brillas, 2012; Wang and Wang, 2016). Wastewater  
69 treatment plants (WWTPs) are considered significant sources of PPCP contamination in water  
70 systems due to the limited removal efficiency of conventional treatment methods (Ramirez-  
71 Morales et al., 2020; Rout et al., 2021). To address this issue, advanced chemical and physical  
72 processes such as ozonation, photolysis, and membrane filtration can be employed (Esplugas et  
73 al., 2007; Zhang et al., 2020; Lozano et al., 2022). However, the cost associated with these  
74 techniques hinders their widespread implementation on a large scale.

75 Constructed wetlands (CWs) have been widely recognized as a promising and cost-effective  
76 phytoremediation technique for removing pharmaceuticals and personal care products (PPCPs)  
77 from effluents. CWs employ a combination of physical, chemical, and biological processes  
78 (Carvalho et al., 2014; Li et al., 2014; Verlicchi and Zambello, 2014; Zhang et al., 2014). The  
79 efficacy of pollutant removal and transformation in CWs relies on the performance of plants, as  
80 well as the interactions between the plants, substrate, and associated microbial communities  
81 (Carvalho et al., 2014). However, excessive amounts of organic compounds, including PPCPs, in  
82 the vicinity of plant roots can have phytotoxic effects. This can make plants more susceptible to  
83 stress conditions, ultimately impacting the overall phytoremediation performance.

84 The proper use of beneficial microbes, in particular bacteria, can help to overcome the effect of  
85 organic pollutants by increasing the phytoremediation potential and enhancing the removal  
86 efficiencies for these pollutants during the remediation process (Becerra-Castro et al. 2013;  
87 Hussain et al., 2018 a&b; Rehman et al., 2018). In this context, bacteria (endophytic or  
88 rhizospheric) can enhance plant growth as well as contribute to the pollutants  
89 detoxification/degradation process to diminish the resulting phytotoxic effect (Khan et al., 2013).



90 However, the role of bacterial inoculation to boost the remediation process of PPCPs by plants is  
91 scantily discussed. For example, Shah and coauthors (2022) explored the beneficial usage of a  
92 bacterial consortium, either free or after immobilization on Fe<sub>3</sub>O<sub>4</sub>-nanoparticles, with *Canna*  
93 *indica* (Indian shot) plants in ciprofloxacin (100 mg L<sup>-1</sup>) removal from water under floating  
94 treatment wetland technique. Another study demonstrated that inoculation of mung bean (*Vigna*  
95 *radiata*) plants grown in triclocarban-contaminated soil with *Pseudomonas fluorescens* MC46  
96 enhances the removal of this compound besides boosting soil enzymes activities (Sipahutar et al.,  
97 2018). An *in vitro* study conducted by Sauvêtre and coauthors (2018) in Murashige and Skoog  
98 medium showed the positive impact of bacterial inoculation of horseradish hairy root cultures in  
99 enhancing the removal of carbamazepine. Other studies reported the ability of *Hydrogenophaga*  
100 sp. YM1 and *Sphingomonas* sp. strain Ibu-2 to degrade atenolol and ibuprofen, respectively  
101 (Murdoch and Hay, 2005; Yi et al., 2022). Moreover, it was shown that *Pseudoxanthomonas* sp.  
102 strain DIN-3 has the ability to degrade naproxen, diclofenac and ibuprofen (Lu et al., 2019).  
103 Thus, we hypothesized that inoculation of plants with bacterial endophytes, previously isolated  
104 from TRD-exposed plants, can boost plant performance in TRD remediation process.

105 The opioid tramadol (TRD) is one of the recalcitrant PPCPs, which have been detected in various  
106 water resources, such as surface, influents and effluents of WWTPs (Kasprzyk-Hordern et al.,  
107 2008&2009; Rúa-Gómez and Püttmann, 2012; Mackuľak et al., 2015; Archer et al., 2017).  
108 Mackuľak and coauthors (2015) showed that conventional WWTPs are not able to efficiently  
109 remove TRD from the influents, however, treating the effluent water from WWTPs using the  
110 aquatic plants *Cabomba caroliniana*, *Limnophila sessiliflora* and *Egeria najas* as an additional  
111 cleaning step increased TRD removal potential (29-59%). Moreover, our previous study  
112 demonstrated the ability of barley seedlings to remove TRD with an efficiency of up to 89.13%  
113 from hydroponic culture experiment under controlled conditions (Khalaf et al., 2022). An *in vitro*  
114 study showed the ability of TRD-acclimatized sludge culture to co-metabolize or degrade TRD  
115 in the presence or absence of glucose, respectively (Kostanjevecki et al., 2019). Therefore, we  
116 hypothesized a possible role of bacterial inoculation which might enhance the metabolization of  
117 TRD inside plant tissues.

118 To the best of our knowledge, there is no information concerning the effect of the bacteria-plant  
119 synergism on TRD removal efficiency as well as the formed metabolites inside the plant tissues.  
120 Thus, this study aims to (1) isolate and screen endophytic bacteria for their plant growth

121 promotion characteristics as well as their ability to remove TRD; (2) explore the effect of  
122 bacterial inoculation on TRD removal efficiency; and (3) identify the possible impact of bacterial  
123 inoculation on the formed metabolites inside plant tissues.

124

## 125 **2. Materials and methods**

### 126 *2.1. Chemicals*

127 Tramadol HCl (TRD, 99%) and cis-Tramadol-<sup>13</sup>C, D<sub>3</sub>-hydrochlorid solution (TRD-D3; 100 µg  
128 mL<sup>-1</sup> in methanol) and N-desmethyl-cis-tramadol HCl (NDTRD, 1 mg mL<sup>-1</sup> in methanol), 1,4-  
129 Piperazinediethanesulfonic acid (PIPES), L(-)malic acid disodium (referred to here as malate)  
130 and R-2A agar were obtained from Sigma-Aldrich (Germany). O-desmethyltramadol HCl  
131 (ODTRD, 98%) was purchased from Focus Biomolecules (BIOZOL Diagnostica Vertrieb  
132 GmbH, Germany). Potassium chloride (KCl) and potassium phosphate monobasic were  
133 purchased from Fluka. Formic acid, acetonitrile (HPLC-grade), absolute ethanol, calcium  
134 chloride dehydrate, Sulphuric acid (H<sub>2</sub>SO<sub>4</sub>, 95-98%), nutrient broth, Nessler's reagent and  
135 formic acid (HPLC-grade) were purchased from Merck (Germany). Ferric chloride, ferrous  
136 sulphate heptahydrate, 5-sulphosalicylic acid (5-SSA), agar and peptone were obtained from Carl  
137 Roth<sup>®</sup> GmbH+Co. KG (Germany). PBS buffer (10X Dulbecco's) powder purchased from  
138 AppliChem (Germany). Acridine-D<sub>9</sub> was obtained from LGC Labor GmbH (Augsburg,  
139 Germany).

140

### 141 *2.2. Isolation of cultivable endophytes from cattail plants exposed to TRD*

142 Cattail plants (*Typha angustifolia* L.) were purchased from Gärtnerei Hollern (Unterschleißheim,  
143 Germany). Cattail cuttings were washed several times with tap water followed by rinsing with  
144 distilled (dist.) water before transferring them to the hydroponic system. Glass containers (3 L)  
145 were used as a growing system for the plants. Cattail plants grown in full-strength (100%)  
146 modified Hoagland's solution supplemented with TRD (5 mg L<sup>-1</sup>) after a period of  
147 acclimatization on half-strength (50%) modified Hoagland's solution (Taiz and Zeiger, 2010).  
148 Plants (3 replicates, 5 plants each) were kept in a growth chamber for one month under the  
149 conditions mentioned in Khalaf et al. (2022), prior to usage. After treatment with TRD (5 mg L<sup>-1</sup>)  
150 for one month, roots were collected from different plants, washed with tap water followed by  
151 rinsing three times with sterile dist. water in sterile conditions. Roots were sliced into 1-2 cm

152 pieces surface sterilized with a sequence of ethyl alcohol (70%, 30 sec), sodium hypochlorite  
153 (NaOCl; 3%, 3 min), ethyl alcohol (70%, 1 min), and then rinsed with sterile dist. water (3 times,  
154 1 min each). The sterile segments were crushed in a sterile mortar using 2 mL of sterile dist.  
155 water, and then, 1 mL aliquot was ten-fold diluted. From serial dilutions ( $10^{-1}$  -  $10^{-6}$ ), 100  $\mu$ L  
156 were taken and spread in duplicate onto nutrient and R-2A (Reasoner's 2A) agar plates  
157 supplemented with TRD. The plates were incubated for 5 days at  $28 \pm 2$  °C. To ensure  
158 sterilization efficiency, R-2A and nutrient agar plates were inoculated with 100  $\mu$ L from the third  
159 rinsing dist. water and used as negative controls. Distinct colonies were picked and subcultured  
160 twice to verify purity before they were preserved on R-2A plates and glycerol stocks.

161

### 162 *2.3. Determination of plant growth promotion traits by endophytic bacterial isolates*

163 For qualitative estimation of phosphate solubilization, freshly cultivated bacterial isolates were  
164 inoculated in triplicate on Pikovskaya's agar plates (10 g L<sup>-1</sup> glucose; 0.5 g L<sup>-1</sup> ammonium  
165 sulphate; 5 g L<sup>-1</sup> Ca<sub>3</sub>(PO<sub>4</sub>)<sub>2</sub>; 0.1 g L<sup>-1</sup> KCl; 0.1 g L<sup>-1</sup> MgSO<sub>4</sub>.7H<sub>2</sub>O; 0.5 g L<sup>-1</sup> yeast extract; 0.0001  
166 g L<sup>-1</sup> MnSO<sub>4</sub>.H<sub>2</sub>O; 0.0001 g L<sup>-1</sup> FeSO<sub>4</sub>.7H<sub>2</sub>O; 15 g L<sup>-1</sup> agar) then incubated for 5 days at  $28 \pm 2$   
167 °C. Isolates which developed a clear zone on the previous medium were considered positive to  
168 the test. Bacterial isolates were assayed for siderophore production according to a modified  
169 method described by Pérez-Miranda et al. (2007) and Louden et al. (2011). Freshly grown  
170 bacterial cultures were inoculated on nutrient agar plates and incubated for 48 h. Following the  
171 protocol described by Louden et al. (2011), the dye mixture was prepared from chrome azurol S  
172 (CAS), FeCl<sub>3</sub> and hexadecyltrimethylammonium bromide (HDTMA). Another solution was  
173 prepared by the addition of piperazine-N,N'-bis(2-ethanesulfonic acid) (PIPES) to dist. water  
174 supplemented with 0.9% agar with a final pH value of 6.8. The two solutions were mixed after  
175 autoclaving and then 10 mL of the mixture was added to the nutrient agar plates containing the  
176 bacterial cultures. These plates were incubated in the dark for 24h at  $28 \pm 2$  °C. Isolates which can  
177 develop colour change from blue to orange-yellow (either under the colony [+] or around it [++])  
178 were considered as positive for siderophore production. For indole acetic acid (IAA) and  
179 ammonia production tests, bacterial isolates were cultivated in nutrient broth for 72 hours. After  
180 centrifugation, bacterial pellets were washed twice with 1X PBS and then resuspended in the  
181 same solution. The suspensions were used for both tests after normalization to equal OD<sub>600</sub>. IAA  
182 production was detected according to Sauvêtre and Schröder, (2015) with some modifications.

183 Bacterial suspensions were inoculated in LB medium (1.2 mL in total) supplemented with 1 mg  
184 mL<sup>-1</sup> tryptophan and incubated for 72 h at 28±2 °C. The bacterial cultures were centrifuged and 1  
185 mL of the supernatant was transferred to a clean tube to which 1 mL of Salkowski reagent (12 g  
186 L<sup>-1</sup> FeCl<sub>3</sub> in 7.9 M H<sub>2</sub>SO<sub>4</sub>; Glickmann and Dessaux, 1995) was added. The previous mixture was  
187 incubated in the dark for 25 min at room temperature and the absorbance of developed pink  
188 colour was read at 530 nm. A calibration curve from pure IAA (ranging from 1 - 10 µg mL<sup>-1</sup>)  
189 was used to calculate the concentration of produced IAA. Ammonia production was determined  
190 as previously described by Ahmad et al. (2008) also with some modifications. Briefly, bacterial  
191 suspensions were inoculated into peptone water medium (10 g L<sup>-1</sup> peptone; 5 g L<sup>-1</sup> NaCl; 1.2 mL  
192 in total) and then incubated for 72 h at 28±2 °C. The cultures were centrifuged, then 50 µL  
193 Nessler's reagent was added to 1 mL of the supernatant. The developed colour (yellow to brown)  
194 was measured at 450 nm. The concentration of ammonia was analysed using a standard curve of  
195 ammonium sulphate (ranging from 1 - 20 µmol L<sup>-1</sup>).

196

#### 197 *2.4. Screening the capability of bacterial endophytes for TRD removal*

198 Bacterial isolates were assessed for their ability to remove TRD (100 µg L<sup>-1</sup>, close to higher  
199 value found in WWTPs; Kasprzyk-Hordern et al., 2009) in liquid media. Initially, freshly  
200 transferred bacterial cultures were cultivated in nutrient broth for 72 hours. Following  
201 incubation, the cultures were subjected to centrifugation, and the resulting bacterial pellets were  
202 washed twice and then resuspended in 1X PBS solution. Subsequently, the bacterial suspensions  
203 (normalised to equal OD<sub>600</sub>) were inoculated into 3 mL of sterile AB minimal medium (to reach  
204 an OD<sub>600</sub> of 0.01), which consisted of the following components per litre: 2 g ammonium  
205 sulphate, 6 g sodium phosphate dibasic, 3 g sodium chloride, 3 g potassium phosphate  
206 monobasic, 200 µL calcium chloride dehydrate (0.5 M), 2 mL magnesium chloride (1 M), and  
207 300 µL ferric chloride (0.01 M). To provide a carbon source, the medium was supplemented with  
208 1 g L<sup>-1</sup> of either glucose or malate. Additionally, 100 µg L<sup>-1</sup> of TRD was added to the medium as  
209 the target compound. For control purposes, tubes containing the corresponding sterile media with  
210 the same concentration of TRD and without bacterial inoculation were also prepared. All tubes  
211 were incubated at a temperature of 28±2 °C under orbital shaking (120 rpm) for 14 days. At the  
212 end of the incubation period, 0.5 mL of each tube's content was subjected to centrifugation at  
213 10000 rpm for 5 min. The resulting supernatant was collected from each tube for subsequent

214 TRD quantification. Prior to analysis, all samples were mixed with 5-SSA (10:1 v/v, 1.9 M in  
215 H<sub>2</sub>O) to precipitate proteins. After centrifugation, the supernatants were acidified using formic  
216 acid (final concentration 0.1%), filtered through 0.2 µm filters (SPARTAN™ 13/0.2 RC), and  
217 spiked with an internal standard (IS; TRD-D3) to achieve a final concentration of 20 µg L<sup>-1</sup>.

218

### 219 *2.5. Molecular identification of endophytic bacterial isolates*

220 Colony PCR was performed following the protocol from Duffner et al. (2022) to amplify a near  
221 full-length 16S rRNA gene. Briefly, the PCR reaction mixture contained (for one reaction);  
222 31.25 µL MiliQ-DEPC water, 0.25 µL dNTPs (10 mM), 5 µL PCR buffer (10X), 5 µL BSA  
223 (3%), 3 µL MgCl<sub>2</sub> (25 mM), 0.5 µL Taq DNA polymerase (5 U), 1 µL forward primer 27f (10  
224 pmol µL<sup>-1</sup>), 1 µL reverse primer 1492r (10 pmol µL<sup>-1</sup>) and 3 µL from diluted bacterial colony  
225 (prepared by picking up single colony using a sterile toothpick and diluted into 30 µL MiliQ-  
226 DEPC water). Afterwards, the amplified DNA, which resulted from the previous reaction, was  
227 purified and then Sanger sequenced. The quality of the sequenced chromatograms was checked  
228 manually using MEGA-X software (Kumar et al., 2018), then forward and reverse reads (except  
229 for TE2, TE10 and TE19 only with forward reads) were merged (to get assembled contig using  
230 BioEdit software) and allied against rRNA/ITS databases from the basic local alignment search  
231 tool for nucleotide (nblast) for taxonomic assignment (NCBI:  
232 <https://blast.ncbi.nlm.nih.gov/Blast.cgi>). Sequences of the used isolates and comparison of these  
233 sequences with rRNA/ITS databases from NCBI website are included in supplementary  
234 materials.

235

### 236 *2.6. Plant growth condition, bacterial endophytes and inoculation*

237 To investigate the role of barley seedlings together with certain bacterial strains (depending on  
238 the results from *in vitro* TRD removal and/or PGP traits) in enhancing the removal and  
239 metabolization of TRD, a hydroponic experiment was performed. Propagation of barley  
240 seedlings was done as described by Khalaf et al. (2022). The acclimatized barley seedlings were  
241 cultivated on 200 mL full-strength (100%) modified Hoagland solution either supplemented with  
242 or without TRD (1 mg L<sup>-1</sup>) and divided into six groups (Fig. S1) as follows; control group (Cont  
243 group; nutrient solution), TRD group (nutrient solution + TRD), TE12 group (nutrient solution +  
244 TRD + inoculation with bacterial isolate TE12), TE17 group (nutrient solution amended + TRD

245 + inoculation with bacterial isolate TE17), Dual group (nutrient solution + TRD + inoculation  
246 with bacterial isolates TE12 + TE17) and Mix group (nutrient solution + TRD + inoculation with  
247 bacterial consortium from TE2 + TE3 + TE6 + TE12 + T E17 + TE20). Bacteria (1 mL from  
248 suspensions having  $OD_{600}$  2) were supplemented two times in the first days. A final abiotic  
249 control group (AB-Cont group; nutrient solution amended with  $1 \text{ mg L}^{-1}$  TRD and without  
250 seedlings) were included to detect the degradation of TRD during the experiment. The  
251 experiment was done for 24 days, where nutrients were added one time in the middle of this  
252 period and water loss was compensated and adjusted to the initial volume using dist.  $\text{H}_2\text{O}$  before  
253 aliquots collection.

254

### 255 *2.7. Sample collection and preparation*

256 Media samples (0.5 mL) were collected at different time intervals and stored at  $-20 \text{ }^\circ\text{C}$ . Before  
257 analyses, samples from 0, 3, 6, 10, 18, 21, 24 days were treated with 5-SSA and followed the  
258 same steps as described previously (section 2.4). By the end of the experiment (24 days),  
259 seedlings were collected and divided into roots (washed 3 times with dist. water) and shoots.  
260 Both roots and shoots were freshly weighed and frozen at  $-80 \text{ }^\circ\text{C}$  till further analysis. Root and  
261 shoot tissues were ground and homogenized using liquid nitrogen. A modified QuEChERS  
262 (Khalaf et al., 2022) was used for the extraction of TRD and metabolites.

263

### 264 *2.8. Analytical instrument and measurements conditions*

265 The samples were injected ( $3 \times 10 \text{ } \mu\text{L}$ ) via autosampler into an UHPLC (Dionex UltiMate  
266 3000RS, Gering, Germany) coupled with a triple quadrupole mass spectrometer (Thermo  
267 Scientific HESI-MS/MS, TSQ Quantum Access Max, San Jose, USA), as described by Khalaf et  
268 al. (2022). For chromatographic separation, an Accucore PFP column (particle size  $100 \text{ mm} \times$   
269  $2.1 \text{ mm}$ ,  $2.6 \text{ } \mu\text{m}$ ) with an Accucore PFP pre-column (particle size  $10 \times 2.1 \text{ mm}$ ,  $2.6 \text{ } \mu\text{m}$ ) at a flow  
270 rate of  $0.45 \text{ mL min}^{-1}$  was used. The mobile phases were Mili-Q water acidified with 0.1%  
271 formic acid (A) and acetonitrile acidified with 0.1% formic acid (B). The mass spectrometer was  
272 operated in positive HESI mode. Media samples were analysed in selected ion monitoring (SIM)  
273 mode to quantify TRD [TRD 264.3 (m/z)], while the root and shoot samples were analysed, for  
274 both TRD and metabolites quantification, using tandem mass spectrometry (MS/MS) mode, as  
275 shown in Table (1). Further to peak integration, area ratios were calculated by dividing the peak

276 area of the targeted compound by the peak area of the IS (TRD-D3) and then quantified against  
 277 calibration curves using six concentrations ranging from 37.5 to 1200  $\mu\text{g L}^{-1}$  (for TRD) and 3.75  
 278 to 120  $\mu\text{g L}^{-1}$  (for ODTRD and NDTRD), where the final concentration of IS was 20  $\mu\text{g L}^{-1}$ . We  
 279 used the software Xcalibur (ver. 4.1) for peak integration, identification and quantification. For  
 280 the quantified pharmaceuticals in root and shoot samples, limits of detection (LODs) and  
 281 quantification (LOQs) were calculated (Table S1), as  $\text{LOD} = 3.3(\alpha/S)$  and  $\text{LOQ} = 10(\alpha/S)$ ; where  
 282  $\alpha$  refers to standard deviation slope and S is the average slopes of the calibration curves.

283 Table 1. Quantification and diagnostic ions of each compound, analysed by HESI-LC-MS/MS,  
 284 from root and shoot samples.

Target compounds	Precursor ion (m/z) [M +H] <sup>+</sup>	Product ions (m/z)	Collision Energy (v)
TRD	264.30	58.35*, 121.29*, 42.45, 56.31	16*, 39*, 74, 48,
ODTRD	250.20	58.29*, 107.34*, 77.22*, 42.29	14*, 17*, 58*, 77
NDTRD	250.13	44.54*, 121.02*, 91.22*, 115.65*	12*, 21*, 41*, 36*
TRD-D3	268.20	58.43*, 125.49*	14*, 20*

Note: The ions used for quantification are denoted by an asterisk (\*)

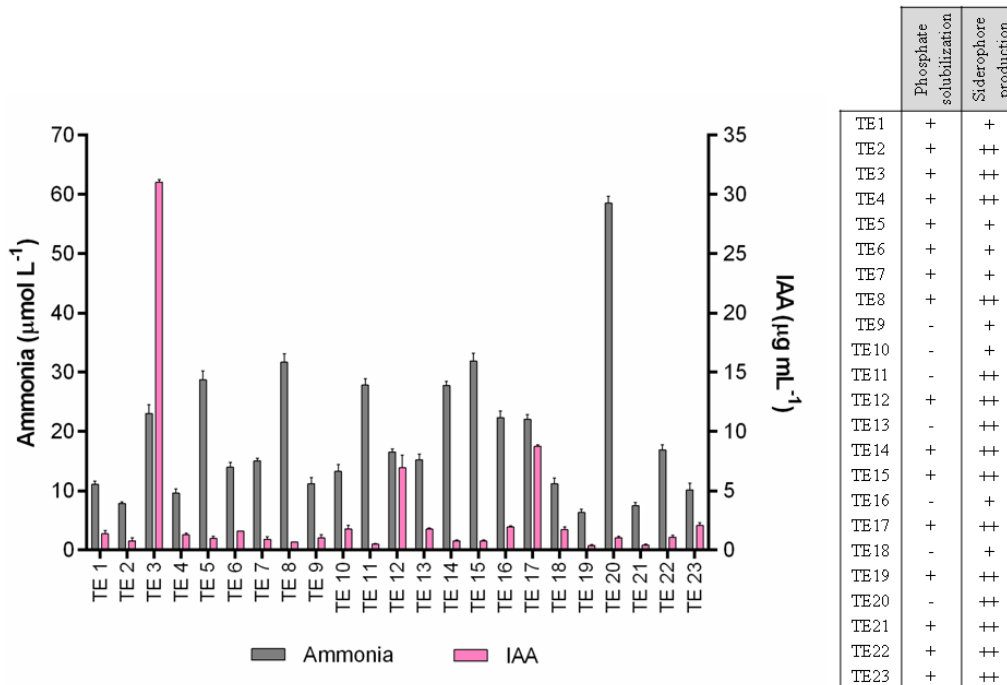
285

### 286 3. Results and Discussion

#### 287 3.1. Plant growth promoting (PGP) traits

288 After purification and subculturing, twenty-three cultivable isolates were obtained and used in  
 289 the *in vitro* studies. No bacterial colonies appeared on the negative control plates indicating a  
 290 high efficiency in the sterilization process. All twenty-three isolates were able to produce  
 291 ammonia, IAA and siderophores, but only 16 isolates were able to solubilize inorganic phosphate  
 292 (Fig. 1).

293



294

295

296 **Fig.1.** Plant growth promoting traits for cattail endophytic bacterial isolates. Measurements are  
 297 shown as ammonia ( $\mu\text{mol L}^{-1}$ ), IAA ( $\mu\text{g mL}^{-1}$ ) production, phosphate solubilization, and  
 298 siderophore production ability. Values are presented as the mean of three replicates  $\pm$  SD.

299

300 Most of the ammonia production values ranged from 3.17 to 15.94  $\mu\text{mol L}^{-1}$ , whereas the highest  
 301 production value (29.26  $\mu\text{mol L}^{-1}$ ) was recorded for isolate TE20 (closely related to *Duganella*  
 302 *aceris* by 98.07%). Concerning IAA production, the bacterial isolates exhibited the ability to  
 303 utilize tryptophan and synthesize IAA, with values ranging from 0.78 to 17.51  $\mu\text{g mL}^{-1}$ . Notably,  
 304 the isolate TE3 (closely related to *Azospirillum palustre* by 98.93%) demonstrated highest  
 305 production level (62.08  $\mu\text{g mL}^{-1}$ ) over this range. Previous studies showed that the recovered  
 306 isolates possess PGP characteristics and can enhance plant growth and performance. As an  
 307 example, *D. aceris* is a beta proteobacterial strain which had been isolated from extracted sap  
 308 of *Acer pictum* tree and identified by Jeon et al. (2021). While little information is available  
 309 about this species, another member from the same genus such as *D. ginsengisoli* was known for  
 310 its ability for IAA and siderophore production (Zhang et al., 2016). Also, Rath and coauthors  
 311 (2020) reported that *D. callida* possesses various genes linked to plant growth promotion. In the



312 case of *Azospirillum* is a well-studied genus used in biofertilization process and known for its  
313 ability to promote plant productivity (Cassán and Diaz-Zorita, 2016), play a role in osmotic  
314 stress mitigation in plants (Cassán et al., 2009), and has potential use in hydrocarbon remediation  
315 and heavy metal tolerance (Cruz-Hernández et al., 2022). *A. palustre* is a methylotrophic  
316 nitrogen-fixing strain, which was isolated by Tikhonova and coauthors (2019) from a *Sphagnum*-  
317 dominated raised bog. *A. palustre* was reported to have the ability to produce indole (Tikhonova  
318 et al., 2019). Naqqash and coauthors (2022) showed the ability of two *Azospirillum* strains  
319 (TN03 and TN09) to produce IAA (30.43  $\mu\text{g mL}^{-1}$ ) and solubilize phosphate (249.38  $\mu\text{g mL}^{-1}$ ),  
320 respectively. Another study revealed that *A. lipoferum* D-2 can produce phenolate siderophores  
321 (Saxena et al., 1986). The previous findings are in accordance with our observations which  
322 showed that the recovered isolates, during this study, possess PGP characteristics depending on  
323 the results from the *in vitro* tests which have been done.

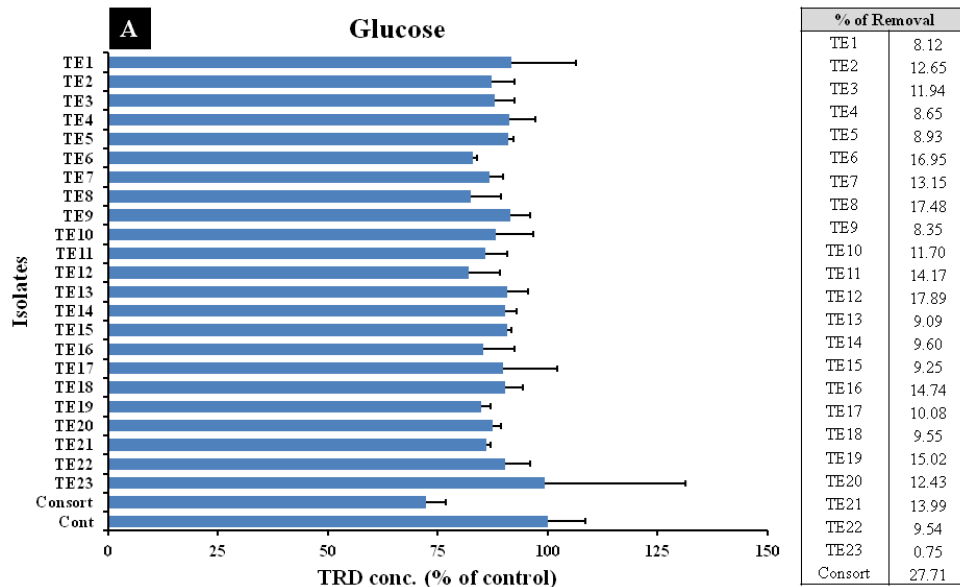
324

### 325 3.2. Screening for the best endophytic bacteria for *in vitro* TRD removal

326 Twenty-three bacterial isolates were examined for TRD (100  $\mu\text{g L}^{-1}$ ) removal, after 14 days of  
327 incubation, using AB minimal medium supplemented either with glucose or malate, as carbon  
328 source (Fig. 2 A&B). Regarding the recovered isolates grown on the medium supplemented with  
329 glucose, the % of TRD removal ranged from 0.75 to 17.89 % where the highest value between  
330 single inoculations was recorded for TE12 (closely related to *M. azadirachtae*;  
331 Microbacteriaceae, Actinomycetia), while the consortium from all bacterial isolates reached  
332 27.71 % TRD removal. When the medium was supplemented with malate, the removal efficiency  
333 ranged between 0.79 to 16.89 %, where the highest value was recorded by TE16 (closely related  
334 to *Paenibacillus curdolanolyticus*; Paenibacillaceae, Bacilli), while the consortium of all bacterial  
335 isolates reached 3.56 % TRD removal. Kostanjevecki and coauthors (2019) showed that using an  
336 original culture from activated sludge (collected from WWTP) was incapable to remove TRD  
337 from a controlled medium containing 20  $\text{mg L}^{-1}$  TRD. This indicates the persistence level of  
338 TRD; however, the same authors recorded biodegradation of TRD by 30 % after seven months of  
339 culture adaptation. This percentage rose to 82 %, after using a one-year optimized culture, in a  
340 TRD medium supplemented with glucose within 14 days incubation time. The same authors  
341 showed that relative abundances of *Bacillus* and *Enterobacter*, as dominant genera, comprised 30  
342 % and 13% of the community composition of the cultures grown on TRD medium amended with

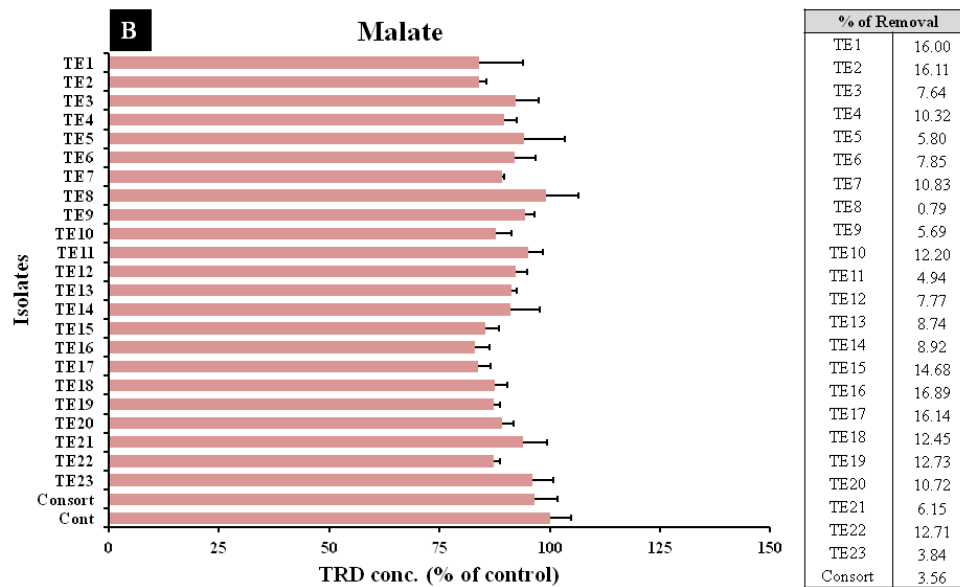
343 glucose. In our study, isolate TE12 (closely related to *M. azadirachtae*), TE8 (closely related to  
344 *B. toyonensis*) and TE6 (closely related to *R. xiangquanii*) recorded removal efficiencies of 17.89  
345 %, 17.48 % and 16.95 %, respectively after supplementation with glucose. Whereas, isolate  
346 TE16 (closely related to *P. curdlanolyticus*), TE17 (closely related to *B. toyonensis*) and TE2  
347 (closely related to *N. coeliaca*) showed removal efficiencies close to 16.89 %, 16.14 % and 16.00  
348 %, respectively after using malate as carbon source. These findings showed the possible  
349 contribution of some of the endophytic isolates in the TRD removal process. Kim and coauthors  
350 (2011) reported that *Microbacterium* sp. (strain 4N2-2) can produce four metabolites from the  
351 fluoroquinolone antibiotic norfloxacin. After comparison with other closely related strains from  
352 *Microbacterium* genus, they found similarities between their isolate and the PGP strain *M.*  
353 *azadirachtae* AI-S262<sup>T</sup> by (99.70 %). *R. xiangquanii* BJQ-6<sup>T</sup> isolated from WWTP-activated  
354 sludge in China, showed a degradation capability to the herbicide anilofos by 85 % from minimal  
355 salt medium supplemented with 50 mg L<sup>-1</sup> of this compound (Zhang et al., 2011). Howell and  
356 coauthors (2014), showed that bacterial strain CCH1, having similarity up to 98 % with  
357 uncultured *Rhodanobacter* sp., was able to degrade the fungicide azoxystrobin. Concerning *N.*  
358 *coeliaca*, a previous study had shown the ability of this bacterium to metabolize side-chains (up  
359 to nine methylene groups) in certain  $\omega$ -phenoxyalkanecarboxylic acids through  $\beta$ -oxidation  
360 (Taylor and Wain, 1962). Another species belonging to the same genus, *N. soli* Y48, exhibited  
361 degradation characteristics nearly to the components of crude oil besides possessing many genes  
362 accountable for degradation of hydrocarbons (Yang et al., 2019). *P. curdlanolyticus* (formerly *B.*  
363 *curdlanolyticus*) exhibits potential to degrade polysaccharides such as the resistant curdlan,  
364 pustulan and pullulan (Kanzawa et al., 1995). Pason and coauthors (2006) reported that a *P.*  
365 *curdlanolyticus* strain B-6 can produce a xylanolytic-cellulolytic multienzyme system, including  
366 xylanase, carboxymethyl cellulose, acetyl esterase, arabinofuranosidase, avicelase, mannanase,  
367 cellobiohydrolase, amylase,  $\beta$ -xylosidase,  $\beta$ -glucosidase, and chitinase, after growing aerobically  
368 on xylan. Besides the plant growth promoting activities that *B. toyonensis* has, Meda and  
369 coauthors (2020), using a response surface methodology, showed that this species was able to  
370 degrade the explosive compound HMX (octahydro-1,3,5,7-tetranitro-1,3,5,7-tetrazocine) by 87.7  
371 % after 15 days incubation when 4 % of bacterial suspension and 2 mg L<sup>-1</sup> HMX concentration  
372 were used. The previous findings are in line with our observations demonstrating the possible  
373 role of these genera in xenobiotics removal/metabolization processes.

374



375

376



377

378 **Fig. 2.** TRD removal from AB minimal medium supplemented with 1 g L<sup>-1</sup> either glucose (A) or  
379 malate (B) as carbon sources. TRD concentrations were calculated as percentages normalised by  
380 the average concentration of the control group. Values are presented as the mean of three  
381 replicates ± SD.

382

383

### 384 3.3. Molecular identification of endophytic bacteria

385 From the twenty-three isolates, twenty-two isolates which showed similarities of more than 98%  
386 to taxa in rRNA/ITS databases from NCBI website were further used. Sequencing from  
387 amplified 16S rRNA genes resulted in 16 species belonging to 13 genera (Table 2). The  
388 identified isolates belong to 12 bacterial families (Nocardiaceae, Microbacteriaceae,  
389 Mycobacteriaceae, Bacillaceae, Paenibacillaceae, Comamonadaceae, Alcaligenaceae,  
390 Oxalobacteraceae, Burkholderiaceae, Sphingomonadaceae, Azospirillaceae and  
391 Rhodanobacteraceae) under 5 classes (Actinomycetia, Bacilli, Betaproteobacteria,  
392 Alphaproteobacteria and Gammaproteobacteria). Given that the roots of cattail plants are the first  
393 point of contact after exposure to TRD, it is crucial to investigate the impact of TRD on the  
394 endophytic community associated with these roots. Plant roots possess the capability to uptake  
395 and accumulate TRD in their tissues, as previously observed by Khalaf et al. (2022; 2023).  
396 Understanding the fate of TRD within root tissues requires a closer examination of the bacterial  
397 endophytes that may play a role in TRD metabolism. In the current study, the isolated genera  
398 belong to three bacterial phyla; Proteobacteria, Actinobacteria and Firmicutes; these results  
399 might reflect the importance of these phyla in cattail plants and their possible contribution in the  
400 TRD removal/adaption process. The previous findings can be strengthened with the research  
401 conducted by Li et al. (2011) who used 16S rDNA sequencing and identified Proteobacteria (161  
402 clones) as the prevalent phylum (87.5%) within the total endophytic bacterial community of  
403 cattail roots grown in a wetland for wastewater treatment. Additionally, Ghosh et al. (2014)  
404 isolated two strains, *Paenibacillus cookii* JGR8 and *Bacillus megaterium* JGR9, belonging to  
405 Firmicutes, from the rhizoplane of heavy metal tolerant cattail plants found in a highly  
406 contaminated area with iron. Saha et al. (2016), successfully isolated ten endophytic bacteria  
407 from cattail plants grown in a Uranium mine area in India, where Firmicutes constituted the  
408 predominant group in the cultivable endophytic bacterial community. The previous data along  
409 with ours show a possible role that might be played by these phyla in xenobiotic adaption.

410

411

412

413

414 **Table 2.** Taxonomic identification of endophytic bacteria from *Typha angustifolia* plants  
 415 exposed to TRD (5 mg L<sup>-1</sup>) based on comparison of 16s rRNA sequences available on NCBI  
 416 database.

Isolates	Closest match	Similarities	Family	Class
TE1	<i>Sphingobium xanthum</i>	99.40%	Sphingomonadaceae	Alphaproteobacteria
TE2	<i>Nocardia coeliaca</i>	99.74%	Nocardiaceae	Actinomycetia
TE3	<i>Azospirillum palustre</i>	98.93%	Azospirillaceae	Alphaproteobacteria
TE4	<i>Microbacterium suwonense</i>	99.26%	Microbacteriaceae	Actinomycetia
TE5	<i>Rhodococcus qingshengii</i>	99.77%	Nocardiaceae	Actinomycetia
TE6	<i>Rhodanobacter xiangquanii</i>	99.71%	Rhodanobacteraceae	Gammaproteobacteria
TE7	<i>Rhodococcus qingshengii</i>	99.93%	Nocardiaceae	Actinomycetia
TE8	<i>Bacillus toyonensis</i>	99.85%	Bacillaceae	Bacilli
TE9	<i>Delftia acidovorans</i>	99.93%	Comamonadaceae	Betaproteobacteria
TE10	<i>Paenibacillus curdolanolyticus</i>	98.80%	Paenibacillaceae	Bacilli
TE11	<i>Bacillus toyonensis</i>	99.79%	Bacillaceae	Bacilli
TE12	<i>Microbacterium azadirachtae</i>	98.83%	Microbacteriaceae	Actinomycetia
TE13	<i>Microbacterium lacus</i>	100%	Microbacteriaceae	Actinomycetia
TE14	<i>Bacillus toyonensis</i>	99.49%	Bacillaceae	Bacilli
TE15	<i>Bacillus toyonensis</i>	99.93%	Bacillaceae	Bacilli
TE16	<i>Paenibacillus curdolanolyticus</i>	99.01%	Paenibacillaceae	Bacilli
TE17	<i>Bacillus toyonensis</i>	99.72%	Bacillaceae	Bacilli
TE19	<i>Achromobacter mucicolens</i>	99.88%	Alcaligenaceae	Betaproteobacteria
TE20	<i>Duganella aceris</i>	98.07%	Oxalobacteraceae	Betaproteobacteria
TE21	<i>Trinickia diaoshuihuensis</i>	99.49%	Burkholderiaceae	Betaproteobacteria
TE22	<i>Rhodanobacter hydrolyticus</i>	98.97%	Rhodanobacteraceae	Gammaproteobacteria
TE23	<i>Mycolicibacterium rhodesiae</i>	99.78%	Mycobacteriaceae	Actinomycetia

417

418

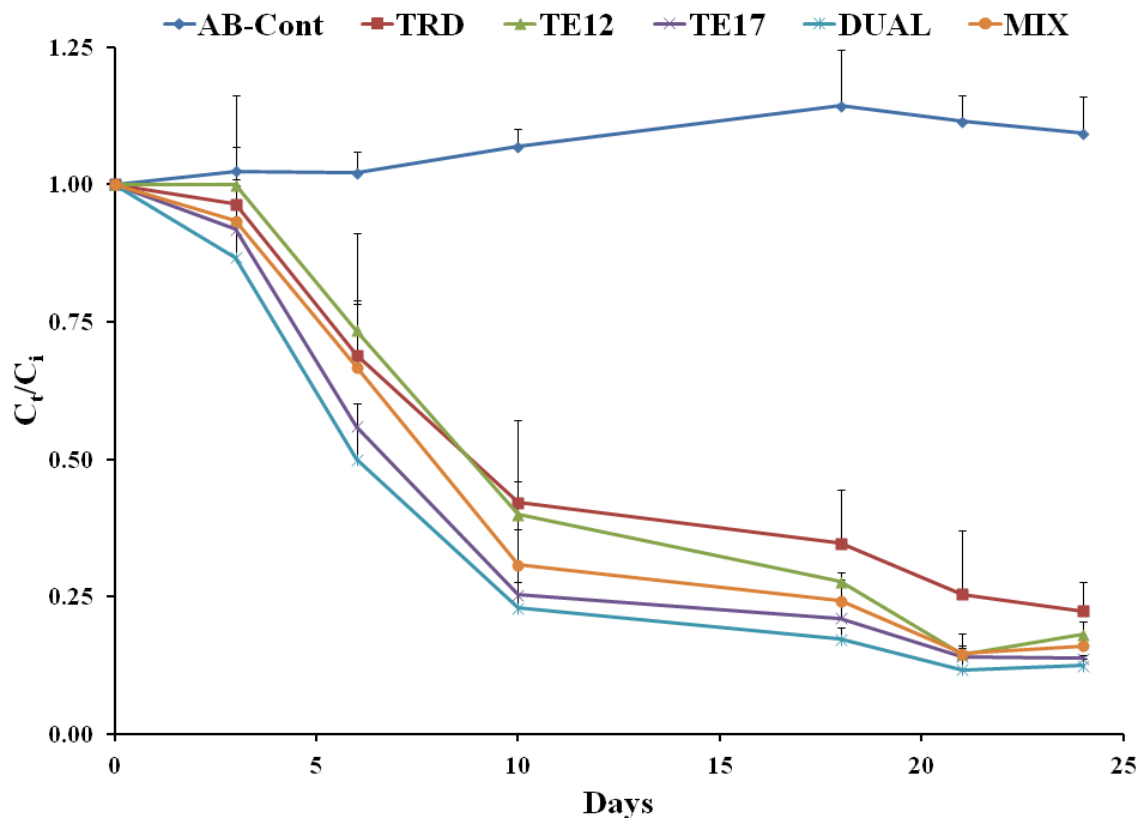
419

420

421 3.4. Removal of TRD from hydroponic cultures under plant-bacterial partnership

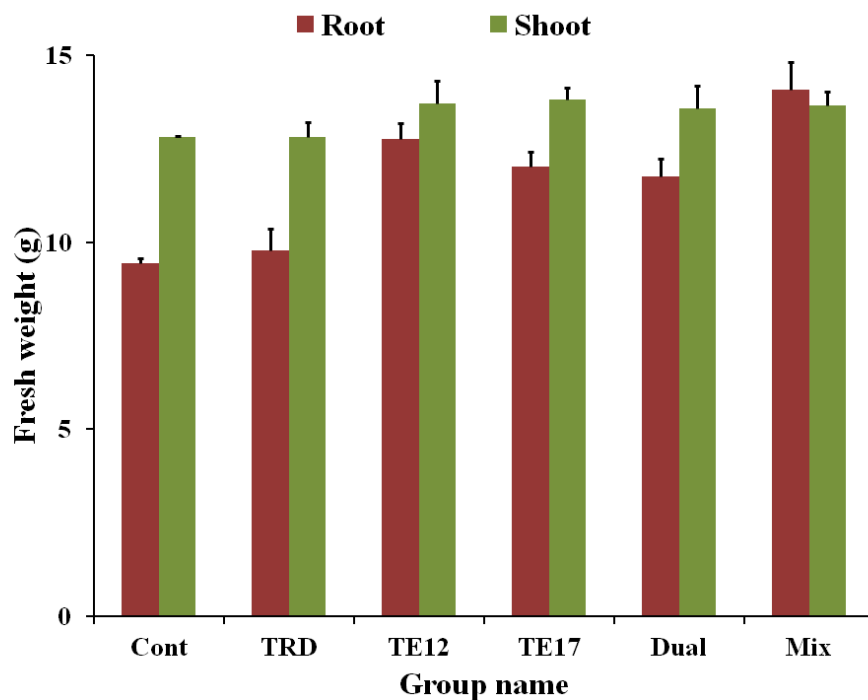
422 The TRD ( $1 \text{ mg L}^{-1}$ ) removal using endophytic bacterial sets (Single, Dual and Mix) of  
423 inoculation to barley seedlings are presented in Fig. 3. The concentration used in this experiment  
424 was higher than the environmentally relevant concentrations. This was done to facilitate  
425 detecting the TRD metabolites inside plant tissues.

426



427  
428 **Fig. 3.** Removal of TRD ( $1 \text{ mg L}^{-1}$ ) from the hydroponic culture over 24 days by barley  
429 seedlings either inoculated with bacterial endophytes or non-inoculated. The figure shows five  
430 groups: TRD (TRD), TE12 (TRD + TE12 bacterial isolate), TE17 (TRD + TE17 bacterial  
431 isolate), Dual (TRD + TE12 + TE17 bacterial isolates), and Mix (TRD + TE2 + TE3 + TE6 +  
432 TE12 + TE17 + TE20 bacterial isolates). An AB-Cont group (TRD + without barley seedlings)  
433 worked as abiotic control.  $C_i$  refers to the initial concentration of TRD, whilst  $C_t$  represents the  
434 residual concentration of TRD at the targeted time (day). Values are presented as the mean of  
435 three replicates  $\pm$  SD.

436 In the TRD group, we observed a removal of up to 77.69 % from the hydroponic cultures after  
437 24 days, whereas inoculation with endophytic bacterial isolates enhanced the removal efficiency  
438 of TRD compared to controls. The highest TRD removal efficiencies were observed in the Dual  
439 and TE17 groups, reaching up to 87.53 % and 86.23 % after 24 days of incubation, respectively.  
440 Moreover, TRD removal efficiencies were 81.85 % and 83.91 % after 24 days exposure period in  
441 the case of TE12 and Mix group, respectively. This might be due to indirect effects like  
442 enhancing plant growth (especially root biomass as shown in Fig. 4) and consequently increasing  
443 uptake rate or direct effect by enhancing co-metabolization of TRD. The isolates used in this  
444 experiment were selected depending on their ability to remove TRD and/or their PGP traits.  
445 Rojas-Solis and coauthors (2020), revealed that inoculating tomato plants with *B. toyonensis*  
446 COPE52 increased both root and shoot biomass as well as chlorophyll content at 0 and 100 mM  
447 NaCl. Another study reported that inoculation with *B. toyonensis* Bt04 resulted in promoting  
448 maize growth and an enhancement of root development under aluminium (Al) toxicity conditions  
449 (Zerrouk et al., 2020). Madhaiyan and coauthors (2010), showed that *M. azadirachtae*, isolated  
450 from neem seedlings' rhizoplane, causes positive *in vitro* reactions concerning plant growth  
451 promotion such as IAA production, ACC deaminase activity, phosphate solubilization and sulfur  
452 oxidation. Perazzolli and coauthors (2022), reported the ability of the endophytic isolate  
453 *Duganella* sp. to colonize different parts of tomato seedlings besides promoting tomato growth at  
454 low temperatures (15±1 °C). Moreover, Alotaibi and coauthors (2022), showed that inoculation  
455 of canola plants that had been grown in 3% n-hexadecane with *Nocardia* sp. WB46 resulted in  
456 increasing root and shoot lengths of canola compared to control plants receiving the same  
457 concentration of n-hexadecane.  
458



459

460

461 **Fig. 4.** Barley seedlings' growth after 24 days of exposure to TRD ( $1 \text{ mg L}^{-1}$ ) either inoculated  
 462 (TE12, TE17, Dual and Mix) or non-inoculated (TRD) with bacterial endophytes. Cont group are  
 463 plants only cultivated on nutrient solution. Values are presented as the mean of three replicates  $\pm$   
 464 SD.

465

### 466 3.5. Quantification of TRD and its main metabolites in barley tissues

467 The contents of TRD and its main metabolites (NDTRD and ODTRD) were detected in root and  
 468 shoot extracts, of barley seedlings, after 24 days of exposure to  $1 \text{ mg L}^{-1}$  TRD, either with or  
 469 without bacterial inoculation (Table 3). Concerning TRD, the highest concentration in root  
 470 tissues was recorded in TE17 and Dual group ( $72.16$  and  $69.90 \mu\text{g}$  in total root FW,  
 471 respectively), while in shoots was detected in the Mix group ( $255.87 \mu\text{g}$  in total shoot FW).  
 472 NDTRD results revealed that the highest contents of NDTRD in root ( $3.58 \mu\text{g}$  in total root FW)  
 473 and shoot ( $11.02 \mu\text{g}$  in total shoot FW) tissues were detected in Mix group, whereas in the case  
 474 of ODTRD, the highest values were found in the root and shoot of Mix and Dual groups,  
 475 respectively. It is well known that TRD metabolizes via O- and N-demethylation followed by  
 476 further metabolization through glucuronide and sulphate conjugation (Gong et al., 2014). O-



477 demethylation is catalyzed by cytochrome P450 (CYP) 2D6 to convert TRD to its main active  
 478 metabolite ODTRD (Paar et al., 1997; Subrahmanyam et al., 2001), while N-demethylation of  
 479 TRD to NDTRD (pharmacologically inactive metabolite) is mediated by CYP3A4 and CYP2B6  
 480 (Subrahmanyam et al., 2001). ODTRD and NDTRD can be further degraded to N,O-  
 481 didesmethyltramadol, N,N-didesmethyltramadol and N,N,O-tridesmethyltramadol  
 482 (Subrahmanyam et al., 2001).

483  
 484 **Table 3.** Concentration of TRD, ODTRD and NDTRD ( $\mu\text{g}$  in total FW) detected in both roots  
 485 and shoots of barley seedlings after exposure to TRD ( $1 \text{ mg L}^{-1}$ ) for 24 days; Values are  
 486 presented as the mean of three replicates  $\pm$  SD.

	Root			Shoot		
	ODTRD	NDTRD	TRD	ODTRD	NDTRD	TRD
<b>TRD</b>	0.79 $\pm$ 0.06	3.43 $\pm$ 1.11	49.11 $\pm$ 11.76	3.20 $\pm$ 0.06*	7.95 $\pm$ 2.56	205.22 $\pm$ 30.57
<b>TE12</b>	1.06 $\pm$ 0.04	3.28 $\pm$ 0.95	60.09 $\pm$ 6.17	3.43 $\pm$ 0.09	8.28 $\pm$ 1.49	206.31 $\pm$ 13.29
<b>TE17</b>	0.96 $\pm$ 0.03	2.81 $\pm$ 0.71	72.16 $\pm$ 8.03	3.42 $\pm$ 0.06	8.39 $\pm$ 0.90	222.82 $\pm$ 20.17
<b>Dual</b>	1.02 $\pm$ 0.06	3.11 $\pm$ 0.22	69.90 $\pm$ 13.27	3.46 $\pm$ 0.17*	8.28 $\pm$ 3.46	226.53 $\pm$ 19.48
<b>Mix</b>	1.06 $\pm$ 0.03	3.58 $\pm$ 0.90	63.10 $\pm$ 8.14	3.37 $\pm$ 0.08*	11.02 $\pm$ 1.54	255.87 $\pm$ 24.95

\* Average value from two replicates

487  
 488 In the current study, all treatments resulted in the accumulation of the parent compound TRD and  
 489 the formation of the first two main metabolites ODTRD and NDTRD in both root and shoot  
 490 tissues (Table 3). These findings show similarities between the plant/bacterial and the  
 491 mammalian system in TRD metabolism. It is worth highlighting that the barley plants inoculated  
 492 with bacteria (Single, Dual, Mix) displayed a trend towards higher concentration values of  
 493 ODTRD, NDTRD, and TRD compared to the non-inoculated ones. The former results revealed  
 494 that plants alone or in combination with bacteria can metabolize TRD through their  
 495 detoxification systems. The metabolization process in barley seedlings is in accordance with the  
 496 “green liver” concept that was first described by Shimabukuro et al. (1979) and confirmed by  
 497 Sandermann (1992 & 1994). This “green liver” concept comprises three phases in which some  
 498 cornerstone enzymes for xenobiotic metabolization, such as cytochrome P450 monooxygenases,

499 peroxidases or enzymes performing oxidation, reduction or hydrolysis reactions and glutathione  
500 S-transferases, can play a crucial role (Sandermann, 1994; Schröder, 1997). Siminszky and  
501 coauthors (2005), reported the crucial role of CYP82E4 (a cytochrome P450 monooxygenase) in  
502 the conversion of nicotine (via N- demethylation) to its metabolite nornicotine in tobacco plants.  
503 Furthermore, Moreland and coauthors (1990), showed that microsomes isolated from sorghum  
504 shoots can O-demethylate the herbicide metolachlor. The former authors also found a lack of  
505 metabolite formation after using compounds that inhibit cytochrome P450 monooxygenases such  
506 as tetraclacis, piperonyl butoxide and tridiphane. Bacterial CYP450 showed also an important  
507 role in pharmaceutical degradation. For example, the crucial role of CYP450 in *B. subtilis* for  
508 diclofenac degradation was recorded (Chen et al., 2020). Moreover, depending on the genome  
509 analysis of the bacterial strain LYK-6 which belongs to *Pseudomonas* genus, carbamazepine  
510 biodegradation was attributed to oxidation reactions caused by CYP450 system (Zhou et al.,  
511 2022). In the current study, it's noteworthy to mention that NDTRD concentrations in both root  
512 and shoot tissues were higher than ODTRD (Table 3). This result reveals the tendency of  
513 inoculated and non-inoculated barley seedlings either to metabolize TRD to NDTRD more than  
514 ODTRD or to further metabolize/conjugate the formed ODTRD. In line with former  
515 observations, Giorgi and coauthors (2009), noticed that the amount of NDTRD formed in the  
516 plasma of dogs, after giving immediate release capsules of TRD by oral administration, was  
517 higher than ODTRD concentration and the same was recorded in their urine.

518

#### 519 **4. Conclusion**

520 The present work was conducted to explore synergistic effects between plants and bacterial  
521 endophytic isolates to enhance the removal of TRD as well as to explore TRD metabolism inside  
522 the plant tissues. Bacterial endophytic isolates obtained from cattail roots showed PGP  
523 characteristics besides an *in vitro* potential to remove TRD. Six bacterial strains were selected  
524 and used in different sets (Single, Dual and Mix) for inoculation experiment with barley  
525 seedlings where the Dual group exhibited the best combination for TRD removal, reflecting the  
526 possible usage of these isolates with plants to enhance TRD remediation from contaminated  
527 water systems. Further trials with different combinations of isolates should be done to test the  
528 removal of TRD alone and together with other contaminants. The metabolization of TRD  
529 through O- and N-demethylations was recorded in all treatments with better advantage for N-

530 demethylation pathway. Concentrations of TRD, NDTRD and ODTRD were higher in the  
531 bacterial inoculated plants compared to non-inoculated plants with higher values detected in  
532 shoots than roots. Overall, cattail root bacterial endophytes showed PGP activities and to some  
533 extent increased the TRD removal and metabolization potential of barley seedlings. The current  
534 study opens the discussion about TRD metabolism in plants and a recommendation for removal  
535 of the compound by phytoremediation, however, further studies should be conducted to see if the  
536 main metabolites found in this study can be subjected to further degradation/conjugation,  
537 forming new metabolites or not.

538

### 539 **References**

540 Afzal, M., Yousaf, S., Reichenauer, T. G., & Sessitsch, A. (2012). The inoculation method  
541 affects colonization and performance of bacterial inoculant strains in the phytoremediation  
542 of soil contaminated with diesel oil. *International Journal of Phytoremediation*, 14, 35-47.  
543 <https://doi.org/10.1080/15226514.2011.552928>

544 Ahmad, F., Ahmad, I., & Khan, M. S. (2008). Screening of free-living rhizospheric bacteria for  
545 their multiple plant growth promoting activities. *Microbiological Research*, 163, 173-181.  
546 <https://doi.org/10.1016/j.micres.2006.04.001>

547 Alotaibi, F., St-Arnaud, M., & Hijri, M. (2022). In-Depth characterization of plant growth  
548 promotion potentials of selected alkanes-degrading plant growth-promoting bacterial  
549 isolates. *Frontiers in Microbiology*, 13. <https://doi.org/10.3389/fmicb.2022.863702>

550 Archer, E., Petrie, B., Kasprzyk-Hordern, B., & Wolfaardt, G. M. (2017). The fate of  
551 pharmaceuticals and personal care products (PPCPs), endocrine disrupting contaminants  
552 (EDCs), metabolites and illicit drugs in a WWTW and environmental waters. *Chemosphere*,  
553 174, 437-446. <https://doi.org/10.1016/j.chemosphere.2017.01.101>

554 Balakrishna, K., Rath, A., Praveenkumarreddy, Y., Guruge, K. S., & Subedi, B. (2017). A review  
555 of the occurrence of pharmaceuticals and personal care products in Indian water bodies.  
556 *Ecotoxicology and Environmental Safety*, 137, 113-120.  
557 <https://doi.org/10.1016/j.ecoenv.2016.11.014>

558 Becerra-Castro, C., Kidd, P. S., Rodríguez-Garrido, B., Monterroso, C., Santos-Ucha, P., &  
559 Prieto-Fernández, Á. (2013). Phytoremediation of hexachlorocyclohexane (HCH)-  
560 contaminated soils using *Cytisus striatus* and bacterial inoculants in soils with distinct

561 organic matter content. Environmental Pollution, 178, 202-210.  
562 <https://doi.org/10.1016/j.envpol.2013.03.027>

563 Carmona, E., Andreu, V., & Picó, Y. (2014). Occurrence of acidic pharmaceuticals and personal  
564 care products in Turia River Basin: from waste to drinking water. Science of the Total  
565 Environment, 484, 53-63. <https://doi.org/10.1016/j.scitotenv.2014.02.085>

566 Carvalho, P. N., Basto, M. C. P., Almeida, C. M. R., & Brix, H. (2014). A review of plant–  
567 pharmaceutical interactions: from uptake and effects in crop plants to phytoremediation in  
568 constructed wetlands. Environmental Science and Pollution Research, 21, 11729-11763.  
569 <https://doi.org/10.1007/s11356-014-2550-3>

570 Cassán, F., & Diaz-Zorita, M. (2016). *Azospirillum* sp. in current agriculture: From the  
571 laboratory to the field. Soil Biology and Biochemistry, 103, 117-130.  
572 <https://doi.org/10.1016/j.soilbio.2016.08.020>

573 Cassán, F., Maiale, S., Masciarelli, O., Vidal, A., Luna, V., & Ruiz, O. (2009). Cadaverine  
574 production by *Azospirillum brasilense* and its possible role in plant growth promotion and  
575 osmotic stress mitigation. European Journal of Soil Biology, 45, 12-19.  
576 <https://doi.org/10.1016/j.ejsobi.2008.08.003>

577 Chen, L., Li, Y., Lin, L., Tian, X., Cui, H., & Zhao, F. (2020). Degradation of diclofenac by *B.*  
578 *subtilis* through a cytochrome P450-dependent pathway. Environmental Technology &  
579 Innovation, 20, 101160. <https://doi.org/10.1016/j.eti.2020.101160>

580 Cruz-Hernández, M. A., Mendoza-Herrera, A., Bocanegra-García, V., & Rivera, G. (2022).  
581 *Azospirillum* spp. from plant growth-promoting bacteria to their use in bioremediation.  
582 Microorganisms, 10, 1057. <https://doi.org/10.3390/microorganisms10051057>

583 Duffner, C., Kublik, S., Fösel, B., Frostegård, Å., Schloter, M., Bakken, L., & Schulz, S. (2022).  
584 Genotypic and phenotypic characterization of hydrogenotrophic denitrifiers. Environmental  
585 Microbiology, 24, 1887-1901. <https://doi.org/10.1111/1462-2920.15921>

586 Esplugas, S., Bila, D. M., Krause, L. G. T., & Dezotti, M. (2007). Ozonation and advanced  
587 oxidation technologies to remove endocrine disrupting chemicals (EDCs) and  
588 pharmaceuticals and personal care products (PPCPs) in water effluents. Journal of  
589 Hazardous Materials, 149, 631-642. <https://doi.org/10.1016/j.jhazmat.2007.07.073>

590 Falahi, O. A. A., Abdullah, S. R. S., Hasan, H. A., Othman, A. R., Ewadh, H. M., Al-Baldawi, I.  
591 A., Kurniawan, S. B., Imron, M. F. & Ismail, N. I. (2021). Simultaneous removal of

592 ibuprofen, organic material, and nutrients from domestic wastewater through a pilot-scale  
593 vertical sub-surface flow constructed wetland with aeration system. *Journal of Water*  
594 *Process Engineering*, 43, 102214. <https://doi.org/10.1016/j.jwpe.2021.102214>

595 Ghosh, U. D., Saha, C., Maiti, M., Lahiri, S., Ghosh, S., Seal, A., & MitraGhosh, M. (2014).  
596 Root associated iron oxidizing bacteria increase phosphate nutrition and influence root to  
597 shoot partitioning of iron in tolerant plant *Typha angustifolia*. *Plant and Soil*, 381, 279-295.  
598 <https://doi.org/10.1007/s11104-014-2085-x>

599 Giorgi, M., Del Carlo, S., Saccomanni, G., Lebkowska-Wieruszewska, B., & Kowalski, C. J.  
600 (2009). Pharmacokinetic and urine profile of tramadol and its major metabolites following  
601 oral immediate release capsules administration in dogs. *Veterinary Research*  
602 *Communications*, 33, 875-885. <https://doi.org/10.1007/s11259-009-9236-1>

603 Glickmann, E., & Dessaux, Y. (1995). A critical examination of the specificity of the Salkowski  
604 reagent for indolic compounds produced by phytopathogenic bacteria. *Applied and*  
605 *Environmental Microbiology*, 61, 793-796. <https://doi.org/10.1128/aem.61.2.793-796.1995>

606 Gong, L., Stamer, U. M., Tzvetkov, M. V., Altman, R. B., & Klein, T. E. (2014). PharmGKB  
607 summary: tramadol pathway. *Pharmacogenetics and Genomics*, 24, 374. doi:  
608 <https://doi.org/10.1097/FPC.0000000000000057>

609 Howell, C. C., Semple, K. T., & Bending, G. D. (2014). Isolation and characterisation of  
610 azoxystrobin degrading bacteria from soil. *Chemosphere*, 95, 370-378.  
611 <https://doi.org/10.1016/j.chemosphere.2013.09.048>

612 Hussain, Z., Arslan, M., Malik, M. H., Mohsin, M., Iqbal, S., & Afzal, M. (2018a). Integrated  
613 perspectives on the use of bacterial endophytes in horizontal flow constructed wetlands for  
614 the treatment of liquid textile effluent: phytoremediation advances in the field. *Journal of*  
615 *Environmental Management*, 224, 387-395. <https://doi.org/10.1016/j.jenvman.2018.07.057>

616 Hussain, Z., Arslan, M., Malik, M. H., Mohsin, M., Iqbal, S., & Afzal, M. (2018b). Treatment of  
617 the textile industry effluent in a pilot-scale vertical flow constructed wetland system  
618 augmented with bacterial endophytes. *Science of the Total Environment*, 645, 966-973.  
619 <https://doi.org/10.1016/j.scitotenv.2018.07.163>

620 Jeon, D., Kim, I. S., Choe, H., Kim, J. S., & Lee, S. D. (2021). *Duganella aceris* sp. nov.,  
621 isolated from tree sap and proposal to transfer of *Rugamonas aquatica* and *Rugamonas*  
622 *rivuli* to the genus *Duganella* as *Duganella aquatica* comb. nov., with the emended

623 description of the genus *Rugamonas*. Archives of Microbiology, 203, 2843-2852.  
624 <https://doi.org/10.1007/s00203-021-02191-z>

625 Kanzawa, Y., Harada, A., Takeuchi, M., Yokota, A., & Harada, T. (1995). *Bacillus*  
626 *curdlanolyticus* sp. nov. and *Bacillus kobensis* sp. nov., which hydrolyze resistant curdlan.  
627 International Journal of Systematic and Evolutionary Microbiology, 45, 515-521.  
628 <https://doi.org/10.1099/00207713-45-3-515>

629 Kasprzyk-Hordern, B., Dinsdale, R. M., & Guwy, A. J. (2007). Multi-residue method for the  
630 determination of basic/neutral pharmaceuticals and illicit drugs in surface water by solid-  
631 phase extraction and ultra performance liquid chromatography-positive electrospray  
632 ionisation tandem mass spectrometry. Journal of Chromatography A, 1161, 132-145.  
633 <https://doi.org/10.1016/j.chroma.2007.05.074>

634 Kasprzyk-Hordern, B., Dinsdale, R. M., & Guwy, A. J. (2008). The occurrence of  
635 pharmaceuticals, personal care products, endocrine disruptors and illicit drugs in surface  
636 water in South Wales, UK. Water Research, 42, 3498-3518.  
637 <https://doi.org/10.1016/j.watres.2008.04.026>

638 Kasprzyk-Hordern, B., Dinsdale, R. M., & Guwy, A. J. (2009). The removal of pharmaceuticals,  
639 personal care products, endocrine disruptors and illicit drugs during wastewater treatment  
640 and its impact on the quality of receiving waters. Water Research, 43, 363-380.  
641 <https://doi.org/10.1016/j.watres.2008.10.047>

642 Khalaf, D. M., Cruzeiro, C., & Schröder, P. (2022). Removal of tramadol from water using  
643 *Typha angustifolia* and *Hordeum vulgare* as biological models: Possible interaction with  
644 other pollutants in short-term uptake experiments. Science of The Total Environment, 809,  
645 151164. <https://doi.org/10.1016/j.scitotenv.2021.151164>

646 Khan, S., Afzal, M., Iqbal, S., & Khan, Q. M. (2013). Plant-bacteria partnerships for the  
647 remediation of hydrocarbon contaminated soils. Chemosphere, 90, 1317-1332.  
648 <https://doi.org/10.1016/j.chemosphere.2012.09.045>

649 Kim, D. W., Heinze, T. M., Kim, B. S., Schnackenberg, L. K., Woodling, K. A., & Sutherland, J.  
650 B. (2011). Modification of norfloxacin by a *Microbacterium* sp. strain isolated from a  
651 wastewater treatment plant. Applied and Environmental Microbiology, 77, 6100-6108.  
652 <https://doi.org/10.1128/AEM.00545-11>

653 Kostanjevecki, P., Petric, I., Loncar, J., Smital, T., Ahel, M., & Terzic, S. (2019). Aerobic

654 biodegradation of tramadol by pre-adapted activated sludge culture: Cometabolic  
655 transformations and bacterial community changes during enrichment. *Science of The Total*  
656 *Environment*, 687, 858-866. <https://doi.org/10.1016/j.scitotenv.2019.06.118>

657 Kumar, S., Stecher, G., Li, M., Knyaz, C., & Tamura, K. (2018). MEGA X: molecular  
658 evolutionary genetics analysis across computing platforms. *Molecular Biology and*  
659 *Evolution*, 35, 1547. <https://doi.org/10.1093/molbev/msy096>

660 Kümmerer, K. (2009). The presence of pharmaceuticals in the environment due to human use-  
661 present knowledge and future challenges. *Journal of Environmental Management*, 90, 2354-  
662 2366. <https://doi.org/10.1016/j.jenvman.2009.01.023>

663 Li, Y. H., Liu, Q. F., Liu, Y., Zhu, J. N., & Zhang, Q. (2011). Endophytic bacterial diversity in  
664 roots of *Typha angustifolia* L. in the constructed Beijing Cuihu Wetland (China). *Research*  
665 *in Microbiology*, 162, 124-131. <https://doi.org/10.1016/j.resmic.2010.09.021>

666 Li, Y., Zhu, G., Ng, W. J., & Tan, S. K. (2014). A review on removing pharmaceutical  
667 contaminants from wastewater by constructed wetlands: design, performance and  
668 mechanism. *Science of the Total Environment*, 468, 908-932.  
669 <https://doi.org/10.1016/j.scitotenv.2013.09.018>

670 Louden, B. C., Haarmann, D., & Lynne, A. M. (2011). Use of blue agar CAS assay for  
671 siderophore detection. *Journal of Microbiology and Biology Education*, 12, 51-53.  
672 <https://doi.org/10.1128/jmbe.v12i1.249>

673 Lozano, I., Pérez-Guzmán, C. J., Mora, A., Mählknecht, J., Aguilar, C. L., & Cervantes-Avilés,  
674 P. (2022). Pharmaceuticals and personal care products in water streams: Occurrence,  
675 detection, and removal by electrochemical advanced oxidation processes. *Science of The*  
676 *Total Environment*, 154348. <https://doi.org/10.1016/j.scitotenv.2022.154348>

677 Lu, Z., Sun, W., Li, C., Ao, X., Yang, C., & Li, S. (2019). Bioremoval of non-steroidal anti-  
678 inflammatory drugs by *Pseudoxanthomonas* sp. DIN-3 isolated from biological activated  
679 carbon process. *Water Research*, 161, 459-472. <https://doi.org/10.1016/j.watres.2019.05.065>

680 Mackuřak, T., Mosný, M., Škubák, J., Grabic, R., & Birošová, L. (2015). Fate of psychoactive  
681 compounds in wastewater treatment plant and the possibility of their degradation using  
682 aquatic plants. *Environmental Toxicology and Pharmacology*, 39, 969-973.  
683 <https://doi.org/10.1016/j.etap.2015.02.018>

684 Madhaiyan, M., Poonguzhali, S., Lee, J. S., Lee, K. C., Saravanan, V. S., & Santhanakrishnan, P.

685 (2010). *Microbacterium azadirachtae* sp. nov., a plant-growth-promoting actinobacterium  
686 isolated from the rhizoplane of neem seedlings. *International Journal of Systematic and*  
687 *Evolutionary Microbiology*, 60, 1687-1692. <https://doi.org/10.1099/ijs.0.015800-0>

688 Meda, A., Sangwan, P., & Bala, K. (2020). Optimization of process parameters for degradation  
689 of HMX with *Bacillus toyonensis* using response surface methodology. *International*  
690 *Journal of Environmental Science and Technology*, 17, 4601-4610.  
691 <https://doi.org/10.1007/s13762-020-02783-0>

692 Moreland, D. E., Corbin, F. T., Novitzky, W. P., Parker, C. E., & Tomer, K. B. (1990).  
693 Metabolism of metolachlor by a microsomal fraction isolated from grain sorghum (*Sorghum*  
694 *bicolor*) shoots. *Zeitschrift für Naturforschung C*, 45, 558-564. [https://doi.org/10.1515/znc-](https://doi.org/10.1515/znc-1990-0544)  
695 [1990-0544](https://doi.org/10.1515/znc-1990-0544)

696 Murdoch, R. W., & Hay, A. G. (2005). Formation of catechols via removal of acid side chains  
697 from ibuprofen and related aromatic acids. *Applied and Environmental Microbiology*, 71,  
698 6121-6125. <https://doi.org/10.1128/AEM.71.10.6121-6125.2005>

699 Naqqash, T., Malik, K. A., Imran, A., Hameed, S., Shahid, M., Hanif, M. K., Majeed, A., Iqbal,  
700 M. J., Qaisrani, M. M., & Van Elsas, J. D. (2022). Inoculation with *Azospirillum* spp. acts as  
701 the liming source for improving growth and nitrogen use efficiency of potato. *Frontiers in*  
702 *Plant Science*, 13. <https://doi.org/10.3389/fpls.2022.929114>

703 Paar, W. D., Poche, S., Gerloff, J., & Dengler, H. J. (1997). Polymorphic CYP2D6 mediates O-  
704 demethylation of the opioid analgesic tramadol. *European Journal of Clinical*  
705 *Pharmacology*, 53, 235-239. <https://doi.org/10.1007/s002280050368>

706 Pason, P., Kyu, K. L., & Ratanakhanokchai, K. (2006). *Paenibacillus curdlanolyticus* strain B-6  
707 xylanolytic-cellulolytic enzyme system that degrades insoluble polysaccharides. *Applied*  
708 *and Environmental Microbiology*, 72, 2483-2490. [https://doi.org/10.1128/AEM.72.4.2483-](https://doi.org/10.1128/AEM.72.4.2483-2490.2006)  
709 [2490.2006](https://doi.org/10.1128/AEM.72.4.2483-2490.2006)

710 Perazzolli, M., Vicelli, B., Antonielli, L., Longa, C. M., Bozza, E., Bertini, L., Caruso, C., &  
711 Pertot, I. (2022). Simulated global warming affects endophytic bacterial and fungal  
712 communities of Antarctic pearlwort leaves and some bacterial isolates support plant growth  
713 at low temperatures. *Scientific Reports*, 12, 1-13. [https://doi.org/10.1038/s41598-022-](https://doi.org/10.1038/s41598-022-23582-2)  
714 [23582-2](https://doi.org/10.1038/s41598-022-23582-2)

715 Pérez-Miranda, S., Cabirol, N., George-Téllez, R., Zamudio-Rivera, L. S., & Fernández, F. J.



716 (2007). O-CAS, a fast and universal method for siderophore detection. Journal of  
717 Microbiological Methods, 70, 127-131. <https://doi.org/10.1016/j.mimet.2007.03.023>

718 Quesada, H. B., Baptista, A. T. A., Cusioli, L. F., Seibert, D., de Oliveira Bezerra, C., &  
719 Bergamasco, R. (2019). Surface water pollution by pharmaceuticals and an alternative of  
720 removal by low-cost adsorbents: A review. Chemosphere, 222, 766-780.  
721 <https://doi.org/10.1016/j.chemosphere.2019.02.009>

722 Ramírez-Morales, D., Masís-Mora, M., Montiel-Mora, J. R., Cambronero-Heinrichs, J. C.,  
723 Briceño-Guevara, S., Rojas-Sánchez, C. E., Méndez-Rivera, M., Arias-Mora, V., Tormo-  
724 Budowski, R., Brenes-Alfaro, L., & Rodríguez-Rodríguez, C. E. (2020). Occurrence of  
725 pharmaceuticals, hazard assessment and ecotoxicological evaluation of wastewater  
726 treatment plants in Costa Rica. Science of the Total Environment, 746, 141200.  
727 <https://doi.org/10.1016/j.scitotenv.2020.141200>

728 Rath, R., Peta, V., & Bücking, H. (2020). *Duganella callida* sp. nov., a novel addition to the  
729 *Duganella* genus, isolated from the soil of a cultivated maize field. International Journal of  
730 Systematic and Evolutionary Microbiology, 71, 004599.  
731 <https://doi.org/10.1099/ijsem.0.004599>

732 Rehman, K., Imran, A., Amin, I., & Afzal, M. (2018). Inoculation with bacteria in floating  
733 treatment wetlands positively modulates the phytoremediation of oil field wastewater.  
734 Journal of Hazardous Materials, 349, 242-251.  
735 <https://doi.org/10.1016/j.jhazmat.2018.02.013>

736 Rojas-Solis, D., Vences-Guzmán, M. A., Sohlenkamp, C., & Santoyo, G. (2020). *Bacillus*  
737 *toyonensis* COPE52 modifies lipid and fatty acid composition, exhibits antifungal activity,  
738 and stimulates growth of tomato plants under saline conditions. Current Microbiology, 77,  
739 2735-2744. <https://doi.org/10.1007/s00284-020-02069-1>

740 Rout, P. R., Zhang, T. C., Bhunia, P., & Surampalli, R. Y. (2021). Treatment technologies for  
741 emerging contaminants in wastewater treatment plants: A review. Science of the Total  
742 Environment, 753, 141990. <https://doi.org/10.1016/j.scitotenv.2020.141990>

743 Rúa-Gómez, P. C., & Püttmann, W. (2012). Impact of wastewater treatment plant discharge of  
744 lidocaine, tramadol, venlafaxine and their metabolites on the quality of surface waters and  
745 groundwater. Journal of Environmental Monitoring, 14, 1391-1399.  
746 <https://doi.org/10.1039/C2EM10950F>

747 Saha, C., Mukherjee, G., Agarwal- Banka, P., & Seal, A. (2016). A consortium of  
748 non- rhizobial endophytic microbes from *Typha angustifolia* functions as probiotic in rice  
749 and improves nitrogen metabolism. *Plant Biology*, 18, 938-946.  
750 <https://doi.org/10.1111/plb.12485>

751 Sandermann Jr, H. (1992). Plant metabolism of xenobiotics. *Trends in Biochemical Sciences*, 17,  
752 82-84. [https://doi.org/10.1016/0968-0004\(92\)90507-6](https://doi.org/10.1016/0968-0004(92)90507-6)

753 Sandermann Jr, H. (1994). Higher plant metabolism of xenobiotics: the 'green liver' concept.  
754 *Pharmacogenetics*, 4, 225-241. <https://doi.org/10.1097/00008571-199410000-00001>

755 Sauvêtre, A., & Schröder, P. (2015). Uptake of carbamazepine by rhizomes and endophytic  
756 bacteria of *Phragmites australis*. *Frontiers in Plant Science*, 6, 83.  
757 <https://doi.org/10.3389/fpls.2015.00083>

758 Sauvêtre, A., May, R., Harpaintner, R., Poschenrieder, C., & Schröder, P. (2018). Metabolism of  
759 carbamazepine in plant roots and endophytic rhizobacteria isolated from *Phragmites*  
760 *australis*. *Journal of Hazardous Materials*, 342, 85-95.  
761 <https://doi.org/10.1016/j.jhazmat.2017.08.006>

762 Saxena, B., Modi, M., & Modi, V. V. (1986). Isolation and characterization of siderophores from  
763 *Azospirillum lipoferum* D-2. *Microbiology*, 132, 2219-2224.  
764 <https://doi.org/10.1099/00221287-132-8-2219>

765 Schröder, P. (1997). Fate of glutathione S-conjugates in plants: Cleavage of the glutathione  
766 moiety. In: Hatzios KK (ed), *Regulation of enzymatic systems detoxifying xenobiotics in*  
767 *plants*. NATO ASI Series Vol. 37, Kluwer Academic Publishers, The Netherlands, pp 233–  
768 244.

769 Shah, S. W. A., Rehman, M. U., Hayat, A., Tahseen, R., Bajwa, S., Islam, E., Naqvi, S. N. H.,  
770 Shabir, G., Iqbal, S., Afzal, M. & Niazi, N. K. (2022). Enhanced degradation of  
771 ciprofloxacin in floating treatment wetlands augmented with bacterial cells immobilized on  
772 iron oxide nanoparticles. *Sustainability*, 14, 14997. <https://doi.org/10.3390/su142214997>

773 Shimabukuro, R. H., Walsh, W. C., & Hoerauf, R. A. (1979). Metabolism and selectivity of  
774 diclofop-methyl in wild oat and wheat. *Journal of Agricultural and Food Chemistry*, 27,  
775 615-623.

776 Siminszky, B., Gavilano, L., Bowen, S. W., & Dewey, R. E. (2005). Conversion of nicotine to  
777 nornicotine in *Nicotiana tabacum* is mediated by CYP82E4, a cytochrome P450

778 monooxygenase. Proceedings of the National Academy of Sciences, 102, 14919-14924.  
779 <https://doi.org/10.1073/pnas.0506581102>

780 Sipahutar, M. K., Piapukiew, J., & Vangnai, A. S. (2018). Efficiency of the formulated plant-  
781 growth promoting *Pseudomonas fluorescens* MC46 inoculant on triclocarban treatment in  
782 soil and its effect on *Vigna radiata* growth and soil enzyme activities. Journal of Hazardous  
783 Materials, 344, 883-892. <https://doi.org/10.1016/j.jhazmat.2017.11.046>

784 Sirés, I., & Brillas, E. (2012). Remediation of water pollution caused by pharmaceutical residues  
785 based on electrochemical separation and degradation technologies: a review. Environment  
786 International, 40, 212-229. <https://doi.org/10.1016/j.envint.2011.07.012>

787 Subrahmanyam, V., Renwick, A. B., Walters, D. G., Young, P. J., Price, R. J., Tonelli, A. P., &  
788 Lake, B. G. (2001). Identification of cytochrome P-450 isoforms responsible for cis-  
789 tramadol metabolism in human liver microsomes. Drug Metabolism and Disposition, 29,  
790 1146-1155.

791 Taiz, L., Zeiger, E. (2010). Plant Physiology, 5th ed. Sinauer Associates, Sunderland, MA, p.  
792 464.

793 Taylor, H. F., & Wain, R. L. (1962). Side-chain degradation of certain  $\omega$ -  
794 phenoxyalkanecarboxylic acids by *Nocardia coeliaca* and other micro-organisms isolated  
795 from soil. Proceedings of the Royal Society of London. Series B. Biological Sciences, 156,  
796 172-186. <https://doi.org/10.1098/rspb.1962.0038>

797 Tikhonova, E. N., Grouzdev, D. S., & Kravchenko, I. K. (2019). *Azospirillum palustre* sp. nov., a  
798 methylotrophic nitrogen-fixing species isolated from raised bog. International Journal of  
799 Systematic and Evolutionary Microbiology, 69, 2787-2793.  
800 <https://doi.org/10.1099/ijsem.0.003560>

801 Verlicchi, P., & Zambello, E. (2014). How efficient are constructed wetlands in removing  
802 pharmaceuticals from untreated and treated urban wastewaters? A review. Science of the  
803 Total Environment, 470, 1281-1306. <https://doi.org/10.1016/j.scitotenv.2013.10.085>

804 Wang, J., & Wang, S. (2016). Removal of pharmaceuticals and personal care products (PPCPs)  
805 from wastewater: a review. Journal of Environmental Management, 182, 620-640.  
806 <https://doi.org/10.1016/j.jenvman.2016.07.049>

807 Yang, R., Liu, G., Chen, T., Li, S., An, L., Zhang, G., Li, G., Chang, S., Zhang, W., Chen, X.,  
808 Wu, X., & Zhang, B. (2019). Characterization of the genome of a *Nocardia* strain isolated

809 from soils in the Qinghai-Tibetan Plateau that specifically degrades crude oil and of this  
810 biodegradation. *Genomics*, 111, 356-366. <https://doi.org/10.1016/j.ygeno.2018.02.010>

811 Yi, M., Sheng, Q., Lv, Z., & Lu, H. (2022). Novel pathway and acetate-facilitated complete  
812 atenolol degradation by *Hydrogenophaga* sp. YM1 isolated from activated sludge. *Science*  
813 of The Total Environment, 810, 152218. <https://doi.org/10.1016/j.scitotenv.2021.152218>

814 Zerrouk, I. Z., Rahmoune, B., Auer, S., Rößler, S., Lin, T., Baluska, F., Dobrev, P. I., Motyka,  
815 V., & Ludwig-Müller, J. (2020). Growth and aluminum tolerance of maize roots mediated  
816 by auxin-and cytokinin-producing *Bacillus toyonensis* requires polar auxin transport.  
817 *Environmental and Experimental Botany*, 176, 104064.  
818 <https://doi.org/10.1016/j.envexpbot.2020.104064>

819 Zhang, D., Gersberg, R. M., Ng, W. J., & Tan, S. K. (2014). Removal of pharmaceuticals and  
820 personal care products in aquatic plant-based systems: a review. *Environmental Pollution*,  
821 184, 620-639. <https://doi.org/10.1016/j.envpol.2013.09.009>

822 Zhang, J., Kim, Y. J., Hoang, V. A., Nguyen, N. L., Wang, C., Kang, J. P., Wang, D. & Yang, D.  
823 C. (2016). *Duganella ginsengisoli* sp. nov., isolated from ginseng soil. *International Journal*  
824 of Systematic and Evolutionary Microbiology, 66, 56-61.  
825 <https://doi.org/10.1099/ijsem.0.000669>

826 Zhang, J., Zheng, J. W., Hang, B. J., Ni, Y. Y., He, J., & Li, S. P. (2011). *Rhodanobacter*  
827 *xiangquanii* sp. nov., a novel anilofos-degrading bacterium isolated from a wastewater  
828 treating system. *Current Microbiology*, 62, 645-649. [https://doi.org/10.1007/s00284-010-](https://doi.org/10.1007/s00284-010-9757-4)  
829 [9757-4](https://doi.org/10.1007/s00284-010-9757-4)






















830 Zhang, K., Zhang, Z. H., Wang, H., Wang, X. M., Zhang, X. H., & Xie, Y. F. (2020). Synergistic  
831 effects of combining ozonation, ceramic membrane filtration and biologically active carbon  
832 filtration for wastewater reclamation. *Journal of Hazardous Materials*, 382, 121091.  
833 <https://doi.org/10.1016/j.jhazmat.2019.121091>

834 Zhou, Z., Wu, Y., Xu, Y., Wang, Z., Fu, H., & Zheng, Y. (2022). Carbamazepine degradation  
835 and genome sequencing of a novel exoelectrogen isolated from microbial fuel cells. *Science*  
836 of The Total Environment, 838, 156161. <https://doi.org/10.1016/j.scitotenv.2022.156161>

837

### **Appendix M3 (Supplements III)**

Khalaf, D. M., Cruzeiro, C., & Schröder, P. (in preparation for publication). Impact of plant-bacterial synergism on removal and metabolization of the recalcitrant tramadol (not submitted yet).

AB-Cont	Cont	TRD	TE12	TE17	Dual (TE12+TE17)	Mix (TE2+TE3+TE6+TE12+TE17+TE20)
						
						
						
No plants, no inoculation	Non-inoculated plants		Plants inoculated with bacteria			

**Fig. S1.** Showing the experimental design of inoculation experiment using barley seedlings which grown either on nutrient medium supplemented with  $1 \text{ mg L}^{-1}$  TRD or without (Cont). Exposed plants to TRD were either inoculated (TE12, TE17, Dual and Mix) or non-inoculated with bacteria (TRD). An AB-Cont group (TRD + without barley seedlings) worked as abiotic control.

**Table S1.** Values of limit of detection (LOD) and limit of quantification (LOQ) for ODTRD, NDTRD and TRD in root and shoot tissues.

	Root ( $\mu\text{g L}^{-1}$ )			Shoot ( $\mu\text{g L}^{-1}$ )		
	ODTRD	NDTRD	TRD	ODTRD	NDTRD	TRD
<b>LOD</b>	0.53	0.12	0.18	0.40	0.04	0.44
<b>LOQ</b>	1.61	0.35	0.55	1.22	0.12	1.33

**Sequences of bacterial endophytic isolates (manually checked with MEGA-X program, forward (F) and reverse (R) sequences assembled using BioEdit sequence alignment editor program) and comparison with NCBI database (Checked on 23-05-2023):**

**TE1 (F+R)**

CATGCAGTCGAACGAGATCTTCGGATCTAGTGGCGCACGGGTGCGTAACGCGTGGGAATC  
TACCCTTGGGTTCGGAATAACAGTTAGAAATGACTGCTAATACCGGATGATGACGTAAGT  
CCAAAGATTTATCGCCAAGGATGAGCCCGCGTAGGATTAGCTAGTTGGTGAGGTAAGG  
CTCACCAAGGCTACGATCCTTAGCTGGTCTGAGAGGATGATCAGCCACACTGGGACTGAG  
ACACGGCCCAGACTCCTACGGGAGGCAGCAGTAGGGAATATTGGACAATGGGCGAAAGCC  
TGATCCAGCAATGCCGCGTGAGCGATGAAGGCCTTAGGGTTGTAAAGCTCTTTTACCCGG  
GATGATAATGACAGTACCGGGAGAATAAGCCCCGGCTAACTCCGTGCCAGCAGCCGCGGT  
AATACGGAGGGGGCTAGCGTTGTTCCGAATTACTGGGCGTAAAGCGCACGTAGGCGGCTA  
TTTAAGTCAGAGGTGAAAGCCCGGGGCTCAACCCCGGAATTGCCTTTGAGACTGGATAGC  
TAGAATCTTGAGAGGCGGGTGAATTCCGAGTGTAGAGGTGAAATTCGTAGATATTCGG  
AAGAACACCAGTGGCGAAGGCGGCCCGCTGGACAAGTATTGACGCTGAGGTGCGAAAGCG  
TGGGGAGCAAACAGGATTAGATACCCTGGTAGTCCACGCCGTAAACGATGATAACTAGCT  
GTCCGGGCTCATAGAGTTTGGGTGGCGCAGCTAACGCATTAAGTTATCCGCCTGGGGAGT  
ACGGTCGCAAGATTA-AACTCAAAGGAATTGACGGGGGCCTGCACAAGCGGTGGAGCATG  
TGGTTTAATTCGAAGCAACGCGCAGAACCTTACCAACGTTTGACATCCCTATCGCGGTTA  
CCAGAGATGGTTTCCTTCAGTTCGGCTGGATAGGTGACAGGTGCTGCATGGCTGTCGTCA  
GCTCGTGTCTGAGATGTTGGGTTAAGTCCCGCAACGAGCGCAACCCTCGCCTTTAGTTG  
CCAGCATTTAGTTGGGTACTCTAAAGGAACCGCCGGTGATAAGCCGGAGGAAGGTGGGGA  
TGACGTCAAGTCCTCATGGCCCTTACGCGTTGGGCTACACACGTGCTACAATGGCGACTA  
CAGTGGGCAGCTATCCCGCGAGGGTGAGCTAATCTCCAAAAGTCGTCTCAGTTCGGATTG  
TTCTCTGCAACTCGAGAGCATGAAGGCGGAATCGCTAGTAATCGCGGATCAGCATGCCGC  
GGTGAATACGTTCCAGGCCTGTACACACCGCCCGTCACACCATGGGAGTTGGTTTCAC  
CCGAAGGCAGTGCCTAACC

Program BLASTN [Citation](#)

Database rRNA\_typestrains/16S\_ribosomal\_RNA [See details](#)

Query ID lc|Query\_127501

Description None

Molecule type dna

Query Length 1340

Other reports [Distance tree of results](#) [MSA viewer](#)

Organism only top 20 will appear  exclude

Type common name, binomial, taxid or group name

[+ Add organism](#)

Percent Identity  to  E value  to  Query Coverage  to

[Filter](#) [Reset](#)

**Descriptions** [Graphic Summary](#) [Alignments](#) [Taxonomy](#)

Sequences producing significant alignments [Download](#) [Select columns](#) Show 100 [?](#)

select all 100 sequences selected [GenBank](#) [Graphics](#) [Distance tree of results](#) [MSA Viewer](#)

Description	Scientific Name	Max Score	Total Score	Query Cover	E value	Per. Ident	Acc. Len	Accession
<input checked="" type="checkbox"/> <a href="#">Sphingobium xanthum strain NL9 16S ribosomal RNA, partial sequence</a>	<a href="#">Sphingobium xanthum</a>	2431	2431	100%	0.0	99.40%	1453	<a href="#">NR_133860.1</a>
<input checked="" type="checkbox"/> <a href="#">Sphingobium vulgare strain HU1-GD12 16S ribosomal RNA, partial sequence</a>	<a href="#">Sphingobium vulgare</a>	2398	2398	100%	0.0	98.96%	1394	<a href="#">NR_116563.1</a>
<input checked="" type="checkbox"/> <a href="#">Sphingobium pinisoli strain ASA28 16S ribosomal RNA, partial sequence</a>	<a href="#">Sphingobium pinisoli</a>	2237	2237	100%	0.0	96.79%	1427	<a href="#">NR_164942.1</a>
<input checked="" type="checkbox"/> <a href="#">Sphingobium herbicidovorans strain NBRC 16415 16S ribosomal RNA, partial sequence</a>	<a href="#">Sphingobium herbicidovorans</a>	2231	2231	100%	0.0	96.72%	1412	<a href="#">NR_113843.1</a>
<input checked="" type="checkbox"/> <a href="#">Sphingobium herbicidovorans strain MBIC 3166 16S ribosomal RNA, partial sequence</a>	<a href="#">Sphingobium herbicidovorans</a>	2231	2231	100%	0.0	96.72%	1438	<a href="#">NR_040807.1</a>



## TE2 (F)

TCGGGGTACACGAGCGGCGAACGGGTGAGTAACACGTGGGTGATCTGCCCTGCACTTCGG  
 GATAAGCCTGGGAAACTGGGTCTAATACGGATATGACCTCAGGTTGCATGACTTGGGGT  
 GGAAAGATTTATCGGTGCAGGATGGGCCCGCGGCCTATCAGCTTGTGGTGGGGTAATGG  
 CCTACCAAGGCGACGACGGGTAGCCGACCTGAGAGGGTGACCGGCCACACTGGGACTGAG  
 ACACGGCCCAGACTCCTACGGGAGGCAGCAGTGGGGAATATTGCACAATGGGCGAAAGCC  
 TGATGCAGCGACCCGCGTGAGGGATGACGGCCTTCGGGTTGTAAACCTCTTTCAGCAGG  
 GACGAAGCGCAAGTGACGGTACCTGCAGAAGAAGCACCGGCTAACTACGTGCCAGCAGCC  
 GCGTAATACGTAGGGTGCAAGCGTTGTCCGGAATTACTGGGCGTAAAGAGTTCGTAGGC  
 GGTTTGTGCGTTCGTTTGTGAAAACCAGCAGCTCAACTGCTGGCTTGCAGGCGATACGGG  
 CAGACTTGAGTACTGCAGGGGAGACTGGAATTCCTGGTGTAGCGGTGAAATGCGCANATA  
 TCAGGAGGAACACCGGTGGCGAAGGCGGGTCTCTGGGCAGTAACTGACGCTGAGGAACGA  
 AAGCGTGGGTAGCGAACAGGATTAGATACCCTGGTAGTCCACGCCGTAACGGTGGGCGCT  
 AGGTGTGGGTTTCCTTCCACGGAATCCGTGCCGTA

Program **BLASTN** [Citation](#) ?

Database **rRNA\_typestrains/16S\_ribosomal\_RNA** [See details](#) ?

Query ID **lc|Query\_349411**

Description **None**

Molecule type **dna**

Query Length **754**

Other reports [Distance tree of results](#) [MSA viewer](#) ?

Organism only top 20 will appear  exclude

Type common name, binomial, taxid or group name

[+ Add organism](#)

Percent Identity  to  E value  to  Query Coverage  to

**Filter** **Reset**

- Descriptions**
- Graphic Summary
- Alignments
- Taxonomy

Sequences producing significant alignments Download ? Select columns ? Show  ?

select all 100 sequences selected [GenBank](#) [Graphics](#) [Distance tree of results](#) [MSA Viewer](#)

	Description	Scientific Name	Max Score	Total Score	Query Cover	E value	Per. Ident	Acc. Len	Accession
<input checked="" type="checkbox"/>	<a href="#">Nocardia coeliaca strain DSM 44595 16S ribosomal RNA, partial sequence</a>	<a href="#">Nocardia coeliaca</a>	1384	1384	100%	0.0	99.74%	1507	<a href="#">NR_104776.1</a>
<input checked="" type="checkbox"/>	<a href="#">Rhodococcus erythropolis strain N11 16S ribosomal RNA, partial sequence</a>	<a href="#">Rhodococcus erythropolis</a>	1380	1380	100%	0.0	99.60%	1476	<a href="#">NR_037024.1</a>
<input checked="" type="checkbox"/>	<a href="#">Rhodococcus erythropolis strain ATCC 4277 16S ribosomal RNA, partial sequence</a>	<a href="#">Rhodococcus erythropolis</a>	1376	1376	100%	0.0	99.47%	1314	<a href="#">NR_119125.1</a>
<input checked="" type="checkbox"/>	<a href="#">Rhodococcus qingshengii strain dj1-6-2 16S ribosomal RNA, partial sequence</a>	<a href="#">Rhodococcus qingshengii</a>	1339	1339	100%	0.0	98.68%	1489	<a href="#">NR_115708.1</a>
<input checked="" type="checkbox"/>	<a href="#">Rhodococcus qingshengii strain CCM 4446 16S ribosomal RNA, partial sequence</a>	<a href="#">Rhodococcus qingshengii</a>	1339	1339	100%	0.0	98.68%	1473	<a href="#">NR_145886.1</a>

### TE3 (F+R)

GCCTTAGTGGCGCACGGGTGAGTAACACGTGGGAACCTGCCTTTCGGTTCGGAATAACGT  
 CTGGAAACGGACGCTAACACCGGATACGCCCTTTGGGGAAAGTTTACGCCGAGAGAGGG  
 GCCC GCGTCGGATTAGGTAGTTGGTGAGGTAATGGCTCACCAAGCCTTCGATCCGTAGCT  
 GGTCTGAGAGGATGATCAGCCACACTGGGACTGAGACACGGCCCAGACTCCTACGGGAGG  
 CAGCAGTGGGGAATATTGGACAATGGGCGCAAGCCTGATCCAGCAATGCCGCGTGAGTGA  
 TGAAGGCCTTAGGGTTGTAAAGCTCTTTCGCACGCGACGATGATGACGGTAGCGTGAGAA  
 GAAGCCCCGGCTAACTTCGTGCCAGCAGCCGCGGTAATACGAAGGGGGCTAGCGTTGTTC  
 GGAATTACTGGGCGTAAAGGGCGCGTAGGGCGCCTGTTTAGTCAGAAGTGAAAGCCCCGG  
 GCTCAACCTGGGAATAGCTTTTGATACTGGCAGGCTTGAGTTCCGGAGAGGATGGTGGAA  
 TTCCAGTGTAGAGGTGAAATTCGTAGATATTGGGAAGAACACCGGTGGCGAAGGCGGCC  
 ATCTGGACGGACACTGACGCTGAGGCGCGAAAGCGTGGGGAGCAAACAGGATTAGATAACC  
 CTGGTAGTCCACGCCGTAAACGATGAATGCTAGACGTCGGGGTGCATGCACTTCGGTGTC  
 GCCGCTAACGCATTAAGCATTCCGCCTGGGGAGTACGGCCGCAAGGTTAAAACCTCAAAGG  
 AATTGACGGGGGCCCGCACAAAGCGGTGGAGCATGTGGTTAATTGAAGCAACGCGCAGA  
 ACCTTACCAACCCTTGACATGTCCACTTTGGGTGAGAGAGATCACACCCTTCAGTTCGGC  
 TGGGTGGAACACAGGTGCTGCATGGCTGTCGTCAGCTCGTGTGAGATGTTGGGTTAA  
 GTCCCGCAACGAGCGCAACCCCTACCGTCAGTTGCCATCATTAGTTGGGCACTCTGGTG  
 GAACCGCCGGTGACAAGCCGGAGGAAGGCGGGGATGACGTCAAGTCCTCATGGCCCTTAT  
 GGGTTGGGCTACACACGTGCTACAATGGCGGTGACAGTGGGACGCGAAGTCGCGAGATGG  
 AGCAAATCCCCAAAAGCCGTCTCAGTTCGGATCGCACTCTGCAACTCGAGTGCCTGAAGT  
 TGAATCGCTAGTAATCGCGGATCAGCACGCCGCGGTGAATACGTTCCCGGGCCTTGTAC  
 ACACCGCCCGTACACCATGGGAGTTGGTTTTACCCGAAGGTGGTGC

Program	BLASTN <a href="#">Citation</a>
Database	rRNA_typestrains/16S_ribosomal_RNA <a href="#">See details</a>
Query ID	lcl Query_368227
Description	None
Molecule type	dna
Query Length	1307
Other reports	<a href="#">Distance tree of results</a> <a href="#">MSA viewer</a>

Organism only top 20 will appear  exclude

Type common name, binomial, taxid or group name

[+ Add organism](#)

Percent Identity  to  E value  to  Query Coverage  to

Descriptions		Graphic Summary	Alignments	Taxonomy				
<b>Sequences producing significant alignments</b>								
<input checked="" type="checkbox"/> select all 100 sequences selected		<a href="#">GenBank</a> <a href="#">Graphics</a> <a href="#">Distance tree of results</a> <a href="#">MSA Viewer</a>						
Description	Scientific Name	Max Score	Total Score	Query Cover	E value	Per. Ident	Acc. Len	Accession
<input checked="" type="checkbox"/> <a href="#">Azospirillum palustre strain B2 16S ribosomal RNA, partial sequence</a>	<a href="#">Azospirillum palustre</a>	2340	2340	100%	0.0	98.93%	1395	<a href="#">NR_178321.1</a>
<input checked="" type="checkbox"/> <a href="#">Azospirillum lipoferum strain NBRC 102290 16S ribosomal RNA, partial sequence</a>	<a href="#">Azospirillum lipoferum</a>	2316	2316	100%	0.0	98.62%	1417	<a href="#">NR_114058.1</a>
<input checked="" type="checkbox"/> <a href="#">Azospirillum lipoferum strain DSM 1691 16S ribosomal RNA, partial sequence</a>	<a href="#">Azospirillum lipoferum</a>	2314	2314	100%	0.0	98.62%	1478	<a href="#">NR_117481.1</a>
<input checked="" type="checkbox"/> <a href="#">Azospirillum lipoferum strain ATCC 29707 16S ribosomal RNA, partial sequence</a>	<a href="#">Azospirillum lipoferum</a>	2314	2314	100%	0.0	98.62%	1377	<a href="#">NR_116846.1</a>
<input checked="" type="checkbox"/> <a href="#">Azospirillum melinis strain TMCY 0552 16S ribosomal RNA, partial sequence</a>	<a href="#">Azospirillum melinis</a>	2287	2287	100%	0.0	98.24%	1414	<a href="#">NR_043483.1</a>

## TE4 (F+R)

GGTGCTTGCATCTGGGGGATTAGTGGCGAACGGGTGAGTAACACGTGAGCAACCTGCCCC  
 TGACTCTGGGATAAGCGCTGGAAACGGTGTCTAATACTGGATATGTCCTATCACCGCATG  
 GTGTGTGGGTGGAAAGATTTTTTCGTTGGGGATGGGCTCGCGGCCTATCAGCTTGTGGT  
 GAGGTAATGGCTACCAAGGCGTCGACGGGTAGCCGGCCTGAGAGGGTGACCGGCCACAC  
 TGGGACTGAGACACGGCCCAGACTCCTACGGGAGGCAGCAGTGGGGAATATTGCACAATG  
 GGCGCAAGCCTGATGCAGCAACGCCGCGTGAGGGATGACGGCCTTCGGGTTGTAACCTC  
 TTTTAGCAGGGAAGAAGCGAGAGTGACGGTACCTGCAGAAAAAGCACCGGCTAACTACGT  
 GCCAGCAGCCGCGGTAATACGTAGGGTGCAAGCGTTATCCGGAATTATTGGGCGTAAAGA  
 GCTCGTAGGCGGTTTGTGCGGTCTGCTGTGAAATCCCCGAGGCTCAACTTCGGGCTTGACG  
 TGGGTACGGGCAGACTAGAGTGCGGTAGGGGAGATTGGAATTCCTGGTGTAGCGGTGGAA  
 TGCGCAGATATCAGGAGGAACACCGATGGCGAAGGCAGATCTCTGGGCCGTAACCTGACGC  
 TGAGGAGCGAAAGGGTGGGGAGCAAACAGGCTTAGATACCCTGGTAGTCCACCCCGTAAA  
 CGTTGGGAACTAGTTGTGGGGTCCCTTCCACGGATTCCGTGACGCAGCTAACGCATTAAG  
 TTCCCCGCCTGGGGAGTACGGCCGCAAGGCTAAAACCTCAAAGGAATTGACGGGGACCCGC  
 ACAAGCGGCGGAGCATGCGGATTAATTCGATGCAACGCGAAGAACCTTACCAAGGCTTGA  
 CATAACCAGAACACCCTGGAAACAGGGGACTCTTTGGACACTGGTGAACAGGTGGTGA  
 TGGTTGTCGTCAGCTCGTGTGCTGAGATGTTGGGTAAAGTCCCGCAACGAGCGCAACCCT  
 CGTTCTATGTTGCCAGCACGTAATGGTGGGAACTCATGGGATACTGCCGGGGTCAACTCG  
 GAGGAAGGTGGGGATGACGTCAAATCATCATGCCCTTATGTCTTGGGCTTCACGCATGC  
 TACAATGGCCGGTACAATGGGCTGCGATACCCTAAGGTGGAGCGAATCCCCAAAAGCCGG  
 TCCCAGTTCGGATTGAGGTCTGCAACTCGACCTCATGAAGTCGGAGTCGCTAGTAATCGC  
 AGATCAGCAACGCTGCGGTGAATACGTTCCCGGGTCTTGTACACACCGCCCGTCAAGTCA  
 TGAAAGTCGGTAACACCTGAAGCCGG

Program [BLASTN](#) [Citation](#) ▼

Database [rRNA\\_typestrains/16S\\_ribosomal\\_RNA](#) [See details](#) ▼

Query ID [|cl|Query\\_44743](#)

Description None

Molecule type dna

Query Length 1346

Other reports [Distance tree of results](#) [MSA viewer](#) ?

Organism only top 20 will appear  exclude

Type common name, binomial, taxid or group name

[+ Add organism](#)

Percent Identity  to  E value  to  Query Coverage  to

[Filter](#) [Reset](#)

**Descriptions** [Graphic Summary](#) [Alignments](#) [Taxonomy](#)

Sequences producing significant alignments [Download](#) [Select columns](#) Show  ?

select all 100 sequences selected [GenBank](#) [Graphics](#) [Distance tree of results](#) [MSA Viewer](#)

Description	Scientific Name	Max Score	Total Score	Query Cover	E value	Per. Ident	Acc. Len	Accession
<input checked="" type="checkbox"/> <a href="#">Microbacterium suwonense strain M1T8B9 16S ribosomal RNA, partial sequence</a>	<a href="#">Microbacterium suwonense</a>	2429	2429	100%	0.0	99.26%	1428	<a href="#">NR_117266.1</a>
<input checked="" type="checkbox"/> <a href="#">Microbacterium arabinogalactanolyticum strain DSM 8611 16S ribosomal RNA, partial sequ...</a>	<a href="#">Microbacterium arabinogalactanolytic...</a>	2361	2361	99%	0.0	98.58%	1462	<a href="#">NR_044932.1</a>
<input checked="" type="checkbox"/> <a href="#">Microbacterium esteraromaticum strain DSM 8609 16S ribosomal RNA, partial sequence</a>	<a href="#">Microbacterium esteraromaticum</a>	2338	2338	99%	0.0	98.28%	1463	<a href="#">NR_026468.1</a>
<input checked="" type="checkbox"/> <a href="#">Microbacterium soli strain DCY17 16S ribosomal RNA, partial sequence</a>	<a href="#">Microbacterium soli</a>	2337	2337	100%	0.0	98.00%	1477	<a href="#">NR_116065.1</a>
<input checked="" type="checkbox"/> <a href="#">Microbacterium jejuense strain THG-C31 16S ribosomal RNA, partial sequence</a>	<a href="#">Microbacterium jejuense</a>	2324	2324	99%	0.0	98.13%	1441	<a href="#">NR_134085.1</a>

## TE5 (F+R)

GAGCGGCGAACGGGTGAGTAACACGTGGGTGATCTGCCCTGCACTTCGGGATAAGCCTGG  
 GAAACTGGGTCTAATACCGGATATGACCTCCTATCGCATGGTGGGTGGTGGAAAGATTTA  
 TCGGTGCAGGATGGGCCCGCGGCCTATCAGCTTGTGGTGGGGTAATGGCCTACCAAGGC  
 GACGACGGGTAGCCGACCTGAGAGGGTGACCGGCCACACTGGGACTGAGACACGGCCCAG  
 ACTCCTACGGGAGGCAGCAGTGGGGAATATTGCACAATGGGCGAAAGCCTGATGCAGCGA  
 CGCCGCGTGAGGGATGACGGCCTTCGGGTTGTAACCTCTTTTCAGCAGGGACGAAGCGCA  
 AGTGACGGTACCTGCAGAAGAAGCACCGGCTAACTACGTGCCAGCAGCCGCGGTAATACG  
 TAGGGTGCAAGCGTTGTCCGGAATTACTGGGCGTAAAGAGTTCGTAGGCGGTTTGTTCGCG  
 TCGTTTGTGAAAACCAGCAGCTCAACTGCTGGCTTGACAGGCGATACGGGCAGACTTGAGT  
 ACTGCAGGGGAGACTGGAATTCCTGGTGTAGCGGTGAAATGCGCAGATATCAGGAGGAAC  
 ACCGGTGGCGAAGGCGGGTCTCTGGGCAGTAACTGACGCTGAGGAACGAAAGCGTGGGTA  
 GCGAACAGGATTAGATACCCTGGTAGTCCACGCCGTAACGGTGGGCGCTAGGTGTGGGT  
 TCCTTCCACGGAATCCGTGCCGTAGCTAACGCATTAAGCGCCCCGCCTGGGGAGTACGGC  
 CGCAAGGCTAAAACCTCAAAGGAATTGACGGGGGCCCGCACAAAGCGGCGGAGCATGTGGAT  
 TAATTCGATGCAACGCGAAGAACCTTACCTGGGTTTGACATATACCGGAAAGCTGCAGAG  
 ATGTGGCCCCCTTGTGGTCGGTATACAGGTGGTGCATGGCTGTCGTCAGCTCGTGTCTGT  
 GAGATGTTGGGTTAAGTCCCGCAACGAGCGCAACCCCTATCTTATGTTGCCAGCACGTTA  
 TGGTGGGGACTCGTAAGAGACTGCCGGGGTCAACTCGGAGGAAGGTGGGGACGACGTCAA  
 GTCATCATGCCCCTTATGTCCAGGGCTTCACACATGCTACAATGGCCAGTACAGAGGGCT  
 GCGAGACCGTGAGGTGGAGCGAATCCCTTAAAGCTGGTCTCAGTTCGGATCGGGGTCTGC  
 AACTCGACCCCGTGAAGTCGGAGTCGCTAGTAATCGCAGATCAGCAACGCTGCGGTGAAT  
 ACGTTCGCCGGGCCTTGTACACACCGCCCGTCAAGTCATGAAAGTCGGAACACCCGAACCG

Program **BLASTN** [Citation](#)

Database **rRNA\_typestrains/16S\_ribosomal\_RNA** [See details](#)

Query ID **lcl|Query\_30459**

Description **None**

Molecule type **dna**

Query Length **1320**

Other reports [Distance tree of results](#) [MSA viewer](#)

Organism *only top 20 will appear*  exclude

Type common name, binomial, taxid or group name

[+ Add organism](#)

Percent Identity  to  E value  to  Query Coverage  to

**Filter** **Reset**

- Descriptions**
- Graphic Summary
- Alignments
- Taxonomy

Sequences producing significant alignments Download Select columns Show

select all 100 sequences selected [GenBank](#) [Graphics](#) [Distance tree of results](#) [MSA Viewer](#)

Description	Scientific Name	Max Score	Total Score	Query Cover	E value	Per. Ident	Acc. Len	Accession
<input checked="" type="checkbox"/> <a href="#">Rhodococcus qingshengii strain dj1-6-2 16S ribosomal RNA, partial sequence</a>	<a href="#">Rhodococcus qingshengii</a>	2423	2423	100%	0.0	99.77%	1489	<a href="#">NR_115708.1</a>
<input checked="" type="checkbox"/> <a href="#">Rhodococcus qingshengii strain CCM 4446 16S ribosomal RNA, partial sequence</a>	<a href="#">Rhodococcus qingshengii</a>	2423	2423	100%	0.0	99.77%	1473	<a href="#">NR_145886.1</a>
<input checked="" type="checkbox"/> <a href="#">Rhodococcus qingshengii JCM 15477 strain dj1-6 16S ribosomal RNA, partial sequence</a>	<a href="#">Rhodococcus qingshengii JCM 15477</a>	2423	2423	100%	0.0	99.77%	1484	<a href="#">NR_043535.1</a>
<input checked="" type="checkbox"/> <a href="#">Rhodococcus erythropolis strain N11 16S ribosomal RNA, partial sequence</a>	<a href="#">Rhodococcus erythropolis</a>	2381	2381	100%	0.0	99.17%	1476	<a href="#">NR_037024.1</a>
<input checked="" type="checkbox"/> <a href="#">Nocardia coeliaca strain DSM 44595 16S ribosomal RNA, partial sequence</a>	<a href="#">Nocardia coeliaca</a>	2379	2379	100%	0.0	99.17%	1507	<a href="#">NR_104776.1</a>

## TE6 (F+R)

GCAGCACAGAGGAGCTTGCTCCTTGGGTGGCGAGTGGCGGACGGGTGAGTAATGCATCGG  
 GATCTACCCTGACGTGGGGGATAACCTCGGGAACCGGGACTAATACCGCATAACGTCCTA  
 CGGGAGAAAGCGGGGGACCTTTTAGGCCTCGCGCGCAGGACGAACCGATGTGCGATTAG  
 CTAGTTGGCGGGTAATGGCCACCAAGGCGACGATCGCTAGCTGGTCTGAGAGGATGAT  
 CAGCCACACTGGGACTGAGACACGGCCCAGACTCCTACGGGAGGCAGCAGTGGGGAATAT  
 TGGACAATGGGCGCAAGCCTGATCCAGCAATGCCGCGTGTGTGAAGAAGGCCCTTCGGGTT  
 GTAAAGCACTTTTATCAGGAGCGAAATCTGCATGCTTAATACGTGTGCAGTCTGACGGTA  
 CCTGAGGAATAAGCACCGGCTAACTTCGTGCCAGCAGCCGCGGTAATACGAAGGGTGCAA  
 GCGTTAATCGGAATTACTGGGCGTAAAGGGTGCGTAGGCGGTTTCGTTAAGTCTGTCTGTA  
 AATCCCCGGGCTCAACCTGGGAATGGCGATGGATACTGGCGAGCTAGAGTGTGTCAGAGG  
 ATGGTGAATTCCCGGTGTAGCGGTGAAATGCGTAGAGATCGGGAGGAACATCAGTGGCG  
 AAGGCGCCATCTGGGACAACACTGACGCTGAAGCACGAAAGCGTGGGGAGCAAACAGGA  
 TTAGATACCCTGGTAGTCCACGCCCTAAACGATGCGAACTGGATGTTGGTCTCAACTCGG  
 AGATCAGTGTGCAAGCTAACGCGTTAAGTTCGCCGCTGGGGAGTACGGTCGCAAGACTG  
 AAACCTCAAAGGAATTGACGGGGGGCCGCACAAGCGGTGGAGTATGTGGTTAATTCGATG  
 CAACGCGAAGAACCCTTACCTGGCCTTGACATGTCCGGAATCCTGCAGAGATGCGGGAGTG  
 CCTTCGGGAATCGGAACACAGGTGCTGCATGGCTGTCGTCAGCTCGTGTCTGAGATGTT  
 GGGTTAAGTCCCAGCAACGAGCGCAACCCCTTGTCTTAGTTGCCAGCGAGTAATGTCGGGA  
 ACTCTAAGGAGACTGCCGGTGACAAACCGGAGGAAGGTGGGGATGACGTCAAGTCTCAT  
 GGCCCTTACGGCCAGGGCTACACACGTAACAATGGTTCGGTACAGAGGGTTGCAATACC  
 GCGAGGTGGAGCCAATCCCAGAAAGCCGATCCCAGTCCGGATTGGAGTCTGCAACTCGAC  
 TCCATGAAGTCGGAATCGCTAGTAATCGCGGATCAGCTATGCCGCGGTGAATACGTTCCC  
 GGGCCTTGTACACACCGCCCGTCACACCATGGGAGTGGGTTGCTCCAGAAGGCGTTAGTC  
 TAA

Program	BLASTN <a href="#">Citation</a> <span>▼</span>
Database	rRNA_typestrains/16S_ribosomal_RNA <a href="#">See details</a> <span>▼</span>
Query ID	lcl Query_115001
Description	None
Molecule type	dna
Query Length	1383
Other reports	<a href="#">Distance tree of results</a> <a href="#">MSA viewer</a> <span>?</span>

Organism only top 20 will appear  exclude

Type common name, binomial, taxid or group name

[+ Add organism](#)

Percent Identity  to  E value  to  Query Coverage  to

[Filter](#) [Reset](#)

- Descriptions**
- Graphic Summary
- Alignments
- Taxonomy

Sequences producing significant alignments Download ▼ Select columns ▼ Show  ?

select all 100 sequences selected [GenBank](#) [Graphics](#) [Distance tree of results](#) [MSA Viewer](#)

Description	Scientific Name	Max Score	Total Score	Query Cover	E value	Per. Ident	Acc. Len	Accession
<input checked="" type="checkbox"/> <a href="#">Rhodanobacter xiangguanii strain BJQ-6 16S ribosomal RNA, partial sequence</a>	<a href="#">Rhodanobacter xiangguanii</a>	2532	2532	100%	0.0	99.71%	1424	<a href="#">NR_132710.1</a>
<input checked="" type="checkbox"/> <a href="#">Rhodanobacter lindaniclasticus strain RP5557 16S ribosomal RNA, partial sequence</a>	<a href="#">Rhodanobacter lindaniclasticus</a>	2531	2531	100%	0.0	99.71%	1503	<a href="#">NR_024878.1</a>
<input checked="" type="checkbox"/> <a href="#">Rhodanobacter rhizosphaerae strain CR164 16S ribosomal RNA, partial sequence</a>	<a href="#">Rhodanobacter rhizosphaerae</a>	2444	2444	100%	0.0	98.56%	1486	<a href="#">NR_156938.1</a>
<input checked="" type="checkbox"/> <a href="#">Rhodanobacter denitrificans strain ZAPBS1 16S ribosomal RNA, partial sequence</a>	<a href="#">Rhodanobacter denitrificans</a>	2372	2372	98%	0.0	98.16%	1527	<a href="#">NR_102497.1</a>
<input checked="" type="checkbox"/> <a href="#">Rhodanobacter denitrificans strain ZAPBS1 16S ribosomal RNA, partial sequence</a>	<a href="#">Rhodanobacter denitrificans</a>	2372	2372	98%	0.0	98.16%	1419	<a href="#">NR_108437.1</a>



## TE7 (F+R)

GGCCTTTCGGGGTACACGAGCGGCGAACGGGTGAGTAACACGTGGGTGATCTGCCCTGCA  
 CTTTCGGGATAAGCCTGGGAAACTGGGTCTAATACCGGATATGACCTCCTATCGCATGGTG  
 GGTGGTGGAAAGATTTATCGGTGCAGGATGGGCCCGCGGCCTATCAGCTTGTGGTGGGG  
 TAATGGCCTACCAAGGCGACGACGGGTAGCCGACCTGAGAGGGTGACCGGCCACACTGGG  
 ACTGAGACACGGCCCAGACTCCTACGGGAGGCAGCAGTGGGGAATATTGCACAATGGGCG  
 AAAGCCTGATGCAGCGACGCCGCGTGAGGGATGACGGCCTTCGGGTTGTAAACCTCTTTC  
 AGCAGGGACGAAGCGCAAGTGACGGTACCTGCAGAAGAAGCACCGGCTAACTACGTGCCA  
 GCAGCCGCGGTAATACGTAGGGTGCAAGCGTTGTCCGGAATTACTGGGCGTAAAGAGTTC  
 GTAGGCGGTTTGTTCGCGTCGTTTGTGAAAACCAGCAGCTCAACTGCTGGCTTGCAGGCGA  
 TACGGGCAGACTTGAGTACTGCAGGGGAGACTGGAATTCCTGGTGTAGCGGTGAAATGCG  
 CAGATATCAGGAGGAACACCGGTGGCGAAGGCGGGTCTCTGGGCAGTAACTGACGCTGAG  
 GAACGAAAGCGTGGGTAGCGAACAGGATTAGATACCCTGGTAGTCCACGCCGTAAACGGT  
 GGGCGCTAGGTGTGGGTTCTTCCACGGAATCCGTGCCGTAGCTAACGCATTAAGCGCCC  
 CGCTGGGGAGTACGGCCGCAAGGCTAAACTCAAAGGAATTGACGGGGGCCCGCACAAAG  
 CGGCGGAGCATGTGGATTAATTCGATGCAACGCGAAGAACCTTACCTGGGTTTGACATAT  
 ACCGAAAGCTGCAGAGATGTGGCCCCCTTGTGGTCGGTATACAGGTGGTGCATGGCTG  
 TCGTCAGCTCGTGTCTGAGATGTTGGGTTAAGTCCCGCAACGAGCGCAACCCCTATCTT  
 ATGTTGCCAGCACGTTATGGTGGGACTCGTAAGAGACTGCCGGGGTCAACTCGGAGGAA  
 GGTGGGGACGACGTCAAGTCATCATGCCCTTATGTCCAGGGCTTCACACATGCTACAAT  
 GGCCAGTACAGAGGGCTGCGAGACCGTGAGGTGGAGCGAATCCCTTAAAGCTGGTCTCAG  
 TTCGGATCGGGTCTGCAACTCGACCCCGTGAAGTCGGAGTCGCTAGTAATCGCAGATCA  
 GCAACGCTGCGGTGAATACGTTCCCGGGCCTGTACACACCGCCCGTCACGTCAGAAAGT  
 CGGTAACACCCGAAGCCGGG

Program	BLASTN <a href="#">Citation</a>
Database	rRNA_typestrains/16S_ribosomal_RNA <a href="#">See details</a>
Query ID	lcl Query_47061
Description	None
Molecule type	dna
Query Length	1340
Other reports	<a href="#">Distance tree of results</a> <a href="#">MSA viewer</a>

Organism only top 20 will appear  exclude

Type common name, binomial, taxid or group name

[+ Add organism](#)

Percent Identity  to  E value  to  Query Coverage  to

- Descriptions**
- Graphic Summary
- Alignments
- Taxonomy

Sequences producing significant alignments Download  Select columns  Show  [?](#)

select all 100 sequences selected [GenBank](#) [Graphics](#) [Distance tree of results](#) [MSA Viewer](#)

Description	Scientific Name	Max Score	Total Score	Query Cover	E value	Per. Ident	Acc. Len	Accession
<input checked="" type="checkbox"/> <a href="#">Rhodococcus qingshengii strain djI-6-2 16S ribosomal RNA, partial sequence</a>	<a href="#">Rhodococcus qingshengii</a>	2468	2468	99%	0.0	99.93%	1489	<a href="#">NR_115708.1</a>
<input checked="" type="checkbox"/> <a href="#">Rhodococcus qingshengii strain CCM 4446 16S ribosomal RNA, partial sequence</a>	<a href="#">Rhodococcus qingshengii</a>	2468	2468	99%	0.0	99.93%	1473	<a href="#">NR_145886.1</a>
<input checked="" type="checkbox"/> <a href="#">Rhodococcus qingshengii JCM 15477 strain djI-6 16S ribosomal RNA, partial sequence</a>	<a href="#">Rhodococcus qingshengii JCM 15477</a>	2468	2468	99%	0.0	99.93%	1484	<a href="#">NR_043535.1</a>
<input checked="" type="checkbox"/> <a href="#">Rhodococcus erythropolis strain N11 16S ribosomal RNA, partial sequence</a>	<a href="#">Rhodococcus erythropolis</a>	2425	2425	99%	0.0	99.33%	1476	<a href="#">NR_037024.1</a>
<input checked="" type="checkbox"/> <a href="#">Nocardia coeliaca strain DSM 44595 16S ribosomal RNA, partial sequence</a>	<a href="#">Nocardia coeliaca</a>	2423	2423	99%	0.0	99.33%	1507	<a href="#">NR_104776.1</a>

## TE8 (F+R)

GGATTGAGAGCTTGCTCTCAGAAGTTAGCGGCGGACGGGTGAGTAACACGTGGGTAACCT  
GCCATAAGACTGGGATAACTCCGGGAAACCGGGGCTAATACCGGATAACATTTTGAAC  
GCATAGTTTCGAAATTGAAAGGCGGCTTCGGCTGTCACTTATGGATGGACCCGCGTCGCAT  
TAGCTAGTTGGTGAGGTAACGGCTCACCAAGGCAACGATGCGTAGCCGACCTGAGAGGGT  
GATCGGCCACACTGGGACTGAGACACGGCCCAGACTCCTACGGGAGGCAGCAGTAGGGAA  
TCTTCCGCAATGGACGAAAGTCTGACGGAGCAACGCCGCGTGAGTGATGAAGGCTTTCGG  
GTCGTAAACTCTGTTGTTAGGGAAGAACAAGTGCTAGTTGAATAAGCTGGCACCTTGAC  
GGTACCTAACAGAAAGCCACGGCTAACTACGTGCCAGCAGCCGCGTAATACGTAGGTG  
GCAAGCGTTATCCGGAATTATTGGGCGTAAAGCGCGCGCAGGTGGTTTCTTAAGTCTGAT  
GTGAAAGCCCACGGCTCAACCGTGGAGGGTCATTGGAACTGGGAGACTTGAGTGCAGAA  
GAGGAAAGTGGAATCCATGTGTAGCGGTGAAATGCGTAGAGATATGGAGGAACACCAGT  
GGCGAAGGCGACTTCTGGTCTGTAAGTACTGACACTGAGGCGCGAAAGCGTGGGGAGCAAAC  
AGGATTAGATACCCTGGTAGTCCACGCCGTAAACGATGAGTGCTAAGTGTAGAGGGTTT  
CCGCCCTTATAGTCTGAAGTTAACGCATTAAGCACTCCGCCTGGGGAGTACGGCCGCAAG  
GCTGAAACTCAAAGGAATTGACGGGGGCCCGCACAAAGCGGTGGAGCATGTGGTTTAATTC  
GAAGCAACGCGAAGAACCTTACCAGGTCTTGACATCCTCTGAAAACCTAGAGATAGGGC  
TTCTCCTTCGGGAGCAGAGTGACAGGTGGTGCATGGTTGTCGTCAGCTCGTGTCTGAGA  
TGTTGGGTTAAGTCCCAGCAACGAGCGCAACCCTTGATCTTAGTTGCCATCATTAAAGTTGG  
GCACTCTAAGGTGACTGCCGGTGACAAACCGGAGGAAGGTGGGGATGACGTCAAATCATC  
ATGCCCTTATGACCTGGGCTACACACGTGCTACAATGGACGGTACAAAGAGCTGCAAGA  
CCGCGAGGTGGAGCTAATCTCATAAAACCGTTCTCAGTTCGGATTGTAGGCTGCAACTCG  
CCTACATGAAGCTGGAATCGCTAGTAATCGCGGATCAGCATGCCGCGGTGAATACGTTCC  
CGGGCCTTGTACACACCGCCCGTCACACCACGAGAGTTTGTAAACCCGAAGTCGGT

Program	BLASTN <a href="#">Citation</a>
Database	rRNA_typestrains/16S_ribosomal_RNA <a href="#">See details</a>
Query ID	lcl Query_65285
Description	None
Molecule type	dna
Query Length	1377
Other reports	<a href="#">Distance tree of results</a> <a href="#">MSA viewer</a>

Organism only top 20 will appear  exclude

  
[+ Add organism](#)

Percent Identity	E value	Query Coverage
<input type="text"/> to <input type="text"/>	<input type="text"/> to <input type="text"/>	<input type="text"/> to <input type="text"/>

Descriptions		Graphic Summary	Alignments	Taxonomy					
Sequences producing significant alignments									
Download									
Select columns									
Show 100									
GenBank Graphics Distance tree of results MSA Viewer									
<input checked="" type="checkbox"/> select all	Description	Scientific Name	Max Score	Total Score	Query Cover	E value	Per. Ident	Acc. Len	Accession
<input checked="" type="checkbox"/>	<a href="#">Bacillus toyonensis strain BCT-7112 16S ribosomal RNA, partial sequence</a>	<a href="#">Bacillus toyonensis</a>	2532	2532	100%	0.0	99.85%	1544	<a href="#">NR_121761.1</a>
<input checked="" type="checkbox"/>	<a href="#">Bacillus thuringiensis strain ATCC 10792 16S ribosomal RNA, partial sequence</a>	<a href="#">Bacillus thuringiensis</a>	2532	2532	100%	0.0	99.85%	1482	<a href="#">NR_114581.1</a>
<input checked="" type="checkbox"/>	<a href="#">Bacillus thuringiensis strain IAM 12077 16S ribosomal RNA, partial sequence</a>	<a href="#">Bacillus thuringiensis</a>	2532	2532	100%	0.0	99.85%	1486	<a href="#">NR_043403.1</a>
<input checked="" type="checkbox"/>	<a href="#">Bacillus thuringiensis strain NBRC 101235 16S ribosomal RNA, partial sequence</a>	<a href="#">Bacillus thuringiensis</a>	2529	2529	100%	0.0	99.78%	1477	<a href="#">NR_112780.1</a>
<input checked="" type="checkbox"/>	<a href="#">Bacillus pacificus strain MCCC 1A06182 16S ribosomal RNA, partial sequence</a>	<a href="#">Bacillus pacificus</a>	2527	2527	100%	0.0	99.78%	1509	<a href="#">NR_157733.1</a>

## TE9 (F+R)

CTTCGGACGCTGACGAGTGGCGAACGGGTGAGTAATACATCGGAACGTGCCAGTCGTGG  
 GGGATAACTACTCGAAAGAGTAGCTAATACCGCATAACGATCTGAGGATGAAAGCGGGGA  
 CCTTCGGGCCTCGCGCGATTGGAGCGGCCGATGGCAGATTAGGTAGTTGGTGGGATAAAA  
 GCTTACCAAGCCGACGATCTGTAGCTGGTCTGAGAGGACGACCAGCCACACTGGGACTGA  
 GACACGGCCCAGACTCCTACGGGAGGCAGCAGTGGGGAATTTTGGACAATGGGCGAAAGC  
 CTGATCCAGCAATGCCGCGTGCAGGATGAAGGCCTTCGGGTTGTAAACTGCTTTTGTACG  
 GAACGAAAAAGCTTCTCCTAATACGAGAGGCCCATGACGGTACCGTAAGAATAAGCACCG  
 GCTAACTACGTGCCAGCAGCCGCGGTAATACGTAGGGTGCAGCGTTAATCGGAATTACT  
 GGGCGTAAAGCGTGCGCAGGCGGTTATGTAAGACAGATGTGAAATCCCCGGGCTCAACCT  
 GGGAACTGCATTTGTGACTGCATGGCTAGAGTACGGTAGAGGGGGATGGAATCCGCGTG  
 TAGCAGTCAAATGCGTAGATATGCGGAGGAACACCGATGGCGAAGGCAATCCCCTGGACC  
 TGTACTGACGCTCATGCACGAAAGCGTGGGGAGCAAACAGGATTAGATACCTGGTAGTC  
 CACGCCCTAACGATGTCAACTGGTTGTTGGGAATTAGTTTTCTCAGTAACGAAGCTAAC  
 GCGTGAAGTTGACCGCCTGGGGAGTACGGCCGCAAGGTTGAAACTCAAAGGAATTGACGG  
 GGACCCGCACAAGCGGTGGATGATGTGGTTTAATTCGATGCAACGCGAAAAACCTTACCC  
 ACCTTTGACATGGCAGGAAGTTTCCAGAGATGGATTCGTGCTCGAAAGAGAACCTGCACA  
 CAGGTGCTGCATGGCTGTCGTCAGCTCGTGTGAGATGTTGGGTTAAGTCCCGCAACG  
 AGCGCAACCCTTGTCAATTAGTTGCTACATTTAGTTGNGCACTCTAATGAGACTGCCGGTG  
 ACAAACCGGAGGAAGGTGGGGATGACGTCAAGTCCTCATGGCCCTTATAGGTGGGGCTAC  
 ACACGTCATAAATGGCTGGTACAGAGGGTTGCCAACCCGCGAGGGGGAGCTAATCCCAT  
 AAAACCAGTCGTAGTCCGGATCGCAGTCTGCAACTCGACTGCGTGAAGTCGGAATCGCTA  
 GTAATCGCGGATCAGCATGCCGCGGTGAATACGTTCCCGGGTCTTGTACACACCGCCCGT  
 CACACCATGGGAGCGGGTCTCGCCAGAAGTAGGTAG

Program	BLASTN <a href="#">Citation</a>
Database	rRNA_tyestrains/16S_ribosomal_RNA <a href="#">See details</a>
Query ID	lc Query_20227
Description	None
Molecule type	dna
Query Length	1356
Other reports	<a href="#">Distance tree of results</a> <a href="#">MSA viewer</a>

Organism only top 20 will appear  exclude

Type common name, binomial, taxid or group name

[+ Add organism](#)

Percent Identity  to  E value  to  Query Coverage  to

[Filter](#) [Reset](#)

- Descriptions**
- Graphic Summary
- Alignments
- Taxonomy

Sequences producing significant alignments Download Select columns Show  [?](#)

select all 100 sequences selected GenBank Graphics Distance tree of results MSA Viewer

Description	Scientific Name	Max Score	Total Score	Query Cover	E value	Per. Ident	Acc. Len	Accession
<input checked="" type="checkbox"/> <a href="#">Delftia acidovorans strain NBRC 14950 16S ribosomal RNA, partial sequence</a>	<a href="#">Delftia acidovorans</a>	2501	2501	100%	0.0	99.93%	1458	<a href="#">NR_113708.1</a>
<input checked="" type="checkbox"/> <a href="#">Delftia lacustris strain 332 16S ribosomal RNA, partial sequence</a>	<a href="#">Delftia lacustris</a>	2468	2468	100%	0.0	99.48%	1534	<a href="#">NR_116495.1</a>
<input checked="" type="checkbox"/> <a href="#">Delftia tsuruhatensis strain NBRC 16741 16S ribosomal RNA, partial sequence</a>	<a href="#">Delftia tsuruhatensis</a>	2464	2464	100%	0.0	99.41%	1458	<a href="#">NR_113870.1</a>
<input checked="" type="checkbox"/> <a href="#">Delftia tsuruhatensis strain T7 16S ribosomal RNA, partial sequence</a>	<a href="#">Delftia tsuruhatensis</a>	2462	2462	100%	0.0	99.41%	1456	<a href="#">NR_024786.1</a>
<input checked="" type="checkbox"/> <a href="#">Delftia acidovorans strain IAM 12409 16S ribosomal RNA, partial sequence</a>	<a href="#">Delftia acidovorans</a>	2453	2453	100%	0.0	99.26%	1522	<a href="#">NR_024711.1</a>



## TE10 (F)

CATGCAGTCGAGCGGACTTGATGGAGTGCTTGCACTCCTGATGGTTAGCGGCGGACGGGT  
 GAGTAACACGTAGGCAACCTGCCCGTAAGACTGGGATAACATTCGAAACGAATGCTAAT  
 ACCGGATACGCGATTTTCTCGCATGAGAGAATCGGGAAAGAAGGAGCAATCTTTCACCTA  
 CGGATGGGCCTGCGGCGCATTAGCTAGTTGGTGGGGTAACGGCTCACCAAGGCGACGATG  
 CGTAGCCGACCTGAGAGGGTGATCGGCCACACTGGGACTGAGACACGGCCCAGACTCCTA  
 CGGGAGGCAGCAGTAGGGAATCTTCCGCAATGGACGAAAGTCTGACGGAGCAACGCCCGC  
 TGAGTGAAGAAGGCTTTCGGGTCGTAAGCTCTGTTGCCAGGGAAGAACAATTGAGAGAG  
 TAACTGCTCTTGAGTTGACGGTACCTGAGAAGAAAGCCCCGGCTAACTACGTGCCAGCAG  
 CCGCGGTAATACGTAGGGGGCAAGCGTTGTCCGGAATTATTGGGCGTAAAGCGCGCGCAG  
 GCGGCTTTGTAAGTCTGTCGTTTAAGTTCGGGGCTCAACCCCGTGTCGCGATGGAAACTG  
 CAAGGCTTGAGTACAGAAGAGGAAAGTGGAATTCCACGTGTAGCGGTGAAATGCGTAGAG  
 ATGTGGAGGAACACCAGTGGCGAAGGCGACTTTCTGGGCTGTAAGTACGCTGAGGCGCG  
 AAAGCGTGGGGAGCAAACAGGATTAGATACCCTGGTAGTCCACGCCGTAACGATGAATG  
 CTAGGTGTTAGGGGTTTCAATACCCTTGGTGCCGAAGTTAACACATTAAGCATTCCGCCT  
 GGGGAGTACGCTCGCAAGAGTGAAACTCAAAGGAATTGACGGGGACCCGCACAAGCAGTG  
 GAGTATGTGGTTTAATTCGAAGCAACGCGAAGAACCTTACCAGGTCTTGACATCCCTCTG  
 ACCGGTCTGGAGACAGGCCTTCCCTTCGGGCAGA

Program [BLASTN](#) [Citation](#)

Database [rRNA\\_typestrains/16S\\_ribosomal\\_RNA](#) [See details](#)

Query ID [Ic|Query\\_24471](#)

Description None

Molecule type dna

Query Length 994

Other reports [Distance tree of results](#) [MSA viewer](#)

Organism only top 20 will appear  exclude

Type common name, binomial, taxid or group name

[+ Add organism](#)

Percent Identity  to  E value  to  Query Coverage  to

[Filter](#) [Reset](#)

- Descriptions**
- Graphic Summary
- Alignments
- Taxonomy

Sequences producing significant alignments Download  Select columns  Show  100

select all 100 sequences selected [GenBank](#) [Graphics](#) [Distance tree of results](#) [MSA Viewer](#)

	Description	Scientific Name	Max Score	Total Score	Query Cover	E value	Per. Ident	Acc. Len	Accession
<input checked="" type="checkbox"/>	<a href="#">Paenibacillus curdlanolyticus strain YK9 16S ribosomal RNA, partial sequence</a>	<a href="#">Paenibacillus curdlanolyticus</a>	1775	1775	100%	0.0	98.80%	1531	<a href="#">NR_040891.1</a>
<input checked="" type="checkbox"/>	<a href="#">Paenibacillus curdlanolyticus strain NBRC 15724 16S ribosomal RNA, partial sequence</a>	<a href="#">Paenibacillus curdlanolyticus</a>	1773	1773	100%	0.0	98.80%	1478	<a href="#">NR_113803.1</a>
<input checked="" type="checkbox"/>	<a href="#">Paenibacillus curdlanolyticus strain YK9 16S ribosomal RNA, partial sequence</a>	<a href="#">Paenibacillus curdlanolyticus</a>	1764	1764	100%	0.0	98.60%	1436	<a href="#">NR_115596.1</a>
<input checked="" type="checkbox"/>	<a href="#">Paenibacillus ginsengiterrae strain DCY89 16S ribosomal RNA, partial sequence</a>	<a href="#">Paenibacillus ginsengiterrae</a>	1683	1683	99%	0.0	97.29%	1495	<a href="#">NR_178650.1</a>
<input checked="" type="checkbox"/>	<a href="#">Paenibacillus xylaniclasticus strain TW1 16S ribosomal RNA, partial sequence</a>	<a href="#">Paenibacillus xylaniclasticus</a>	1672	1672	100%	0.0	96.99%	1513	<a href="#">NR_116719.1</a>

## TE11 (F+R)

CATGCAGTCGAGCGAATGGATTGAGAGCTTGCTCTCAAGAAGTTAGCGGCGGACGGGTGA  
GTAACACGTGGGTAACCTGCCATAAGACTGGGATAACTCCGGGAAACCGGGGCTAATAC  
CGGATAACATTTTGAAGTGCATAGTTCGAAATTGAAAGGCGGCTTCGGCTGTCACCTTATG  
GATGGACCCGCGTCGATTAGCTAGTTGGTGAGGTAACGGCTCACCAAGGCAACGATGCG  
TAGCCGACCTGAGAGGGTGATCGGCCACACTGGGACTGAGACACGGCCCAGACTCCTACG  
GGAGGCAGCAGTAGGGAATCTTCCGCAATGGACGAAAGTCTGACGGAGCAACGCCGCGTG  
AGTGATGAAGGCTTTCGGGTCTGAAAACCTCTGTTGTTAGGGAAGAACAAGTGCTAGTTGA  
ATAAGCTGGCACCTTGACGGTACCTAACCAGAAAGCCACGGCTAACTACGTGCCAGCAGC  
CGCGGTAATACGTAGGTGGCAAGCGTTATCCGGAATTATTGGGCGTAAAGCGCGCGCAGG  
TGGTTTCTTAAGTCTGATGTGAAAGCCCACGGCTCAACCGTGGAGGGTCATTGGAACTG  
GGAGACTTGAGTGCAGAAGAGGAAAGTGGAATTCCATGTGTAGCGGTGAAATGCGTAGAG  
ATATGGAGGAACACCAGTGGCGAAGGCGACTTCTGGTCTGTAAGTACTGACACTGAGGCGCG  
AAAGCGTGGGGAGCAAACAGGATTAGATACCCTGGTAGTCCACGCCGTAACGATGAGTG  
CTAAGTGTTAGAGGGTTTCCGCCCTTATGCTGAAGTTAACGCATTAAGCACTCCGCCT  
GGGAGTACGGCCGCAAGGCTGAAACTCAAAGGAATTGACGGGGGCCCGCACAAAGCGGTG  
GAGCATGTGGTTTAATTCGAAGCAACGCGAAGAACCTTACCAGGTCTTGACATCCTCTGA  
AAACCCTAGAGATAGGGCTTCTCCTTCGGGAGCAGAGTGACAGGTGGTGCATGGTTGTCG  
TCAGCTCGTGTCTGAGATGTTGGGTTAAGTCCCGCAACGAGCGCAACCCTTGATCTTAG  
TTGCCATCATTAAAGTTGGGCACTCTAAGGTGACTGCCGGTGACAAACCGGAGGAAGGTGG  
GGATGACGTCAAATCATCATGCCCTTATGACCTGGGCTACACACGTGCTACAATGGACG  
GTACAAAGAGCTGCAAGACCGCGAGGTGGAGCTAATCTCATAAAACCGTTCTCAGTTCGG  
ATTGTAGGCTGCAACTCGCCTACATGAAGCTGGAATCGCTAGTAATCGCGGATCAGCATG  
CCGCGGTGAATACGTTCCCGGGCCTTGTACACACCGCCCGTCACACCACGAGAGTTTGTA  
ACACCCGAAGTCGGTGGGGTAACCTTTTGGAGCCAG

Program	BLASTN <a href="#">Citation</a>
Database	rRNA_tpestrains/16S_ribosomal_RNA <a href="#">See details</a>
Query ID	lcl Query_121993
Description	None
Molecule type	dna
Query Length	1416
Other reports	<a href="#">Distance tree of results</a> <a href="#">MSA viewer</a>

Organism only top 20 will appear  exclude

Type common name, binomial, taxid or group name

[+ Add organism](#)

Percent Identity  to  E value  to  Query Coverage  to

[Filter](#) [Reset](#)

- Descriptions**
- Graphic Summary
- Alignments
- Taxonomy

Sequences producing significant alignments Download Select columns Show  [?](#)

select all 100 sequences selected [GenBank](#) [Graphics](#) [Distance tree of results](#) [MSA Viewer](#)

Description	Scientific Name	Max Score	Total Score	Query Cover	E value	Per. Ident	Acc. Len	Accession
<input checked="" type="checkbox"/> <a href="#">Bacillus toyonensis strain BCT-7112 16S ribosomal RNA, partial sequence</a>	<a href="#">Bacillus toyonensis</a>	2601	2601	100%	0.0	99.79%	1544	<a href="#">NR_121761.1</a>
<input checked="" type="checkbox"/> <a href="#">Bacillus thuringiensis strain ATCC 10792 16S ribosomal RNA, partial sequence</a>	<a href="#">Bacillus thuringiensis</a>	2601	2601	100%	0.0	99.79%	1482	<a href="#">NR_114581.1</a>
<input checked="" type="checkbox"/> <a href="#">Bacillus thuringiensis strain IAM 12077 16S ribosomal RNA, partial sequence</a>	<a href="#">Bacillus thuringiensis</a>	2601	2601	100%	0.0	99.79%	1486	<a href="#">NR_043403.1</a>
<input checked="" type="checkbox"/> <a href="#">Bacillus thuringiensis strain NBRC 101235 16S ribosomal RNA, partial sequence</a>	<a href="#">Bacillus thuringiensis</a>	2597	2597	100%	0.0	99.72%	1477	<a href="#">NR_112780.1</a>
<input checked="" type="checkbox"/> <a href="#">Bacillus pacificus strain MCCC 1A06182 16S ribosomal RNA, partial sequence</a>	<a href="#">Bacillus pacificus</a>	2595	2595	100%	0.0	99.72%	1509	<a href="#">NR_157733.1</a>

## TE12 (F+R)

ATGCAGTCGACGATGAACCAGAGTGCTTGCACCTGGGGATTAGTGGCGAACGGGTGAGTA  
ACACGTGAGCAACCTGCCCTCACTCTGGGATAAGCGCTGGAAACGGCGTCTAATACTGG  
ATACGAGGCACAACCGCATGGTTAGTGTCTGGAAAGATTTTTTGGTGGGGGATGGGCTCG  
CGGCCTATCAGCTTGTGGTGAGGTAATGGCTACCAAGGCGTCGACGGGTAGCCGGCCT  
GAGAGGGTGACCGGCCACACTGGGACTGAGACACGGCCCAGACTCCTACGGGAGGCAGCA  
GTGGGGAATATTGCACAATGGGCGGAAGCCTGATGCAGCAACGCCGCGTGAGGGATGACG  
GCCTTCGGGTGTAAACCTCTTTTAGCAGGGAAGAAGCGAAAGTGACGGTACCTGCAGAA  
AAAGCACCGGCTAACTACGTGCCAGCAGCCGCGGTAATACGTAGGGTGCAAGCGTTATCC  
GGAATTATTGGGCGTAAAGAGCTCGTAGGCGGTTTGTGCGCTCTGCTGTGAAATCCCGAG  
GCTCAACCTCGGGCCTGCAGTGGGTACGGGCAGACTAGAGTGCGGTAGGGGAGATTGGAA  
TTCTGGTGTAGCGGTGGAATGCGCAGATATCAGGAGGAACACCGATGGCGAAGGCAGAT  
CTCTGGGCCGTAACCTGACGCTGAGGAGCGAAAGGGTGGGGAGCAAACAGGCTTAGATACC  
CTGGTAGTCCACCCGTAACGTTGGGAACTAGTTGTGGGGTCCCTTCCACGGATCCCGT  
GACGCAGCTAACGCATTAAGTTCCCCGCCTGGGGAGTACGGCCGCAAGGCTAAAACCTCAA  
AGGAATTGACGGGGACCCGCACAAGCGGCGGAGCATGCGGATTAATTTCGATGCAACGCGA  
AGAACCTTACCAAGGCTTGACATACAGGAAACGGGCCAGAAATGGTCAACTCTTTGGAC  
ACTCGTGAACAGGTGGTGCATGGTTGTCGTCAACTCGTGTCTGAGATGTTGGGTTAAGT  
CCCGCAACGAGCGCAACCCTCGTTCTATGTTGCCAGCACGTAATGGTGGGAACTCATGGG  
ATACTGCCGGGTCAACTCGGAGGAAGGTGGGGATGACGTCAAATCATCATGCCCTTAT  
GTCTTGGGCTTCACGCATGCTACAATGGCCGTACAAAGGGCTGCAATACCGTGAGGTGG  
AGCGAATCCCAAAAAGCCGGTCCCAGTTCGGATTGAGGTCTGCAACTCGACCTCATGAAG  
TCGGAGTCGCTAGTAATCGCAGATCAGCAACGCTGCGGTGAATACGTTCCCGGGTCTTGT  
ACACACCGCCCGTCAAGTCATGAAAGTCGGTAACACCTGAAGCCGG

Program	BLASTN <a href="#">?</a> <a href="#">Citation</a> <a href="#">v</a>
Database	rRNA_typestrains/16S_ribosomal_RNA <a href="#">See details</a> <a href="#">v</a>
Query ID	lcl Query_301989
Description	None
Molecule type	dna
Query Length	1366
Other reports	<a href="#">Distance tree of results</a> <a href="#">MSA viewer</a> <a href="#">?</a>

Organism only top 20 will appear  exclude

Type common name, binomial, taxid or group name

[+ Add organism](#)

Percent Identity  to  E value  to  Query Coverage  to

**Descriptions** [Graphic Summary](#) [Alignments](#) [Taxonomy](#)

Sequences producing significant alignments [Download](#) [Select columns](#) Show  [?](#)

select all 100 sequences selected [GenBank](#) [Graphics](#) [Distance tree of results](#) [MSA Viewer](#)

	Description	Scientific Name	Max Score	Total Score	Query Cover	E value	Per. Ident	Acc. Len	Accession
<input checked="" type="checkbox"/>	<a href="#">Microbacterium azadirachtae strain AI-S262 16S ribosomal RNA, partial sequence</a>	<a href="#">Microbacterium azadirachtae</a>	2435	2435	99%	0.0	98.83%	1373	<a href="#">NR_116502.1</a>
<input checked="" type="checkbox"/>	<a href="#">Microbacterium resistens strain DMMZ 1710 16S ribosomal RNA, partial sequence</a>	<a href="#">Microbacterium resistens</a>	2361	2361	100%	0.0	97.81%	1461	<a href="#">NR_026437.1</a>
<input checked="" type="checkbox"/>	<a href="#">Microbacterium lumbae strain T7528-3-6b 16S ribosomal RNA, partial sequence</a>	<a href="#">Microbacterium lumbae</a>	2357	2357	97%	0.0	98.65%	1448	<a href="#">NR_156954.1</a>
<input checked="" type="checkbox"/>	<a href="#">Microbacterium xylanilyticum strain S3-E 16S ribosomal RNA, partial sequence</a>	<a href="#">Microbacterium xylanilyticum</a>	2357	2357	100%	0.0	97.81%	1476	<a href="#">NR_042350.1</a>
<input checked="" type="checkbox"/>	<a href="#">Microbacterium insulae strain DS-66 16S ribosomal RNA, partial sequence</a>	<a href="#">Microbacterium insulae</a>	2357	2357	100%	0.0	97.81%	1447	<a href="#">NR_044440.1</a>

## TE13 (F+R)

AGCTTGCTCTCTGGATCAGTGGCGAACGGGTGAGTAACACGTGAGCAATCTGCCCTGAC  
TCTGGGATAAGCGCTGGAACGGCGTCTAATACCGGATACGAGCTGCGAAGGCATCTTCA  
GCAGCTGGAAAGAACTTCGGTCAGGGATGAGCTCGCGGCCTATCAGCTAGTTGGTGAGGT  
AATGGCTCACCAAGGCGTCGACGGGTAGCCGGCCTGAGAGGGTGACCGGCCACACTGGGA  
CTGAGACACGGCCCAGACTCCTACGGGAGGCAGCAGTGGGGAATATTGCACAATGGGCGC  
AAGCCTGATGCAGCAACGCCGCGTGAGGGACGACGGCCTTCGGGTTGTAACCTCTTTTA  
GCAGGGAAGAAGCGAAAGTGACGGTACCTGCAGAAAAAGCACCGGCTAACTACGTGCCAG  
CAGCCGCGTAATACGTAGGGTGCAAGCGTTATCCGGAATTATTGGGCGTAAAGAGCTCG  
TAGGCGGTTTGTGCGTCTGCTGTGAAAAGTGGGGCTCAACCCCAGCCTGCAGTGGGT  
ACGGGCAGACTAGAGTGCGGTAGGGGAGATTGGAATTCCTGGTGTAGCGGTGGAATGCGC  
AGATATCAGGAGGAACACCGATGGCGAAGGCAGATCTCTGGGCCGTAACTGACGCTGAGG  
AGCGAAAGGGTGGGGAGCAAACAGGCTTAGATACCCTGGTAGTCCACCCCGTAAACGTTG  
GGAAGTGTGGGGTCCATTCCACGGATTCCGTGACGCAGCTAACGCATTAAGTTCCC  
CGCCTGGGGAGTACGGCCGCAAGGCTAAAAGTCAAAGGAATTGACGGGGACCCGCACAAG  
CGCGGAGCATGCGGATTAATTCGATGCAACGCGAAGAACCTTACCAAGGCTTGACATAT  
ACGAGAACGGCCAGAAATGGTCAACTCTTTGGACTCGTAAACAGGTGGTGCATGGTT  
GTCGTCAGCTCGTGTGCTGAGATGTTGGGTTAAGTCCCGCAACGAGCGCAACCCTCGTTC  
TATGTTGCCAGCACGTAATGGTGGGAACTCATGGGATACTGCCGGGGTCAACTCGGAGGA  
AGGTGGGGATGACGTCAAATCATCATGCCCTTATGTCTTGGGCTTCACGCATGCTACAA  
TGGCCGGTACAAAGGGCTGCAATACCGTAAGGTGGAGCGAATCCCAAAAAGCCGGTCCCA  
GTTCCGATTGAGGTCTGCAACTCGACCTCATGAAGTCGGAGTCGCTAGTAATCGCAGATC  
AGCAACGCTGCGGTGAATACGTTCCCGGGTCTTGTACACACCGCCCGTCAAGTCATGAAA  
GTCGGTAACACCTGAAGCCGG

Program	BLASTN <a href="#">?</a> <a href="#">Citation</a> <a href="#">v</a>
Database	rRNA_typestrains/16S_ribosomal_RNA <a href="#">See details</a> <a href="#">v</a>
Query ID	lcl Query_347961
Description	None
Molecule type	dna
Query Length	1341
Other reports	<a href="#">Distance tree of results</a> <a href="#">MSA viewer</a> <a href="#">?</a>

Organism only top 20 will appear  exclude

Type common name, binomial, taxid or group name

[+ Add organism](#)

Percent Identity  to  E value  to  Query Coverage  to

[Filter](#) [Reset](#)

<b>Descriptions</b>	Graphic Summary	Alignments	Taxonomy
---------------------	-----------------	------------	----------

Sequences producing significant alignments Download Select columns Show  [?](#)

select all 100 sequences selected [GenBank](#) [Graphics](#) [Distance tree of results](#) [MSA Viewer](#)

	Description	Scientific Name	Max Score	Total Score	Query Cover	E value	Per. Ident	Acc. Len	Accession
<input checked="" type="checkbox"/>	<a href="#">Microbacterium lacus strain A5E-52 16S ribosomal RNA, partial sequence</a>	<a href="#">Microbacterium lacus</a>	2477	2477	100%	0.0	100.00%	1463	<a href="#">NR_041563.1</a>
<input checked="" type="checkbox"/>	<a href="#">Microbacterium aoyamense strain KV-492 16S ribosomal RNA, partial sequence</a>	<a href="#">Microbacterium aoyamense</a>	2433	2433	100%	0.0	99.40%	1443	<a href="#">NR_041332.1</a>
<input checked="" type="checkbox"/>	<a href="#">Microbacterium aurum strain DSM 8600 16S ribosomal RNA, partial sequence</a>	<a href="#">Microbacterium aurum</a>	2423	2423	100%	0.0	99.25%	1472	<a href="#">NR_044933.1</a>
<input checked="" type="checkbox"/>	<a href="#">Microbacterium pumilum strain KV-488 16S ribosomal RNA, partial sequence</a>	<a href="#">Microbacterium pumilum</a>	2410	2410	100%	0.0	99.11%	1403	<a href="#">NR_041331.1</a>
<input checked="" type="checkbox"/>	<a href="#">Microbacterium paulum strain 2C 16S ribosomal RNA, complete sequence</a>	<a href="#">Microbacterium paulum</a>	2405	2405	100%	0.0	99.03%	1524	<a href="#">NR_181679.1</a>

## TE14 (F+R)

GCTTGCTCTCAAGAAGTTAGCGGGCGGACGGGTGAGTAACACGTGGGTAACCTGCCCATAA  
 GACTGGGATAACTCCGGGAAACCGGGGCTAATACCGGATAACATTTTGAAGTGCATAGTT  
 CGAAATTGAAAGGCGGCTTCGGCTGTCACTTATGGATGGACCCGCGTCGCATTAGCTAGT  
 TGGTGAGGTAACGGCTACCAAGGCAACGATGCGTAGCCGACCTGAGAGGGTGATCGGCC  
 AACTGGGACTGAGACACGGCCCAGACTCCTACGGGAGGCAGCAGTAGGGAATCTTCCGC  
 AATGGACGAAAGTCTGACGGAGCAACGCCGCGTGAGTGATGAAGGCTTTCGGGTGCTAAA  
 ACTCTGTTGTTAGGGAAGAACAAGTGCTAGTTGAATAAGCTGGCACCTTGACGGTACCTA  
 ACCAGAAAGCCACGGCTAACTACGTGCCAGCAGCCGCGGTAATACGTAGGTGGCAAGCGT  
 TATCCGGAATTATTGGGCGTAAAGCGCGCGCAGGTGGTTTCTTAAGTCTGATGTGAAAGC  
 CCACGGCTCAACCGTGGAGGGTCATTGGAACTGGGAGACTTGAGTGCANAANAGGAAAG  
 TGGAATTCCATGTGTANCGGTGAAATGCGTAGAGATATGGAGGAACACCAGTGGCGAAGG  
 CGACTTTTCTGGTCTGTAAGTACTGACACTGAGGCGNGAAAGCGTGGGGAGCAAACAGGATTN  
 GATACCCTGGTAGTCCACGCCGTAAACGATGAGTGCTAAGTGTTAGAGGGTTTCCGCCCT  
 TTAGTGCTGAAGTTAACGCATTAAGCACTCCGCCTGGGGAGTACGGCCGCAAGGCTGAAA  
 CTCAAAGGAATTGACGGGGGCCCGCACAAAGCGGTGGAGCATGTGGTTTAATTCGAAGCAA  
 CGCGAAGAACCTTACCAGGTCTTGACATCCTCTGAAAACCCTAGAGATAGGGCTTCTCCT  
 TCGGGAGCAGAGTGACAGGTGGTGCATGGTTGTCGTCAGCTCGTGTCTGAGATGTTGGG  
 TTAAGTCCCAGCAACGAGCGCAACCCTTGATCTTAGTTGCCATCATTAAAGTTGGGCACTCT  
 AAGGTGACTGCCGGTGACAAACCGGAGGAAGGTGGGGATGACGTCAAATCATCATGCCCC  
 TTATGACCTGGGCTACACACGTGCTACAATGGACGGTACAAAGAGCTGCAAGACCGCGAG  
 GTGGAGCTAATCTCATAAAACCGTTCTCAGTTCGGATTGTAGGCTGCAACTCGCCTACAT  
 GAAGCTGGAATCGCTAGTAATCGCGGATCAGCATGCCGCGGTGAATACGTTCCCGGGCCT  
 TGTACACACCGCCCGTCACACCAGAGAGTTTGTAAACACCCGAAGT

Program [BLASTN](#) [Citation](#)

Database [rRNA\\_tpestrains/16S\\_ribosomal\\_RNA](#) [See details](#)

Query ID [|cl|Query\\_44357](#)

Description None

Molecule type dna

Query Length 1366

Other reports [Distance tree of results](#) [MSA viewer](#)

Organism only top 20 will appear  exclude

Type common name, binomial, taxid or group name

[+ Add organism](#)

Percent Identity  to  E value  to  Query Coverage  to

[Filter](#) [Reset](#)

- Descriptions**
- Graphic Summary
- Alignments
- Taxonomy

Sequences producing significant alignments Download Select columns Show

select all 100 sequences selected [GenBank](#) [Graphics](#) [Distance tree of results](#) [MSA Viewer](#)

Description	Scientific Name	Max Score	Total Score	Query Cover	E value	Per. Ident	Acc. Len	Accession
<input checked="" type="checkbox"/> <a href="#">Bacillus toyonensis strain BCT-7112 16S ribosomal RNA, partial sequence</a>	<a href="#">Bacillus toyonensis</a>	2492	2492	100%	0.0	99.49%	1544	<a href="#">NR_121761.1</a>
<input checked="" type="checkbox"/> <a href="#">Bacillus thuringiensis strain ATCC 10792 16S ribosomal RNA, partial sequence</a>	<a href="#">Bacillus thuringiensis</a>	2492	2492	100%	0.0	99.49%	1482	<a href="#">NR_114581.1</a>
<input checked="" type="checkbox"/> <a href="#">Bacillus thuringiensis strain IAM 12077 16S ribosomal RNA, partial sequence</a>	<a href="#">Bacillus thuringiensis</a>	2492	2492	100%	0.0	99.49%	1486	<a href="#">NR_043403.1</a>
<input checked="" type="checkbox"/> <a href="#">Bacillus thuringiensis strain NBRC 101235 16S ribosomal RNA, partial sequence</a>	<a href="#">Bacillus thuringiensis</a>	2488	2488	100%	0.0	99.41%	1477	<a href="#">NR_112780.1</a>
<input checked="" type="checkbox"/> <a href="#">Bacillus pacificus strain MCCC 1A06182 16S ribosomal RNA, partial sequence</a>	<a href="#">Bacillus pacificus</a>	2486	2486	100%	0.0	99.41%	1509	<a href="#">NR_157733.1</a>



## TE15 (F+R)

GGATTGAGAGCTTGCTCTCAAGAAGTTAGCGGCGGACGGGTGAGTAACACGTGGGTAACC  
 TGCCATAAGACTGGGATAACTCCGGGAAACCGGGGCTAATACCGGATAACATTTTGAAC  
 TGCATAGTTGAAATTGAAAGGCGGCTTCGGCTGTCACTTATGGATGGACCCGCGTCGCA  
 TTAGCTAGTTGGTGAGGTAACGGCTACCAAGGCAACGATGCGTAGCCGACCTGAGAGGG  
 TGATCGGCCACACTGGGACTGAGACACGGCCCAGACTCCTACGGGAGGCAGCAGTAGGGA  
 ATCTTCCGCAATGGACGAAAGTCTGACGGAGCAACGCCGCGTGAGTGATGAAGGCTTTTCG  
 GGTCGTAAAACCTCTGTTGTTAGGGAAGAACAAGTGCTAGTTGAATAAGCTGGCACCTTGA  
 CGGTACCTAACCAGAAAGCCACGGCTAACTACGTGCCAGCAGCCGCGGTAATACGTAGGT  
 GGCAAGCGTTATCCGGAATTATTGGGCGTAAAGCGCGCGCAGGTGGTTTCTTAAGTCTGA  
 TGTGAAAGCCCACGGCTCAACCGTGGAGGGTCATTGGAAACTGGGAGACTTGAGTGCAGA  
 AGAGGAAAGTGGAATTCCATGTGTAGCGGTGAAATGCGTAGAGATATGGAGGAACACCAG  
 TGGCGAAGGCGACTTTCTGGTCTGTAAGTACTGACACTGAGGCGCGAAAGCGTGGGGAGCAA  
 CAGGATTAGATACCCTGGTAGTCCACGCCGTAACGATGAGTGCTAAGTGTTAGAGGGTT  
 TCCGCCCTTTAGTGCTGAAGTTAACGCATTAAGCACTCCGCCTGGGGAGTACGGCCGCAA  
 GGCTGAAACTCAAAGGAATTGACGGGGGCCCGCACAAAGCGGTGGAGCATGTGGTTAATT  
 CGAAGCAACGCGAAGAACCCTACCAGGTCTTGACATCCTCTGAAAACCCCTAGAGATAGGG  
 CTTCTCCTTCGGGAGCAGAGTGACAGGTGGTGCATGGTTGTCGTCAGCTCGTGTCGTGAG  
 ATGTTGGGTTAAGTCCCGCAACGAGCGCAACCCTTGATCTTAGTTGCCATCATTAAAGTTG  
 GGCACCTAAGGTGACTGCCGGTGACAAACCGGAGGAAGGTGGGGATGACGTCAAATCAT  
 CATGCCCTTATGACCTGGGCTACACACGTGCTACAATGGACGGTACAAAGAGCTGCAAG  
 ACCGCGAGGTGGAGCTAATCTCATAAAACCGTTCTCAGTTCGGATTGTAGGCTGCAACTC  
 GCCTACATGAAGCTGGAATCGCTAGTAATCGCGGATCAGCATGCCGCGGTGAATACGTTCC  
 CCGGGCCTTGACACACCGCCCGTCACACCACGAGAGTTTGTAACACCCGAAGTCGGTGG  
 GGTAAC

Program	BLASTN <a href="#">?</a> <a href="#">Citation</a> <a href="#">v</a>
Database	rRNA_typestrains/16S_ribosomal_RNA <a href="#">See details</a> <a href="#">v</a>
Query ID	lcl Query_33623
Description	None
Molecule type	dna
Query Length	1386
Other reports	<a href="#">Distance tree of results</a> <a href="#">MSA viewer</a> <a href="#">?</a>

Organism only top 20 will appear  exclude

Type common name, binomial, taxid or group name

[+ Add organism](#)

Percent Identity  to  E value  to  Query Coverage  to

[Filter](#) [Reset](#)

- Descriptions**
- Graphic Summary
- Alignments
- Taxonomy

Sequences producing significant alignments Download [v](#) Select columns [v](#) Show  [?](#)

select all 100 sequences selected [GenBank](#) [Graphics](#) [Distance tree of results](#) [MSA Viewer](#)

Description	Scientific Name	Max Score	Total Score	Query Cover	E value	Per. Ident	Acc. Len	Accession
<input checked="" type="checkbox"/> <a href="#">Bacillus toyonensis strain BCT-7112 16S ribosomal RNA, partial sequence</a>	<a href="#">Bacillus toyonensis</a>	2555	2555	100%	0.0	99.93%	1544	<a href="#">NR_121761.1</a>
<input checked="" type="checkbox"/> <a href="#">Bacillus thuringiensis strain ATCC 10792 16S ribosomal RNA, partial sequence</a>	<a href="#">Bacillus thuringiensis</a>	2555	2555	100%	0.0	99.93%	1482	<a href="#">NR_114581.1</a>
<input checked="" type="checkbox"/> <a href="#">Bacillus thuringiensis strain IAM 12077 16S ribosomal RNA, partial sequence</a>	<a href="#">Bacillus thuringiensis</a>	2555	2555	100%	0.0	99.93%	1486	<a href="#">NR_043403.1</a>
<input checked="" type="checkbox"/> <a href="#">Bacillus thuringiensis strain NBRC 101235 16S ribosomal RNA, partial sequence</a>	<a href="#">Bacillus thuringiensis</a>	2551	2551	100%	0.0	99.86%	1477	<a href="#">NR_112780.1</a>
<input checked="" type="checkbox"/> <a href="#">Bacillus pacificus strain MCCC 1A06182 16S ribosomal RNA, partial sequence</a>	<a href="#">Bacillus pacificus</a>	2549	2549	100%	0.0	99.86%	1509	<a href="#">NR_157733.1</a>

## TE16 (F+R)

ACATGCAGTCGAGCGGACTTGATGGAGTGCTTGCACTCCTGATGGTTAGCGGCGGACGGG  
TGAGTAACACGTAGGCAACCTGCCCGTAAGACTGGGATAACATTGCGAAACGAATGCTAA  
TACCGGATACGCGATTTTCTCGCATGAGAGAATCGGGAAAGAAGGAGCAATCTTTCACCT  
ACGGATGGGCCTGCGGCGCATTAGCTAGTTGGTGGGGTAACGGCTCACCAAGGCGACGAT  
GCGTAGCCGACCTGAGAGGGTGATCGGCCACACTGGGACTGAGACACGGCCCAGACTCCT  
ACGGGAGGCAGCAGTAGGGAATCTTCCGCAATGGACGAAAGTCTGACGGAGCAACGCCGC  
GTGAGTGAAGAAGGCTTTCGGGTCGTAAAGCTCTGTTGCCAGGGAAGAACAACCTTGAGAGA  
GTAAGTCTTGGAGTTGACGGTACCTGAGAAGAAAGCCCCGGCTAACTACGTGCCAGCA  
GCCGCGGTAATACGTAGGGGGCAAGCGTTGTCCGGAATTATTGGGCGTAAAGCGCGCGCA  
GGCGGCTTTGTAAGTCTGTCGTTTAAGTTCGGGGCTCAACCCCGTGTCGCGATGGAACT  
GCAAGGCTTGAGTACAGAAGAGGAAAGTGAATTCACGTGTAGCGGTGAAATGCGTAGA  
GATGTGGAGGAACACCAGTGGCGAAGGCGACTTCTGGGCTGTAAGTACGCTGAGGCGC  
GAAAGCGTGGGGAGCAAACAGGATTAGATACCCTGGTAGTCCACGCCGTAAACGATGAAT  
GCTAGGTGTTAGGGGTTTCAATACCCTTGGTGCCGAAGTTAACACATTAAGCATTCCGCC  
TGGGGAGTACGCTCGCAAGAGTAAACTCAAAGGAATTGACGGGGACCCGCACAAGCAGT  
GGAGTATGTGGTTTAATTCGAAGCAACGCGAAGAACCTTACCAGGTCTTGACATCCCTCT  
GACCGGTCTGGAGACAGGCCTTCCCTTCGGGGCAGAGGAGACAGGTGGTGCATGGTTGTC  
GTCAGCTCGTGTCTGAGATGTTGGGTTAAGTCCCACAACGAGCGCAACCCCTGATTTTA  
GTTGCCAGCACATCATGGTGGGCACTCTAGAATGACTGCCGGTGACAAACCGGAGGAAGG  
CGGGGATGACGTCAAATCATCATGCCCTTATGACCTGGGCTACACACGTACTACAATGG  
CCGGTACAACGGGCTGCGAAAGAGCGATCTGGAGCGAATCCTATAAAGCCGGTCTCAGTT  
CGGATTGCAGGCTGCAACTCGCTGCATGAAGTCGGAATTGCTAGTAATCGCGGATCAGC  
ATGCCGCGGTGAATACGTTCCCGGGTCTTGTACACACCGCCCGTCACACCACGAGAGTTT  
ACAACACCCGAAGCCGGTGGGGTAACCGCAAGGAGCCA

Program	BLASTN <a href="#">Citation</a>
Database	rRNA_typestrains/16S_ribosomal_RNA <a href="#">See details</a>
Query ID	Ic Query_22255
Description	None
Molecule type	dna
Query Length	1418
Other reports	<a href="#">Distance tree of results</a> <a href="#">MSA viewer</a>

Organism only top 20 will appear  exclude

Type common name, binomial, taxid or group name

[+ Add organism](#)

Percent Identity  to  E value  to  Query Coverage  to

[Filter](#) [Reset](#)

- Descriptions** | [Graphic Summary](#) | [Alignments](#) | [Taxonomy](#)

Sequences producing significant alignments [Download](#) [Select columns](#) Show

select all 100 sequences selected [GenBank](#) [Graphics](#) [Distance tree of results](#) [MSA Viewer](#)

Description	Scientific Name	Max Score	Total Score	Query Cover	E value	Per. Ident	Acc. Len	Accession
<input checked="" type="checkbox"/> <a href="#">Paenibacillus curdianolyticus strain YK9 16S ribosomal RNA, partial sequence</a>	<a href="#">Paenibacillus curdianolyticus</a>	2547	2547	100%	0.0	99.01%	1531	<a href="#">NR_040891.1</a>
<input checked="" type="checkbox"/> <a href="#">Paenibacillus curdianolyticus strain NBRC 15724 16S ribosomal RNA, partial sequence</a>	<a href="#">Paenibacillus curdianolyticus</a>	2543	2543	100%	0.0	99.01%	1478	<a href="#">NR_113803.1</a>
<input checked="" type="checkbox"/> <a href="#">Paenibacillus curdianolyticus strain YK9 16S ribosomal RNA, partial sequence</a>	<a href="#">Paenibacillus curdianolyticus</a>	2466	2466	97%	0.0	98.63%	1436	<a href="#">NR_115596.1</a>
<input checked="" type="checkbox"/> <a href="#">Paenibacillus cellulosilyticus strain PALXIL08 16S ribosomal RNA, partial sequence</a>	<a href="#">Paenibacillus cellulosilyticus</a>	2409	2409	100%	0.0	97.32%	1546	<a href="#">NR_043789.1</a>
<input checked="" type="checkbox"/> <a href="#">Paenibacillus ginsengiterrae strain DCY89 16S ribosomal RNA, partial sequence</a>	<a href="#">Paenibacillus ginsengiterrae</a>	2407	2407	100%	0.0	97.26%	1495	<a href="#">NR_178650.1</a>

## TE17 (F+R)

CATGCAGTCGAGCGAATGGATTGAGAGCTTGCTCTCAAGAAGTTAGCGGCGGACGGGTGA  
GTAACACGTGGGTAACCTGCCATAAGACTGGGATAACTCCGGGAAACCGGGGCTAATAC  
CGGATAACATTTTGAAGTGCATAGTTCGAAATTGAAAGGCGGCTTCGGCTGTCACCTTATG  
GATGGACCCCGTTCGATTAGCTAGTTGGTGAGGTAACGGCTCACCAAGGCAACGATGCG  
TAGCCGACCTGAGAGGGTGATCGGCCACACTGGGACTGAGACACGGCCCAGACTCCTACG  
GGAGGCAGCAGTAGGGAATCTTCCGCAATGGACGAAAGTCTGACGGAGCAACGCCCGCTG  
AGTGATGAAGGCTTTCGGGTTCGTA AAACTCTGTTGTTAGGGAAGAACAAGTGCTAGTTGA  
ATAAGCTGGCACCTTGACGGTACCTAACCAGAAAGCCACGGCTAACTACGTGCCAGCAGC  
CGCGGTAATACGTAGGTGGCAAGCGTTATCCGGAATTATTGGGCGTAAAGCGCGCGCAGG  
TGGTTTCTTAAGTCTGATGTGAAAGCCCCACGGCTCAACCGTGGAGGGTCATTGGAAACT  
GGGAGACTTGAGTGCAGAAGAGGAAAGTGGAATTCCATGTGTAGCGGTGAAATGCGTAGA  
GATATGGAGGAACACCAGTGGCGAAGGCGACTTCTGGTCTGTA ACTGACACTGAGGCGC  
GAAAGCGTGGGGAGCAAACAGGATTAGATACCCTGGTAGTCCACGCCGTAAACGATGAGT  
GCTAAGTGTTAGAGGGTTTCCGCCCTT TAGTGCTGAAGTTAACGCATTAAGCACTCCGCC  
TGGGGAGTACGGCCGCAAGGCTGAAACTCAAAGGAATTGACGGGGGCCCGCACAAAGCGGT  
GGAGCATGTGGTTTAATTCGAAGCAACGCGAAGAACCTTACCAGGTCTTGACATCCTCTG  
AAAACCCTAGAGATAGGGCTTCTCCTTCGGGAGCAGAGTGACAGGTGGTGCATGGTTGTC  
GTCAGCTCGTGTCGTGAGATGTTGGGTTAAGTCCC GCAACGAGCGCAACCCTTGATCTTA  
GTTGCCATCATTAAGTTGGGCACTCTAAGGTGACTGCCGGTGACAAACCGGAGGAAGGTG  
GGATGACGTCAAATCATCATGCCCTTATGACCTGGGCTACACACGTGCTACAATGGAC  
GGTACAAAGAGCTGCAAGACCGCGAGGTGGAGCTAATCTCATAAAACCGTTCTCAGTTCCG  
GATTGTAGGCTGCAACTCGCCTACATGAAGCTGGAATCGCTAGTAATCGCGGATCAGCAT  
GCCGCGGTGAATACGTTCCCGGGCCTTGACACACCGCCCGTACACCACGAGAGTTTGT  
AACACCCGAAGTCGGTGGGGTAACCTTTTGGAGCCA

Program	BLASTN <a href="#">Citation</a>
Database	rRNA_tyestrains/16S_ribosomal_RNA <a href="#">See details</a>
Query ID	Ic Query_11995
Description	None
Molecule type	dna
Query Length	1416
Other reports	<a href="#">Distance tree of results</a> <a href="#">MSA viewer</a>

Organism only top 20 will appear  exclude

Type common name, binomial, taxid or group name

[+ Add organism](#)

Percent Identity  to  E value  to  Query Coverage  to

[Filter](#) [Reset](#)

<b>Descriptions</b>	Graphic Summary	Alignments	Taxonomy
---------------------	-----------------	------------	----------

Sequences producing significant alignments Download Select columns Show  [?](#)

select all 100 sequences selected [GenBank](#) [Graphics](#) [Distance tree of results](#) [MSA Viewer](#)

	Description	Scientific Name	Max Score	Total Score	Query Cover	E value	Per. Ident	Acc. Len	Accession
<input checked="" type="checkbox"/>	<a href="#">Bacillus toyonensis strain BCT-7112 16S ribosomal RNA, partial sequence</a>	<a href="#">Bacillus toyonensis</a>	2593	2593	100%	0.0	99.72%	1544	<a href="#">NR_121761.1</a>
<input checked="" type="checkbox"/>	<a href="#">Bacillus thuringiensis strain ATCC 10792 16S ribosomal RNA, partial sequence</a>	<a href="#">Bacillus thuringiensis</a>	2593	2593	100%	0.0	99.72%	1482	<a href="#">NR_114581.1</a>
<input checked="" type="checkbox"/>	<a href="#">Bacillus thuringiensis strain IAM 12077 16S ribosomal RNA, partial sequence</a>	<a href="#">Bacillus thuringiensis</a>	2593	2593	100%	0.0	99.72%	1486	<a href="#">NR_043403.1</a>
<input checked="" type="checkbox"/>	<a href="#">Bacillus thuringiensis strain NBRC 101235 16S ribosomal RNA, partial sequence</a>	<a href="#">Bacillus thuringiensis</a>	2590	2590	100%	0.0	99.65%	1477	<a href="#">NR_112780.1</a>
<input checked="" type="checkbox"/>	<a href="#">Bacillus pacificus strain MCCC-1A06182 16S ribosomal RNA, partial sequence</a>	<a href="#">Bacillus pacificus</a>	2588	2588	100%	0.0	99.65%	1509	<a href="#">NR_157733.1</a>



## TE19 (F)

CCATGCAGTCGAACGGCAGCACGGACTTCGGTCTGGTGGCGAGTGGCGAACGGGTGAGTA  
ATGTATCGGAACGTGCCTAGTAGCGGGGATAACTACGCGAAAGCGTAGCTAATACCGCA  
TACGCCCTACGGGGAAAGCAGGGGATCGCAAGACCTTGCACTATTAGAGCGGCCGATAT  
CGGATTAGCTAGTTGGTGGGGTAACGGCTACCAAGGCGACGATCCGTAGCTGGTTTGAG  
AGGACGACCAGCCACACTGGGACTGAGACACGGCCCAGACTCCTACGGGAGGCAGCAGTG  
GGGAATTTTGGACAATGGGGGAAACCCTGATCCAGCCATCCC GCGTGTGCGATGAAGGCC  
TTCGGGTTGTAAAGCACTTTTGGCAGGAAAGAAACGTTCCGGGTTAATACCCCGGGAAAC  
TGACGGTACCTGCAGAATAAGCACCGGCTAACTACGTGCCAGCAGCCGCGGTAATACGTA  
GGGTGCAAGCGTTAATCGGAATTACTGGGCGTAAAGCGTGCGCAGGCGGTTTCGGAAAGAA  
AGATGTGAAATCCCAGAGCTTAACTTTGGAAGTGCATTTTTAACTACCGAGCTAGAGTGT  
GTCAGAGGGAGGTGGAATTCGCGTGTAGCAGTGAATGCGTAGATATGCGGAGGAACAC  
CGATGGCGAAGGCAGCCTCCTGGGATAAACTGACGCTCATGCACGAAAGCGTGGGGAGC  
AAACAGGATTAGATACCCTGGTAGTCCACGCCCTAAACGATGTCAACTAGCTGTTGGGGC  
CTTCGGGCCTTGGTAGCGCAGCTAACGCGTGAAGTTGACCGCCTGGGGAGTACGGTCGCA  
AGATTA AAACTCAA

Program	BLASTN <a href="#">?</a> <a href="#">Citation</a> <a href="#">v</a>
Database	rRNA_typestrains/16S_ribosomal_RNA <a href="#">See details</a> <a href="#">v</a>
Query ID	lcl Query_116343
Description	None
Molecule type	dna
Query Length	855
Other reports	<a href="#">Distance tree of results</a> <a href="#">MSA viewer</a> <a href="#">?</a>

Organism only top 20 will appear  exclude

Type common name, binomial, taxid or group name

[+ Add organism](#)

Percent Identity  to  E value  to  Query Coverage  to

[Filter](#) [Reset](#)

**Descriptions** | Graphic Summary | Alignments | Taxonomy

Sequences producing significant alignments Download Select columns Show  [?](#)

select all 100 sequences selected [GenBank](#) [Graphics](#) [Distance tree of results](#) [MSA Viewer](#)

	Description	Scientific Name	Max Score	Total Score	Query Cover	E value	Per. Ident	Acc. Len	Accession
<input checked="" type="checkbox"/>	<a href="#">Achromobacter mucicolens strain R-46658 16S ribosomal RNA, partial sequence</a>	<a href="#">Achromobacter mucicolens</a>	1572	1572	99%	0.0	99.88%	1507	<a href="#">NR_117613.1</a>
<input checked="" type="checkbox"/>	<a href="#">Achromobacter deleyi strain LMG 3458 16S ribosomal RNA, partial sequence</a>	<a href="#">Achromobacter deleyi</a>	1546	1546	99%	0.0	99.30%	1483	<a href="#">NR_152014.1</a>
<input checked="" type="checkbox"/>	<a href="#">Achromobacter pestifer strain LMG 3431 16S ribosomal RNA, partial sequence</a>	<a href="#">Achromobacter pestifer</a>	1544	1544	99%	0.0	99.30%	1483	<a href="#">NR_152016.1</a>
<input checked="" type="checkbox"/>	<a href="#">Achromobacter kerstersii strain LMG 3441 16S ribosomal RNA, partial sequence</a>	<a href="#">Achromobacter kerstersii</a>	1544	1544	99%	0.0	99.30%	1483	<a href="#">NR_152015.1</a>
<input checked="" type="checkbox"/>	<a href="#">Achromobacter agilis strain LMG 3411 16S ribosomal RNA, partial sequence</a>	<a href="#">Achromobacter agilis</a>	1544	1544	99%	0.0	99.30%	1483	<a href="#">NR_152013.1</a>

## TE20 (F+R)

GCAACCTGGCGGCGAGTGGCGAACGGGTGAGTAATATATATCGGAACGTACCCTGGAGTGGG  
GGATAACGTAGCGAAAGTTACGCTAATACCGCATAACGATCCAAGGATGAAAGCAGGGGAC  
CTTCGGGCCTTGTGCTCCTGGAGCGGCCGATATCTGATTAGCTAGTTGGTGGGGTAAAGG  
CCCACCAAGGCATCGATCAGTAGCTGGTCTGAGAGGACGACCAGCCACACTGGAAGTGGAG  
ACACGGTCCAGACTCCTACGGGAGGCAGCAGTGGGGAATTTTGGACAATGGGCGCAAGCC  
TGATCCAGCAATGCCGCGTGAGTGAAGAAGGCCCTTCGGGTTGTAAGCTCTTTTGTGTCAGG  
GAAGAAACGGTGAGGGTTAATACCTCTTGCTAATGACGGTACCTGAAGAATAAGCACCGG  
CTAACTACGTGCCAGCAGCCGCGGTAATACGTAGGGTGCAAGCGTTAATCGGAATTACTG  
GGCGTAAAGCGTGCGCAGGCGGTTTTGTAAGACTGTCGTGAAATCCCCGGGCTCAACCTG  
GGAATGGCGATGGTGACTGCAAGGCTAGAGTTTGGCAGAGGGGGGTAGAATTCCACGTGT  
AGCAGTGAAATGCGTAGATATGTGGAGGAACACCGATGGCGAAGGCAGCCCCCTGGGTCA  
AAACTGACGCTCATGCACGAAAGCGTGGGGAGCAAACAGGATTAGATACCCTGGTAGTCC  
ACGCCCTAAACGATGTCTACTAGTTGTCGGGTCTTAATTGACTTGGTAACGCAGCTAACG  
CGTGAAGTAGACCGCCTGGGGAGTACGGTCGCAAGATTAAACTCAAAGGAATTGACGGG  
GACCCGCACAAGCGGTGGATGATGTGGATTAATTCGATGCAACGCGAAAAACCTTACCTA  
CCCTTGACATGGAAGGAATCCCTGAGAGATTGGGGAGTGCTCGAAAGAGAACCTTTACAC  
AGGTGCTGCATGGCTGTCGTGAGCTCGTGTGTCGTGAGATGTTGGGTTAAGTCCCGCAACGA  
GCGCAACCCCTTGTCATTAGTTGCTACGAAAGGGCACTCTAATGAGACTGCCGGTGACAAA  
CCGGAGGAAGGTGGGGATGACGTCAAGTCCTCATGGCCCTTATGGGTAGGGCTTCACACG  
TCATAAATGGTACATACAGAGGGCCGCCAACCCGCGAGGGGGAGCTAATCCAGAAAGT  
GTATCGTAGTCCGGATTGTAGTCTGCAACTCGACTGCATGAAGTTGGAATCGCTAGTAAT  
CGCGGATCAGCATGTCGCGGTGAATACGTTCCCGGGTCTTGTACACACCGCCCGTACAC  
CATGGGAGCGGGTTTTACCAGAAGTAG

Program	BLASTN <a href="#">?</a> <a href="#">Citation</a> <a href="#">v</a>
Database	rRNA_tpestrains/16S_ribosomal_RNA <a href="#">See details</a> <a href="#">v</a>
Query ID	lc Query_112169
Description	None
Molecule type	dna
Query Length	1347
Other reports	<a href="#">Distance tree of results</a> <a href="#">MSA viewer</a> <a href="#">?</a>

Organism only top 20 will appear  exclude

Type common name, binomial, taxid or group name

[+ Add organism](#)

Percent Identity  to  E value  to  Query Coverage  to

[Filter](#) [Reset](#)

- Descriptions**
- Graphic Summary
- Alignments
- Taxonomy

Sequences producing significant alignments Download Select columns Show  [?](#)

select all 100 sequences selected [GenBank](#) [Graphics](#) [Distance tree of results](#) [MSA Viewer](#)

Description	Scientific Name	Max Score	Total Score	Query Cover	E value	Per. Ident	Acc. Len	Accession
<input checked="" type="checkbox"/> <a href="#">Duganella aceris strain SAP-35 16S ribosomal RNA, partial sequence</a>	<a href="#">Duganella aceris</a>	2344	2344	100%	0.0	98.07%	1459	<a href="#">NR_180977.1</a>
<input checked="" type="checkbox"/> <a href="#">Duganella qianjiadongensis strain CY13W 16S ribosomal RNA, partial sequence</a>	<a href="#">Duganella qianjiadongensis</a>	2340	2340	99%	0.0	98.14%	1495	<a href="#">NR_170537.1</a>
<input checked="" type="checkbox"/> <a href="#">Duganella margarita strain FT109W 16S ribosomal RNA, partial sequence</a>	<a href="#">Duganella margarita</a>	2338	2338	100%	0.0	98.00%	1493	<a href="#">NR_170536.1</a>
<input checked="" type="checkbox"/> <a href="#">Pseudoduganella namucuoensis strain 333-1-0411 16S ribosomal RNA, partial sequence</a>	<a href="#">Pseudoduganella namucuoensis</a>	2338	2338	100%	0.0	98.00%	1490	<a href="#">NR_118215.1</a>
<input checked="" type="checkbox"/> <a href="#">Rugamonas aquatica strain FT29W 16S ribosomal RNA, partial sequence</a>	<a href="#">Rugamonas aquatica</a>	2337	2337	100%	0.0	97.92%	1493	<a href="#">NR_180583.1</a>

## TE21 (F+R)

GCAGCACGGGGCAACCCTGGTGGCGAGTGGCGAACGGGTGAGTAATACATCGGAACGTG  
TCCTAGAGTGGGGGATAGCCCGGCCAAAGCCGGATTAATACCGCATAACGCTCGAGAGAGG  
AAAGCGGGGGATCTTCGGACCTCGCGCTCAAGGGGCGGCCGATGGCGGATTAGCTAGTTG  
GTGGGGTAAAGGCCTACCAAGGCGACGATCCGTAGCTGGTCTGAGAGGACGACCAGCCAC  
ACTGGGACTGAGACACGGCCCAGACTCCTACGGGAGGCAGCAGTGGGGAATTTGGACAA  
TGGGGGCAACCCTGATCCAGCAATGCCGCGTGTGTGAAGAAGGCCTTCGGGTTGTAAGC  
ACTTTTGTCCGAAAGAAATCCTCTGGGTTAATACCTCGGGGGGATGACGGTACCGGAAG  
AATAAGCACCGGCTAACTACGTGCCAGCAGCCGCGGTAATACGTAGGGTGCAGAGCGTTAA  
TCGGAATTACTGGGCGTAAAGCGTGCGCAGGCGGTTTCGCTAAGACCGATGTGAAATCCCC  
GGGCTTAACCTGGGAACTGCATTGGTACTGGCGAGCTAGAGTGTGGCAGAGGGGGGTAG  
AATCCACGTGTAGCAGTCAAATGCGTAGAGATGTGGAGGAATACCGATGGCGAAGGCAG  
CCCCCTGGGCTAACACTGACGCTCATGCACGAAAGCGTGGGGAGCAAACAGGATTAGATA  
CCCTGGTAGTCCACGCCCTAAACGATGTCAACTAGTTGTTGGGGATTCATTTCTTAGTA  
ACGTAGCTAACGCGTGAAGTTGACCGCCTGGGGAGTACGGTCGCAAGATTA AAAACTCAA  
GGAATTGACGGGGACCCGCACAAGCGGTGGATGATGTGGATTAATTCGATGCAACGCGAA  
AAACCTTACCTACCCTTGACATGGACGGAACCTCCGCTGAGAGGTGAAGGTGCTCGAAAGA  
GAACCGTCGCACAGGTGCTGCATGGCTGTCGTCAGCTCGTGTGAGATGTTGGGTTAA  
GTCCCGCAACGAGCGCAACCCTTGTCTCTAGTTGCTACGAAAGGGCACTCTAGAGAGACT  
GCCGGTGACAAACCGGAGGAAGGTGGGGATGACGTCAAGTCCTCATGGCCCTTATGGGTA  
GGGCTTACACGTCATAAATGGTCGGAACAGAGGGTTGCCAACCCGCGAGGGGGAGCTA  
ATCCAGAAAACCGATCGTAGTCCGGATTGCACTCTGCAACTCGAGTGCATGAAGCTGGA  
ATCGCTAGTAATCGCGGATCAGCATGCCGCGGTGAATACGTTCCCGGGTCTTGTACACAC  
CGCCCGTCACACCATGGGAGTGGGTTTTACCAGAAGTGGCTAGTC

Program	BLASTN <a href="#">?</a> <a href="#">Citation</a> <a href="#">v</a>
Database	rRNA_tpestrains/16S_ribosomal_RNA <a href="#">See details</a> <a href="#">v</a>
Query ID	lc Query_48179
Description	None
Molecule type	dna
Query Length	1365
Other reports	<a href="#">Distance tree of results</a> <a href="#">MSA viewer</a> <a href="#">?</a>

Organism only top 20 will appear  exclude

Type common name, binomial, taxid or group name

[+ Add organism](#)

Percent Identity  to  E value  to  Query Coverage  to

[Filter](#) [Reset](#)

- Descriptions**
- Graphic Summary
- Alignments
- Taxonomy

Sequences producing significant alignments Download Select columns Show  [?](#)

select all 100 sequences selected [GenBank](#) [Graphics](#) [Distance tree of results](#) [MSA Viewer](#)

	Description	Scientific Name	Max Score	Total Score	Query Cover	E value	Per. Ident	Acc. Len	Accession
<input checked="" type="checkbox"/>	<a href="#">Trinickia diaoshuihuensis strain NEAU-SY24 16S ribosomal RNA, partial sequence</a>	<a href="#">Trinickia diaoshuihuensis</a>	2483	2483	100%	0.0	99.49%	1524	<a href="#">NR_171504.1</a>
<input checked="" type="checkbox"/>	<a href="#">Trinickia dabaoshanensis strain GIMN1.004 16S ribosomal RNA, partial sequence</a>	<a href="#">Trinickia dabaoshanensis</a>	2449	2449	100%	0.0	99.05%	1437	<a href="#">NR_133711.1</a>
<input checked="" type="checkbox"/>	<a href="#">Trinickia soli strain GP25-8 16S ribosomal RNA, partial sequence</a>	<a href="#">Trinickia soli</a>	2449	2449	100%	0.0	99.05%	1480	<a href="#">NR_043872.1</a>
<input checked="" type="checkbox"/>	<a href="#">Trinickia dinghuensis strain DHOM06 16S ribosomal RNA, partial sequence</a>	<a href="#">Trinickia dinghuensis</a>	2444	2444	100%	0.0	98.97%	1492	<a href="#">NR_171482.1</a>
<input checked="" type="checkbox"/>	<a href="#">Trinickia caryophylli strain ATCC 25418 16S ribosomal RNA, partial sequence</a>	<a href="#">Trinickia caryophylli</a>	2344	2344	100%	0.0	97.66%	1448	<a href="#">NR_040806.1</a>

## TE22 (F+R)

AGTAGCAATACCGGGTGGCGAGTGGCGGACGGGTGAGTAATGCATCGGGATCTACCCAAA  
CGTGGGGGATAACGTAGGGAACTTACGCTAATACCGCATACTCCATGGGAGAAAGCG  
GGGGCTCGCAAGACCTCGCGCGGTTGGACGAACCGATGTGCGATTAGCTAGTTGGTAGGG  
TAATGGCCTACCAAGGCGACGATCGCTAGCTGGTCTGAGAGGATGATCAGCCACACTGGG  
ACTGAGACACGGCCCAGACTCCTACGGGAGGCAGCAGTGGGGAATATTGGACAATGGGCG  
CAAGCCTGATCCAGCAATGCCGCGTGTGTGAAGAAGGCCTTCGGGTTGTAAAGCACTTTT  
ATCAGGAGCGAAATACTGCGGGTTAATACCCTGCGGGGCTGACGGTACCTGAGGAATAAG  
CACCGGCTAACTTCGTGCCAGCAGCCGCGTAATACGAAGGGTGCAAGCGTTAATCGGAA  
TTACTGGGCGTAAAGGGTGCCTAGGCGGTTTCGTTAAGTCTGTCGTGAAATCCCCGGGCTC  
AACCTGGGAATGGCGATGGATACTGGCGAGCTAGAGTGTGTCAGAGGATGGTGGAAATCC  
CGGTGTAGCGGTGAAATGCGTAGAGATCGGGAGGAACATCAGTGGCGAAGGCGGCCATCT  
GGGACAACACTGACGCTGAAGCACGAAAGCGTGGGGAGCAAACAGGATTAGATACCCTGG  
TAGTCCACGCCCTAAACGATGCGAACTGGATGTTGGTCTCAACTCGGAGATCAGTGTGCA  
AGCTAACGCGTTAAGTTCGCCGCCTGGGGAGTACGGTTCGCAAGACTGAAACTCAAAGGAA  
TTGACGGGGGCCCGCACAAAGCGGTGGAGTATGTGGTTTAATTCGATGCAACGCGAAGAAC  
CTTACCTGGGCCTTGACATGTCCGGAATCCTGCAGAGATGCGGGAGTGCCTTCGGGAATC  
GGAACACAGGTGCTGCATGGCTGTCGTCAGCTCGTGTGTCGTGAGATGTTGGGTTAAGTCCC  
GCAACGAGCGCAACCCTTGTCTTAGTTGCCAGCACGTAATGGTGGGAACTCTAAGGAGA  
CTGCCGGTGACAAACCGGAGGAAGGTGGGGATGACGTCAAGTCTCATGGCCCTTACGGC  
CAGGGCTACACACGTAATAACAATGGTTCGGTACAGAGGGTTGCAATACCGCGAGGTGGAGC  
CAATCCCAGAAAGCCGATCCCAGTCCGGATTGGAGTCTGCAACTCGACTCCATGAAGTCG  
GAATCGCTAGTAATCGCAGATCAGCTATGCTGCGGTGAATACGTTCCCGGGCCTTGACA  
CACCGCCGTCACACCATGGGAGTGAGTTGCTCCAGAAGCCGTTAG

Program	BLASTN <a href="#">?</a> <a href="#">Citation</a> <a href="#">v</a>
Database	rRNA_tyestrains/16S_ribosomal_RNA <a href="#">See details</a> <a href="#">v</a>
Query ID	lc Query_60379
Description	None
Molecule type	dna
Query Length	1366
Other reports	<a href="#">Distance tree of results</a> <a href="#">MSA viewer</a> <a href="#">?</a>

**Organism** only top 20 will appear  exclude

Type common name, binomial, taxid or group name

[+ Add organism](#)

---

**Percent Identity**  to  **E value**  to  **Query Coverage**  to

[Filter](#) [Reset](#)

Descriptions		Graphic Summary	Alignments	Taxonomy				
<b>Sequences producing significant alignments</b> <span style="float: right;">Download <a href="#">v</a> Select columns <a href="#">v</a> Show <input type="text" value="100"/> <a href="#">?</a></span>								
<input checked="" type="checkbox"/> select all <small>100 sequences selected</small> <span style="float: right;"><a href="#">GenBank</a> <a href="#">Graphics</a> <a href="#">Distance tree of results</a> <a href="#">MSA Viewer</a></span>								
Description	Scientific Name	Max Score	Total Score	Query Cover	E value	Per. Ident	Acc. Len	Accession
<input checked="" type="checkbox"/> <a href="#">Rhodanobacter hydrolyticus strain G-5-5 16S ribosomal RNA, partial sequence</a>	<a href="#">Rhodanobacter hydrolyticus</a>	2442	2442	99%	0.0	98.97%	1478	<a href="#">NR_179070.1</a>
<input checked="" type="checkbox"/> <a href="#">Dyella agri strain DKC-1 16S ribosomal RNA, partial sequence</a>	<a href="#">Dyella agri</a>	2422	2422	99%	0.0	98.68%	1479	<a href="#">NR_158147.1</a>
<input checked="" type="checkbox"/> <a href="#">Dyella japonica strain XD53 16S ribosomal RNA, partial sequence</a>	<a href="#">Dyella japonica</a>	2346	2346	100%	0.0	97.66%	1485	<a href="#">NR_040974.1</a>
<input checked="" type="checkbox"/> <a href="#">Dyella japonica strain NBRC 102414 16S ribosomal RNA, partial sequence</a>	<a href="#">Dyella japonica</a>	2346	2346	100%	0.0	97.66%	1465	<a href="#">NR_114075.1</a>
<input checked="" type="checkbox"/> <a href="#">Dyella kyungheensis strain THG-B117 16S ribosomal RNA, partial sequence</a>	<a href="#">Dyella kyungheensis</a>	2340	2340	99%	0.0	97.86%	1454	<a href="#">NR_109691.1</a>

## TE23 (F+R)

AAGGCCCTTCGGGGTACTCGAGTGGCGAACGGGTGAGTAACACGTGGGTGATCTGCCCTG  
CACTTTGGGATAAGCCTGGGAAACTGGGTCTAATACCGAATATGATCATGGCCTGCATGG  
GTTGTGGTGGAAAGCTTTTGCGGTGTGGGATGGGCCCGCGCCTATCAGCTTGTGGTGG  
GGTAATGGCCTACCAAGGCGACGACGGGTAGCCGGCCTGAGAGGGTGACCGGCCACACTG  
GGACTGAGATACGGCCCAGACTCCTACGGGAGGCAGCAGTGGGGAATATTGCACAATGGG  
CGCAAGCCTGATGCAGCGACGCCGCGTGAGGGATGACGGCCTTCGGGTTGTAAACCTCTT  
TCAGTAGGGACGAAGCGCAAGTGACGGTACCTATAGAAGAAGGACCGGCCAACTACGTGC  
CAGCAGCCGCGGTAATACGTAGGGTCCGAGCGTTGTCCGGAATTACTGGGCGTAAAGAGC  
TCGTAGGTGGTTTGTGCGGTTGTTTCGTGAAAACCTCACAGCTCAACTGTGGGCGTGCGGGC  
GATACGGGCAGACTTGAGTACTGCAGGGGAGACTGGAATTCCTGGTGTAGCGGTGGAATG  
CGCAGATATCAGGAGGAACACCGGTGGCGAAGGCGGGTCTCTGGGCAGTAACTGACGCTG  
AGGAGCGAAAGCGTGGGGAGCGAACAGGATTAGATACCCTGGTAGTCCACGCCGTAAACG  
GTGGGTACTAGGTGTGGGTTTCCTTCCCTGGGATCCGCGCCGTAGCTAACGCATTAAGTA  
CCCCGCCTGGGGAGTACGGCCGCAAGGCTAAAACCTCAAAGAAATTGACGGGGGCCCGCAC  
AAGCGGCGGAGCATGTGGATTAATTTCGATGCAACGCGAAGAACCTTACCTGGGTTTGACA  
TGCACAGGACGCCGGCAGAGATGTCGGTTCCTTGTGGCCTGTGTGCAGGTGGTGCATGG  
CTGTCGTCAGCTCGTGTGAGATGTTGGGTTAAGTCCCGCAACGAGCGCAACCCTTGT  
CTCATGTTGCCAGCACGTTATGGTGGGACTCGTGAGAGACTGCCGGGGTCAACTCGGAG  
GAAGGTGGGGATGACGTCAAGTCATCATGCCCTTATGTCCAGGGCTTACACATGCTAC  
AATGGCCGTACAAAGGGCTGCGATGCCGTGAGGTGGAGCGAATCCTTTCAAAGCCGGTC  
TCAGTTCGGATCGGGTCTGCAACTCGACCCCGTGAAGTCGGAGTCGCTAGTAATCGCAG  
ATCAGCAACGCTGCGGTGAATACGTTCCCGGGCCTTGTACACACCGCCCGTCACGTCATG  
AAAGTCGGTAACACCCGAAGCCGGTGGCCTAACCC

Program	BLASTN <a href="#">?</a> <a href="#">Citation</a> <a href="#">v</a>
Database	rRNA_tyestrains/16S_ribosomal_RNA <a href="#">See details</a> <a href="#">v</a>
Query ID	lc Query_20203
Description	None
Molecule type	dna
Query Length	1355
Other reports	<a href="#">Distance tree of results</a> <a href="#">MSA viewer</a> <a href="#">?</a>

Organism only top 20 will appear  exclude

Type common name, binomial, taxid or group name

[+ Add organism](#)

Percent Identity  to  E value  to  Query Coverage  to

[Filter](#) [Reset](#)

- Descriptions**
- Graphic Summary
- Alignments
- Taxonomy

Sequences producing significant alignments Download Select columns Show  [?](#)

select all 100 sequences selected [GenBank](#) [Graphics](#) [Distance tree of results](#) [MSA Viewer](#)

	Description	Scientific Name	Max Score	Total Score	Query Cover	E value	Per. Ident	Acc. Len	Accession
<input checked="" type="checkbox"/>	<a href="#">Mycolicibacterium rhodesiae strain DSM 44223 16S ribosomal RNA, partial sequence</a>	<a href="#">Mycolicibacteriu...</a>	2486	2486	100%	0.0	99.78%	1485	<a href="#">NR_025529.1</a>
<input checked="" type="checkbox"/>	<a href="#">Mycolicibacterium helvum strain JCM 30396 16S ribosomal RNA, partial sequence</a>	<a href="#">Mycolicibacteriu...</a>	2440	2440	100%	0.0	99.19%	1459	<a href="#">NR_152647.1</a>
<input checked="" type="checkbox"/>	<a href="#">Mycolicibacterium setense strain CJP.109395 16S ribosomal RNA, partial sequence</a>	<a href="#">Mycolicibacteriu...</a>	2436	2436	100%	0.0	99.11%	1442	<a href="#">NR_116291.1</a>
<input checked="" type="checkbox"/>	<a href="#">Mycolicibacterium aichiense strain 49005 16S ribosomal RNA, partial sequence</a>	<a href="#">Mycolicibacteriu...</a>	2433	2433	100%	0.0	99.11%	1456	<a href="#">NR_029219.1</a>
<input checked="" type="checkbox"/>	<a href="#">Mycolicibacterium luletiense strain 071 16S ribosomal RNA, partial sequence</a>	<a href="#">Mycolicibacteriu...</a>	2425	2425	100%	0.0	98.97%	1471	<a href="#">NR_151953.1</a>